Quantifying Wave Attenuation by Nature-based Solutions in the Galveston Bay

M. Godfroy

Technische Universiteit Delft

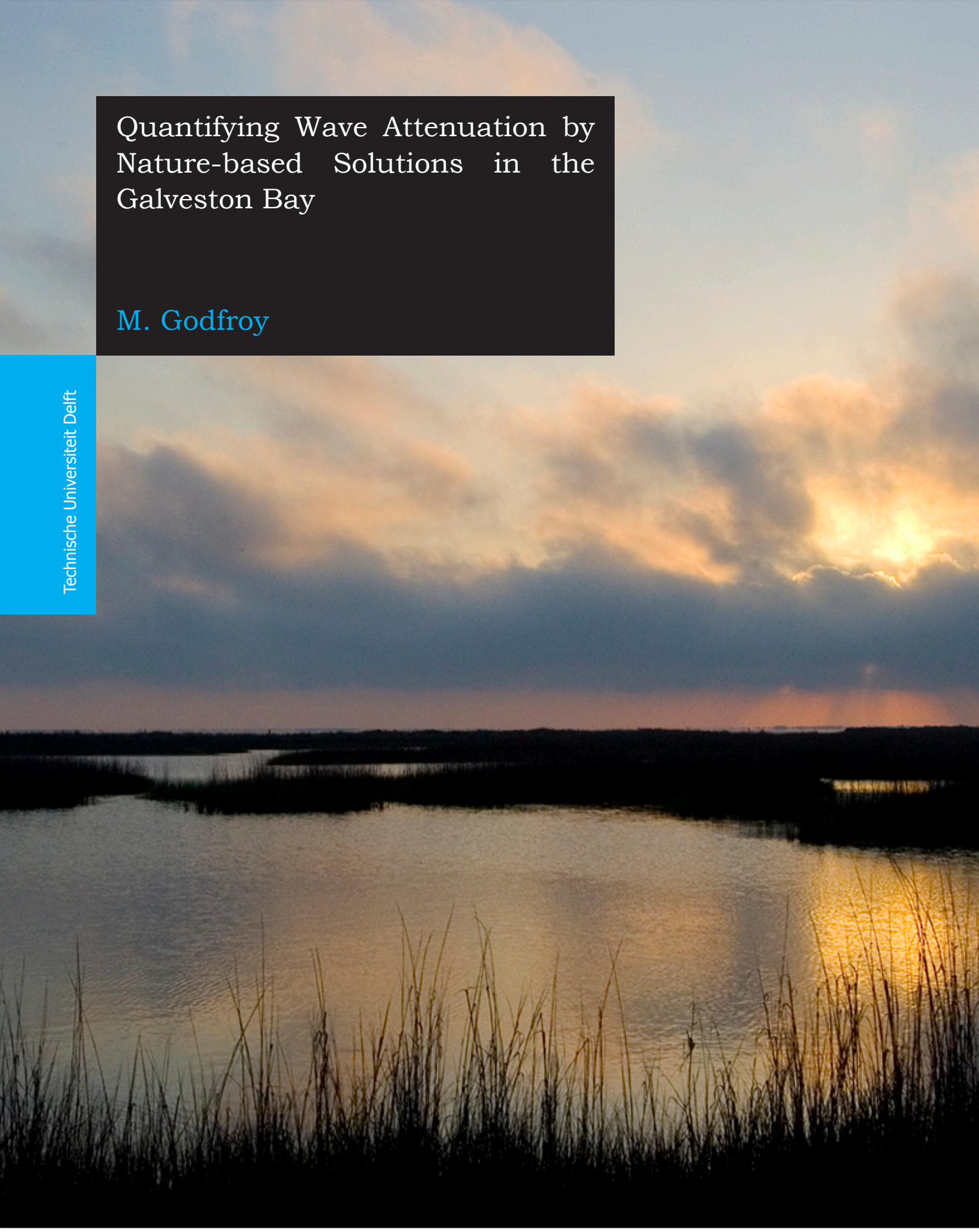

TU Delft Delft University of Technology

Challenge the future

Quantifying Wave Attenuation by Nature-based Solutions in the Galveston Bay

by

M. Godfroy

in partial fulfillment of the requirements for the degree of

Master of Science
in Civil Engineering

at the Delft University of Technology,
to be defended publicly on November 15, 2017.

Supervisor:	Prof. S.N. Jonkman
Thesis committee:	Ir. E.C. Van Berchum
	Ir. V. Vuik
	Ir. H.J. Verhagen

TU Delft Delft University of Technology

Summary

Flood risk is one of the largest natural threats in coastal areas world wide. Significant drivers are storms and hurricanes causing extreme precipitation, storm surge and waves. The latter can result in considerable damage to coastal structures during flood event, especially by energy dissipation due to adverse wave breaking. Nature-based Solutions (NbS) are a promising type of flood mitigation measures that gained significance in recent years. It aims to address flood risk with a sustainable approach and consist of natural or nature-inspired processes and actions. Although many Nature-based Solutions show potential for wave height reduction, their effects are not yet fully quantified. Moreover, research was primarily conducted for mild wave conditions, which further complicates their successful application as flood risk reduction measure.

The Galveston Bay on the upper Texas coast is regularly hit by tropical storms and hurricanes, and large parts of the area are prone to flood risk due to storm surge and wave action. The Federal Emergency Agency (FEMA) indicated flood risk areas in the Bay with a return period of 100 years or shorter in flood maps. Areas with additional risk due to storm waves are explicitly marked. Wave height reduction is furthermore relevant in combination with dikes and levees, as it reduces run-up and overtopping.

The main objective of this thesis is to assess the effectiveness of Nature-based Solutions in reducing flood risk in the Galveston Bay by means of wave attenuation. To achieve this, four sub-research questions were formulated that address (1) the selection of Nature-based Solutions that show promise in reducing wave height, (2) the quantitative description of wave attenuating mechanisms of Nature-based Solutions, (3) the extend of wave-induced flood risk in the Galveston Bay and (4) the effectiveness of Nature-based Solutions in attenuating waves in the Galveston Bay.

The methodology to answer these questions consists of both literature review and numerical modeling. Reference studies show that marsh vegetation, seagrass meadows and oyster reefs are promising NbS with the capability to attenuate waves. Their dissipating mechanisms can be described with depth-induced breaking, bottom friction and vegetation-induced drag. A vegetation-induced drag model is selected to describe the wave energy dissipation by marsh vegetation and seagreass meadows whereas a combination of depth-induced breaking and bottom friction is used to describe the dissipation by an oyster reef. Expressions that describe these hydrodynamic processes are included in a 1D numerical wave propagation model. The numerical model is validated with data from reference studies and the sensitivity for several assumptions is checked.

Next, the model is used to asses the effectiveness of the selected NbS in the Galveston Bay at two locations that are prone to wave action during storm conditions. For both locations, a schematized cross-shore section and hydrodynamic boundary conditions were derived, being water level, wave height, wave period and wind speed, for return periods varying from 10 to 500 years. During these extreme conditions, storm surge causes flooding of the hinterland and waves can travel inland. The wave height at the first line of houses on shore was compared for the situation with and without Nature-based Solutions.

At the first location, the urbanized shore of San Leon in the western part of the Bay, Nature-based Solutions were found not effective in reducing the wave height at the output location. The platform-like bathymetry of the location causes sharp depth-induced breaking, regardless of the Nature-based Solutions. Nevertheless, the NbS did reduces the wave height on the part of the bathymetry leading up to the bank, which suggest that the natural measures can reduce wave breaking on the bank and subsequently wave-induced erosion of the banks.

At the second location, the northern shore of Galveston Island, the implementation of Nature-based Solutions proved more effective. The natural measures were situated on a 500 meter wide, gradually

sloping foreshore. Marsh vegetation makes the largest difference for all return periods, with a reduction rate between 52% and 75%. The reduction is strongest in small water depths but remains significant as the return periods, and thus water depth and wave height, increase. The wave height reduction by seagrass meadows is observed to be minor and decreases even further for increasing water depths and wave heights. An oyster reef locally induces a significant reduction in wave height. If the waves have passed the reef, no additional wave height reducing mechanisms are in action and the wave height increases again. At the output location, i.e. first line of houses on shore, the effect of the oyster reef is almost completely canceled out. Additionally, the effect of oyster reefs varies considerably for a varying water depth with decreasing effectiveness for larger water depths.

Several limitation factors and optimization strategies for the application of Nature-based Solutions were investigated. It was found that the wave attenuating effect of NbS can improve significantly if their location is close to the location of interest, because the reduction is strongest directly behind the NbS. This effect is particularly strong with oyster reefs: the results of the simulation showed that the relocation of a reef to 100 m from the output location, increased the wave height reduction at the output location from 9% to 64%. Furthermore, the tidal range is important for the distribution pattern of the selected Nature-based Solutions. The distribution range of all three species increases with a larger tidal range.

Preliminary results indicate that stem breakage is of significant influence on the capacity of marsh vegetation to reduce storm waves. This is caused by the strong orbital wave velocity of storm waves that exert a force that exceeds the strength of the stems. For the case of the Galveston Bay, large-scale stem breakage will probably occur during conditions with a return period of 100 years or higher. However, the properties of the marsh vegetation can be optimized in order to reduce the expected stem breakage rate. The results suggest that an optimum for the vegetation height can be found that minimizes the stem breakage rate and maximizes wave energy dissipation.

Overall, marsh vegetation is most effective at reducing the wave height (up to 75%), but stem breakage becomes a dominant mechanism for hydrodynamic conditions with a very long return period (>100 years). The expected stem breakage can be reduced with shorter vegetation. Oyster reefs are effective at reducing wave height, provided that their location is close to intended area of wave height reduction. They are especially effective for hydrodynamic conditions with shorter return periods (<100 years). Seagrass meadows do not significantly attenuate storm waves. Marsh vegetation can reduce the required Base Floor Elevation at wave action prone locations in the Galveston Bay with up to three feet (0.91 m). Marsh vegetation proves especially effective in combination with a levee, because it reduces run-up and overtopping. It was found that a marsh of 100 meters in front of a dike reduces the maximum overtopping as much as a crest raise of 1.13 meter. This shows that application of natural measures can increase the reliability of existing flood protection structures, and allows new structures to be designed lower while maintaining the same flood safety requirements.

Recommendations and opportunities for further research include:

- Expand the model to two dimensions. Wave processes such as oblique incident waves, refraction and diffraction can be of particular significance in a semi-enclosed water body with and irregular coastline, such as the Galveston Bay.
- Investigate the behavior of waves around oyster reefs with use of physical experiments to expand the knowledge on its limits of effectiveness.
- Develop a more complete flood risk framework for the Galveston Bay by assessing the damage reduction and implementation costs associated with Nature-based Solutions.

To conclude, this research shows that Nature-based Solutions have great potential to contribute to flood risk reduction in the Galveston Bay due to their capability to significantly contribute to wave height reduction during storm conditions. However, it is emphasized that the limitations and optimizations with respect to their location, strength and biological requirements must be taken into account in order to maximize their effectiveness.

Preface

This thesis forms the last step to complete the MSc programme of Hydraulic Engineering at Delft University of Technology. The research is part of the research programme BE SAFE, financed primarily by the Netherlands Organisation for Scientific Research (NWO).

This report is the result of nine months work, which were both challenging and exiting. I encountered a lot of 'firsts' during the research process, which made me step out of my comfort zone again and again. For instance, my knowledge on Nature-based Solutions was limited to the mere basics and I had very little experience with Matlab coding. Moreover, the entire process of setting up a research study was a new experience. This all added to a steep learning curve and made my thesis research the most instructive part of my time at TU Delft.

I was well on my way towards my midterm meeting in June when the Atlantic hurricane season started. I started checking the forecast website of NOAA on a daily base because it was predicted that this would be an intense hurricane year. Texas was, fortunately, not hit by a major hurricane in over a decade but nobody knew for how long this streak would continue. Several hurricanes had formed and dissipated when I saw a depression in the Gulf of Mexico on the NOAA satellite image near the end of August. It was rapidly transforming into a major hurricane and was called 'Harvey'. It was headed for Texas, and within a few days, it swept over the Upper Gulf Coast causing major floodings and damage.

This destructive event underlined, once more, the relevance of flood risk reduction research. With renewed motivation I continued my graduation research, in the hope to contribute to the reduction of the devastating consequences of hurricanes. Furthermore, it sparked a fact-finding research on the aftermath of Hurricane Harvey by several sections from TU Delft. It gave me the opportunity to work together with excellent researchers in a multidisciplinary team. This experience made it even more clear why I started with the Hydraulic Engineering MSc programme in the first place.

I owe many thanks to everybody who helped me during my research. I would like to thank the members of my committee for their guidance and constructive feedback throughout my research process. Erik, thank you for patiently answering all my question and explaining what was going on in the Galveston Bay in the first place. Your help with setting up a structured research proved very valuable. Vincent, thank you for helping me with the numerical model and for your knowledge on wave dissipation in vegetation fields. Discussing your model sparked my motivation to finally, just before graduating, learn Matlab thoroughly. Henk Jan, thank you for sharing your years of experience and for making me zoom out and consider practical aspects that would otherwise be forgotten. This not only holds for my thesis research: throughout my master's studies you were always available to answer my questions. Bas, many thanks for your feedback on my work. Despite your busy schedule, you always found time to reply to my e-mails and answer my questions. I appreciate how you are able to quickly address the key issues and ask the right questions.

Last but foremost, I would like to thank Teun, Gerty, Frans, Hanneke, Noëlle, Michelle, Maartje, Marc and Bram for telling me over and over again that everything is going to be alright.

M. Godfroy
Delft, November 2017

Contents

List of Abbreviations

DFE	- **D**esign **F**lood **E**levation
BFE	- **B**ase **F**loor **E**levation
FEMA	- **F**ederal **E**mergency **M**anagement **A**gency
GCCDRP	- **G**ulf **C**oast **C**ommunity **P**rotection and **R**ecovery **D**istrict
GLO	- **G**eneral **L**and **O**ffice of Texas
GEV	- **G**eneralized **E**xtreme **V**alue distribution
HGBR	- **H**ouston-**G**alveston **B**ay **R**egion
MLLW	- **M**ean **L**ower **L**ow **W**ater
MSL	- **M**ean **S**ea **L**evel
NbS	- **N**ature-**b**ased **S**olution(s)
NAVD-88	- **N**orth **A**merican **V**ertical **D**atum of **1988**
NOAA	- **N**ational **O**ceanic and **A**tmospheric **A**dministration
TAMUG	- **T**exas **A&M U**niversity - **G**alveston
TCHFP	- **T**exas **C**ity **H**urricane **F**lood **P**rotection
SSPEED	- **S**evere **S**torm **P**rediction, **E**ducation, and **E**vacuation from **D**isasters
SWAN	- **S**imulating **WA**aves **N**earshore
USACE	- **U**nited **S**tates **A**rmy **C**orps of **E**ngineers

Terminology

Although consistency is endeavored throughout the report, some sources use the U.S. customary system and others the metric system. The latter is the main system that was used throughout the report. However, in some parts the U.S. customary values are provided as well.

1 inch =	0.0254 meter
1 feet =	0.3048 meter
1 mile =	1,609.3 meter
1 knot =	0.5144 meter per second
1 mile per hour =	0.44704 meter per second

The datum that is used in the report is the North American Vertical Datum of 1988, which is abbreviated as 'NAVD-88'. It is sometimes inevitable, due to the source, to denote water levels with respect to M.L.L.W or M.S.L. Throughout the report the tidal datums of the NOAA station 'Eagle Point' are used. They relate to NAVD-88 as follows:

Mean Higher High Water	NAVD-88 +0.264 m	MHHW
Mean Sea Level	NAVD-88 +0.108 m	MSL
Mean Lower-Low Water	NAVD-88 -0.074 m	MLLW

Furthermore, different parameters for wave height and wave period are used. Generally, the significant wave height is used (H_s). An alternative expression for the significant wave height is the spectral wave height H_{m0}, based on the zeroth-moment of the wave spectrum. It is assumed that $H_s = H_{m0}$. When considering wave energy, the root-mean-square wave height is often used. It relates to the significant wave height as follows: $H_{rms} = 0.5\sqrt{2}H_s$.

For the wave period, the significant wave period T_s is used, which is the mean period of the highest one-third of the waves of a record. The peak wave period T_p is also used, which is almost identical to the significant wave period (Van der Meer et al., 2016).

1

Introduction

1.1. Waves in coastal flood risk

Flood risk is one of the largest hazards in coastal areas. Approximately 40% of the world population lives within a range of 100 km of a coast. In addition, the increase in population in coastal areas is higher than the overall increase in world population (Nicholls & Small, 2002). A number of recent studies suggest that climate change will further increase flood risk in the near future. This is, among others, due to sea level rise, land subsidence and more extreme weather events.

Significant drivers for coastal flood risk are storms and hurricanes. They are accompanied by heavy precipitation and strong wind. The latter generates storm surge and extreme waves in coastal waters, which form a threat in various ways. Hydrodynamic wave loads can inflict considerable damage on coastal constructions such as houses, levees and bridges (Jin et al., 2010). Especially breaking waves, that release large amounts of concentrated wave energy at once, can be hazardous. This is illustrated in figures 1.1 and 1.2. Furthermore, strong wave action can cause erosion of beaches, banks and shorelines. The wave height is, among others, limited by the water depth. Therefore storm surge, resulting in larger water depths during a flood event, causes waves to grow in height and travel further inland.

Figure 1.1: Waves hammering a pier in Ventura, CA. Source: Rob Varela, The Star

Figure 1.2: A lighthouse is battered during a storm in Newhaven, England. Source: Glyn Kirk, AFP

Waves can also cause wave run-up on a slope and overtopping of hydraulic structures. These mechanisms can inflict damage to a levee and ultimately flooding of the hinterland. Run-up can be defined as the maximum water level on an slope; the incoming wave crest propagates on a slope to a higher level than the original wave crest. This is shown in figures 1.3 and 1.4. If the wave run-up level exceeds the crest level of a dike, overtopping occurs. The resulting discharge over the dike can lead to erosion of the landward slope and, in severe cases, to inundation of the hinterland. The severity of both overtopping and run-up depends largely on the wave height (Verhagen, d'Angremond, & van Roode, 2012).

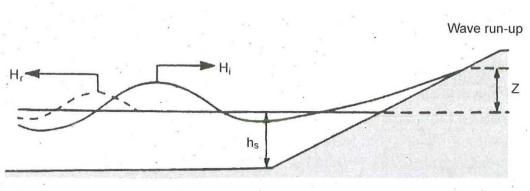

Figure 1.3: Run-up on a slope.
Source: (Verhagen et al., 2012)

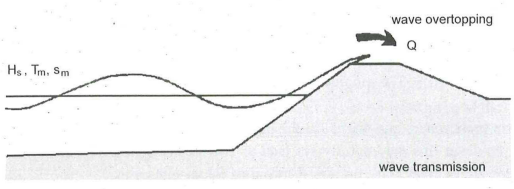

Figure 1.4: Wave overtopping.
Source: (Verhagen et al., 2012)

1.2. Flood risk reduction by Nature-based Solutions

Flood risk can be defined as the product of the probability of a flood event and the consequence of a flood event. In order to reduce flood risk the two components of risk can be addressed. Hence flood risk mitigation measures aim to diminish the probability, the consequence or both. Flood protection measures that aim to reduce to probability of a flood event, often rely on water retaining structures such as levees, dikes and seawalls. They are generally designed to withstand an extreme water level that includes a characteristic storm surge level and wave height. Structures that only reduce wave action are, for example, breakwaters.

Apart from structural protection against flood risk, natural mitigation measures have gained relevance in recent years. Nature-based Solutions (NbS) address a variety of environmental and societal challenges with a sustainable approach. They consist of natural or nature-inspired processes and actions (Krull et al., 2015). Such natural measures can contribute in meeting a wide range of challenges, from resilience to climate change to flood risk reduction.

One of the challenges of NbS is the difficulty of quantifying their effects. In recent years, Nature-based Solutions have been researched to get more insight in their application possibilities and effectiveness (i.e. Narayan et al. (2016), Krull et al. (2015)). NbS that reduce flood risk are interesting from a hydraulic engineering perspective. They can be applied in combination with regular measures, as is shown in figure 1.5: a flood risk protection system is presented that comprises several 'layers'. The red rectangle contains the Nature-based Solutions that contribute flood protection.

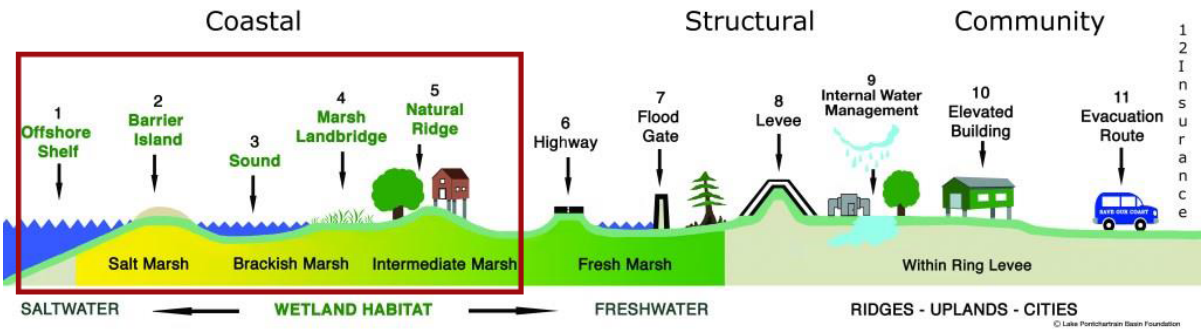

Figure 1.5: A flood risk protection system containing structural measures (e.g. levee), policy measures (e.g. evacuation) and Nature-based Solutions (e.g. marsh vegetation) . Source: Lake Pontchartrain Basin Foundation

Examples of NbS that have potential in reducing surge height or wave action are marsh vegetation, coral reefs or sand nourishments (i.e. Scyphers et al. (2011), Borsje et al. (2011), de Vriend et al. (2015)). Although the mitigating effects of Nature-based Solutions on flood risk is widely acknowledged, many have not been measured and documented thoroughly. This certainly holds for their behavior under extreme conditions (e.g. large wave heights and storm surge). This is nevertheless highly relevant, as design requirements for flood risk protection are based on extremely high water levels and low-probability behavior in general.

Apart from field and laboratory observations, numerical models can assist in gaining insight into the influence of Nature-based Solutions on hydrodynamic processes. In order to assess the effect of NbS on wave action, numerical models are available. For instance, the SWAN model (Simulating WAves Nearshore, (Booij, Ris, & Holthuijsen, 1999)) is widely used to simulate wave behavior in coastal areas,

and offers possibilities to include the effect of vegetation on waves (Suzuki, Zijlema, Burger, Meijer, & Narayan, 2012). Additional research on the flood reducing mechanisms of Nature-based Solutions can contribute to their effective and successful application in flood prone areas. This can be achieved by additional field observations, laboratory experiments and further development of numerical simulation tools for Nature-based Solutions. Eventually, this could lead to generally applicable and substantiated design guidelines for the implementation of Nature-based Solutions in flood risk reducing systems.

1.3. Flood risk in the Galveston Bay

The Houston-Galveston Bay Region (HGBR), shown in figure 1.6 is prone to flood risk and situated in a complex coastal environment, due to the variety of land use (heavy industry in the vicinity of nature reserves) and a densely populated area. The situation is further complicated by a combination of stakeholders with contradicting interests and the large amount of funding that is needed for flood risk reduction. Hurricane Harvey in 2017 and Hurricane Ike in 2008 made it clear that the current protection of the region is substandard. It led to dozens of fatalities and billions of damages even though both events were not worst-case scenarios. In the US, the Federal Emergency Management Agency (FEMA) is responsible for disaster response and pre-disaster mitigation programs. They have been mapping the flood risk in the HGBR and found that, additionally to storm surge, large parts of the Bay are threatened by wave action in case of a storm or hurricane (FEMA, 2017).

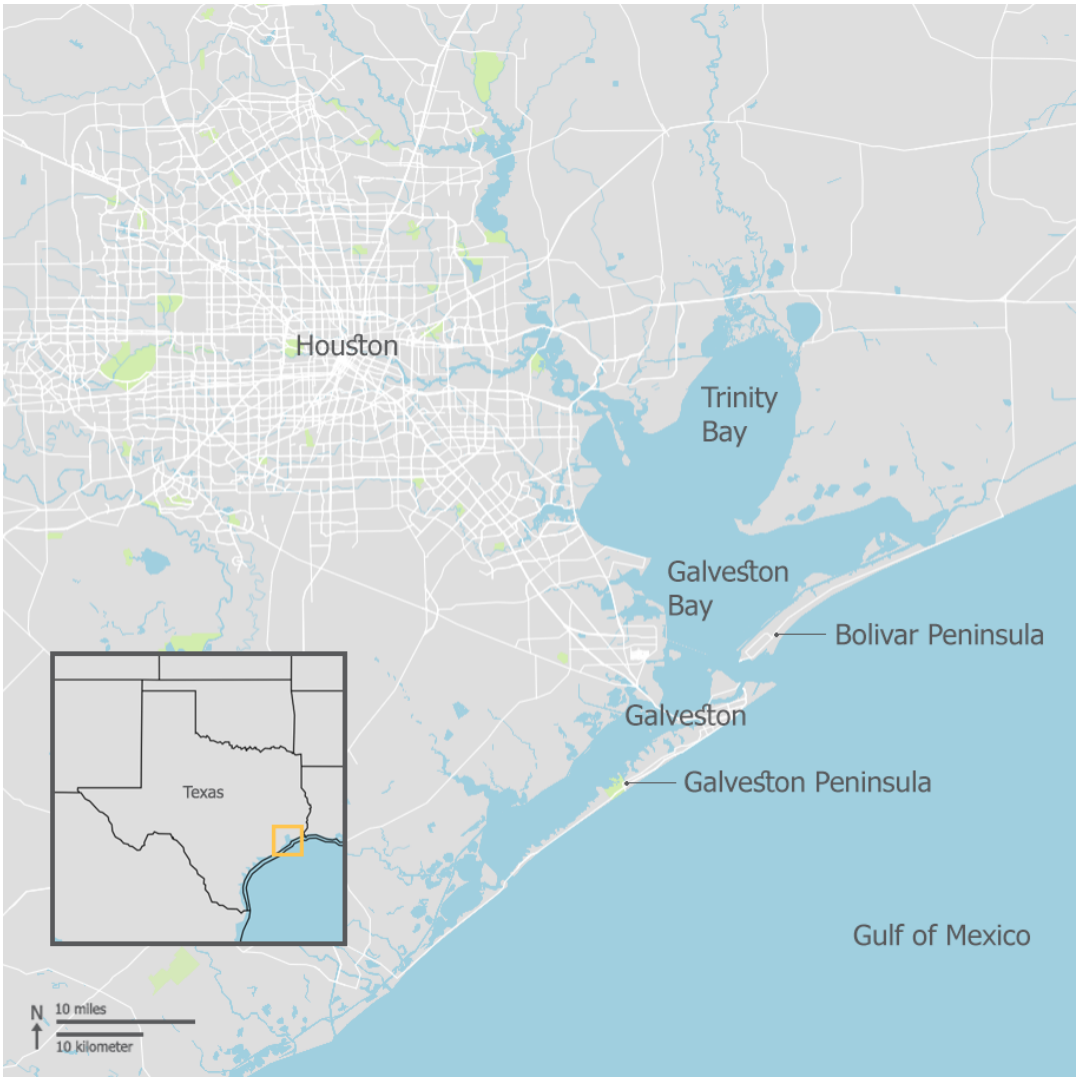

Figure 1.6: Houston-Galveston Bay Region with several relevant components.

Currently, the emphasis of flood risk mitigation in the area is on individual measures such as house elevation and flood risk insurance. Locally, structural measures are in place, for instance a seawall in the city of Galveston. Counties around the Galveston Bay provide awareness programs, dictate building codes and arrange evacuations in case of a flood event, all with varying levels of obligation. As the level of protection for the total area is still inadequate, research on large-scale flood risk reduction has been ongoing for years and several types of mitigation measures have been suggested. The options include among others several levee-type structures, storm surge barriers, expanding of natural measures and adjustment of building regulations (GCCPRD (2016), Taylor et al. (2016), SSPEED (2015)).

Although a range of possible flood risk reducing measures are available for the area, selecting an optimal solution is complicated. This is largely due to the size of the area that is at risk: a single mitigation measure is not enough to reduce the flood risk significantly in the entire area. Suggested measures have been investigated independently and each measure favors a different zone and different stakeholders. To investigate the optimal risk reduction strategy, a research was started on the flood risk reduction system optimization in the Galveston Bay Area that aimed to investigate how different mitigation measures work in combination. Van Berchum and Mobley (2017) developed a model that evaluates a range of combinations of both structural and non-structural measures. It calculates the economic impact of a strategy in terms of investment costs and expected damage. Non-economic performance indicators can also be included. However, in order to assess the feasibility of Nature-based Solutions in a flood risk reduction strategy in the Galveston Bay, their ability to contribute to flood risk reduction should be quantified.

De Boer (2015) mapped the flood risk in the Galveston Bay in his MSc-thesis and investigated vulnerable areas with respect to storm surge and wave action. He explored the opportunities for implementation of Nature-based Solutions for flood risk reduction in the HGBR. He developed conceptual designs for implementation of Nature-based Solutions and investigated storm surge reduction due to Nature-based Solutions quantitatively. In his recommendations, he suggests to do the same for wave height reduction. He used qualitative analysis to evaluate the different Nature-based Solutions for wave height reduction and he concluded that NbS alone cannot sufficiently reduce the flood risk in the HGBR but that they can significantly contribute to flood risk reduction and can add extra value to the region.

1.4. Objective of research

As previously explained, many studies have already indicated the flood risk reducing properties of Nature-based Solutions. Despite this research, the mechanisms of Nature-based Solutions that contribute to flood risk reduction due to wave attenuation are not fully understood. In addition to de Boer (2015), who simulated the effect of different types of NbS on storm surge levels, the objective of this thesis is to quantify the wave height reduction due to Nature-based Solutions. It focuses on waves due to storms and hurricanes. Since extreme conditions are of particular interest from an engineering perspective, it is important to further research the limits of effectiveness of the Nature-based Solutions.

The Houston-Galveston Bay Region is a flood prone area, and research on flood risk reducing measures has been ongoing for years. Large parts of the Bay area are threatened by wave action. Although implementation of Nature-based Solutions to lower wave-related risks has been acknowledged as a solution, their effectiveness has not been studies thoroughly and quantitatively. As a result, it is unknown if NbS are effective in the Galveston bay and, in case they are, how they can best be implemented.

Considering the above, there is a need for quantitative assessment of the wave height reducing capacities of Nature-based Solutions. This contributes to the effective implementation of Nature-based Solutions in flood prone areas, such as the Galveston Bay. Quantitative assessment can contribute to objective design guidelines for Nature-based Solutions.

To conclude, the research objective for this thesis is twofold:

- Quantify wave height reduction by Nature-based Solutions.
- Assess the effectiveness of Nature-based Solutions in reducing flood risk in the Galveston Bay by means of wave attenuation.

1.4.1. Research question

In order obtain the objective, a main research question is formulated along with several sub-questions.

How effective are Nature-based Solutions in reducing flood risk in the Galveston Bay by means of wave attenuation?

This question is separated in four sub-questions, which provide betters guidance to the research. Sub-question one and two refer to the first objective, subquestion three and four refer to the second research objective.

1. Which Nature-based Solutions can reduce wave height?
2. What are wave attenuating mechanisms of Nature-based Solutions and how can they be described quantitatively?
3. How does wave attenuation contribute to flood risk reduction in the Galveston Bay?
4. How effective are Nature-based Solutions in reducing wave height in the Galveston Bay?

1.5. Research approach

Both literature review and numerical modeling will be used to analyze the wave attenuating mechanisms of Nature-based Solutions and simulate wave height reduction in the Galveston Bay. Literature of previous research will be used to select Nature-based Solutions that show promise of wave height reduction. As the case study of this research will focus on the Galveston Bay, the selection of NbS also links to the environmental and climatic conditions of that region.

Next, the wave height reducing processes that can be recognized in the selected Nature-based Solutions will be schematized. These schematized processes will be included in a numerical wave propagation model. The use of a numerical model makes sense because it allows for prediction of behavior of Nature-based Solutions beyond that of the field measurements, on conditions of accurate validation. Further, the numerical model can be used as a tool to gain insight into the wave interaction with the Nature-based Solutions. Both support the optimization of the implementation of NbS in flood prone areas. The predictive properties of the model help to assess the effectiveness of Nature-based Solutions in the Galveston Bay.

The SWAN-model (Simulating WAves Nearshore, Booij et al. (1999)) was developed to simulate wave propagation in shallow waters, which makes it a very suitable model to simulate wave reduction by Nature-based Solutions. The inclusion of some types of Nature-based Solutions (e.g. vegetation) in SWAN have been validated before (i.e. Suzuki et al. (2012), Vuik et al. (2016)), which supports the choice to use a SWAN-based numerical model.

The case study on the Galveston Bay starts with a system analysis based on literature and observations from the NOAA (the U.S. governmental scientific agency that focuses on meteorological, climatic and oceanographic conditions). The level of flood risk in the Bay is evaluated and the contribution of waves in flood risk is assessed. Next, the numerical model is used to simulate and assess the wave behavior under influence of Nature-based Solutions at two normative locations in the Bay. The characteristics of the simulated Nature-based Solutions are hypothetical but realistic, as they are based on previous field observations. For various return periods, the model input parameters for the wave climate are derived, with use of literature and extrapolation of historic observations. This is done because flood risk is often explained in terms of return periods (e.g. 'a 1 in 100 year water level').

The results of the simulations can be used to assess the potential wave reduction in that Bay due to NbS. As the simulations are conducted for various return periods, and the resulting wave reduction rates indicate potential flood risk reduction in the Galveston Bay. Subsequently, the results are further refined through optimization of the configuration of the Nature-based Solutions. The limitation of applicability of the Nature-based Solutions will be investigated, which helps to indicate promising locations for Nature-based Solutions in the Bay.

1.6. Thesis outline

This research report consists of three parts, shown in figure 1.7. The first part contains a literature review of potential Nature-based Solutions (chapter 2) and their wave height reducing mechanisms (chapter 3). Next, a numerical model is introduced to simulate the effect of Nature-based Solutions on wave action (chapter 4). Part I provides a theoretical framework and the methodology that are both used later on in the research.

Part II focuses on the Galveston Bay. A system analysis of the area gives an overview of its relevant hydraulic phenomena and the potential for Nature-based Solutions (chapter 5). It further includes the results of the numerical simulation of wave behavior under influence of Nature-based Solutions at two locations in the bay (chapter 6). The model that was elaborated in Part I, was used for these simulations (as shown by the arrow in figure 1.7). Next, it is investigated how the configuration of the natural measures at the two location could be further optimized (chapter 7). Finally, two possible application of Nature-based Solutions in the Galveston Bay are discussed (chapter 8).

Part III covers the discussion (chapter 10), conclusion (chapter 9) and recommendations (chapter 11).

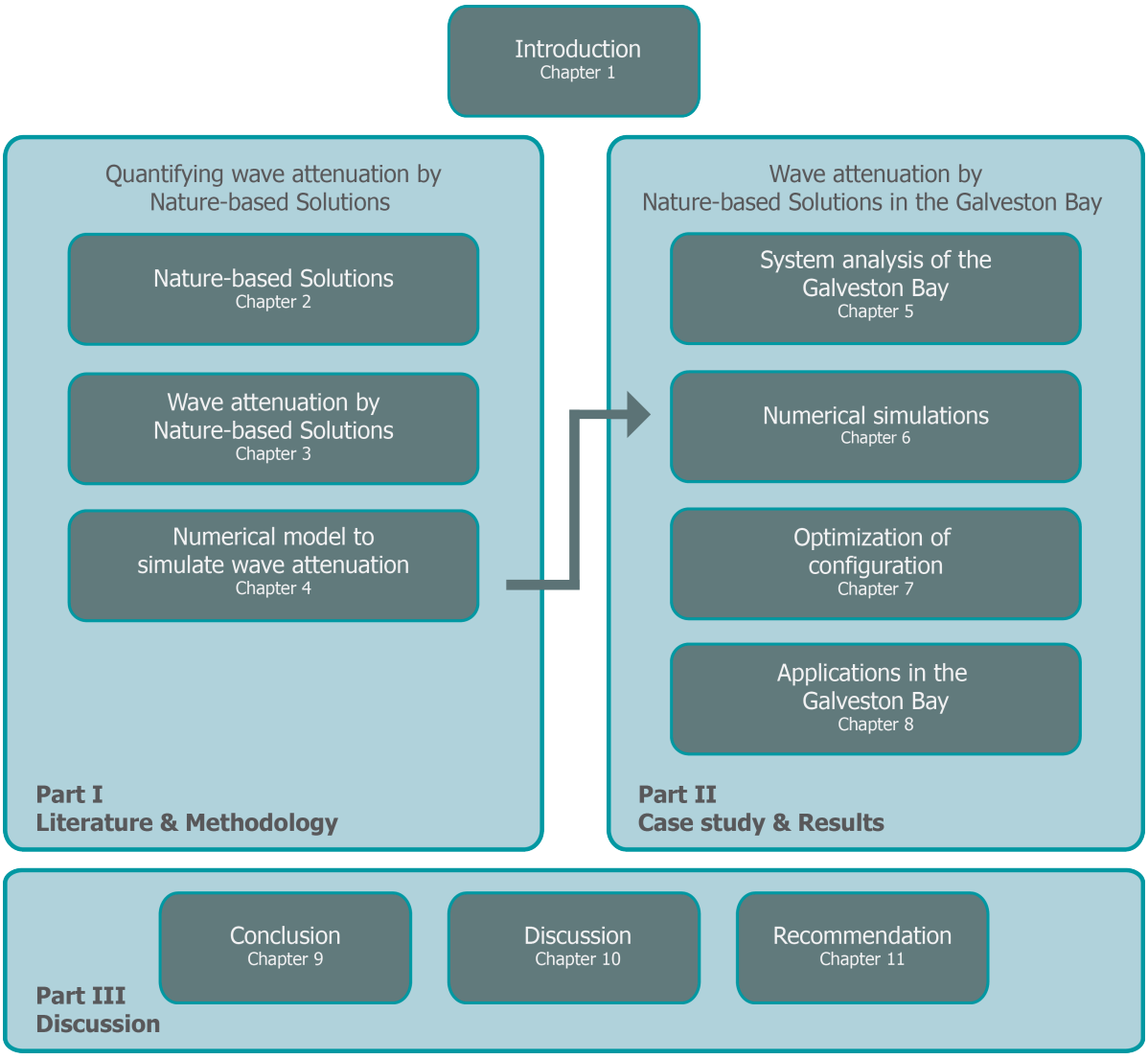

Figure 1.7: Visual overview of the thesis outline.

I

Wave height reduction by Nature-based Solutions

2

Nature-based solutions

In this chapter, it is explained what Nature-based Solutions are and which types of NbS are available. It provides an overview of NbS that, according to literature, can contribute to wave attenuation. An overview of additional properties and benefits are given, as well as restrictions with respect to environmental and climatic conditions in context of the Galveston Bay. This helps to determine what Nature-based Solutions have most potential for further research.

2.1. Classification

Nature-based Solutions have a broad range of applications and appear in various forms. Therefore a clear definition of a NbS is not so straightforward. Moreover, various institutions use different definitions of NbS and place emphasis on diverse aspects. The International Union for Conservation of Nature, an authority in the field of nature conservation, adopted the concept of NbS and defines them as: *"Actions to protect, sustainably manage and restore natural or modified ecosystems that address societal challenges effectively and adaptively, simultaneously providing human well-being and biodiversity benefits."* (Cohen-Shacham, Walters, Janzen, & Maginnis, 2016). The following characteristics are a useful complement to define NbS:

- They address environmental and societal challenges with a sustainable approach.
- They consist of natural or nature-inspired processes and actions.
- They are mostly self-maintaining and resilient to change.

Apart from IUCN, other leading institutions have similar concepts as topics of interest. For instance, Nature-based Solutions are one of the topics of research of the European Commission. Additionally, the Partnership for Environment and Disaster Risk Reduction, which includes UNESCO, uses ecosystems-based disaster risk reduction approaches in their recommendations. Although different terminology is used, the goals of the organizations are similar (Cohen-Shacham et al. (2016) and Krull et al. (2015)).

In engineering context Nature-based Solutions are closely related to the Building with Nature concept. This is a design philosophy that adopts the properties of natural processes and phenomena in a design plan. NbS can be seen as building blocks in a Building with Nature design strategy. However, currently Building with Nature mainly focuses on projects that are related to water safety, whereas nature-based solutions are used in a variety of disciplines (Deltares, 2015).

Nature-based Solutions can help to mitigate, restore, reduce and manage all kinds of challenges and hazards. These environmental and societal challenges include among others:

- **Air pollution** - Remove chemicals and fine particles from the air and diminish emission of such particles.
- **Climate change** - Regulate climate change due to greenhouse gasses by regulating emission and removal of gasses from the atmosphere.
- **Disease regulation** - Prevent spreading of diseases of crops and trees, enhance capacity of an ecosystem to prevent human diseases.

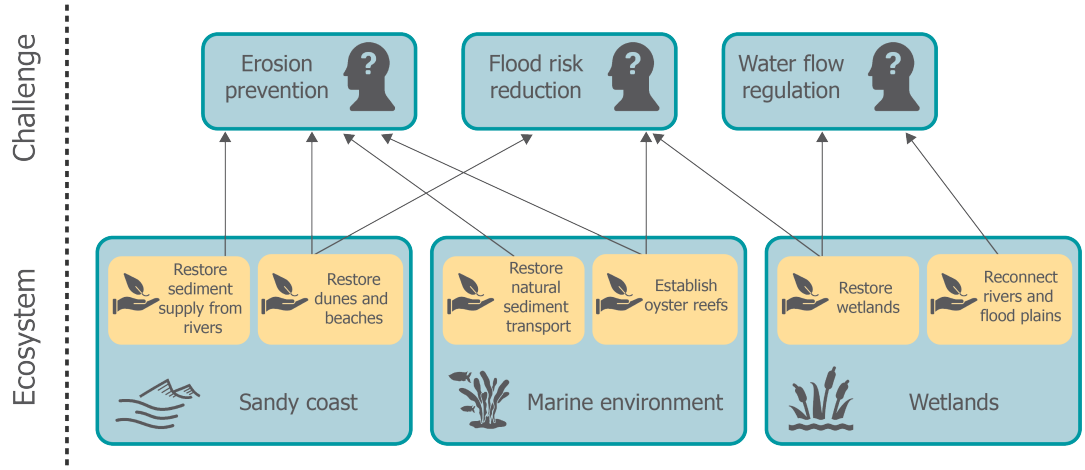

Figure 2.1: An example of Nature-based Solutions (in yellow blocks) in various ecosystems that address several challenges.

- **Disaster risk** - Reduce the impact of disasters such as floods, fires and hurricanes.
- **Erosion prevention** - Reduce structural erosion of soil and establish a morphodynamic equilibrium in coastal areas and inland waters.
- **Food security** -Monitor and balance wild species and distribute food production sustainably and equally.
- **Water flow regulation** - Dampen run-off peaks and related flooding and recharge aquifers.
- **Waste water treatment** - Remove chemicals from water bodies and prevent accumulation of chemicals in sediment en soil.

Nature-based Solutions can be classified in several ecosystems. Multiple groupings can be made: some habitats might overlap depending on the definition. Examples of ecosystems are coastal areas, forests, agricultural zones, urban zones, marine environments, terrestrial wetlands and freshwater zones (Krull et al., 2015). An example of Nature-based Solutions categorized in ecosystems that mitigate challenges is given in figure 2.1.

This study focuses on Nature-based Solutions that mitigate flood risk in a coastal environment. This includes terrestrial wetlands, the coastal areas and the marine environment. For simplicity the combination of these ecosystem is henceforth referred to as 'coastal zone'.

2.2. Categories of flood risk reducing Nature-based Solutions

In recent years natural solutions have been gaining recognition for their ability of coastal protection. Natural coastal and marine ecosystems can act as a buffer between land and sea and damp the hazardous effects of, for instance, hurricanes or erosion. When considering coastal protection, three often heard functions of Nature-based Solutions are their potential for surge reduction, wave attenuation and sediment trapping (Narayan et al., 2016). When considering flood risk reducing Nature-based Solutions in the coastal zone, four categories can be distinguished, based upon a specific ecosystem:

- Biogenic reefs
- Submerged vegetation
- Semi-submerged vegetation
- Sand nourishment measures

The location of the categories is roughly consecutive in the coastal zone, as visualized in figure 2.2. All four categories will be subsequently treated in the following paragraphs and for each category some examples are given. Furthermore the relevance of each category for the case study in the Houston-Galveston Bay Region will be shortly evaluated.

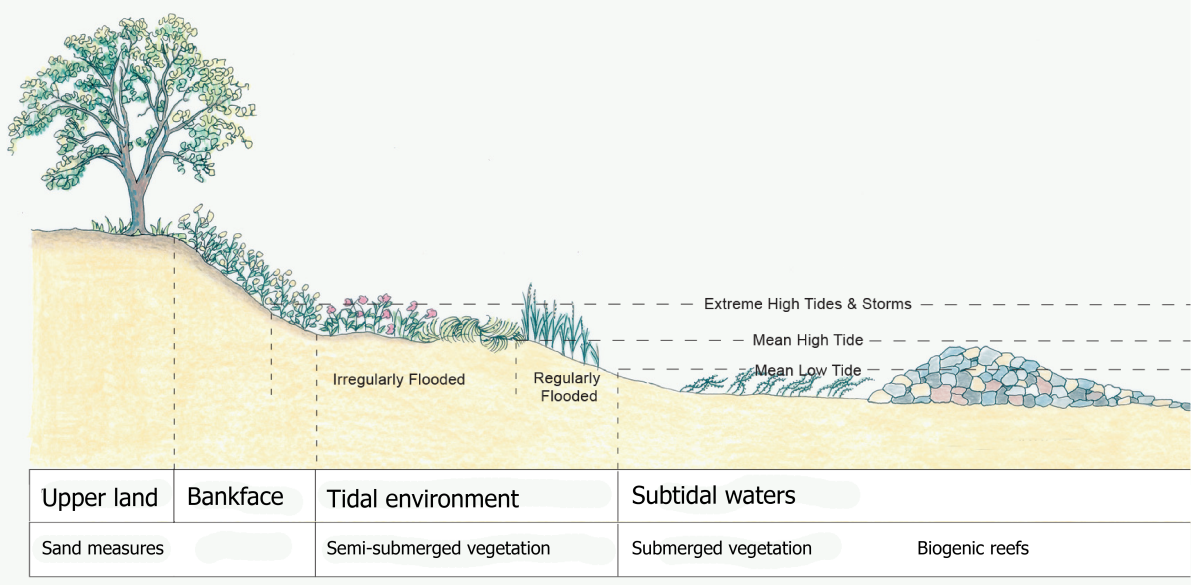

Figure 2.2: Overview of four categories of Nature-based Solutions in the coastal zone. Adapted from Burke Environmental Associates.

2.2.1. Biogenic reefs

Biogenic reefs are hard structures that rise from the sea bed. It is a marine habitat that consists of a biological rocky coalescence. The term 'biogenic' refers to the fact that the hard structure is actually created by organisms, in contrast to already existing rocky structures on which some animals and plants attach.

Reefs are known to be very useful ecosystems. They protect the coastal zone from erosion by regulating sediment transport and attenuating wave energy (Narayan et al., 2016). Furthermore, they are able to filter the water from different types of pollutants and are able to contribute to carbon sequestration, although it is a topic of ongoing discussion in literature whether reefs are a net sink or source for carbon (Wyatt, Lowe, Humphries, & Waite, 2013). They attract a wide rang of fish species, adding to the biodiversity. A range of reef-building species are known. Important types of biogenic reefs are coral reefs, vermetid reefs and oyster reefs.

Coral reefs

Coral reefs are found in tropical climates. They consist of coral in the form of colonies of polyps and various types live in close vicinity. Reef-building types secrete calcium carbonate and thus construct the rock-like structures that primarily function as protection for the organism. Over the years they can form large rocky protrusions on the sea bed. Extensive research has been done on properties and additional functions of coral reefs. They are for instance very effective at attenuating waves, due to their breakwater-like features (Narayan et al., 2016). Coral reefs do occur in the Bay of Mexico but not in the immediate vicinity of the Galveston Bay. The largest coral reef environment in the Bay of Mexico, the Flower Garden Banks, is situated almost 200 kilometer from the Galveston Bay (NOAA, 2016).

Vermetid reefs

Vermetidae are marine worm snails that cannot move by themselves. They live together in large colonies and cement their snail shells together, thus creating a rock-like structure. Sometimes they attach themselves to existing rock formations or grow on top of oysters. Large colonies are located in the Mediterranean Sea and near Florida. It is unknown to what extend vermetid reefs occur in the Galveston Bay. It is known that many of the colonies are declining and research has been done to indicate the cause. As far as literature suggest, no restoration projects for vermetid reefs have been started as they were only recently recognized as a productive and bio-diverse ecosystem (Milazzo, Fine, Marca, Alessi, and Chemello (2016), Milazzo et al. (2014), Balistreri, Chemello, and Mannino (2015)).

Figure 2.3: Coral reef.
Source: Scripps Institution of Oceanography

Figure 2.4: Oyster reef.
Source: Jerod Foster, The Nature Conservancy

Oyster reefs

An oyster reef is a type of shellfish reef. When oyster larvae develop, they attach to a hard substrate for further development. Oysters often attach to other shells, thus forming a column and ultimately a three dimensional reef structure. They are usually found in temperate climate. Oyster reefs can form a natural breakwater-like structure in coastal zones and can diminish wave action. Oyster reefs acts as an important ecosystem for other species and for the environment in general. They prevent erosion, trap sediment and filter water. Harvesting of oysters is a lucrative business for the fishing industry, so regulation and research is conducted in order to realize sustainable oyster farming (Walles et al., 2016). Oyster reefs are abundant in the Galveston Bay and form an important source of income and employment in the area (Scyphers et al., 2011).

2.2.2. Submerged vegetation

Submerged vegetation or 'Submerged Aquatic Vegetation' is a category of plants that is adapted to living in a salt or fresh water environment. Submerged vegetation in coastal areas includes varying types of seagrasses and seaweeds. Seaweeds are typically classified among the algae and seagrasses among the plants. Both types can only survive in shallow waters as the need sunlight for photosynthesis. Submerged vegetation influences wave propagation. It can generate flow resistance and bottom friction that leads to wave attenuation (Fonseca & Cahalan, 1992).

Kelp

Kelp is a large type of seaweed that prevails in relative shallow waters. They grow in colonies known as 'kelp forests'. Smaller patches are called 'kelp meadows'. Kelp forests function as habitat for a range of marine species and are a very productive ecosystem. One of the best known subspecies is the fast-growing Giant Kelp, that can grow as long as 45 meters. Kelp occurs mostly in cool and nutrient-rich waters. Although kelp forests are abundant on the North American west coast, they do not occur in the Gulf of Mexico. Deforestation of kelp forests occurs on several locations around the world, among others due to global warming and overfishing. Although it is widely assumed that global warming and human impact on the environment will increase in the near future, it is not sure if this will cause further degradation of kelp forests, as kelp forest on some location seems highly adaptive to a changing environment. Colonies that harbor a high biodiversity seems to be more adaptive to change (Steneck et al. (2002), Chung et al. (2013)).

Seagrass

Seagrass is a small aquatic flowering plant that can be classified in dozens of species. Most of them prefer a saline environment. They have long, thin leafs and grow in vast colonies called meadows. They resemble terrestrial grass meadows, hence the name 'seagrass'. Seagrass occurs in shallow water as they need sunlight for photosynthesis. Seagrass beds help reduce the wave action on a coast (Narayan et al., 2016). They contribute to stabilization of sediment transport, offer shelter and functions as food source for fish and other marine animals. Furthermore seagrasses can sequester carbon (Fonseca

Figure 2.5: Kelp.
Source: Bluewater Photo Store

Figure 2.6: Seagrass bed.
Source: Michael Patrick O'Neill, New Scientist

& Cahalan, 1992). Seagrass beds once flourished in the Galveston Bay but over the past decades seagrass meadows have largely vanished (Pulich et al., 1996).

2.2.3. Semi-submerged vegetation

Semi-submerged vegetation is vegetation that is partly submerged, or is part of the time submerged, for instance due to the tide. Their oxygen requirement largely defines their adaptions to this specific habitat. Two important ecosystems consisting of semi-submerged vegetation are mangrove forests and wetlands. Vegetation influences wave propagation. It can generate flow resistance and friction that leads to wave attenuation (Möller, Spencer, French, Leggett, & Dixon, 1999). There are indications that vegetation affects surge height but the exact effect is hard to predict on beforehand: spatial and location-specific factors play an important role.

Mangroves trees

Mangrove trees are a type of vegetation that lives exclusively in coastal zones. They are found in tropical climates and have a tolerance for salt or brackish water and for tidal inundation. Mangrove trees are known to need quite strict boundary conditions in order to thrive. Literature suggests that there are several useful functions that mangrove forests fulfill in coastal zones, such as erosion prevention and reduction of wave action. Mangroves occur on the Texas coast but not as abundant as the typical marsh plants. However, ongoing research is investigating the possibilities of expanding the mangroves on the Texas coast because viability could increase as a result of climate change (Armitage, Highfield, Brody, & Louchouarn, 2015).

Wetland vegetation

Wetlands form a habitat in a transition zone from land to water. They can contain fresh, salt or brackish water and are usually found in temperate climate. One of the main wetland types are marshes. Specific herbaceous vegetation (no woody plants like the mangrove tree) distinguishes a marsh from other wetland types. Marshes tend to attenuate wave action and trap and stabilize sediment. They can also store storm surge water, however, previous research suggest that the degree of reduction heavily depends on local circumstances (Bosboom and Stive (2013), Laffoley and Grimsditch (2009)). Wetlands are abundant on the Upper Texas Coast. Towards the coastline the salinity rate increases and this influences the type of wetland, it shifts from prairie (grasslands) to fresh water marshes, to brackish marshes, to salt marshes and eventually to the marine environment.

2.2.4. Sand nourishment measures

A sand nourishment is the placement of a certain volume of sediment (i.e. sand, clay, silt) on- or offshore. A nourishment is mainly aimed to counteract erosion but it can also reduce wave action. Different types of nourishment are applied. Dunes and berms form a natural barrier on a coast against storm surge and wave action. Barrier islands form robust barrier against storm surge and wave action and increase resilience to waves and storm surge. Sand nourishment usually attract a variety of new species (de Boer (2015), Bosboom and Stive (2013)).

Figure 2.7: Wetlands.
Source: Texas Coastal Watershed Program, TAMUG

Figure 2.8: Mangroves.
Source: American Bee Project

Examples of sand nourishments are:

- Beach nourishment (artificial replenishment of beaches)
- Vegetated dunes
- Dredge spoils
- Interitdal muds

2.3. Selection of Nature-based Solutions

It follows from the previous sections that most NbS can contribute to wave attenuation and have multiple additional benefits. While contributing to various challenges, they can add value to a habitat or system in terms of environment, ecology and society. In this chapter, several types of natural measures in the coastal zone were elaborated on. Their characteristics, their wave attenuating properties and their beneficial functions were qualitatively described. Furthermore their presence in and around the Galveston Bay was checked. This is further elaborated in section 5.5. The findings are summarized in table 2.1.

Taking the result of this analysis in account, the focus of further research in this thesis will solely be on Nature-based Solutions that have potential for wave reduction and can prevail in the Houston-Galveston Bay Region. Sand nourishment measures, although potentially effective, will not be further investigated in this study, because of their very broad range of applicability and implementation. The Nature-based Solutions that will be researched in more detail on their wave attenuating abilities are as follows:

- Marsh vegetation
- Seagrass meadows
- Oyster reefs

A more detailed description of the wave reducing mechanisms will be given in the next chapter. Other mechanisms, such as sediment stabilization and storm surge reduction, although perhaps beneficial to flood risk reduction, will not be further studied. Other NbS will be disregarded due to their low prospects of wave attenuation in the HGBR.

Table 2.1: Summary of findings on the considered Nature-based Solutions in the coastal zone.

Nature-based Solutions for flood risk reduction in the coastal zone								
		Habitat	**Flood risk reduction**		**Other benefits**			**Occurence in Galveston Bay**
			Wave attenuation	Surge reduction	Sediment stabilization	Support of species	Water quality	Carbon sequestration	
Reefs									
	Vermetid reef	Marine	+	-	+	+	?	?	Unknown
	Coral reef	Marine	+	-	+	+	+	+/-	No
	Oyster reef	Marine	+	-	+	+	+	+/-	Yes
Submerged vegetation									
	Kelp forest	Marine	?	-	+	+	+	+	No
	Seagrass meadow	Marine	+/-	-	+	+	+	+	Yes
Semi-submerged vegetation									
	Marsh	Wetland	+	+/-	+	+	+	+	Yes
	Mangrove forest	Wetland	+	+/-	+	+	+	+	No
Nourishments									
	Dredge spoils	Coast	+	+/-	-	+/-	-	-	Yes
	Berms	Coast	+	+/-	-	+	-	?	Yes

+	Various sources confirm the effect. It holds for most conditions.
+/-	There are indications for the effect. It holds for specific conditions.
-	The effect is absent or very small.
?	Too little literature on the effect to confirm or refute it.

3

Wave height reduction

This chapter focuses on the potential of oyster reefs, seagrass meadows and marshes to attenuate waves. Although their ability to reduce wave height is widely recognized, quantification of the responsible mechanisms is a topic of ongoing research. Moreover, the extend of their effects under extreme conditions has not been thoroughly investigated. In fact, very few observations are available for large wave heights and high water levels.

Nowadays, numerical modeling tools can simulate the behavior of waves quite accurately. This helps in predicting the effect of Nature-based Solutions on wave propagation. However, to accurately include natural measures in a numerical model, the underlying hydrodynamic processes need to be clear. Therefore, in section 3.1 and 3.2 a short introduction on wave behavior and a concise overview of relevant hydrodynamic processes are given.

In section 3.3, the governing hydrodynamic mechanisms are described that can be recognized in marsh vegetation, seagrass meadows and oyster reefs, and a selection is made in section 3.4. This systematization will be used in the next chapter, where the mechanisms for wave attenuation by Nature-based Solutions are incorporated in a numerical model.

3.1. Wave energy balance

This section addresses the behavior of waves in coastal waters. Wave generation, transformation and dissipation are a result of a complex interaction between hydraulic processes. Holthuijsen (2010) summarizes the main processes clearly in table 3.1. As can be seen, process dominance depends on the hydraulic environment. He relates the mechanisms to energy transference.

For a random wave field in the coastal zone, waves can be described in terms of an energy balance. The wave energy flux remains constant if no energy is generated or dissipated. However, if processes that affect the wave energy are included, the balance can gain or lose energy, which translates to an increase or decrease in wave height. If the governing energy fluxes are represented in the wave energy balance, the corresponding wave height can be calculated. The wave energy balance in cross shore x-direction can be described as follows:

$$\frac{\delta(Ec_g)}{\delta x} = S_{in} + S_{ds,br} + S_{ds,bf} + S_{ds,veg} \tag{3.1}$$

with total wave energy:

$$E = \frac{1}{8}\rho g H_{rms}^2 \tag{3.2}$$

and wave group celerity c_g [m/s], root-mean-square wave height H_{rms} [m], water density ρ [kg/m^3], gravitational acceleration g [m^2/s], distance x [m], energy source wind S_{in} [J/m^2], energy sink depth-induced breaking $S_{ds,br}$ [J/m^2], energy sink bottom friction $S_{ds,bf}$ [J/m^2] and energy sink vegetation induced drag $S_{ds,veg}$ [J/m^2]. A visualization of the energy balance is given in figure 3.1.

Table 3.1: Relative importance of wave-related processes. Processes in a red block are significant in this study, that focuses on nearshore coastal waters (blue block). Adapted from: (Holthuijsen, 2010)

Process	Oceanic waters	Coastal waters		
		Shelf seas	Nearshore	Harbour
Wind generation	●●●	●●●	●	○
Quadruplet wave–wave interactions	●●●	●●●	●	○
White-capping	●●●	●●●	●	○
Bottom friction	○	●●	●●	○
Current refraction / energy bunching	○/●	●	●●	○
Bottom refraction / shoaling	○	●●	●●●	●●
Breaking (depth-induced; surf)	○	●	●●●	○
Triad wave–wave interactions	○	○	●●	●
Reflection	○	○	●/●●	●●●
Diffraction	○	○	●	●●●

●●● = dominant, ●● = significant but not dominant, ● = of minor importance, ○ = negligible.

In the following section the different relevant fluxes will be explored. First, wave generation in the Galveston Bay will be elaborated. Next, the three dominant wave dissipation processes are described, i.e. bottom friction, depth-induced wave breaking and vegetation induced drag (the latter is not included in table 3.1). Wave transformation by shoaling, which is neither an energy source nor an energy sink, is described in appendix A.

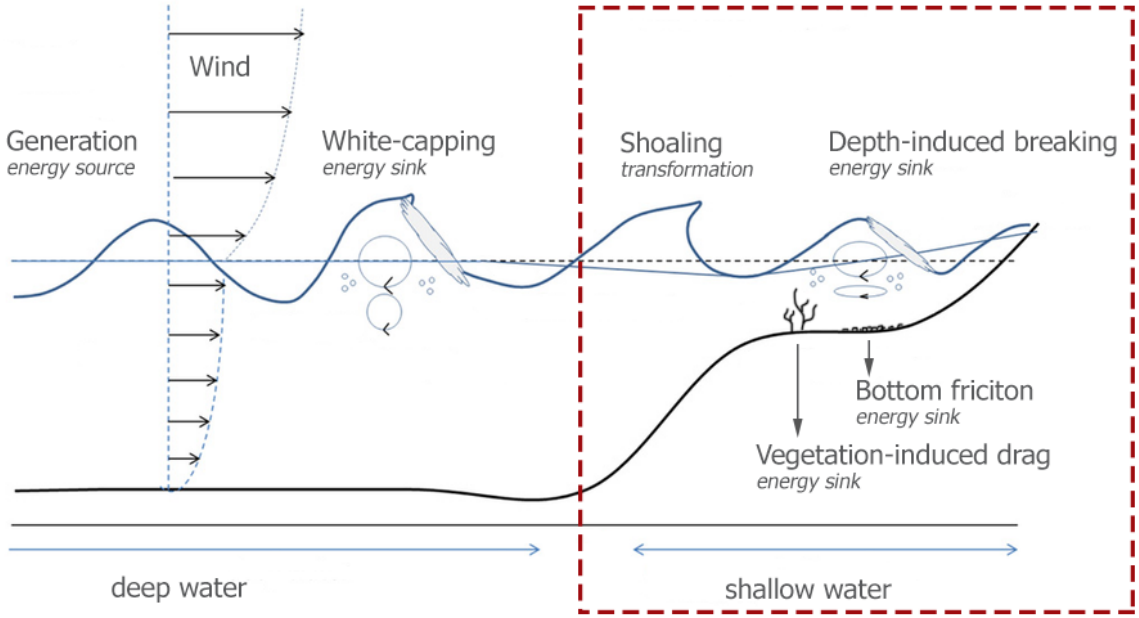

Figure 3.1: Visualization of the wave energy balance (not all processes are included). The dotted rectangle encompasses shallow water wave processes. Adapted from Lee (2013).

3.1.1. Wave generation

Waves are generated by wind that passes over a water surface and exerts pressure and shear forces on the surface. The wave generation depends on the fetch length, wind speed and wind duration. The wind speed is denoted as U_{10}, the wind speed at 10 m above the surface. In coastal waters, wave generation is also influenced (i.e. limited) by the water depth. In a semi-enclosed bay, the fetch length is confined as well.

In an idealized case, a wave field can be described with a characteristic wave height and wave period. These values correspond with a generalized wave spectrum. A practical method to calculate wave growth for depth-depended waves was introduced by Bretschneider (1958). For an idealized case, the significant wave height and wave period can be calculated with only the wind speed, fetch length and the water depth. The velocity and direction are assumed to be constant. A relation for the dimensionless growth curve of the significant wave height for all water depths and all sea states was derived by (Young & Verhagen, 1996) and reads as follow:

$$\widetilde{H} = \widetilde{H}_{\infty}\left[tanh(k_3\widetilde{d}^{m_3})tanh\left(\frac{k_1\widetilde{F}^{m_1}}{tanh(k_3\widetilde{d}^{m_3})}\right)\right]^{p}$$

with the dimensionless significant wave height $\widetilde{H}$, dimensionless deep water limit significant wave height $\widetilde{H}_{\infty}$ [0.24], dimensionless fetch $\widetilde{F}$, dimensionless water depth $\widetilde{d}$ and dimensionless coefficients k_1, k_3, m_1, m_3 and p.

The coefficients for this method were updated by (Breugem & Holthuijsen, 2007). A similar expression is available for the wave period. For comprehensive explanation and application of this method, please refer to appendix E.

3.2. Dissipation mechanisms

The dissipation of wave energy in the coastal zone is effectively obtained by three processes being: depth-induced breaking, bottom friction and vegetation induced drag. All three processes, as illustrated in figure 3.2, are considered separately and subsequently discussed in the following sections.

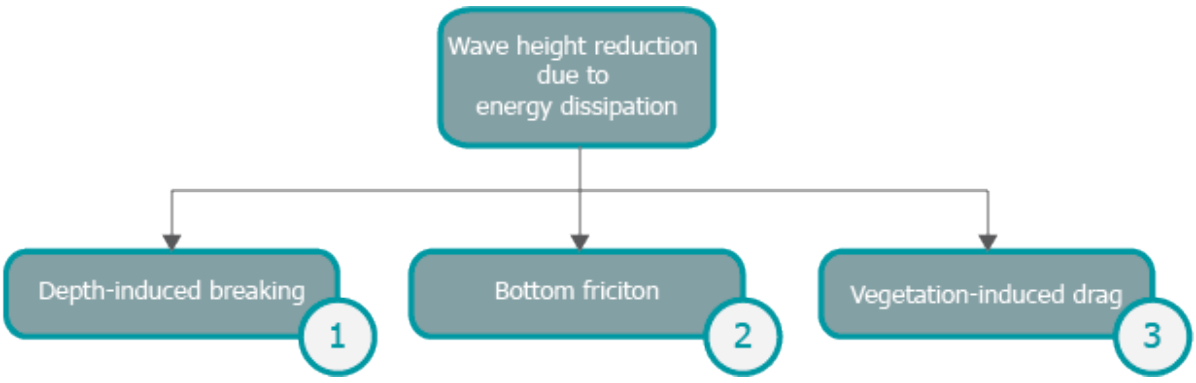

Figure 3.2: Processes that cause wave energy dissipation.

3.2.1. Depth-induced breaking

In near-shore waters, the maximum possible wave height depends on the water depth. Waves will heighten and steepen in water that becomes shallow. If the ratio of wave height over wave length becomes too large, the steepness will cause the wave to break. The combination of increasing wave height and decreasing water depth causes an increase in horizontal particle velocity, that eventually exceeds the wave celerity. At that point, the wave is unstable, breaks and dissipates energy (similar to dissipation in a bore). This turning point in wave stability can be described by the breaker index γ.

The breaker index depends on the wave steepness and the relative slope of the bottom (given by the Iribarren number). It is not an universal constant, one of the expressions that is often used comes from J. A. Battjes and Stive (1985):

$$\gamma = 0.5 + 0.4 \tanh(33 s_0) \tag{3.3}$$

where the incident wave steepness is given by

$$s_0 = \frac{H_{rms}}{L_0} \tag{3.4}$$

with root-mean-square wave height H_{rms} [m] and deep water wave length L_0 [m].

Since H_S is a characteristic value that represents the wave height of a random wave field, most of the observed individual waves are higher ór lower than this value. Therefore, only a fraction of all waves will break. This fraction is used to calculated that amount of energy that is dissipated on average. For further details on depth-induced breaking, please refer to the excellent explanation of Holthuijsen (2010).

3.2.2. Bottom friction

The second energy sink for waves is bottom friction. Wave-related bottom friction on a rough bed can be significant. It depends both on the hydrodynamic wave properties and the bottom characteristics. A rough bottom dissipates wave energy in shallow and intermediate water conditions. The bed friction can be caused by bars and ripples, rocks, shells or vegetation. Additionally, bottom shear stress under (short) waves is usually much larger than bottom shear stresses under a current (Schiereck & Verhagen, 2012).

Wave energy dissipation due to bottom friction is a subject of ongoing research. However, an often used expression to account for bottom friction energy dissipation was formulated by Jonsson (1966) as:

$$S_{ds,bf} = \frac{2}{3}\rho_w \pi f_w \left(\frac{\pi H_{rms}}{T_p sinh(kh)} \right)^3 \tag{3.5}$$

where $S_{ds,bf}$ [J/m^2] is the rate of energy dissipation, ρ_w is the water density [kg/m^3] and $f_w[-]$ is the friction coefficient . The last term in 3.13 represents the near-bottom orbital velocity and includes the root-mean-square wave height H_{rms} [m], the wave period T_p [s], the water depth h [m] and the wave number k [m^{-1}].

Models tend to use a friction coefficient (f_w) to account for bed friction, as the detailed modeling of the mechanisms in the turbulent boundary layer above the bed are complex. Jonsson (1966) derived an empirical formula for the friction factor by relating the bottom roughness characteristics to the wave field characteristics. It approximates the bottom shear stresses, that cause energy dissipation. The expression is specifically meant for wave induced bottom friction in a turbulent, hydraulically rough regime. It was later adapted by Swart (1974) to a more practical formula:

$$f_w = \exp\left[5.213 \left(\frac{k_s \omega}{\hat{a}_b} \right)^{-0.914} - 5.977 \right] \tag{3.6}$$

with

$$f_w, max = 0.3 \tag{3.7}$$

where ω represents the angular wave frequency [s^{-1}], $\hat{a}_b$ the near-bottom maximum orbital amplitude [m], f_w the fiction coefficient [-] and k_s the Nikuradse coefficient (sometimes called 'equivalent roughness length') [m].

The near-bottom maximum orbital amplitude $\hat{a}_b$ is given by:

$$\hat{a}_b = \frac{\hat{u}_b}{\omega} \tag{3.8}$$

with near-bottom maximum orbital velocity:

$$\hat{u}_b = \frac{H_{rms}\omega}{2sin(hk)} \tag{3.9}$$

with the root-mean-square wave height H_{rms} [m], the water depth h [m] and the wave number k [m^{-1}].

The next step is the determination of the Nikuradse coefficient k_s. It is a characteristic roughness parameter that represents the irregularity of the bed. In a perfectly flat bed consisting of uniform spheres, the k_s would be the diameter of the sphere. Since this situation does not exist in nature, representative values for the coefficient have been empirically determined with experiments for a range of bed conditions (rough, even, sloping, ripples etc.). Because the Nikuradse coefficient was originally derived for the roughness of sediment of a bed, it is not clear to what extend it can be applied to vegetated beds; vegetation is not as rigid as sediment and rocks.

The formula for the friction factor depends on the flow regime. Formula 3.6 holds for *a turbulent, hydraulically rough regime*. The other regime is *hydraulically smooth*. The two regimes for turbulent flow are shown in figure 3.3. The boundary layer, δ, can be thought of as the region in the flow where shear stresses play a role. Here, the orbital wave velocity quickly drops to zero. The highly turbulent regime in the this layer dissipates energy. A measure for the characteristic roughness of the bed is the Nikuradse coefficient k_s. If it is higher than the boundary layer, a flow is considered hydraulically rough. An elaboration of the underlying physical processes and derivations of these regimes will not be given here, J. Battjes (2002) gives a very clear explanation of the different regimes.

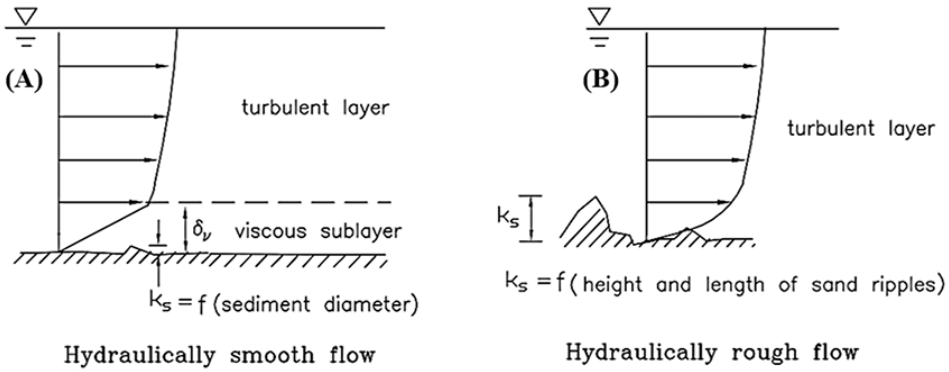

Figure 3.3: A hydraulically smooth and a hydraulically rough regime. Source: Chirol et al. (2011)

For this study, it is important that due to the orbital character of waves, the wave-induced flow velocity near the bed changes direction during a wave period. Therefore the boundary layer never fully develops. That causes high bed shear stresses; the thinner the boundary layer, the larger the shear stress (Nielsen, 1992). Furthermore, a highly turbulent flow and a thin boundary layer move the flow into a hydraulically rough regime, even for small Nikuradse coefficients. The main takeaway is that the friction coefficient is influenced by both the intensity of the waves, expressed as the near-bed orbital velocity and the roughness of the bed, expressed as the Nikuradse coefficient.

Bottom friction becomes a significant wave energy sink on a large length scale. Furthermore, waves need to 'feel' the bottom in order for a rough bottom to dissipate energy. This means that bottom friction is most effective for high waves in shallow water conditions.

3.2.3. Vegetation induced drag

Surface waves that perform work on a vegetation field lose energy, resulting in vegetation-related wave dissipation. The forces are induced by a range of characteristics of both the plant and the wave field. A uniformly valid relation to accurately describe wave energy dissipation by vegetation is not yet available. However, Mendez and Losada (2004) show that accurate prediction of dissipation by stiff vegetation is possible: in that case the plants resemble rigid cylinders, and a valid drag model can be applied (figure 3.4).

Formula 3.10 was composed by Mendez and Losada (2004) and build upon Dalrymple, Kirby, and Hwang (1984), who first proposed this type of formula. It assumes that energy dissipation is only due

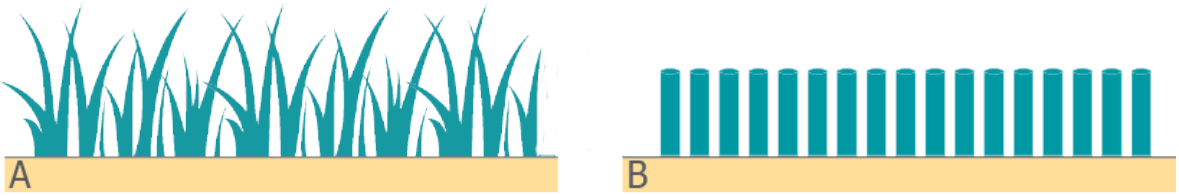

Figure 3.4: A. Schematizing of submerged vegetation field. B. Schematizing of the vegetation as rigid cylinders.

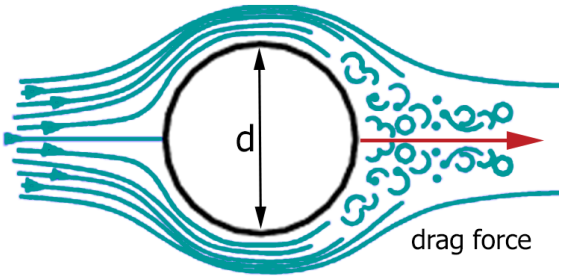

Figure 3.5: Form drag of a cylinder in a flow. Adapted from roymech.co.uk.

to drag forces and depends on both the biodynamic characteristics of the plant and the hydrodynamics characteristics of the wave field.

The equation relates the energy dissipation rate to the wave characteristics and vegetation features:

$$S_{ds,veg} = \frac{1}{2\sqrt{(\pi)}}\rho\widetilde{C_D}b_v N_v(\frac{gk}{2\omega})^3\left(\frac{(\sinh^3(k\alpha h) + 3\sinh(k\alpha h)}{(3k\cosh^3(kh))}\right)H_{rms}^3 \tag{3.10}$$

where $S_{ds,veg}$ is the rate of energy dissipation per unit area over the entire height of the vegetation [J/m^2], $\widetilde{C_D}$ is the bulk drag coefficient [-], b_v is the stem diameter [m], ρ is the fluid density [kg/m^3], N_v is is the number of plants per square meter [m^{-2}], k is the wave number [m^{-1}], ω is the wave angular frequency [s^{-1}], α is the relative vegetation height (hv/h) and $\alpha < 1$, h is the water depth [m], and H_{rms} is the root-mean-square wave height [m]. The expression can be used for both flat and sloping areas and accounts for irregular waves. Reflection by the vegetation is disregarded, but Mendez and Losada (2004) show that this is usually negligible.

A crucial component of the formula is the bulk drag coefficient $\widetilde{C_D}$. It accounts for the drag induced by the the stem, branches and leaves and for additional physical processes that are not accounted for otherwise. A species and site specific calibration is therefore necessary. Literature shows a wide range of values and definitions for $\widetilde{C_D}$. A more detailed description of the physical meaning of the bulk drag coefficient is given in appendix A.

In most studies where expression 3.10 is used, an empirically relation between the $\widetilde{C_D}$ and the vegetation Reynolds number is derived. This relation is calibrated by the authors with their measurements, and enables them to predict the wave attenuation for a variety of conditions. The form of this relation is:

$$\widetilde{C_D} = a + (\frac{b}{Re_v})^c \tag{3.11}$$

where a, b and c are empirical coefficients and the vegetation Reynolds number $Re_v c$ is given by:

$$Re_v = \frac{b_v * u_c}{\mu} \tag{3.12}$$

where b_v is the stem diameter, u_c is the maximum near-bed horizontal orbital velocity and μ is the dynamic viscosity.

The vegetation Reynolds number is a specification of the 'general' Reynolds number. Its characteristic linear dimension is reduced to the diameter of the stems of the vegetation and the flow velocity is expressed as near-bed orbital velocity. A high Reynolds number is an indication for a high-energetic environment, e.g. large waves. If expression 3.12 is calibrated, and site and vegetation specific characteristics are known, it can be used to predict the wave attenuation due to vegetation.

Cases with a large wave height and water depth are of interest for design conditions of coastal protection. In recent years research has been conducted on the validity of formula 3.10 for these extreme situations. The large scale laboratory experiments of Möller et al. (2014) shows that, although vegetation is flattened due to strong waves, the energy reduction is still significant. She also says that breaking of vegetation during storm conditions decreases the dissipation capacity, but that the vegetation field largely withstood storm wave forces. Vuik et al. (2016) further investigated wave damping during high energy conditions and found that marsh vegetation significantly decreases wave heights for storm conditions. Nevertheless, in most studies the calibration of C_D is done for low-energetic regimes, and if its value is extrapolated to high energetic regimes, it tends to give an overestimation of the reduction capacity of vegetation.

3.3. Wave energy dissipation by selected Nature-based Solutions

In the following sections, the previous described wave energy dissipating mechanisms will be connected with the selected nature-based Solutions (marsh vegetation, seagrass meadows and oyster reefs). For each NbS a governing mechanisms will be chosen.

3.3.1. Marsh vegetation

In order to accurately describe the wave attenuation by marsh vegetation, two methods are available: the bottom friction approach and the vegetation induced drag approach.

- The first one describes the influence of vegetation in terms of bottom friction. A friction parameter accounts for the total dissipation of the vegetation. This is for instance done by (Möller et al., 1999). It is a relative simple method to account for vegetation since all characteristics of a plant species at a specific site are merged in one friction coefficient (f_w). This is also the downside of the method: it is not very detailed or flexible. Moreover, extensive reliable data are necessary to validate and verify the friction coefficient. The predictive value of the method is limited, a slight change in conditions asks for a new calibration of f_w. The method also simplifies the flow through a vegetation field to a friction layer above the bed, no matter the vegetation occupancy rate of the water column.

- The second method described the influence of vegetation in terms of vegetation induced drag. It regards each plant as an individual element and takes in account vegetation specific properties, such as the number of stems per m^2 and the height of the vegetation. The method assumes all energy dissipation by vegetation is a result of drag. It was used by Mendez and Losada (2004), Vuik et al. (2016) and many others. A species and site specific calibration of the bulk drag coefficient C_d is necessary. This approach represents the physical mechanisms that occur in the vegetation field more accurately than the bottom friction method.

Typical marsh vegetation consists of different types of bulrush and marsh grasses (both reed-like plant types), which can be represented with the cylinder method quite accurately due to their upright, stiff stems. Marsh vegetation is typically uniform in diameter and height, which further supports the selection of the vegetation-induced drag approach. The field width ranges from 50 to several hundred of meters and the vegetation is often densely packed. Several authors found that typical marsh vegetation is effective in reducing wave height (Jadhav and Chen (2012), Ysebaert et al. (2011)). Vuik et al. (2016) says that even if the vegetation is deeply submerged, it can still attenuate wave significantly.

The average dimensions of a vegetation field (density, height, stem diameter) are input parameters for the method of vegetation induced drag and are not too difficult to observe of estimate. As significant challenge however, is the determination of the drag coefficient C_D. Local wave and vegetation characteristics determine the bulk drag coefficient C_D. Several authors found an empirical relation

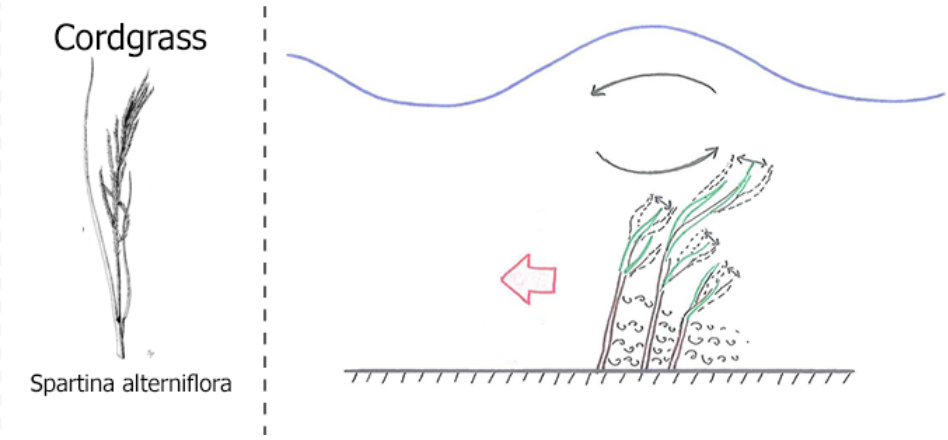

Figure 3.6: Wave dissipation by cord grass due to vegetation induced drag.

between the C_D to the Reynolds number of the flow, as explained in section 3.2.3. A difficulty is that most experiments were conducted for low wave heights and small water depths. There are a few exceptions. The large-scale experiments of Möller et al. (2014) focused explicitly on a high energetic environment. Vuik et al. (2016) also looked into vegetation under storm conditions. Apart from his own measurements, he reanalyzed the data set of Yang, Shi, Bouma, Ysebaert, and Luo (2011), in which smooth cordgrass (Spartina Alterniflora) was the principal species. After calibrating his model with the observations, he proposed a drag coefficient of 0.4 for marsh vegetation under high-energetic conditions (Re > 1000). Paul and Amos (2011) compared several Re-Cd relations and showed that for high Reynolds numbers (Re > 1000) the Cd converges to a constant value. Since this study looks mainly into storm conditions, a C_d of 0.4 seems as valid estimate.

3.3.2. Seagrass meadows

The vegetation induced drag approach, described by the expression of Mendez and Losada (2004), is used often to describe wave attenuation by sea grass. It is an accurate method as long as details of the vegetation field are available. As several reference projects with comprehensive data on seagrass meadows are available, the vegetation induced drag method will be used in this study as well.

Similar to marshes, little research has been done on the effect of seagrass meadows on wave attenuation under storm condition. However, Infantes et al. (2012) investigated the behavior of waves over deeply submerged seagrass meadows (less than 20% of the water column occupied) and found that the wave reduction was significant. He adopted the formula of Mendez and Losada (2004) and used his measurements to calibrate the drag coefficient C_D.

Bradley and Houser (2009) investigated a specific type of seagrass under low-energy conditions. With respect to the wave height, he found that the wave attenuation is relatively larger under low energy conditions. He use the expression formulated by Mendez and Losada (2004) and found that the measured drag coefficient C_D varied significantly for different hydrodynamic conditions. He observed that the assumption of rigid columns for individual stems became more valid for more turbulent conditions (Re > 400). However, he also suggests that a relative large part of the energy dissipation is generated by swaying and leaf motion, in contrast to a drag force afforded by rigid stems.

The prediction of energy dissipation based on the rigid cylinder approach is thus less accurate for sea grass, in comparison to stiff marsh vegetation. Consequently, site-specific calibration of C_D is increasingly important for sea grass meadows.

Bradley and Houser (2009) research a specific type of seagrass called Turtle Grass (Thalassia testudinum). This is one of the species that was historically dominant in the Galveston Bay. He states that its strap-like leaves make the cylinder approach less appropriate. Additionally, he found a decrease in effective bed roughness for more turbulent conditions, as the vegetation becomes more streamlined, which leads to reduced drag.

He used his measurements to find and empirical formula for C_D based on the vegetation Reynolds number of the flow. His calibrated the formula for a low-energetic environment: none of the measure wave height were higher than 0.1 meter. Extrapolation of this expression to waves of several

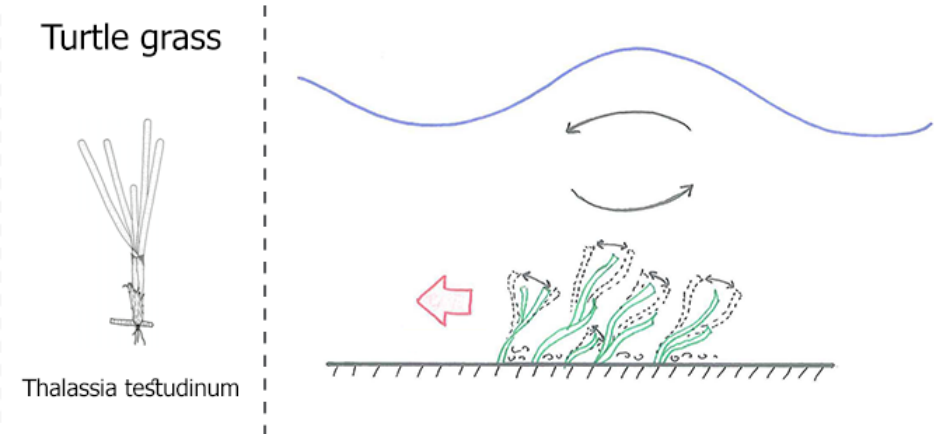

Figure 3.7: Wave dissipation by turtle grass due to vegetation induced drag.

meters (e.g. a very high Reynolds number) leads to a severe overestimation of the wave reduction capacity of seagrass. Paul and Amos (2011) observed a larger water depth and larger waves, although nowhere near several meters. He also calibrated the C_d in his study and compared it with several other calibrations. His expression leads to more conservative and more realistic results.

$$C_D = 0.06 + \left(\frac{153}{Re}\right)^{1.45} \tag{3.13}$$

A vegetation Reynolds number of 1000 is chosen. This is a reasonable value for storm conditions (Vuik et al., 2016). This assumptions is further supported by the fact that for high Reynolds numbers (Re > 1000) the C_D converges to a constant value. This returns a value of 0.13 for C_D.

3.3.3. Oyster reefs

Oyster reefs thrive in salt and shallow water in the tidal zone. Reefs can occupy vast stretches of a bay if the conditions are favorable. They hatch on hard substrate such as rock and old shells, and are able to form columns. Oyster reefs form rocky structures that protrude from the sea bed. They can act as a natural breakwater. Scyphers et al. (2011) investigated oyster reefs acting as a natural breakwater and, apart from confirming their wave attenuating capacities, found that the reefs indeed trap sediment and thus prevent shoreline erosion. After the first substrates and juvenile oysters were establishes, the reef expanded itself.

Although sediment stabilization of oyster reefs have been researched extensively, insight into wave attenuating processes is limited. The wave attenuating effect of oyster reefs is often acknowledged but seldom measured. An exception is Borsje et al. (2011), who observed a wave reduction of up to 40% percent in a flume experiment with oyster beds. However, the underlying hydrodynamic processes are not discussed. The experiment were conducted under calm conditions (average wave height of 0.07 m).

Styles (2015) researched the hydrodynamic processes induced by oysters and found that the main effect of an oyster reef is an increased 'bottom' roughness and a change in bathymetry. He accounts for a flat oyster bed by empirically adapting the Nikuradse roughness K_s of the bottom. He found that a value of 5 times the length of an average oyster gives an acceptable fit for the Nikuradse roughness for the bottom friction. He explains that the situation is more complex if the oysters form columns that together make a reef structure. The reliability of the value depends also on the oyster density of the bed. He further mentions the importance of the hydrodynamic conditions and the configuration of the oysters with respect to the flow. This implies that an oyster reef only affects waves if the waves can 'feel' the reef. Consequently a large water depth will decrease the effect of an oyster reef. This assumption was confirmed by Volp, van Prooijen, Ysebeart, and Dijkstra (2012), who found a linear maximum for the influence of an oyster reef, depending on the height of the reef and the water depth.

Nevertheless, it is assumed that a bottom roughness of 0.3 m for an average oyster bed to give a acceptable first estimate to account for the bottom roughness. Ecoshape (n.d.) also uses an increase

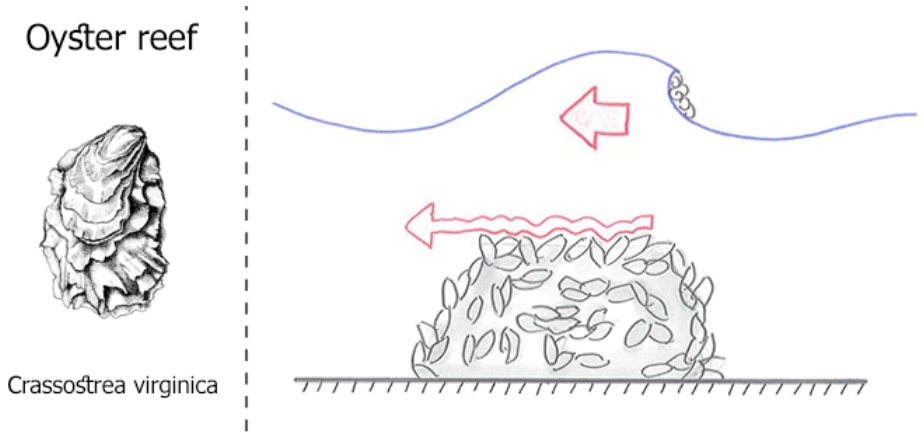

Figure 3.8: Wave dissipation by an oyster reef due to depth induced breaking and bottom friction.

bottom roughness for different types of shellfish in a roughness module that can be included in the numerical model Delft3D. They suggest a K_S of 0.15 m for mussels, which supports the assumption of 0.3 for oysters (being rougher and larger than mussels).

If the bed (in this case, the top of the reef) is at a higher level than its surroundings, depth-induced breaking may occur locally. Volp et al. (2012) found that for deeply submerged reefs, wave reflection can be neglected. The height of reefs lies generally between 0.2 an 0.7 meter, but reports of reefs that have reached a height of over a meter are known. The height of a reef is limited by the diurnal maximum water level, which depends on the local tidal range, because oysters need to be alternately emerged and submerged. The extent of the reef depends mostly on its age: a reef can be decades old and cover several square kilometers. However, artificial reefs are usually constructed along a line parallel to the coast. They can be hundreds of meters long and are mostly between 5 and 30 meter wide.

3.4. Selection of energy dissipation methods

One of the aims of this study was to investigate how the wave height reducing capacities of the selected Nature-based Solutions can be described quantitatively. The previous sections have explored the available methods and elaborated on the most suitable mechanisms and expressions. The selection of the governing mechanism to account for wave height reduction by Nature-based Solutions was not only based on its accuracy but also on how well it can be applied in a numerical model and how well it is equipped to account for highly energetic conditions (e.g. storm conditions). This led to the following choice, which is also shown in figure 3.9:

- Wave attenuation by **marsh vegetation** can be described with the method of Mendez and Losada (2004) that is based on vegetation-induced drag. A bulk drag coefficient of 0.4 is selected.
- Wave attenuation by **seagrass meadows** can be described with the method of Mendez and Losada (2004) that is based on vegetation-induced drag. A bulk drag coefficient of 0.13 is selected.
- Wave attenuation by **oyster reefs** can be described with a combination of depth-induced breaking and an enhanced bottom friction coefficient. A bottom roughness of 0.3 m is selected.

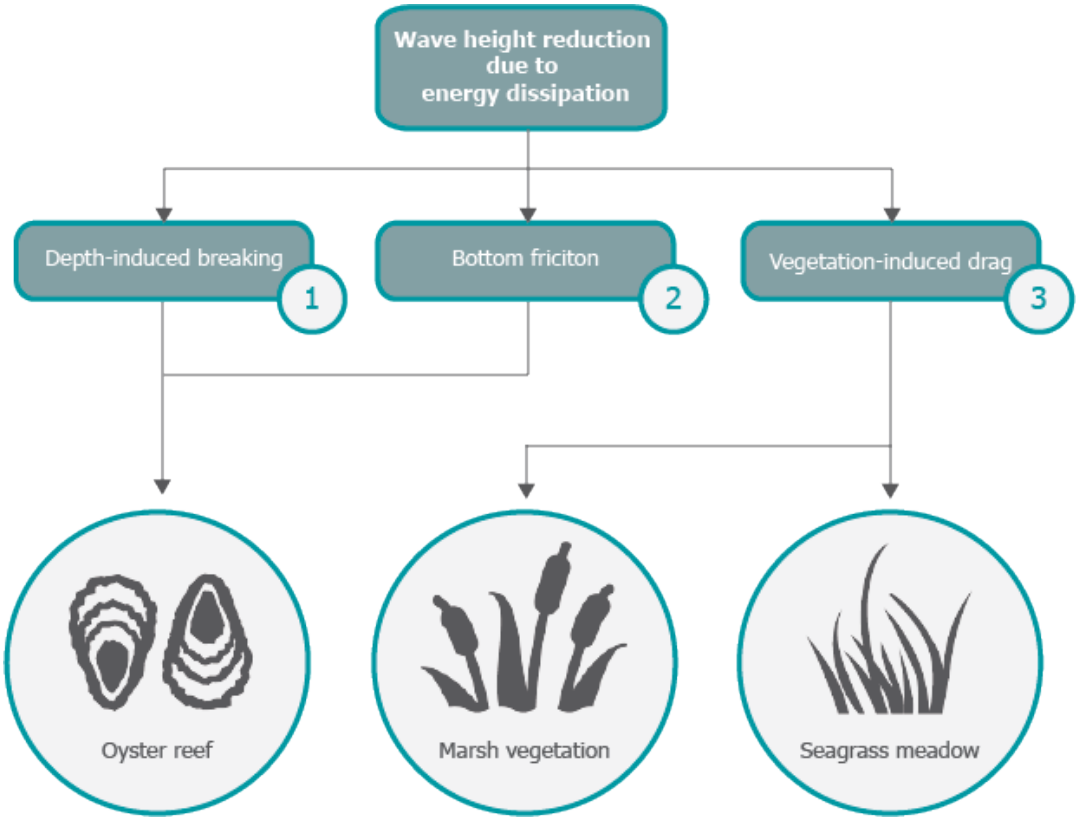

Figure 3.9: Overview of wave energy dissipation by specific Nature-based Solutions

4

Numerical model to simulate wave attenuation

The previous chapter elaborated on the governing processes that induce wave energy reduction. These processes where linked to marsh vegetation, seagrass meadows and oyster reefs. A numerical model can be an effective tool to predict wave attenuation by Nature-based Solutions. It increases the understanding of the hydrodynamics across a Nature-based Solution and it can assist in the optimization of application of these measures. This chapter describes the set-up of the numerical model and the inclusion of Nature-based Solutions. It furthermore discusses the verification of the model. Results and application in the Galveston Bay are covered extensively in part II of this study.

4.1. Model description

The numerical modeling was conducted with a Matlab-based model for 1D wave propagation in coastal waters. It is entirely based on the principles of SWAN (Simulating WAves Nearshore). SWAN is a numerical wave model that can predict wave parameters in near-shore and inland waters, given incoming wind, wave and bathymetry conditions. It is based on the wave energy balance and includes several hydrodynamic processes that influence the wave energy (sources and sinks).

The model used in this research has been adopted from Vuik et al. (2016), where it was used to assess wave attenuation by marsh vegetation in the Netherlands. The model simulates 1D wave propagation by evaluating the wave energy balance, for each grid point. It makes use of characteristic wave parameters (H_s and T_p) that represent a wave spectrum. This implies that certain frequency dependent processes are not captured in the model. Although the model is very well capable of simulating the effect of vegetation on wave energy, the model was slightly altered in this study to also account for oyster reefs. This will be discussed in section 4.1.2. The model is a representation of an idealized situation and includes simplifications and assumptions.

4.1.1. Basic wave propagation model

Before the inclusion of Nature-based Solutions is described, the basic wave modeling is described. The basic principle is that for each succeeding grid point the wave energy balance is evaluated. At the seaward boundary, wave input parameters are dictated and these are translated into wave energy. The wave energy is subsequently transformed under the influence of boundary conditions (bathymetry, wind velocity, water level) and hydrodynamic processes. Together, they can be seen as the energy sources and sinks. The output value for wave energy functions as input for the next grid point, where the calculations are repeated. This continues until the output location (i.e. the location where one want to know the wave height) is reached. Here, the wave energy is translated back into the wave height. This is shown in figure 4.1, that shows the simplified set-up of the model.

Input parameters

The input parameter for the model consist of the wave input parameters and the boundary conditions. The wave input parameters are the initial significant wave height H_s and the peak wave period T_p.

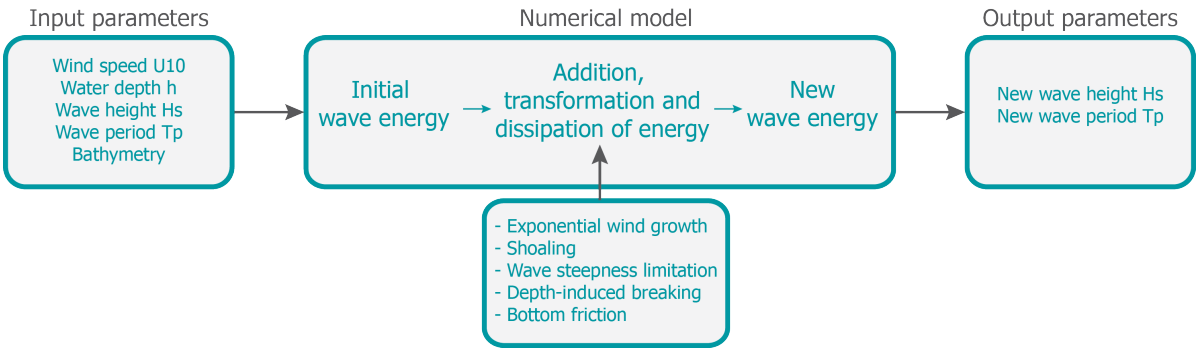

Figure 4.1: Schematized set-up for the basic wave propagation model.

Note that these parameters represent a random wave field: actual measurements would show a variety of periods and wave heights. The significant wave height H_s and the peak wave period T_p can for instance be extracted from a data set of measurements or can be calculated with wave generation expressions.

The dictated boundary conditions consist of the local bathymetry, a representative water level h and a representative wind speed U_{10}.

Wave height to wave energy

As explained in section 3.1 the wave height is directly related to the wave energy. Thus the initial wave height that is dictated as input parameter is translated into a value for wave energy. While the wave height is directly related to the wave energy, the peak period influences the energy balance via the wave number $k[m^{-1}]$: several energy dissipation processes are related to the wave number.

Hydrodynamic processes

The physical background of the processes is given in the previous chapter, section 3.1. Each hydrodynamic process that influences the energy balance can be switch on or off in the model. For most hydrodynamic processes, several methods to describe them are available. One can dictate in the model which formulation must be used. For this study, the following processes were active in the model:

- **Wave generation by wind** is an energy source. Snyder, Dobson, Elliott, and Long (1981) describes this momentum transference from wind to water surface and his expressions are included in the model.
- **Shoaling** is neither a source or a sink. It is included in the model via the constant energy flux along the wave ray, explained in appendix A.1.
- **Wave steepness limitation** is included via the criterion of J. A. Battjes and Stive (1985). The wave height in the model cannot exceed this maximum.
- **Depth-induced breaking** is an energy sink and is account for via the breaker parameter γ derived by J. A. Battjes and Stive (1985). This parameter is then included in the wave breaking model of widely used model of Battjes and Janssen (J. Battjes & Janssen, 1978). This method was explained in section 3.2.1.
- **Bottom friction** is an energy sink and is included via the method of Jonsson (1966), which was explained in section 3.2.2.

For an additional explanation of the available expressions and methods in the model, refer to the complete online scientific documentation of SWAN (SWANteam, 2017).

4.1.2. Inclusion of Nature-based Solutions

In section 3.2.3 on vegetation-induced wave height reduction, the physical background of the formula of Mendez and Losada (2004) was explained. This method returns a value for energy reduction based on hydrodynamic and biomechanical input parameters. The expression (formula 3.10, section 3.2.3)

was included in the model, and added to the list of hydrodynamic processes that influence the wave energy.

In contrast to the basic processes, one has to dictate for which part of the grid the vegetation induced drag model is active. For these grid point, the vegetation induced energy dissipation is added to the energy balance. The characteristics of the vegetation field are included via the input parameters of expression 3.10: vegetation density N_v, vegetation length h_v, stem width b_v and vegetation drag parameter C_D. The latter is important and uncertain because it cannot be measured directly, but must be calibrated with field measurements at the location of interest. If no such measurements are available, a value from reference literature can be used, although results should be interpreted with care.

Oyster reefs can be included in the model via an increased bottom friction coefficient (3.3.3). If the oysters form a protruding structure of significant height, the dimensions of the reef can be incorporated in the bathymetry of the model because depth-induced breaking becomes a significant process. For deeply submerged reefs (e.g. high storm surge), wave reflection is not significant and can be disregarded (Volp et al., 2012). This implies that for regular and stormy hydrodynamic conditions, different processes are relevant and should be incorporated in the model accordingly. Similar to the vegetation drag parameter, the increased roughness coefficient for an oyster reef cannot be measured directly and should be calibrated with field measurements. Again, if no such observations are available, a value from reference literature can be used. However, for oyster reefs these measurements are rather scarce.

4.2. Model assumptions

Assumptions for the model were explained in previous sections and can be summarized as follows:

- The wave propagation is modeled in one dimension: perpendicular on the coastline.
- The wave field is described with a significant wave height and peak wave period that represents a spectrum.
- The wind field is unidirectional and constant.
- The still water level is constant over the cross section.
- The wave height responds instantaneously.
- Nonlinear wave-wave interactions are disregarded.
- Currents are disregarded.
- Diffraction and refraction are disregarded.
- White capping is disregarded.

Assumptions considering the inclusion of vegetation in the model can be summarized as follows:

- The vegetation field is homogeneous.
- The vegetation resists the wave force and plants do not break.
- All plants have the same length and stem width.
- Wave reflection on vegetation is disregarded.

Assumptions considering the inclusion of an oyster reef in the model can be summarized as follows:

- Wave reflection on the reef is negligible for deeply submerged reefs.
- Energy loss due to the seawards and landwards vortex is disregarded.
- The reef can be modeled as an impermeable part of the bathymetry.
- The rough structure of the reef can be modeled with a Nikuradse roughness coefficient.
- The reef has a homogeneous roughness.

4.3. Model verification

The SWAN model for coastal wave behavior have been used extensively in academic and engineering context. It has proven to be robust and to produce reliable results, especially for a first order assessment such as this study. However, the inclusion of Nature-based Solutions is a rather new and ongoing development. Thus a short explanation on the validity of the model with inclusion of vegetation and oyster reefs is useful and necessary.

4.3.1. Validation: vegetation induced energy dissipation

The formula of Mendez and Losada (2004) for vegetation related energy dissipation was included in SWAN and validated by Suzuki et al. (2012). It was then included in the official SWAN model and documentation as the *SWAN-VEG module*.

Vuik et al. (2016) used measurements of stormy conditions to validate the model for the influence of vegetation for a large water depth and wave height. He chose the bulk drag coefficient C_D as main calibration parameter and used three data sets with field observations, this is shown in figure 4.2. One of his calibration results was a C_D of 0.4 for high Reynolds numbers (e.g. stormy conditions).

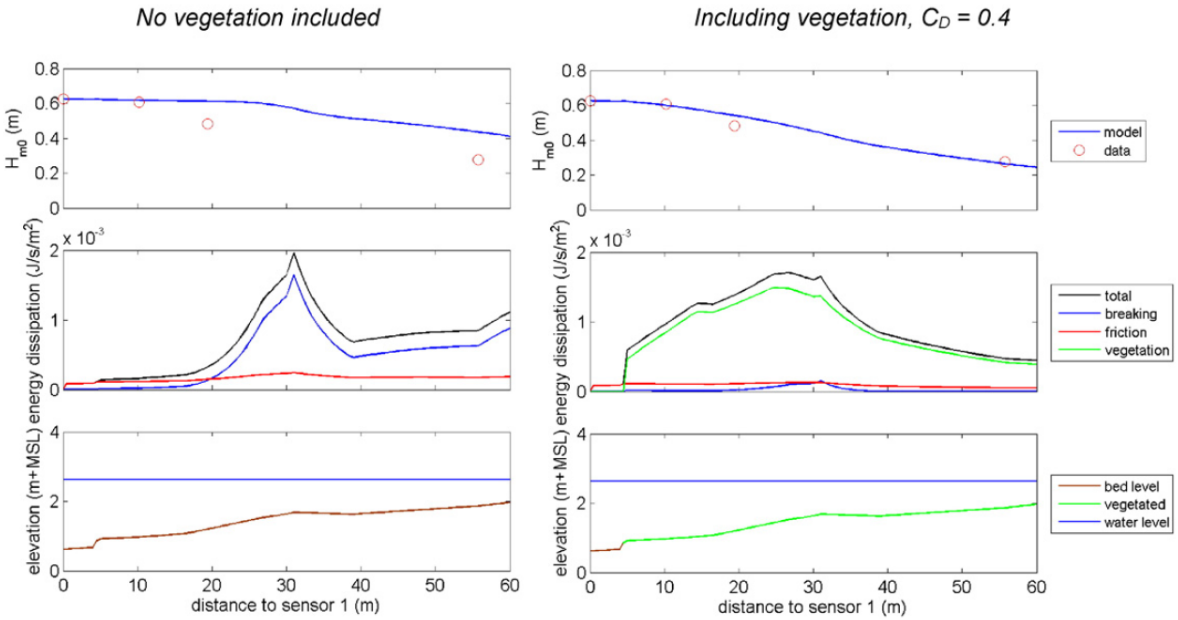

Figure 4.2: The upper panels show an example of a comparison of one of the field observations (red markers) and the model reproduction with (right) and without (left) vegetation. The middle panels show the relative effect per dissipation process, modeled with the SWAN. The lower panels show the bathymetry and water depth at the specific site. Source: Vuik et al. (2016)

Since Vuik et al. (2016) performed a thorough validation and calibration of the model for the effect of vegetation, and this study uses the same model, a new calibration is not conducted. Keeping in mind his recommendations and conclusions, it is assumed the model was accurate enough for the scope of this study.

4.3.2. Validation: oyster reef energy dissipation

The implementation of an oyster reef in the model, although based on existing mechanisms, should be tested, as it is new. However, published data of experiments on wave attenuation by oyster reefs are scarce. Two sets of published measurements were used to validate the method of modeling wave height dissipation due to an oyster reef. Both are laboratory observations, made in a flume. Unfortunately, no published observations of wave attenuation over oyster reefs for stormy conditions are available.

The first one is the study of Borsje et al. (2011) that reviews implementation of Nature-based Solutions in coastal protection. It briefly explains a flume experiment with a mussel bed and an oyster bed and concluded that oysters are more effective in attenuating waves than mussels. It described the oyster density and length, wave input parameters and dimensions of the flume. Results were displayed

in a percentage graph. Disadvantages of the experiment were that the wave height is very low (0.0334 m) and that only one test series is mentioned.

The second one is the study of Manis, Garvis, Jachec, and Walters (2014) that assesses wave attenuation over oyster beds of varying age. It explains the methodology of the experiment in detail. In a wave tank, a slope was constructed on which mats with oysters were anchored. Wave gauges registered water displacement, this data was transformed to wave height and wave energy. The results were given as average values in a table. Downsides of the experiment were that some of the dimension descriptions were contradictory, making it difficult to mimic the set-up of the experiment in the model. Furthermore, no height of the oyster bed was given, only a average oyster shell length.

The model was configured to match the given boundary conditions as closely as possible. The input parameters that were given in both studies are shown in 4.1. In the model, the Nikuradse roughness for both studies was kept constant at 0.3 m. The height of the oyster bed for Manis et al. (2014) was estimated as half the length of the average oyster shell (for Borsje et al. (2011), the height was given as 0.071 m, which is approximately half the length of a shell of an adult oyster).

Table 4.1: Comparison of the wave height reduction between the observed values from two reference studies and the values modeled in this study (on the bottom row). The input parameters are given in the papers.

	Borsje et al. (2011)	**Manis et al. (2014)**	
Input parameters			
Wave height H_s	0.0334 m	0.16 m	
Water depth	0.25 m	0.30 m	
Wave period	1.0 s	1.8 s	
Output parameters	Reduction	Value	Reduction
H_s, observations	-50%	0.09	-45 %
H_s, **modeled**	-26%	0.08	-49%

The study of Borsje et al. (2011) observed a significant wave height reduction of 50% at the output location under influence of an oyster bed. The modeled return a reduction of 26% at the output location (table 4.1). Although this is a significant difference, absolutely spoken the difference is less than 0.01 m.

The study of Manis et al. (2014) used larger wave heights. The observed wave height at the output location was 0.09 m (-45%) whereas the model returned a wave height of 0.08 m (-49%). The absolute difference here is also 0.01 m, but the relative difference is much smaller. Since the latter study uses higher wave heights and a sloping bathymetry, it suits the objective of this research better than Borsje et al. (2011). Both model simulations follow the general behavior of a gradually reducing wave height and of a significant total reduction.

II

Case study: Galveston Bay

5

System analysis of the Galveston Bay

The objective of this chapter is to understand how the hydraulic system of the Galveston Bay works, both under mild and under extreme conditions, and to find out where flood risk due to wave action is present in the Bay. It furthermore investigates if and where marsh vegetation, seagrass meadows and oyster reefs were historically and currently present in the Bay.

This chapter provides a system analysis of the Houston-Galveston Bay Region, with emphasis on the hydraulic analysis and the flood risk related challenges in the area. It gives a general overview of the area in section 5.1 to place the case study in context. In section 5.2, a concise hydraulic analysis is carried out that focuses on regular, mild conditions. In section 5.3, extreme hydraulic conditions caused by hurricanes and storm are discussed. It also highlights vulnerable areas with respect to flood risk and wave action in the Bay. Lastly, it gives an introduction to the current flood risk protection in the Bay. Section (5.5) gives an analysis of natural habitats and environmental threats in the area. This includes an overview of current Nature-based Solutions in the Bay. The last section (5.6) concludes with the main findings of the analysis.

5.1. Location description

The Houston-Galveston Bay Region is an urban area in the U.S. that has around 5.5 million inhabitants. It houses the largest petro-chemical complex in the U.S. In contrast to this urban and industrial region, the east of the area is rural and houses several protected wildlife reserves and coastal marches (GCCPRD, 2016). The region is prone to hurricanes and has been hit severely in the past. A notable high-impact hurricane was Ike in 2008, that let to 74 fatalities in the state of Texas. It resulted in an estimated 28 billion USD in damages. Storm surge was as high as to 15 - 20 feet (4.6 to 6.1 m) and large areas in the HGBR were flooded. More recently Hurricane Harvey hit the area and caused severe flooding due to extreme precipitation rates. Ongoing research is carried out in both the Netherlands and Texas on how to most effectively reduce the flood risk in the area.

The Galveston Bay is a large estuary system in connection with the Gulf of Mexico. It is shown in figure 5.1. The barrier islands in front of the Galveston Bay are called Galveston Island and Bolivar Peninsula. Such islands are present along the entire Upper Texas Coast, where the Galveston Bay system is located. The sandy barrier islands were formed by wave action and longshore transport that deposited sediment along the coast. This is typical for a wave-dominated coast with enough fluvial sediment supply and a small tidal range. The barrier islands in front of the Galveston Bay give the system a lagoon-like character. Furthermore the Bay can be marked as a drowned river valley that developed due to ongoing sea level rise. This rising started near the end of the last glacial period ('ice age'), some 18,000 years ago.

Along the coastline near Galveston Bay, the prevailing winds are from the south-east and so are the alongshore currents. The yearly net transport of sediment is towards the west at most locations. The region is a relatively flat coastal plain area and has a humid subtropical climate. It is part of the Western Gulf Coastal Plain of which its main natural vegetation is grassland. Typical habitats in the

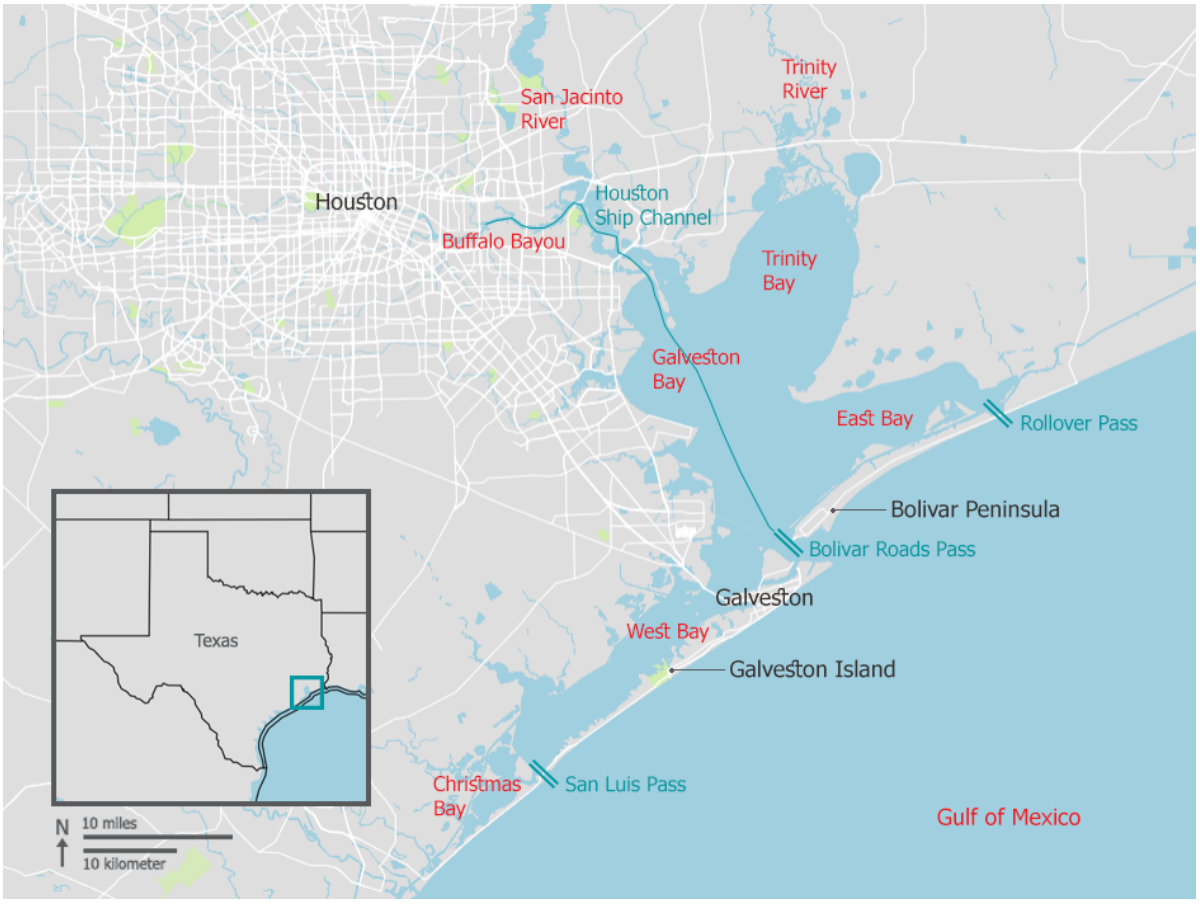

Figure 5.1: Houston-Galveston Bay Region with several relevant components.

vicinity of the Galveston bay are swamps, salt marshes and freshwater wetlands. Industrial and urban land use has expanded greatly in recent decades (EPA, 2013).

5.2. Hydraulic characteristics

The Galveston Bay is an interconnected system of 5 bays: Christmas Bay, West Bay, Galveston Bay, East Bay and Trinity Bay (shown in figure 5.1). Its total surface is approximately 1.600 square kilometers (600 sq miles). Two significant rivers flow in the Bay, Trinity River and San Jacinto River, which account respectively for 28% and 54% of the fresh water inflow). The Buffalo Bayou flows through Houston and merges into the Houston Ship Channel. A bayou is a slow-moving river under strong influence of the tide (Phillips, 2005).

Barrier Islands separate the Bay from the Gulf of Mexico: Galveston Island in the south and Bolivar Peninsula in the north. The islands are separated by the Bolivar Roads Pass, which allows nautical traffic in and out of the Bay and also ensures exchange of water between the Gulf of Mexico and the Bay through tidal motion. Two extra passages that allow for smaller shipping are Rollover Pass in Bolivar Peninsula and San Luis Pass in Galveston Island. The Bay is in connection with a number of smaller adjacent bays and lagoons. These features are shown in figure 5.1.

The Bay is characterized by low wave action, a micro-tidal environment and mostly brackish water. The average depth is 1.8 meter (6 feet) and the maximum undredged depth of 3 meter (10 feet). The navigation channels in the bay are regularly dregded to maintain greater depths. The Houston Shipping Channel is 14 meters (45 feet) deep. An elevation map of the Bay is shown in figure 5.2.

5.2.1. Tidal character

The Gulf of Mexico has a micro-tidal character and this holds for the Galveston Bay as well. Due to the relative small inlets, the tidal range inside the Galveston Bay, being 0.4 m, is smaller compared

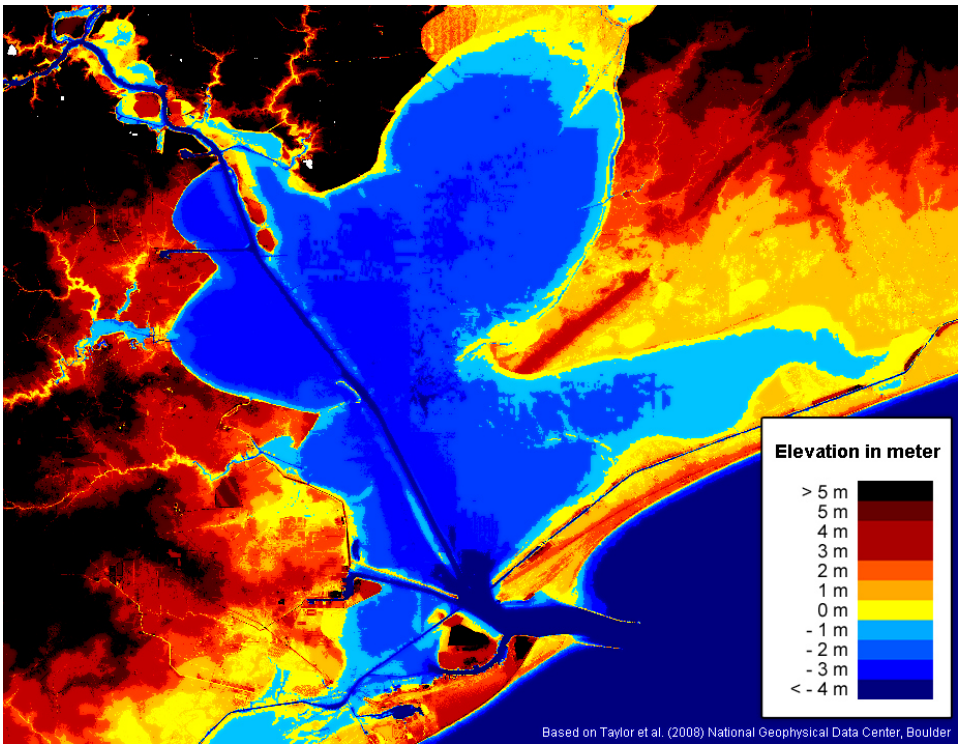

Figure 5.2: Elevation map of the Galveston Bay (datum NAVD-88). Based on Taylor et. al. (2008).

Table 5.1: Datum at Eagle Point inside Galveston Bay, 1983-2001 epoch

Datum	Bay side: Eagle Point	Abbreviation
Mean Higher High Water	NAVD-88 +0.264	MHHW
Mean Sea Level	NAVD-88 +0.108	MSL
Mean Lower-Low Water	NAVD-88 -0.074	MLLW
Great Diurnal Range of Tide	0.338	GT
Mean Range of Tide	0.310	MN

to range in the Gulf, being 0.6 m. Likewise, the tidal motion lags behind in the bay. Its character is predominantly semi-diurnal.

In Texas the Mean Lower Low Water is often used as a reference for dredging works and nautical charts. All datums in the U.S. are based upon the National Tidal Datum Epoch, a specific multi-annual period that is revised every 20-25 years. It includes the 18.6 year astronomical cycle and contributes to correct adjustment of the mean sea level. It is revised every two decades to account for sea level rise and subsidence. The tidal predictions in table 5.1 are based on the still widely used 1983-2001 Epoch. The datums are extracted from the NOAA station Eagle Point, that has the longest data record in the bay (NOAA, 2017). Water levels in this report are relative to either NAVD-88 or MLLW. Although the tidal range is small and the Bay is very shallow, the water level can increase significantly during storm conditions. This is further explained in the section on hurricane conditions (5.3).

5.2.2. Wave climate

In the Galveston Bay, wave generation is depth limited or fetch limited, depending on the location. The maximum fetch in the bay is approximately 30 kilometers. It has a maximum undredged depth of 3 meters. Very little wave data of the sheltered environment of the Galveston bay is available, in contrast to the near shore wave climate of the upper Texas Coast, that has been extensively observed and studied. An exception is (Dupuis & Anis, 2013), who observed the wave climate of the Bay under regular conditions and found that it can be simulated accurately with the modeling tool SWAN for

shallow water environments. To this end, he measured the dynamic pressure and orbital wave velocity at one location on ten separate dates. Unfortunately, the sample rate of the regular observation stations of NOAA in the Bay is too low to distinguish waves. However, the stations do capture wind data and water levels, thus simulating wave data is possible. Dupuis and Anis (2013) described the wave climate in the bay in terms of a significant wave height and a peak wave period, based upon his measurements. The significant wave height ranged from 0.01 to 0.84 meter and the peak period from 1.9 to 3.2 s. During storm conditions wave heights in the bay can become very large. This caused by both a large wind speed and an increased water level. This will be explained further in the section 5.3 discussing hurricane conditions.

de Boer (2015) investigated in his thesis which part of the Galveston Bay is most vulnerable for wave impact. He looked both at the wave climate and the resilience of the coastline. He found that the west part of the bay is most threatened by wave impact. This is because the shoreline is strongly developed, there is no buffer zone and there is little bank protection. He suggested that the main threat would be erosion.

5.3. Hurricane conditions

Significant drivers of flooding in coastal areas are storms and hurricanes. This is of particular importance for the tropical regions on earth. A tropical storm is a closed, rotating storm system accompanied by heavy precipitation, strong winds and a low atmospheric pressure in its center. They have a diameter of hundreds of kilometers. Typically, tropical storms form between 5 and 30 degrees latitude north and south, as can be seen in figure 5.3. This band overlaps with the tropical and subtropical zones on earth. On higher latitudes the water temperature is generally too low to form depressions that lead to tropical storm systems. Since the main driver of the rotating nature of a tropical storm is the Coriolis effect and the Coriolis effect is weakest at the equator, close to the equator no such systems arise. The terminology of tropical storm systems is based on geographic characteristics and intensity. System that arise in the western North Pacific are called typhoons, in the Indian Ocean and South Pacific they are called cyclones and near the North-America they are known as hurricanes. In this report they will henceforth be addressed as hurricanes. They are furthermore categorized based on occurring wind speed. From weakest to strongest they are called tropical depressions, tropical storms, hurricanes and major hurricanes.

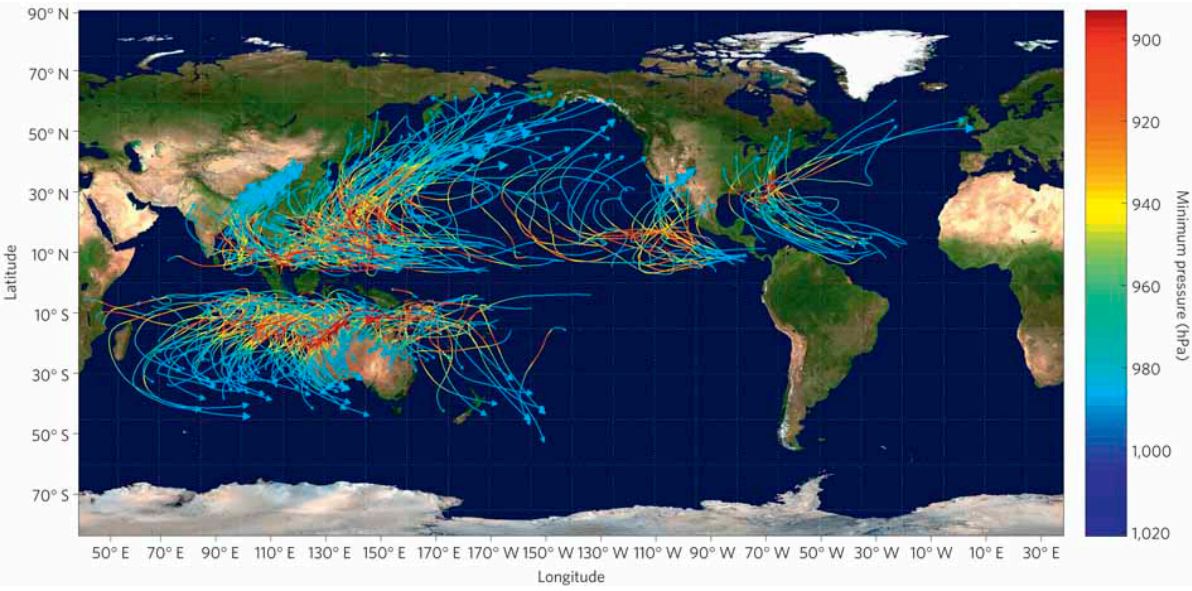

Figure 5.3: Synthetically generated storms using the properties of the current climate. Source: Mendelsohn, Emanuel, Chonabayashi, and Bakkensen (2012)

Major hurricanes have swept over the Galveston Bay region in the past, and it will certainly happen again. They cause severe rainfall and extreme wind. The latter induces storm surge and high waves. The hurricane season in the Atlantic basin occurs between June and November. Between ten and

twenty tropical storms arise each season, of which a minority develops to a full-scale hurricane. Not every hurricane makes landfall at continental U.S. and the few that do can hit the Gulf coast anywhere. This combination of uncertainty leads to the rule of thumb that a major hurricane hits Texas each decade.

Another complexity is that hurricane paths are hard to predict. The location of landfall is of major importance to take precautions at the right location, but a hurricane that heads towards the coast can change its track abruptly. Its exact landfall can only be forecasted a couple of hours in advance. The hydraulic response of the Galveston bay system is very sensitive to its landfall location. This is illustrated in figure 5.4, where the Galveston Bay is simplistically modeled and a land fall east and west of the Bay are shown. If a hurricane passes on the west, the water level in the Bay will rise significantly due to inflow. Wind set-up and waves will threaten mainly the north and west side of the bay. If a hurricane passes on the east, the hurricane will drain the bay by pushing the water out. Waves and wind set-up will be most severe at the east and south side of the Bay.

Effects of storms and hurricanes that lead to hazard can generally be divided in two categories, each causing several sub-effects:

- High wind speed
  - Direct damages due to high wind speed.
  - Storm surge at sea.
  - High waves at sea.
- High precipitation rates
  - Flash floods due to heavy rain and high run-off rates.
  - High discharges in streams and canals.

Storm surge, extreme waves and high precipitation rates will shortly be discussed in the context of the Galveston Bay .

5.3.1. Storm surge

Surge is defined as the observed water level at sea minus the calculated astronomical tide. Storm surge refers to an extreme water level during storm or hurricane conditions. The storm surge level in the Galveston Bay is a result of wind set-up and inflow and overwash from the Gulf. Locally wave set-up can play a role. The inflow and overwash are in strong relation with the water level at the open coast, which is a function of wind set-up, barometric set-up, wave set-up and astronomical tide. Typically the astronomical tide is not included in the calculation for the storm surge, considering its definition. It is nevertheless included in the absolute calculation of the water depth. Increased water levels due to sea level rise, precipitation and fresh water inflow are not included in the calculation for surge.

Extreme water levels in the Bay can be predicted in terms of return periods: the water level that occurs only once every 100 year is higher than the water level that occurs once every 10 year. Since the extreme water levels in the Bay are mainly caused by inflow and local wind set-up, the values differ throughout the Bay. Stoeten (2013) simulated the storm surge levels in the bay and at the open coast with statistical extreme value analysis. The results are shown in figure 5.5. These findings are in line with the notion that a hurricane passing on the west will lead to the highest water levels (in the north and west of the bay).

Another useful source is the report of FEMA (2012). It is a very detailed study of water levels in the bay and inundation levels during flood events. It gives still water levels at dozens of locations around the Bay for four different return periods. FEMA (2012) based its extreme water levels on an USACE study for statistical distributions of hurricane input variables and local bathymetry. It includes tidal elevation, wind set-up, wave set-up and barometric pressure elevation. It was calibrated with five hurricanes, namely Carla (1961), Allen (1980), Bret (1999), Rita (2005) and Ike (2008)).

These two sources turn out to be in good agreement with each other, which suggests reliability of the values (table 5.2).

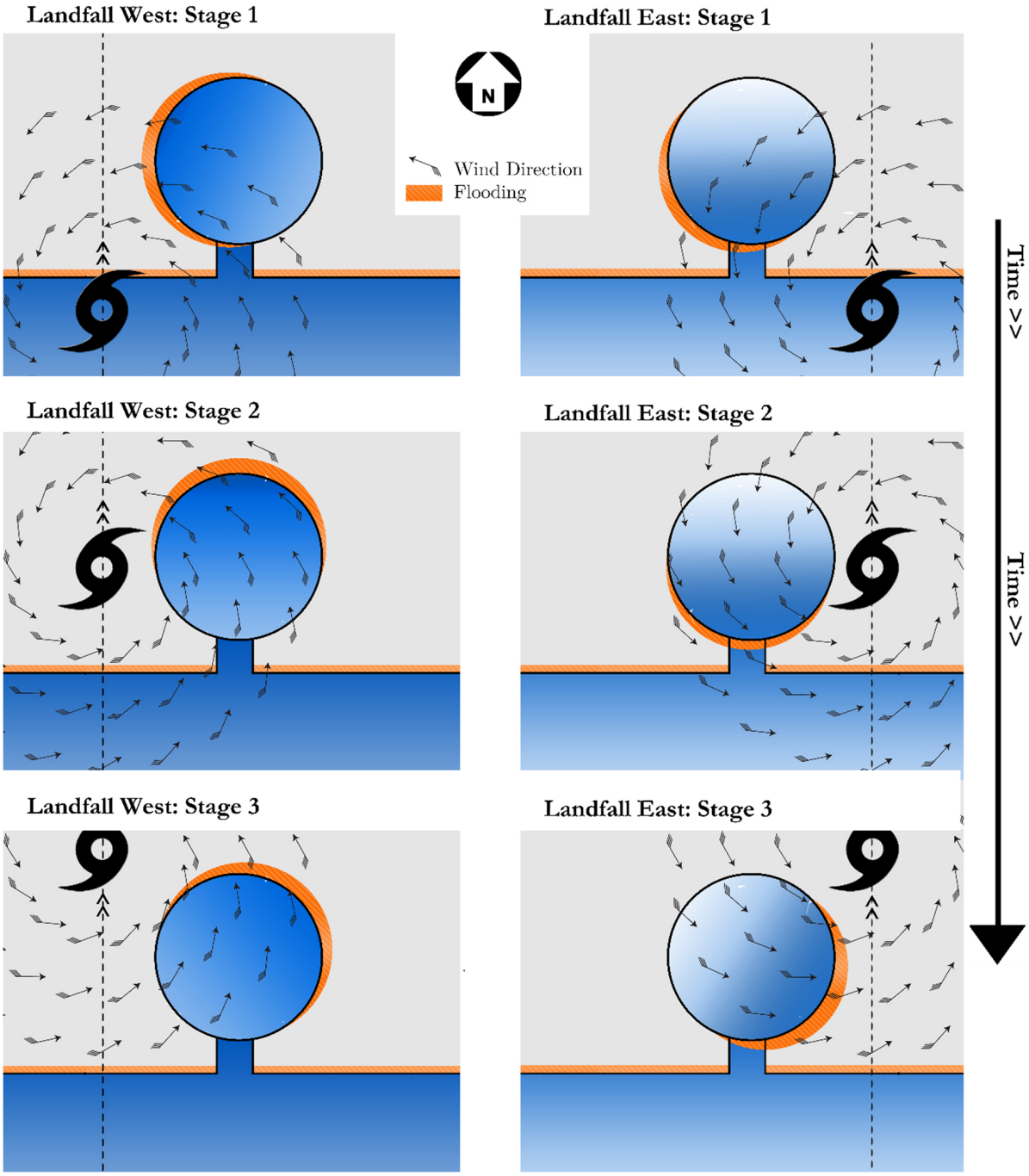

Figure 5.4: Surge and flood prone areas based on the location of landfall of a hurricane in the Galveston Bay. Source: Stoeten (2013)

5.3.2. Precipitation

Hurricanes can generate enormous precipitation volumes. Very recently, Hurricane Harvey caused severe flooding in Houston due to ongoing rain. At some locations the total precipitation exceeded 1.3 meter (50 inch) in 5 days. The combination of heavy rain and storm surge at sea can cause compound flooding in coastal areas. This forms a serious risk during hurricanes, especially in areas with limited buffer capacity. Compound flooding happened during Hurricane Harvey in the Houston-Galveston Bay Region, as the water piled up in Houston due to heavy precipitation, but could not drain to the Bay and the Gulf due to storm surge. Precipitation, although an important cause for urban flooding, will not be further addressed in this thesis.

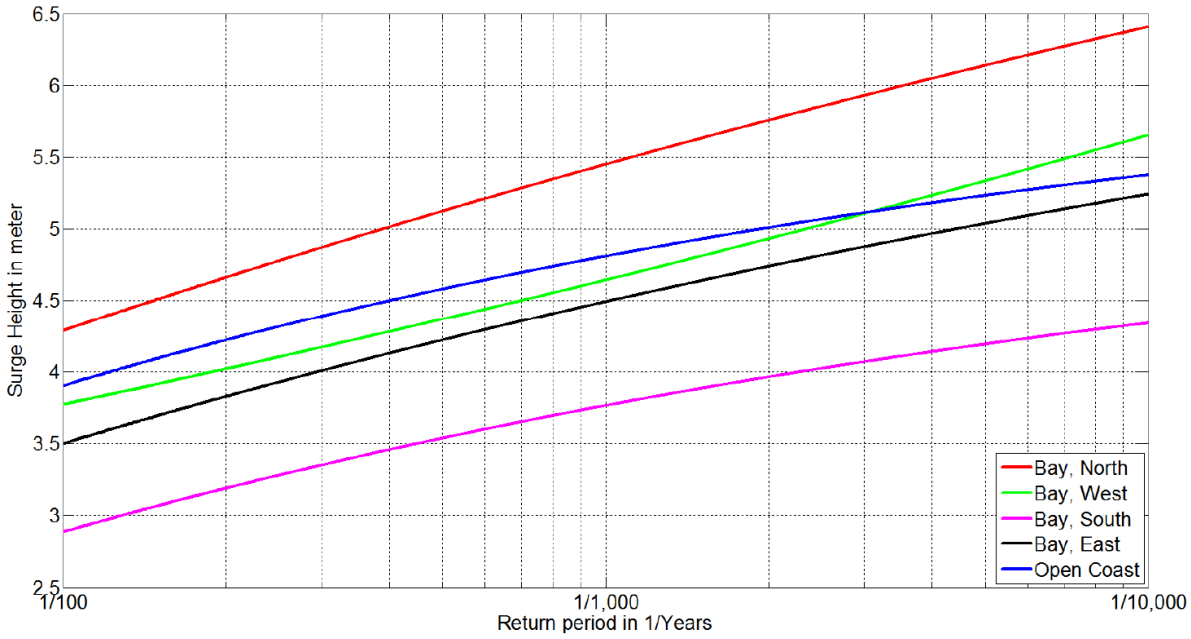

Figure 5.5: Return periods for storm surge in the Galveston Bay, relative to NAVD-88. Source: Stoeten (2013)

Table 5.2: Comparison of water levels [m] for different return periods, at the west side of the Galveston Bay, relative to NAVD-88.

	10 years	**50 years**	**100 years**	**500 years**
FEMA (2012)	2.4	2.9	3.6	4.6
Stoeten (2013)	-	-	3.8	4.4

5.3.3. Waves

Wave heights can become very large during storms and hurricanes. This is due to the high wind speed and storm surge that accompanies a hurricane and fuels wave energy. (Jin et al., 2010) modeled waves heights for different wind conditions at three locations in the Galveston Bay. He found that under storm conditions, wave height in the Galveston Bay mostly relates to the water depth. Because the Galveston Bay is relatively shallow (2 m), the depth limits the wave height. While storm surge can raise the water level by several meters, the depth is still the limiting factor for wave growth, even under intense hurricane wind velocities.

This is illustrated in figure 5.6. Jin et al. (2010) simulated the maximum wave height at the Galveston Causeway, the main connection between Galveston Island and the mainland. As can be seen, the maximum wave height grows with increasing storm surge levels and seems to be less depended on the wind speed.

Waves in Galveston Bay are locally generated, waves from the open coast do not significantly propagate into the bay under regular conditions. Wave penetration could occur in extreme situations were larges parts of Galveston Island or Bolivar Peninsula are heavily inundated.

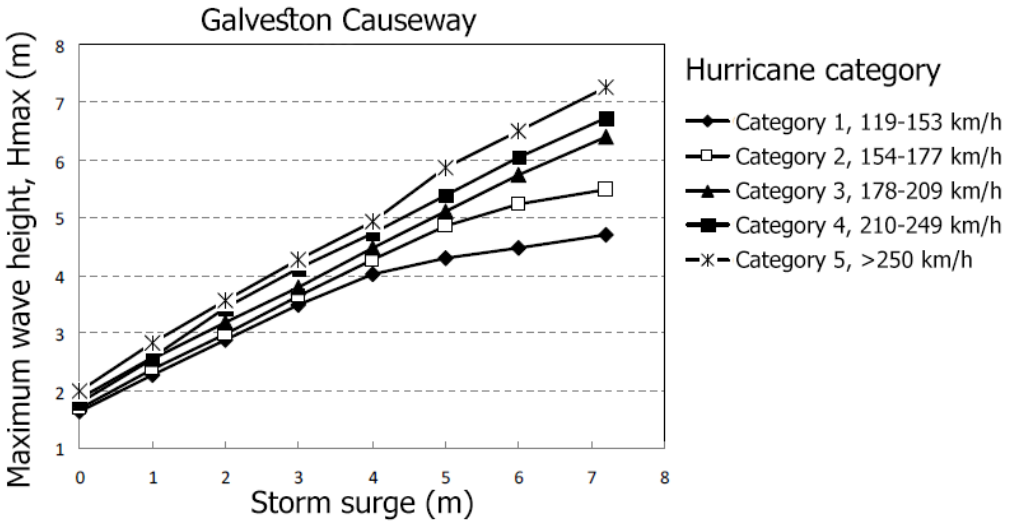

Figure 5.6: Maximum possible wave height related to storm surge for different hurricane categories. Adapted from: Jin et al. (2010)

5.4. Flood risk protection in the Galveston Bay

Flood risk reduction regulation is organized different in the US in comparison to the Netherlands. While there is little focus on large-scale structural prevention, in the United States more emphasis is placed on the policy and emergency measures. For instance, many people have flood insurance and rebuild their homes in case of destruction due to flooding. Large scale evacuations are carried out regularly. Other non-structural flood protection measures consist of building regulations, which is in close accordance to the insurance system.

The institution that governs the national insurance system is the Federal Emergency Management Agency (FEMA). More specifically, it obligates residents of flood prone areas to buy flood insurance and to adhere to the building regulations. If residents do not, they cannot access federal emergency funds that are made available by FEMA in case of a flood disaster. On its flood insurance program FEMA states: *"The National Flood Insurance Program aims to reduce the impact of flooding on private and public structures. It does so by providing affordable insurance to property owners and by encouraging communities to adopt and enforce floodplain management regulations. These efforts help mitigate the effects of flooding on new and improved structures. Overall, the program reduces the socio-economic impact of disasters by promoting the purchase and retention of general risk insurance, but also of flood insurance, specifically."* (FEMA, 2017)

In order to assess which residents need to buy flood insurance, FEMA has defined coastal high hazard zones. The prescribed precautions for these zones are based upon a flood with a return period of 100 years. The zones contain so-called *Base Flood Elevations*, which is a buidling regulation that prescribes the minimum elevation of the house. FEMA (2017) defines the different categories as follows:

- **A** - The flood insurance rate zone that corresponds to the 100 year return period flood zone. Determined by approximate methods.
- **AE** - The flood insurance rate zones that correspond to the 100 year return period flood zone. Determined by detailed methods with inclusion of Base Flood Elevations for houses.
- **V** - Similar to A, with additional risks associated with storm wave action.
- **VE** - Similar to AE, with additional risks associated with storm wave action.
- **X** - The flood insurance rate zones that correspond to areas outside the 100-year floodplains, no mandatory flood insurance.

These zones are shown in figure 5.7. The main take away from the map is that pink areas are flood zones with a 100 year return period (or shorter). Brown areas are zones with additional hazard due to

storm waves (3 ft or higher). The brown areas in the map are of particular interest in this research, since they show were strong wave action is expected during storms and hurricanes.

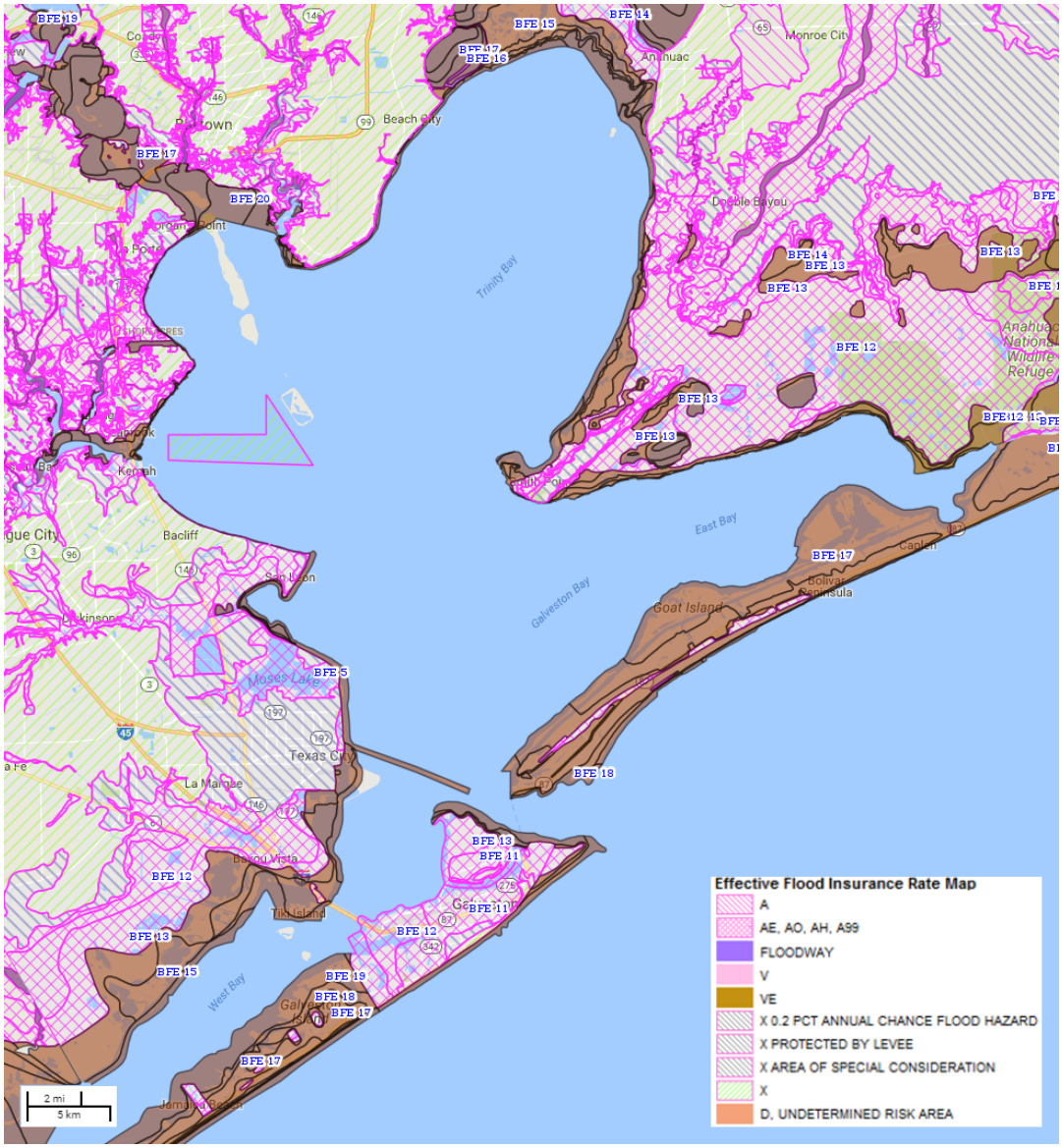

Figure 5.7: Effective flood hazard areas around the Galveston Bay, designated by FEMA. Pink areas are flood zones with a 100 year return period (or shorter). Brown areas are zones with additional hazard due to storm waves (3 ft or higher). Adapted from: FEMA (2017)

It is custom in large parts of coastal US to elevate your house by several feet, depending on the hazard zones and prescribed Base Flood Elevation. The FEMA is responsible for disaster response and pre-disaster mitigation programs. As to flood prove housing, it aims for safer construction of houses and accordingly provides design guidelines for house elevation. The required level is called the Base Flood Elevation (BFE). This level varies per area and is based on a return period of a water level (for instance 1 in 100 year water level). It is determined by a local floodplain management ordinance or law and comprises three components: the ground level, the normative water level and the normative wave height. According to FEMA, waves of 1.5 feet (0.46 m) and higher can cause significant damage to structures. It stresses that breaking waves produce the largest loads on structures. The minimum of 1.5 feet is used to spatially compartmentalize different flood zones. These zones and the BFE are shown in figure 5.8. Hence if the wave height would decrease, the zones would shift in seaward direction and the Design Flood Elevation of a house would be lower.

The FEMA determines the normative wave height based upon the water depth. As shown in figure

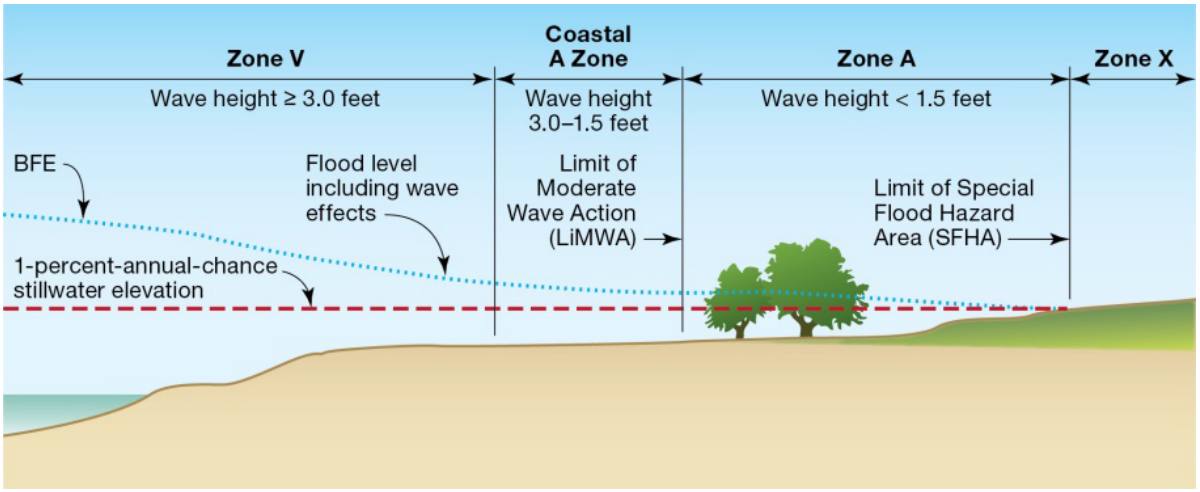

Figure 5.8: Flood zones based on wave height. Source: FEMA (2015)

5.9, the breaking wave height is 0.78% of the still water level. Subsequently, 70 % percent of this value is added to the still water level. As a normative wave height represents a random wave field, singular waves can be higher than this value. Thus, elevated houses can still be hit by waves, especially if a storm has a long duration. Nevertheless, the BFE will be regarded as a normative level in this report.

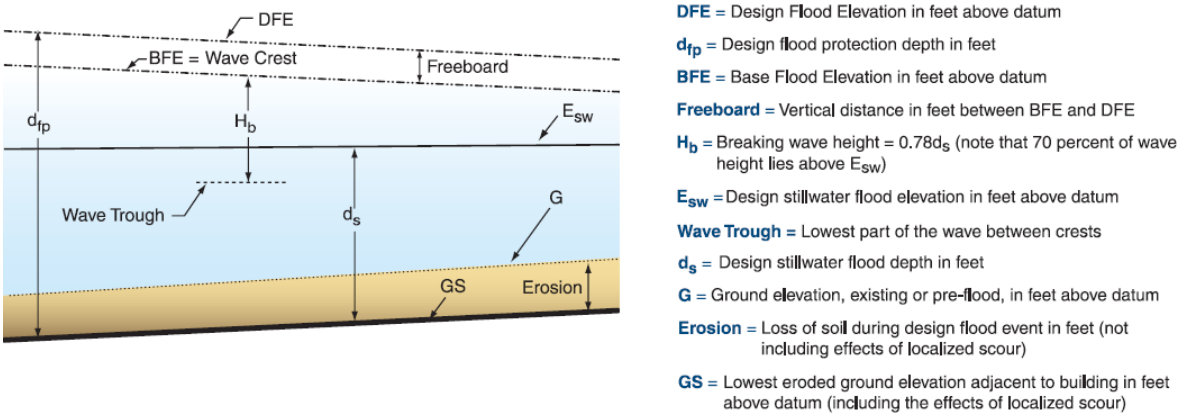

Figure 5.9: Parameters that determine the Base Floor Elevation is flood prone areas in the U.S. Source: FEMA (2015)

Collective, structural flood mitigating measures are exception rather than the rule in the US. Two notable exceptions in the Houston-Galveston Bay Region are the Texas City Hurricane Flood Protection and the Galveston Seawall. However, more and more stakeholders in the Houston-Galveston Bay Region see utility and necessity in collective flood protection. A more thorough elaboration on the hurricanes that have hit the Houston-Galveston Bay Region in the past and the recently proposed counter measures can be found in appendix .

5.5. Environmental analysis

Due to urban and industrial development in the area, natural habitats have been declining and several environmental issues threat the area. The bay area has since long been inhabited. In the 18th century the area was explored by both the Spanish and the French. It was part of Mexico both during the colonization of Mexico by the Spanish and during the first decade of Mexico's independence. In 1836 Texas became independent of Mexico and in 1845 it became a part of the United States of America. Around that time circa 4.000 people lived in city of Galveston, as a reference, in 2016 its population was almost 330.000. The settlements around the bay started to exploit the bay and Galveston became an important transport node for shipping and trade. When more infrastructure for the shipping industry

was built in the bay, Galveston became the largest city in Texas. When in 1900 a severe hurricane struck, Galveston was devastated, which was one of the main factors for Galveston's perish as principal city. Other factors were the construction of the Houston Ship Channel and the rise of the rail network, which further favored Houston over Galveston. Nowadays Houston is the largest city in the area by far.

In the beginning of the 20th century the petro-chemical industry arose around the Galveston Bay. This let to the intensification of the shipping activity and construction of port and shipping infrastructure. This is also the point from which the urban and industrial activity around the bay would lead to more and more impact on the ecology of the Bay area. However, awareness also grew, partly because the fishing industry started to notice the decline in fish stock and blamed the ever-growing petro-chemical companies. It let to the establishment of several stakeholder organizations that served the environmental interest of the Galveston Bay (for instance the Galveston Bay Foundation). The organizations try to obtain sustainable use of resources in the Bay region while respecting both nature, industry and local communities (Gonzalez and Lester (2011), Smith (2013)). Apart from environmental issues, the area is prone to fluvial, coastal and pluvial flood hazard. Even though industry, urban development and natural habitat pursue widely diverging interests, they acknowledged that they all benefit by higher safety from flooding and collaboration in adresses environmental issues.

A report on environmental issues in the bay indicates the following threats (GalvestonBayFoundation, 2016):

- **Water quality** - The overall quality as been improving in recent years.
- **Contaminated sediment** - Due to decades of industrial pollution, the sediment in the Galveston Bay is contaminated. The area around the Houston Shipping Channel is effected most.
- **Oil spills** - Regular oil spills hit the Bay, with severe negative impact on the environment. Notable is the Marsh 2014 oil spill, where 168,000 gallons fuel oil leaked into the Bay (Yin, Hayworth, & Clement, 2015).
- **Biodiversity** - Although it varies per species, a significant number of species has been deteriorating in recent years. This holds especially for shellfish.
- **Loss of habitat** - Most natural habitats in and around the Galveston Bay are under stress. Although there have been recovery projects in recent years, overall, natural habitats are declining. Additional attention will be paid to seagrass, marshes and oysters in the next sections.
- **Erosion** - Rising sea levels and decline of vegetation is causing erosion problems in the Bay. Apart from the decreasing coastal resilience, erosion in the Bay also causes release of pollutants and carbon dioxide.

5.5.1. Marshes in the Houston-Galveston Bay Region

Wetland areas in the HGBR in 2010 are shown in figure 5.10, and consists of different types of marshes. Marshes are typical for the upper Texas coast. Towards the coast the salinity increases and this influences the type of habitat, it shifts from prairie (grasslands) to fresh water marshes, to brackish marshes, to salt marshes and eventually to the marine environment. Fresh water marshes are dependent on precipitation accumulation, stream and rivers and the ground water level. Brackish and salt marshes (together called estuarine wetlands) are under influence of the tide, they are found at locations were inland fresh water mixes with salt water from the sea. Each habitat attracts its own vegetation and species. The dominant species in the estuarine wetlands of the Upper Texas Coast is smooth cord grass (Spartina alterniflora). In the HGBR, large areas of fresh water marshes were lost over the last century due to urbanization. Closer to the coastline, estuarine wetlands are prone to erosion, mainly due to sea level rise. A large part of them is appointed as nature reserve (Laffoley and Grimsditch (2009), HoustonWilderness (2007)).

5.5.2. Seagrass meadows in the Galveston Bay

Seagrass beds once flourished in the Galveston Bay and were mostly found in the southern part of the Bay due to its higher salinity. Over the past decades seagrass meadows have largely vanished. Dredging activity and pollution of the water degraded the natural occurrence of seagrass meadows. Literature also suggests that natural disasters such as floods and hurricanes can damage seagrass meadows. Furthermore, turbid water and extensive boating negatively impacts seagrass. Nowadays meadows can only be found in Christmas Bay in the west of the Galveston Bay system. It has a

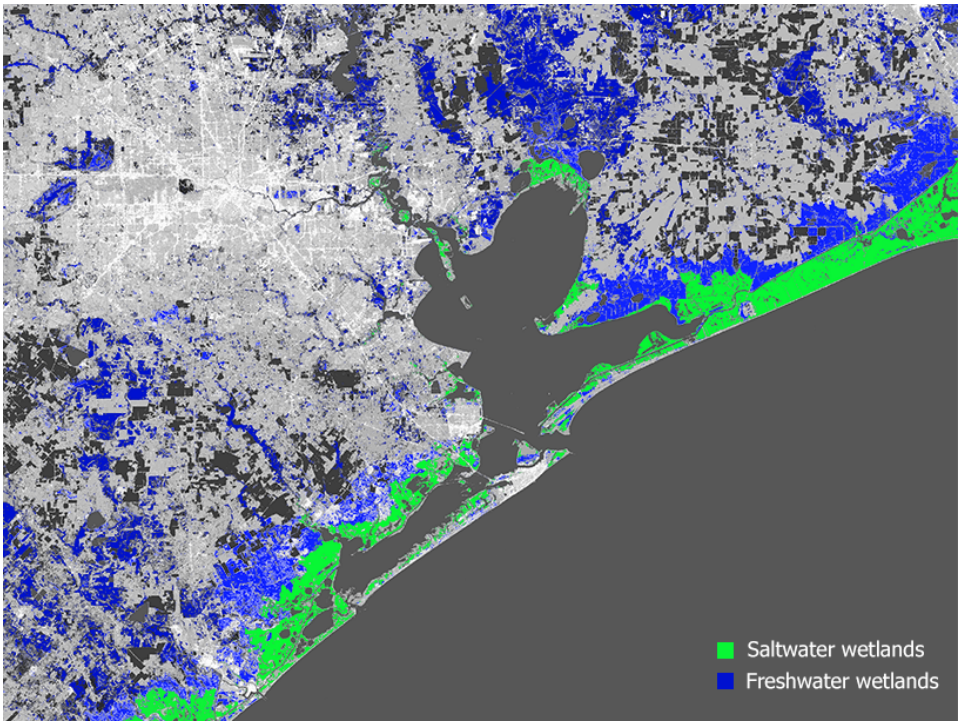

Figure 5.10: Distribution of wetlands in the HGBR. Input data from (NOAACCAP, 2010)

high salinity and in mostly untouched by the impact of the shipping and industry (Pulich et al., 1996). Current and historical presence of seagrass is mapped in figure 5.11. In 1999 a Seagrass Conservation Plan for Texas was initiated. Since then the distribution of seagrass along the Texas coast has been monitored more consequently. Legislation has been implemented in order to protect existing seagrass meadows and prevent further degradation (Gonzalez and Lester (2011), Pulich et al. (1996)).

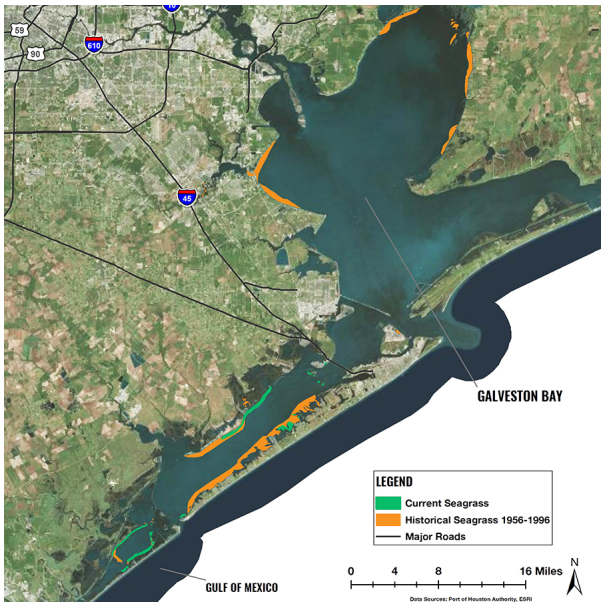

Figure 5.11: Historical and present locations of seagrass meadows in the Galveston Bay. Orange areas are locations where seagrass was present between 1956 and 1996. Green areas are locations where seagrass was present in 1996. Source: GalvestonBayFoundation (2016)

5.5.3. Oyster reefs in the Galveston Bay

The prevalent species in the Galveston Bay is the eastern oyster (Crassostrea virginica), which is harvested on large scale for consumption. Vast oyster beds are present in the Bay, but their development and exact location is not profoundly monitored. Historical presence of oyster beds is mapped in figure 5.12. Oysters form an important source of income and employment in the area but overharvesting of oyster shells decimated the population. As oysters also filter water and trap sediment, and thus contribute to the environmental welfare of the bay, several oyster restoration project were conducted in the Galveston Bay in recent years.

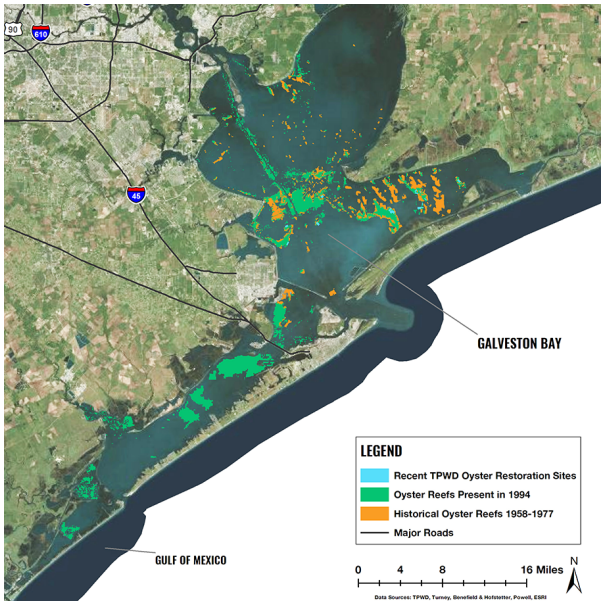

Figure 5.12: Historical and present locations of oyster colonies in the Galveston Bay. Orange areas are locations where oyster beds were present between 1958 and 1977. Green areas are locations were oyster beds were present in 1996. Blue areas are oyster restoration locations. Source: GalvestonBayFoundation (2016)

5.6. Conclusion

- The Galveston Bay is a shallow semi-enclosed bay system characterized by low wave action, a micro-tidal environment and brackish water. The area is prone to hurricanes and tropical storms. During storms, the water level in Galveston Bay can rise significantly due to inflow and locally due to wind set-up. This is especially the case during a hurricane that passes the Galveston Bay on the west.
- Although water levels in the Bay are extensively documented, there is a lack of wave height observations. There are no publicly accessible or published observations of wave heights during extreme conditions in the Galveston Bay.
- Despite the lack of data, the FEMA located flood risk areas around the Bay with additional risk due to storm waves. These zones include the area around the Houston Shipping Channel and large parts of Galveston Island and Bolivar Peninsula. The FEMA relates the expected wave height directly to the water level. Additionally, de Boer (2015) pointed out several locations in the Bay that are prone to wave action. He found that the west part of the bay is at danger due to its urbanized coast line.
- Historically, oyster reefs, seagrass meadows and marsh vegetation have been present in the Galveston Bay. Lack of monitoring hampers a thorough analysis of their current location and development, but it is clear that due to environmental threats their habitat has been declining for decades. Recently, more attention is drawn toward restoration of nature habitats in the Galveston Bay, both for environmental reasons as for their potential in flood risk reduction strategies.

6

Numerical simulations for the Galveston Bay

The numerical model that was covered in chapter 4 was used to increase the understanding of the behavior of Nature-Based Solutions in the Galveston Bay with respect to wave attenuation. In section 6.1, the general approach of the case study is elaborated.

In section 6.2, two locations in the Galveston Bay were selected to serve as a test site for Nature-based Solutions with use of numerical modeling. The first site is at the west side of the Galveston Bay near San Leon. The second site is at the northern coastline of Galveston Island. Both locations are prone to wave action. The hydraulic boundary conditions at the two locations are discussed in section 6.3. They serve as input parameters for the numerical model.

Next, in section 6.4, the configuration of the three types of Nature-based Solutions was explained, namely marsh vegetation, seagrass meadows and oyster reefs. Their inclusion in the numerical model was covered in section 4.1.2. Since their implementation is hypothetical, the properties that function as input parameters are based on reference projects. Finally, the results of the numerical simulations for the two locations are described in section 6.5.

6.1. Approach for simulations

In figure 6.1 the schematic approach for the simulations is shown. The numerical model can return the simulated wave height at any given location. In order to asses the effect of the Nature-based Solutions, an output location was selected (i.e. the first line of houses at the coast) where the wave height with and without influence of Nature-based Solutions are compared. The simulations are based on the current state of the Bay, potential future project (e.g. the coastal spine) are not included.

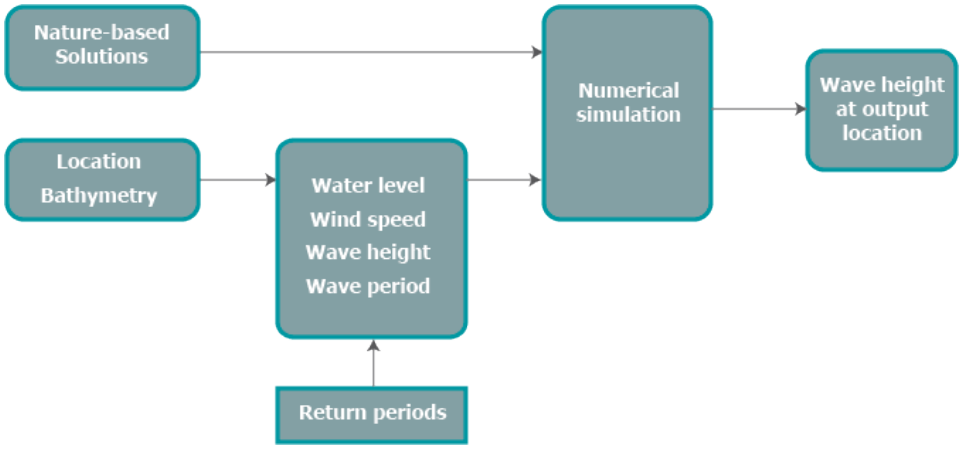

Figure 6.1: Overview of input for numerical simulations.

6.1.1. Return periods

Flood defence systems are often based on return periods of water levels or hydraulic loads. Thus it make sense evaluate the case study for different return periods. In order to do so, the boundary input parameters of the model are related to their return period. The standard return period in the U.S. is 100 years (i.e. every year the probability that the 100 year water level is equaled or exceeded, is 1%). Areas that harbor special buildings, such as nuclear plants or hospitals, sometimes adopt a 500 year return period. The return periods that are considered in this study are 10, 50, 100 and 500 years.

A complexity is the mutual dependence of the parameters of the boundary input. The parameters are positively correlated to a certain level, but the levels of dependency are unknown. In this study it is assumed that a 1-100 year wave height can only happen simultaneously with a 1-100 year water level (i.e. a high level of dependency is assumed). This assumption is supported by the conclusions of Jin et al. (2010), who found that the maximum wave height in Galveston Bay is much more related to the water level than to the wind speed.

Assuming a high dependency between parameters results in a conservative approach. If the parameters were completely independent, their combined return period would be much longer than 100 year (e.g. 100 times 100 years), thus leading to lower values for the 1 in 100 year wave height and water level. However, dependent parameters have a return period in the order of magnitude of the return period of each individual parameter. This could lead to a slight overestimation of the wave height and water depth, which could lead to a conservative design. However, this preferable over an underestimation of the values. The choice of assuming a high dependency was preferred in other studies as well, for instance Suzuki et al. (2012).

Calculating the value of a parameter for a certain return period can be done with the use of Extreme Value Theory. This theory and the calculations made for this study are covered extensively in appendix E. However, two or more parameters that shows extremal dependence should be analyzed with specific methods. The tail dependency of the parameters could for instance be be further investigated with use of multivariate copulas (Coles, 2001). However, an accurate calculation of the correlation of the extreme values of the parameters is outside the scope of this study.

6.2. Location and bathymetry

FEMA has indicated zones in the Galveston Bay that are prone to dangerous wave action in case of a 1 in 100 year flood event, as was discussed in section 5.4. Additionally, de Boer (2015) suggested locations for Nature-based Solutions in the Galveston Bay. He predicted the largest wave impact at the west side of the bay.

Therefore, two locations are selected for the case study. One near San Leon, a town on a peninsula-like area in the Galveston Bay, shown in figure 6.2. The other at the northern side of Galveston Island, west of the city of Galveston. San Leon is home to a meteorological station of the NOAA with a measuring record of over twenty years. This further supports the location selection. The two locations are described in the next sections.

6.2.1. San Leon

The shoreline at San Leon is completely developed; it is dotted with houses. The first line of houses is constructed between 10 and 20 meter from the water line. A number of them have small, private jetties that give access to the bay. Collective flood protection is absent, most houses are constructed on piles, although at different levels. The bank protection consists of loose rock and its top is at ground level (Google Maps). A simplified cross section of the coastal zone was derived from NationalOceanService (2016) and is shown in figure 6.3. The depth of the bay gradually decreases from -3 m to 0 over a length of approximately 1000 meter. The 200 meters directly in front of the shore line can be schematized as a flat foreshore. The bathymetry shown in figure 6.3 is used in the numerical model.

Figure 6.2: Location of San Leon in the west of Galveston Bay.

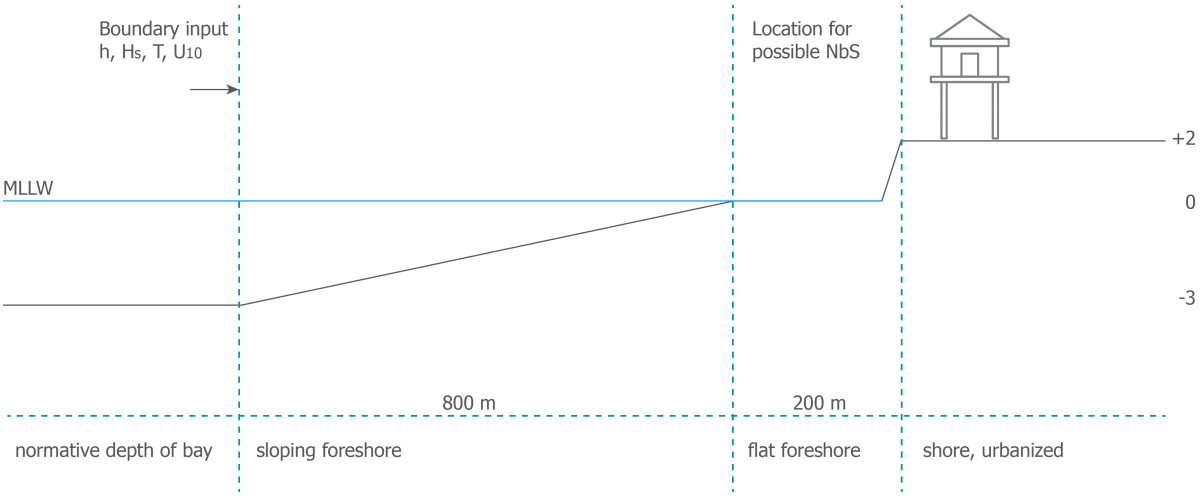

Figure 6.3: Schematized cross section of San Leon location.

6.2.2. Galveston Island

Galveston Island is largely protected from extreme surge and waves at the Gulf-side by the Galveston seawall. However, the backside is vulnerable to both surge and waves. As explained in section 5.3 this is especially the case when a hurricane moves over the area, due to its rotating character. Both waves and surge can be piled up against the backside of the Island. Another property that makes the location an interesting case, is its bathymetry. It has a gradually sloping shore, opposite to the location at San Leon. This makes is possible to better assess the effect of the Nature-Based Solutions, as the abrupt change is bathymetry is absent.

The selected location is to the southwest of the city of Galveston. It is mapped in figure 6.4. The area is characterized by wetlands and small stretches of land that are urbanized. A very gradual transition from bay and wetlands to urbanization is present. The area lacks collective flood protection, and most houses have been elevated to withstand extreme conditions. The characteristic shoreline can

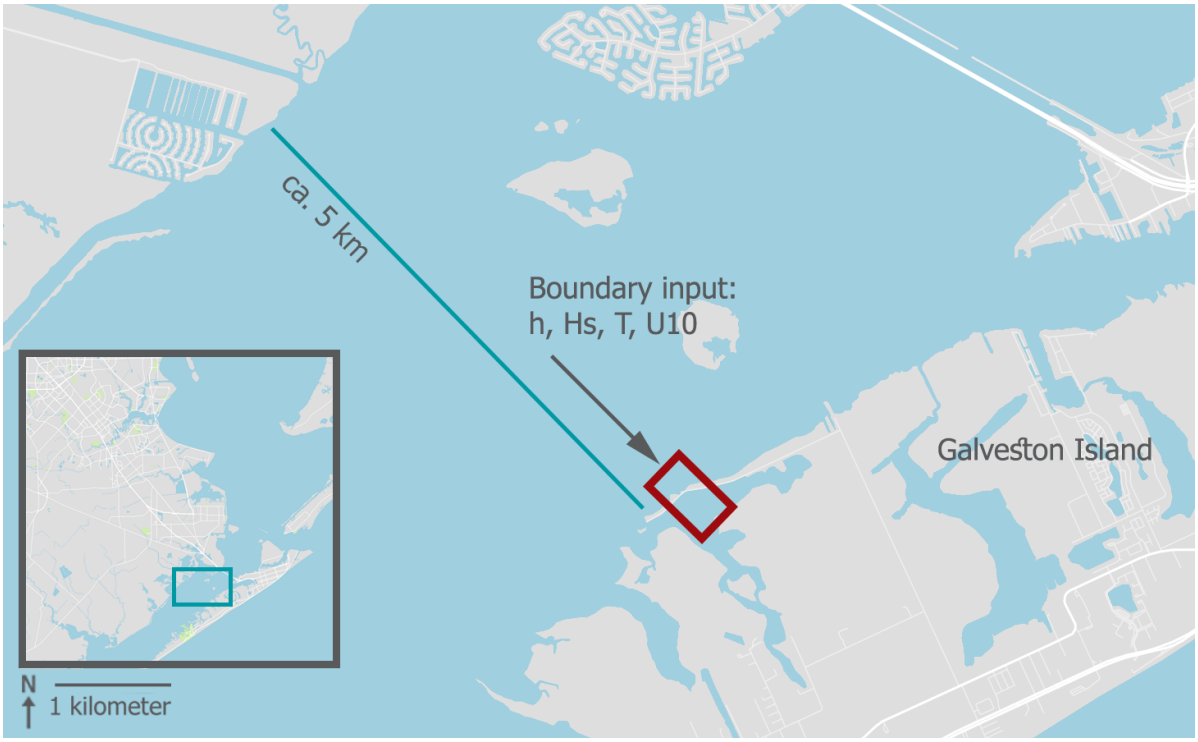

Figure 6.4: Location at northern shore line of Galveston Island

be schematized as shown in figure 6.5.

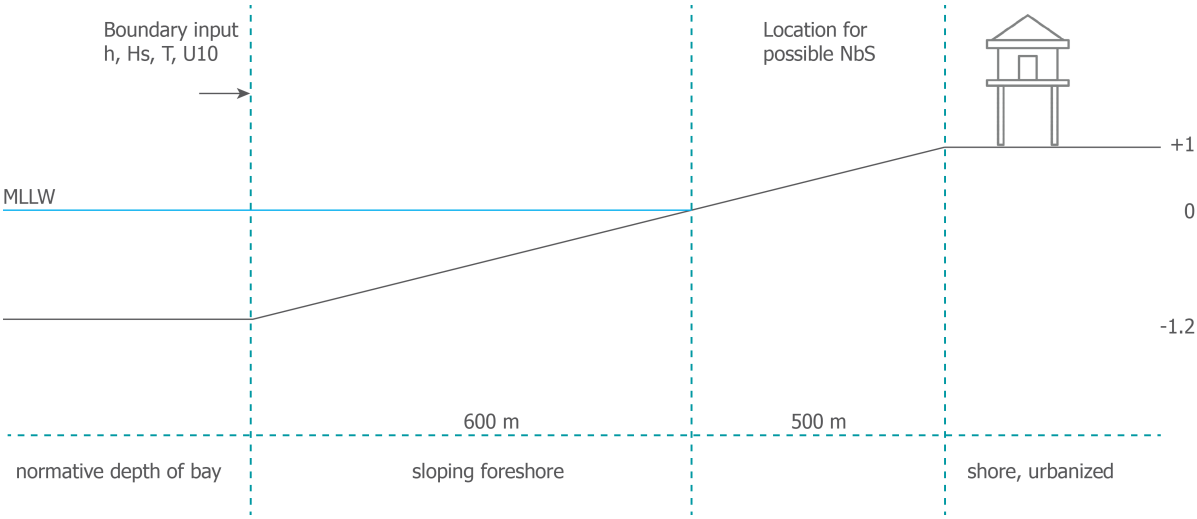

Figure 6.5: Schematized cross section of Galveston Island location.

6.3. Input parameters

The hydrodynamic input parameters for the numerical simulation are location-specific and should subsequently be derived for both locations. As mentioned in figures 6.2 to 6.5, the parameters are water level h, wind speed U_{10}, significant wave height H_s and significant wave period T_s.

6.3.1. Water levels

As explained in section 5.3, Stoeten (2013) and FEMA (2012) derived storm surge levels in the same range for different return periods and locations in the Galveston Bay. The values of FEMA (2012) will be

used as input for the simulations, and are provided in table 6.1. The water level is assumed constant over the considered cross section (see figures 6.3 and 6.5). This is a simplification, as in reality the wind and wave set-up would induce a water level gradient over the cross section.

Table 6.1: Normative water levels with return period for San Leon and Galveston Island locations.

Return period Years	**Water level, San Leon** m w.r.t. NAVD-88	**Water level, Galveston Island** m w.r.t. NAVD-88
10	2.41	2.59
50	2.96	3.17
100	3.66	4.09
500	4.70	5.34

6.3.2. Wind speed

The wind speed in the Galveston Bay is one of the parameters that can be extracted directly from the NOAA database (NOAA, 2017). The NOAA station near to San Leon, called Eagle Point, has kept a wind speed record since November 1995. This is one of the longest measurement periods of meteorologic stations in the Galveston Bay. However, the characteristic wind speed at San Leon for return periods up to 500 year are needed, thus the observed data needs to be extrapolated with Extreme Value Analysis.

Yearly wind speed records of station eagle Point were extracted from the NOAA website (NOAA, 2017) for the period 1996 - 2016. Extreme value theory (EVT) was used to investigate the extreme behaviour of the wind speed. EVT allows us to extrapolate expected values for the wind speed to very small probabilities. From these probabilities, the return periods for extreme values for wind speed were obtained. The results for the San Leon locations are shown in figure 6.6, which shows the wind speed for different return periods. Note that an extrapolation with EVT is based on historical observation and, in this case, a rather limited data set. The results should thus be interpreted with care.

The observations of NOAA station Eagle Point will be used for the Galveston Island location as well. The distance from the station to the location at Galveston Island is approximately 25 kilometers. NOAA stations closer to Galveston Island have much shorter measurement periods, which make them less suitable for data extrapolation. The fact that the fetch (30 km) used in the calculations at San Leon is longer than the distance between San Leon and the location at Galveston Island, further supports this assumption.

The details on the method to determine the normative extrapolated wind speeds and the exact calculations per location are explained comprehensively in appendix E.

A significant assumptions considers the wind direction. As the model approximates a 1-D situation, the wind is assumed perpendicular to the coast line. In reality, the directions of the yearly maxima are scattered on the compass card. Nevertheless, since 1D waves propagating perpendicular to the coast line is considered, only wind coming from the direction of the bay is taken into account.

The main assumptions were as follows:

- Only the wind coming from the Bay (180 degrees limit) is taken into account.
- The wind field is unidirectional (perpendicular to the coastline) and constant.
- Although the data base (NOAA, 2017) contains gaps of several months, the 21 annual maximum values are representative.
- The data from Eagle Point is used for both the San Leon location as the Galveston Island location.

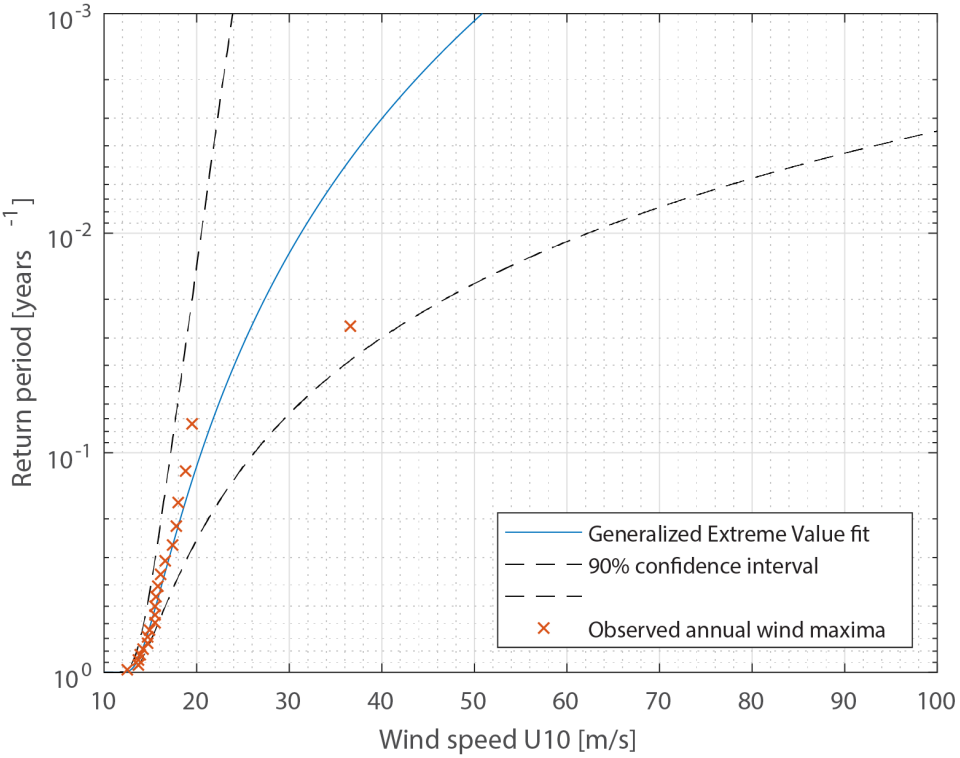

Figure 6.6: Cumulative distribution function for the GEV fit for the San Leon annual maximum wind speed. Plotting position of observed data is obtained with Gringorten method. The data point at U_{10} = 36.6 m/s represents Hurricane Ike (2008).

Table 6.2: Normative simulations for the wind speed with return period for San Leon and Galveston Island.

Return period Years	**Wind speed U_{10}, San Leon** m/s	**Wind speed U_{10}, Galveston Island** m/s
10	20.5	18.9
50	27.3	24.7
100	31.3	28.0
500	43.6	37.8

6.3.3. Wave height

No long term records of the wave height in the Galveston Bay are available, mainly because the frequency of the regular water elevation measurements of NOAA is too low. No additional wave measuring equipment was installed in the Galveston Bay. So in order to generated wave data, the normative wave height and period is calculated with the method of Young and Verhagen (1996) for wave growth for coastal waters.

Young and Verhagen (1996) explicated an adequate method to model wave growth for cases similar to the Galveston Bay. Their results were further refined by Breugem and Holthuijsen (2007). It is tailored to describe wave growth in enclosed water bodies with shallow water conditions, and is thus particularly suitable to derive wave characteristics for the Galveston Bay. The idealized significant wave height and wave period can be calculated with the fetch length, the water depth and the wind speed.

The previously provided values for water level and wind speed are used as input parameters. A fetch length of 30 km is used for the San Leon location and a fetch length of 4 km for the Galveston Island location. For the wave period, a method similar to the wave height calculation was used. The calculations and additional information on the method can be found in appendix E. The main assumptions were as follows:

- The wave height and period depend on wind speed, water depth, fetch and gravitational acceleration only.
- The fetch is small enough to assume an idealized wind field, even during hurricanes.
- Duration is taken infinitely, so that the duration becomes non-essential.
- Turbulence in the air flow, atmospheric instability and wind gusts are disregarded.

6.3.4. Overview of input parameters

The overview of all input parameters is given in table 6.3 for the two locations. An important note is that the simulations were done for specific return periods. This translates to specific, fixed sets of conditions that were statistically obtained. That means that with an increasing return period, not only the wave height increases, but all input parameters become larger.

Table 6.3: Simulated significant wave height and significant wave period for idealized conditions near San Leon and Galveston Island.

	San Leon					**Galveston Island**				
Return period years	h m	U_{10} m/s	H_s m	T_s s	H/h_{abs} -	h m	U_{10} m/s	H_s m	T_s s	H_s/h_{abs} -
10	2.41	20.5	1.43	4.79	0.26	2.59	18.9	0.81	3.14	0.21
50	2.96	27.3	1.87	5.34	0.31	3.17	24.7	1.08	3.55	0.25
100	3.66	31.3	2.21	5.76	0.33	4.09	28.0	1.27	3.76	0.24
500	4.70	43.6	3.07	6.61	0.40	5.34	37.8	1.76	4.32	0.27

6.4. Configuration of Nature-based Solutions

In this section, the configuration of the Nature-based Solutions in the numerical simulations is explained. Figures 6.7 and 6.8 show the hypothetical location of the marsh vegetation, seagrass meadow and oyster reef. At the San Leon location, the natural measures are placed on the flat foreshore in the tidal zone that has a length of 200 meters. The natural measures at the Galveston Island location are positioned on a slope that is 500 meter long. The dimensions and properties of the Nature-based Solutions that were used in the model are described in the next section.

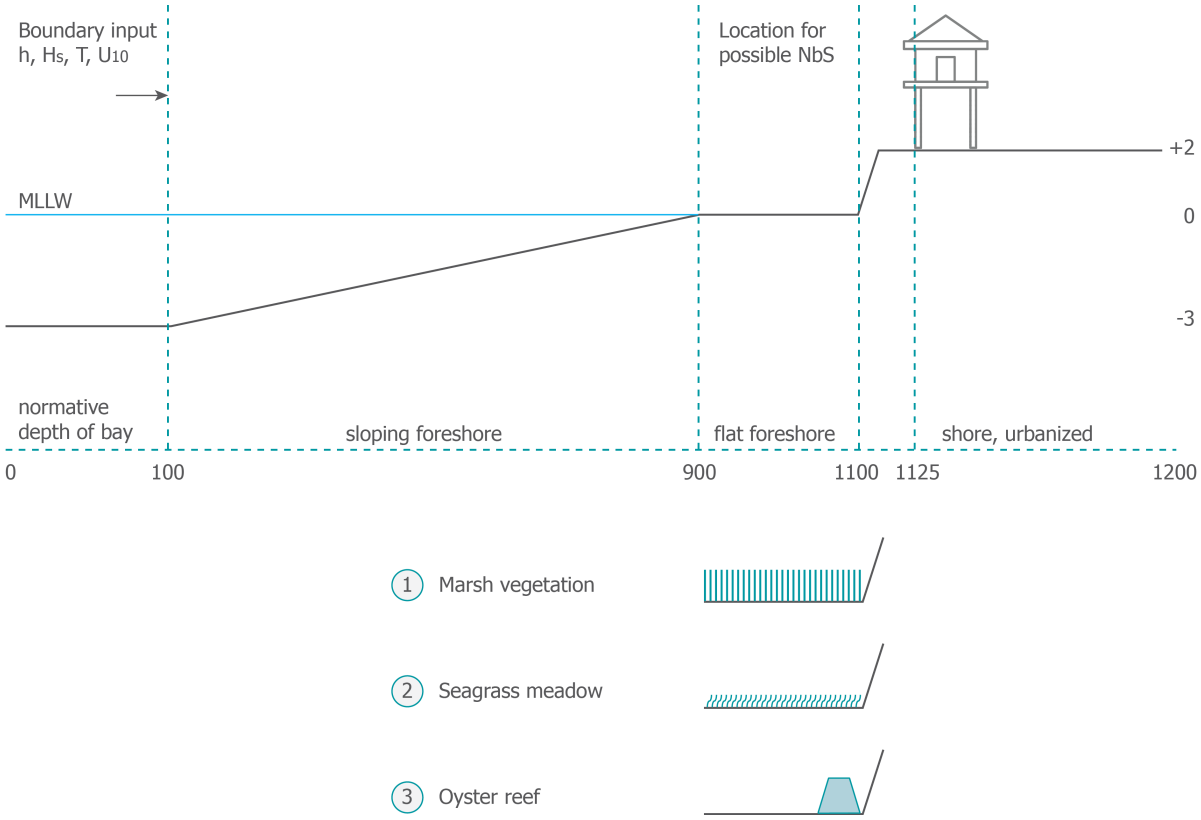

Figure 6.7: Schematized cross section at the San Leon location, as included in the numerical model. Configurations of Nature-based Solutions are shown below the cross section and their properties and dimensions are discussed in the next subsections. The output location, which is ten meters from the edge of the bank, is visualized as the elevated house. The cross shore distance in meters corresponds to the grid points in the numerical model.

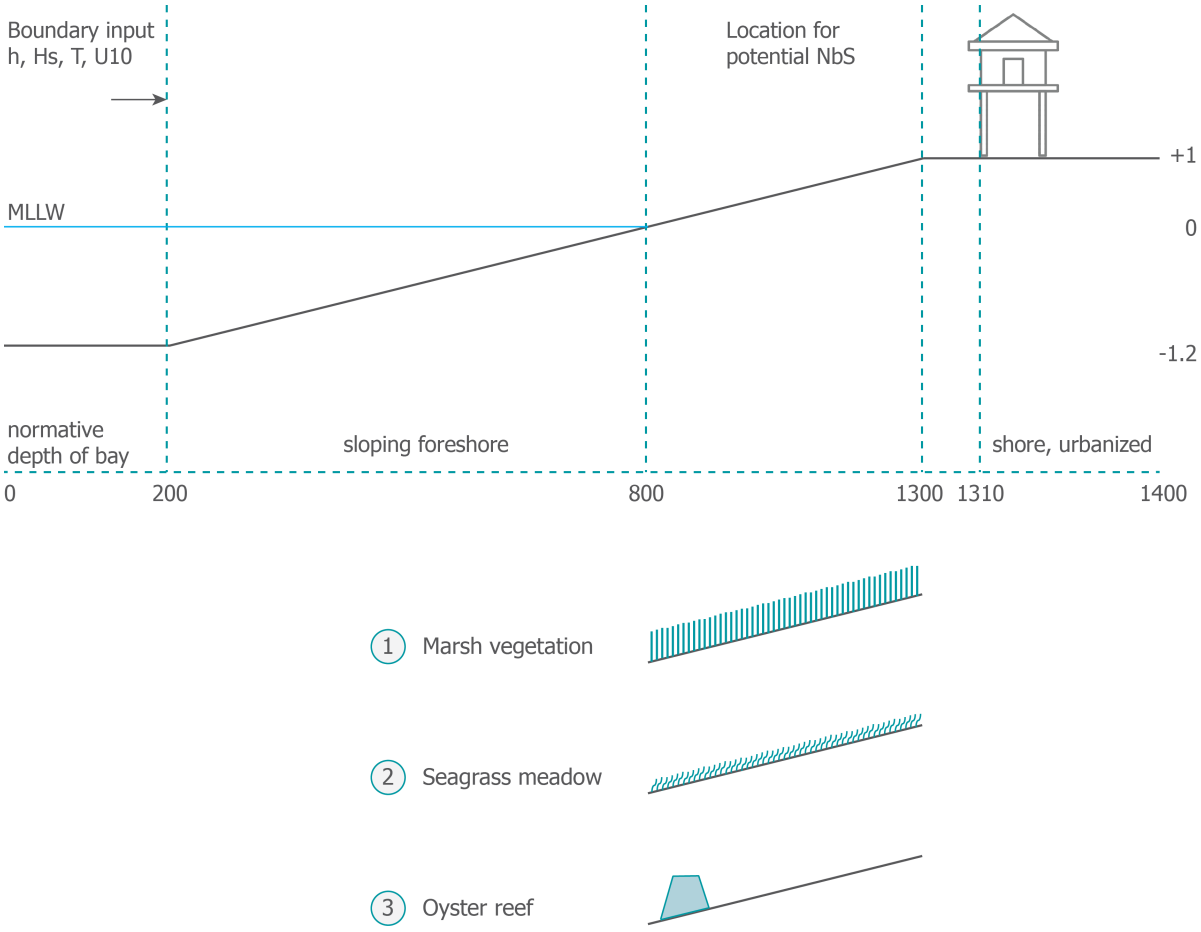

Figure 6.8: Schematized cross section of the Galveston Island location, as included in the numerical model. Configurations of Nature-based Solutions are shown below the cross section and their properties and dimensions are discussed in the next subsections. The output location, which is ten meters from the shore line, is visualized as the elevated house. The cross shore distance in meters corresponds to the grid points in the numerical model.

6.4.1. Marsh configuration

The Galveston Bay region, salt marshes dominate the areas close to the water line. Smooth cord grass (Spartina alterniflora) is the dominant shoreline species. It was used as the reference species in this study because several reference studies are available in which Spartina Alterniflora has the lead, and it is the dominant species in the Galveston Bay.

A hypothetical marsh is incorporated in the model to investigate the effect of marsh vegetation on wave height. Nevertheless, the used values should be realistic. Therefore values for marsh characteristics from reference studies with actual measurements were used. These values are shown in table 6.4 and are averages of the values in table 6.5. The parameters form the vegetation-specific input of formula 3.10 of Mendez and Losada (2004).

At the San Leon location, the vegetation is incorporated on the flat foreshore. At the Galveston Island location, it is assumed that the vegetation field stretches from the MLLW line to the level at which urbanization starts, the length of the field is 500 meter. Smooth cord grass (S. alterniflora) is known to grow above and in the intertidal zone. This is the natural habitat of the species.

Table 6.4: Charcateristics of S. Alterniflora. N_v is density in stems per m^2, b_v is the stem diameter in m, h_v is the vegetation height in m

Location	**Species**	N_v	b_v	h_v	**Author**
Chesapeake Bay, VA/MD, USA	S. Alterniflora	506	0.0043	0.51	(Keefer, 2017)
Hellegat, the Netherlands	S. Angelica	529	0.0072	0.22	(Vuik et al., 2016)
Chongming, China	S. Alterniflora	508	0.0039	0.97	(Yang et al., 2011)
Terrebonne Bay, LA, USA	S. Alterniflora	422	0.008	0.63	(Jadhav & Chen, 2012)

Table 6.5: Marsh vegetation parameters used in the numerical model.

Density N_v m^{-2}	**Stem diameter** b_v m	**Vegetation height** h_v m	**Drag coefficient** C_D
491	0.006	0.58	0.4

6.4.2. Seagrass meadow configuration

Similar to marsh vegetation, a hypothetical -but realistic- seagrass meadow is incorporated in the model. As explained, the dominant species in the Galveston Bay is Thalassia testudinum (turtle grass). Specific characteristics of the vegetation that stem from observations from reference studies were used. These values are shown in table 6.7 and are averages of the values from table 6.6. Previous studies show that the density and height are varying significantly for different sites. This is mostly due to seasonal variation and local conditions of the water and subsoil. All studies present a thickness near the leaf meristem in the range of 0.0035 m.

For the San Leon location, the seagrass meadow is located on the flat foreshore around MLLW. For the location of Galveston Island, the hypothetical meadow stretches out over the upper slope of the bathymetry. Seagrass is known to be able to survive in shallow tidal pools or on dry ground during ebb tide for several hours (Pedersen, Colmer, Borum, Zavala-Perez, & Kendrick, 2016). Nevertheless it is not clear to what extend this applies to T. testudinum (turtle grass).

Table 6.6: Charcateristics of T. testudinum

Location	**Density**	**Height**	**Author**
Santa Rosa Island, Florida	1100	0.27	(Bradley & Houser, 2009)
Florida Keys (moved to lab)	1133	0.19	(Fonseca & Cahalan, 1992)
Coastal Bend, Texas	-	0.30	(Congdon & Dunton, 2016)
Lower Laguna Madre, Texas	-	0.20	(Medina-Gómez, 2016)
Bahia de la Ascension, Mexico	592	0.12	(Vidal & Basurto, 2003)

Table 6.7: Seagrass meadow parameters used in the numerical model.

Density N_v m^{-2}	**Stem diameter** b_v m	**Vegetation height** h_v m	**Drag coefficient** C_D
941	0.0035	0.21	0.13

6.4.3. Oyster reef configuration

The third Nature-based Solution that was incorporated in the numerical model is an oyster reef. Although vast oyster banks are present in the Galveston Bay, it lacks thorough and consequent monitoring of their location and development. Several reference studies were used to compose a realistic oyster reef to include in the numerical model. In view of wave reduction, relevant characteristics of an oyster reef are its location, dimensions and roughness. In the numerical model, we include an artificially constructed reef. The dimensions of the hypothetical reef that were used in the numerical model are shown in table 6.8 and were chosen based on the findings discussed in section 3.3.3.

The height of the reef depends on the growth ceiling. As shown in figure 6.7, the toe of the oyster reef is located at MLLW. A tidal range of approximately 0.35 and the fact that the average observed water level is approximately a feet higher than the predicted tidal level, justifies the choice for a reef with a height of 0.5 meter. These dimensions are incorporated in the bathymetry of the model, thus assuming the reef to be impermeable. This assumption is acceptable with regard to wave attenuation, but cannot automatically be applied in other hydraulics models. Since a reef is actually porous, it will not function as a levee or retain water, so in a model on storm surge reduction, it cannot be incorporated in the bathymetry.

Adult oysters can reach a shell length of ten centimeter in two years, depending upon the local conditions. Their roughness depends on their position with respect to the flow direction and their shell length. Styles (2015) studied the roughness of C. virginica in Winyah Bay, South Carolina and found an empirical value of five times the shell length. Thus a roughness of 0.3 m is a conservative first estimate for the hypothetical reef in the numerical model.

For the Galveston Island location, the growth ceiling of the reef is also relevant, thus its toe is located around the MLLW line.

Table 6.8: Oyster reef parameters used in the numerical model.

Height top h_{top} m	**Height toe** h_{toe} m	**Width** b m	**Nikuradse roughness of reef** k m
0.5	20	30	0.30

6.5. Results

The results of the numerical model were made visual in graphs that show the development of the significant wave height over the cross section for each Nature-based Solutions, grouped per return period. The return periods represent a specific combination of input parameters (h, U_{10},H_s and T_s). Percentage and absolute results are based upon the output location, which is the first line of houses at both locations. This is also visible in the graphs. The bottom panel of each figure shows the bathymetry, water level and location of Nature-based Solutions. The three top panels show the development of the significant wave height with and without the Nature-based Solution.

6.5.1. San Leon

The results at San Leon for a 10 year return period are shown in figure 6.10, for a 100 year return period in figure 6.11. The vertical dotted line at grid point [1125] shows the output location where the wave heights are compared. The grid points in cross shore direction correspond to the cross shore distance shown in figure 6.7. An overview of the results is given in table 6.9 and figure 6.9. The graphical results for the 1 in 50 year and 1 in 500 year situation are presented in appendix F.

The residual wave heights in table 6.9 show that all Nature-based Solutions are capable of reducing

the wave height. For every return period, the marsh vegetation reduces the wave height most, both in relative as in absolute terms. The reduction due to seagrass meadows is small for every return period, the absolute reduction of wave height in meter does not exceed 0.12 m. The oyster reef reduced the wave height in the 1 in 10 year situation significantly, but for larger return periods, thus larger wave height and water depth, the wave height reduction is negligible. The decrease of effect with an increasing return period is present for all three Nature-based Solutions, however, the reduction rates for 1 in 50 year conditions are relatively even smaller.

The maximum difference between the wave height without NbS and wave height as a result of Nature-based Solutions, was not reached at the output location [1125]. Several meters before the output location, the wave height began to reduce sharply due to depth-induced breaking on the platform-like bathymetry transition. This holds for the wave height both with and without Nature-based Solutions. Indeed, just before this bathymetry change (starting at [1100]), the difference between the original wave height and the NbS-influenced wave height is largest. For 1 in 100 year conditions, the reduction percentage at [1100] due to marsh vegetation is 50%. For the seagrass meadows and the oyster reef the reduction is 10%.

Because of the strong depth-induced breaking on the bank (visible on the interval [1100 - 1125]), the effect of Nature-Based Solutions was overruled. The residual wave height further land inwards (grid point [1200]) shows no difference between the case with and without Nature-based Solutions.

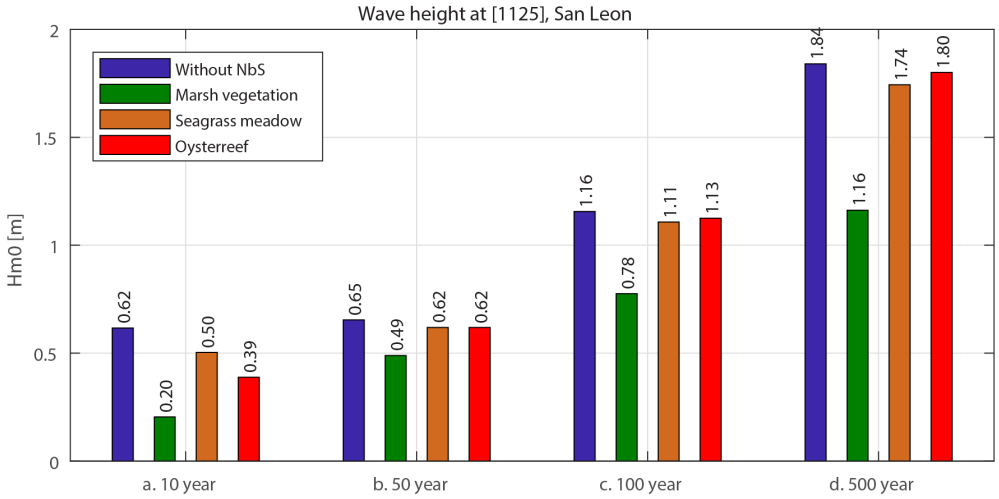

Figure 6.9: Residual significant wave height at output location, gridpoint [1125], for San Leon location.

Table 6.9: Residual significant wave height at output location, gridpoint [1125], for San Leon location.

Return period years	**Without NbS** m	**Marsh vegetation** m	**Seagrass meadow** m	**Oysterreef** m
10	0.62 (100%)	0.20 (-67%)	0.50 (-18%)	0.39 (-37%)
50	0.65 (100%)	0.49 (-25%)	0.62 (-5%)	0.62 (-5%)
100	1.16 (100%)	0.78 (-34%)	1.11 (-4%)	1.13 (-3%)
500	1.84 (100%)	1.16 (-37%)	1.74 (-5%)	1.80 (-2%)

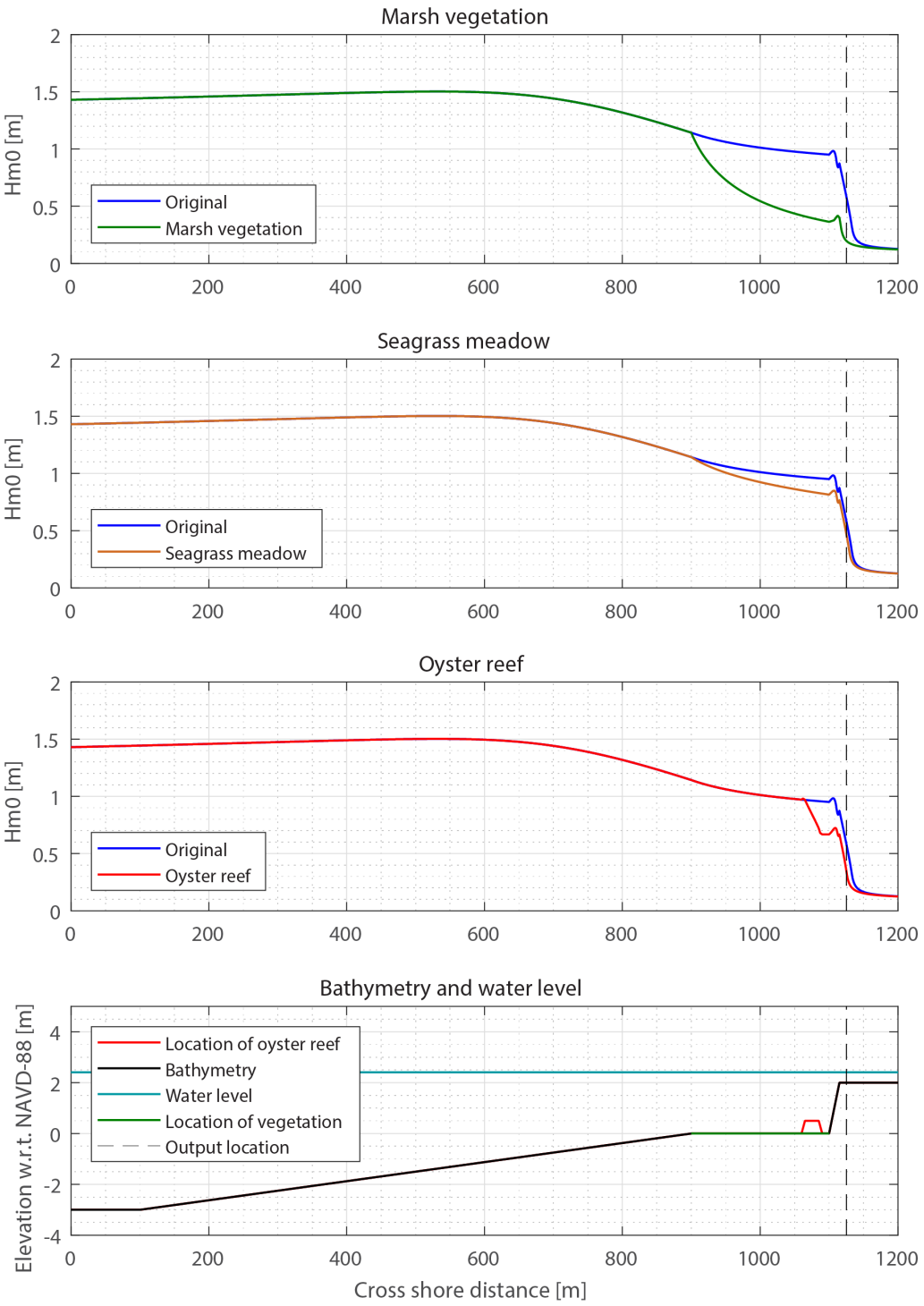

Figure 6.10: Resulting wave heights over the San Leon cross section in a 1 in 10 years situation.

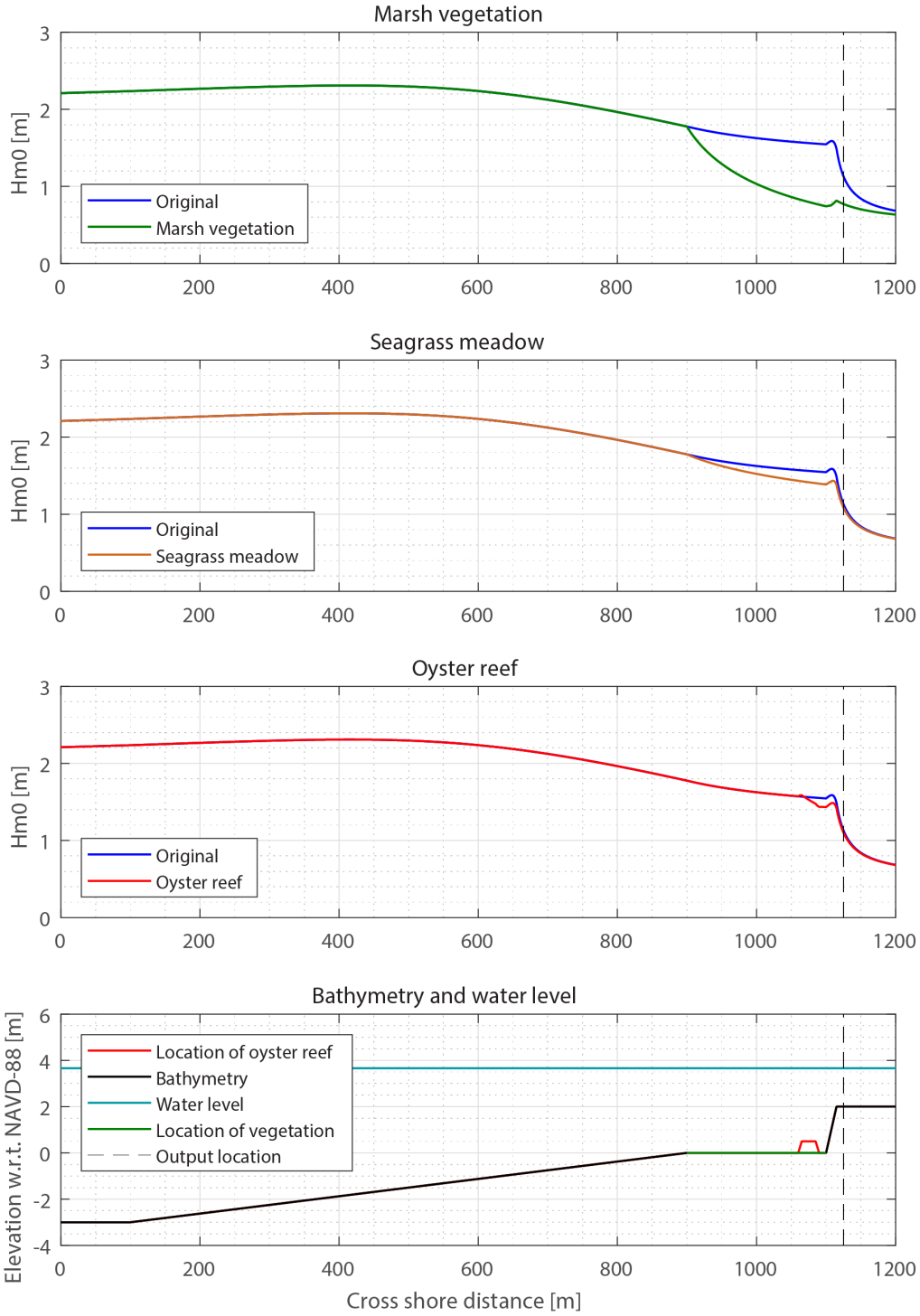

Figure 6.11: Resulting wave heights over the San Leon cross section in a 1 in 100 years situation.

6.5.2. Galveston Island

The results at Galveston Island for a 10 year return period are shown in figure 6.13, for a 1 in 100 year in figure 6.14. The grid points in cross shore direction in these graphs correspond to the cross shore distance shown in figure 6.8. An overview of the results is given in table 6.10 and figure 6.12. The graphical results for the 1 in 50 year and 1 in 500 year conditions are presented in appendix F.

The wave height reducing effect of the Nature-based Solutions is more clearly visible in the figures at this location. Because the waves do not break on an abrupt changing bathymetry, as was the case at the San Leon location, the effect of the NbS on the wave height is more clearly distinguishable. Again, marsh vegetation makes the largest difference for all return periods, with a reduction rate between 52% and 75%. The reduction is strongest in small water depth (see table 6.10) but remains significant as the return periods, and thus water depth and wave height, increase. The seagrass meadow reduces the wave height slightly. Its effect decreases with increasing water depth and wave height.

Figure 6.13 clearly shows the effect of an oyster reef; it locally induces a significant reduction in wave height. Whereas the marsh vegetation and the seagrass meadow stretch for hundreds of meters, the length of the oyster reef is only 30 m. If the waves have passed the reef, there are no additional wave reducing mechanisms in action and the wave height increases again. At the first line of houses on shore (output location [1310]), the effect of the oyster reef is almost completely canceled out. Additionally, the effect of oyster reefs varies considerably for a varying water depth. The larger the water column above the reef, the smaller the reduction. The initial reduction, directly behind the reef (aroung grid point [830]) is 44% for the 1 in 10 year situation and 5% for the 1 in 500 year situation.

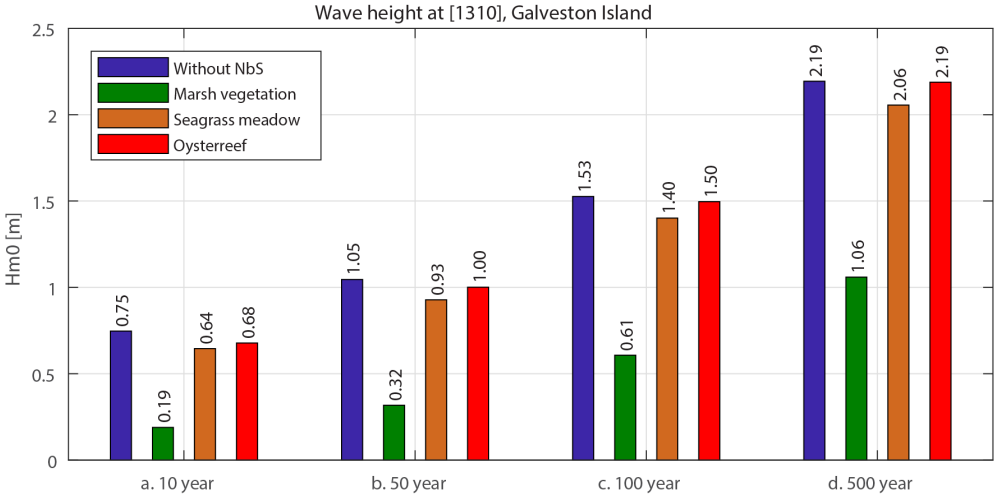

Figure 6.12: Residual significant wave height at output location, gridpoint [1310], for Galveston Island location.

Table 6.10: Residual significant wave height at output location, gridpoint [1310], for Galveston Island location

Return period years	**Without NbS** m	**Marsh vegetation** m	**Seagrass meadow** m	**Oysterreef** m
1-10	0.75	0.19 (-75%)	0.64 (-14%)	0.68 (-9%)
1-50	1.05	0.32 (-70%)	0.93 (-11%)	1.00 (-4%)
1-100	1.53	0.61 (-60%)	1.40 (-8%)	1.50 (-2%)
1-500	2.19	1.06 (-52%)	2.06 (-6%)	2.19 (-0%)

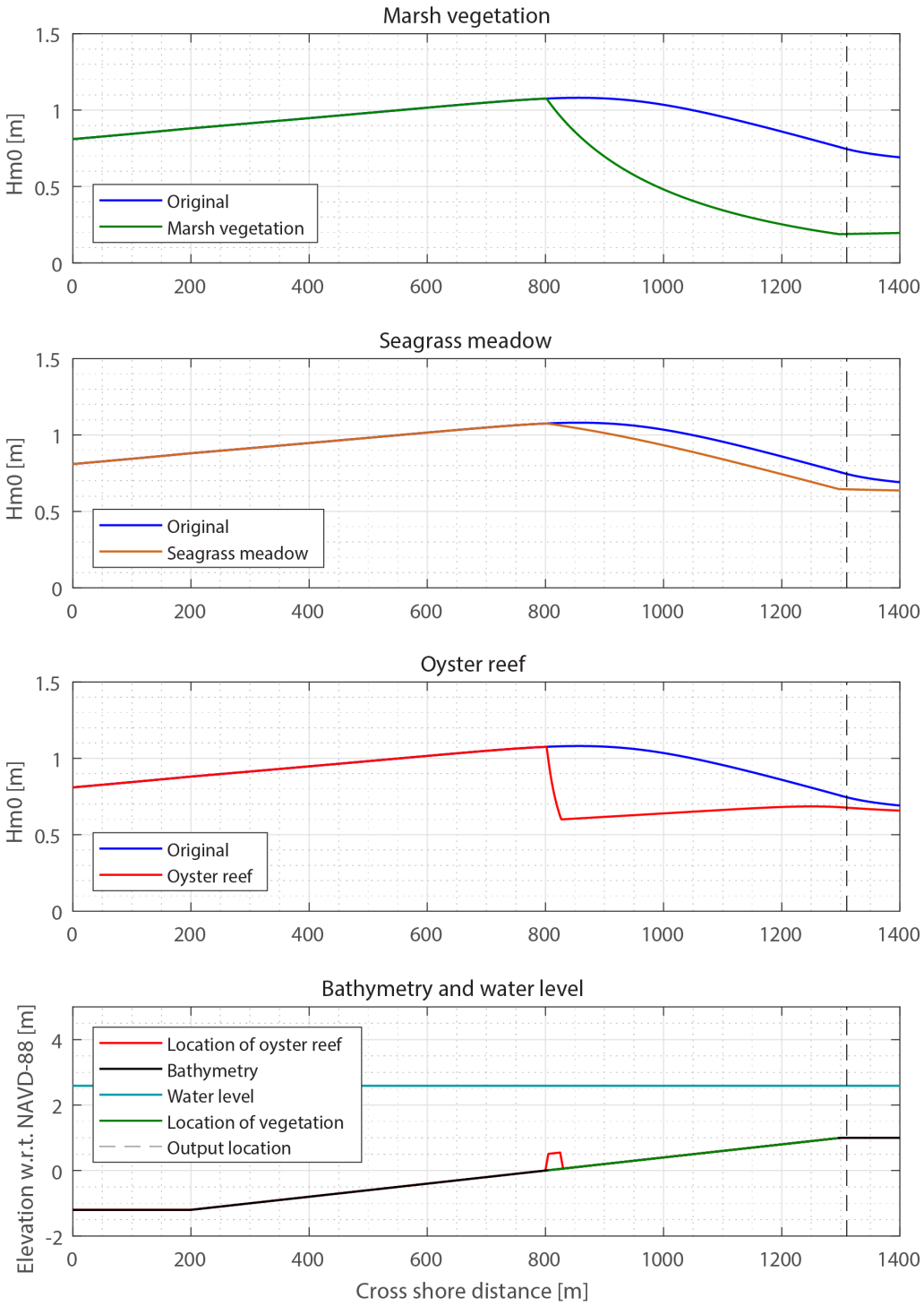

Figure 6.13: Resulting wave heights over the Galveston Island cross section in a 1 in 10 years situation.

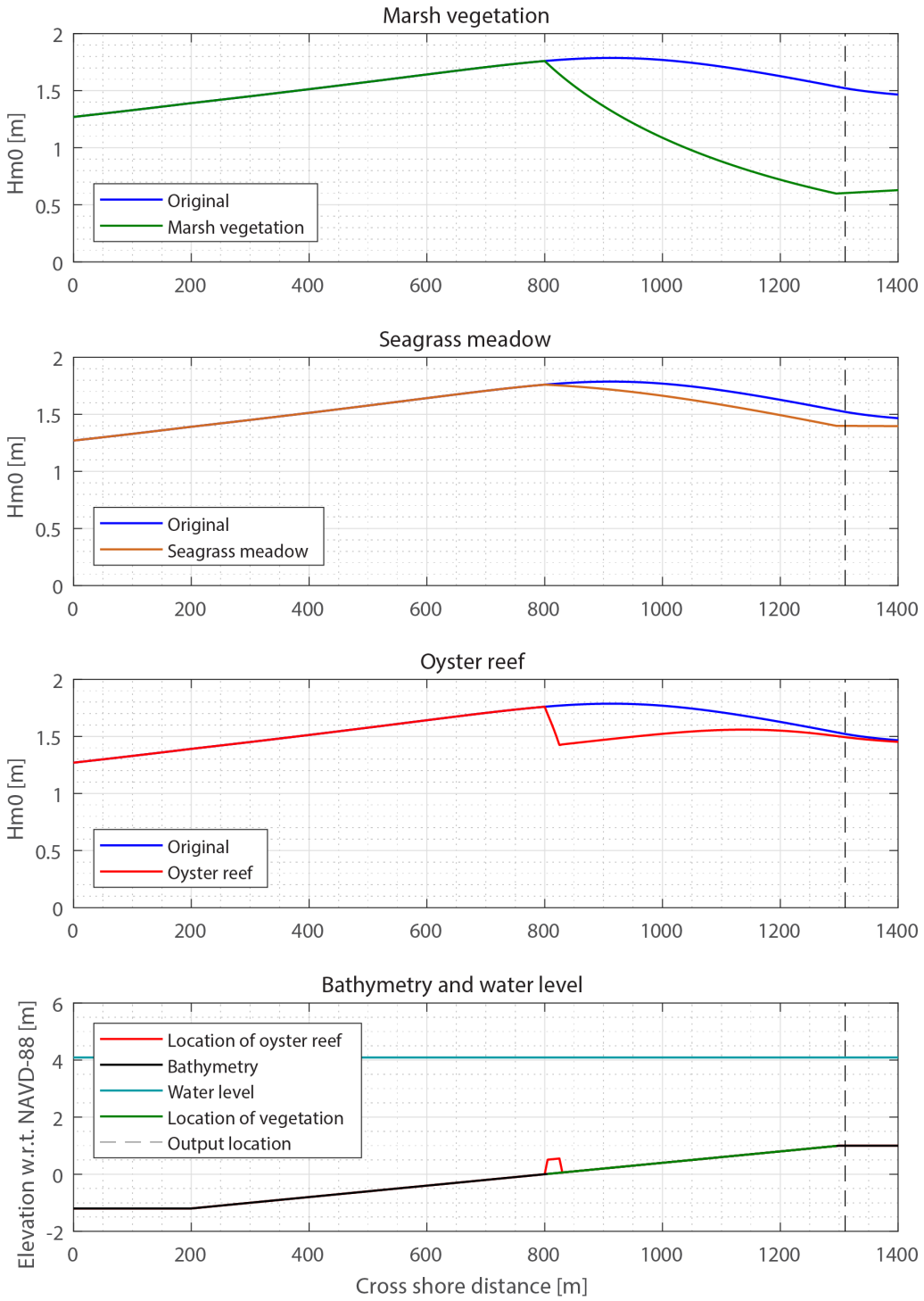

Figure 6.14: Resulting wave heights over the Galveston Island cross section in a 1 in 100 years situation.

6.6. Interpretation of results

The wave height grows over the first part of the cross-section (for Galveston Island until grid point [900], for San Leon until grid point [550] approximately) due to energy input by wind and wave energy bundling by shoaling. Then, in the situation without NbS (the dark blue line in all figures), the wave height cannot grow any further because the maximum wave steepness is reached and waves start to break and dissipate energy.

At San Leon, the waves will break on the bathymetry change either way (the bank at [1100 - 1115]), subsequently the Nature-based Solutions do not have significant effect on the wave height at the first line of houses (i.e. the output location at [1125]). Nevertheless, the measures, especially marsh vegetation, gradually decrease the significant wave height towards the bank. This means that less force is exerted on the bank, in contrast to the breaking waves in the original configuration. Breaking waves can cause erosion and instability of the bank. This suggest that marsh vegetation could contribute to erosion protection at San Leon.

Furthermore, the grid point where maximum reduction due to NbS occurs [1100], does not coincide with the output location [1125]. This suggest that the configuration and location of the Nature-based Solutions is important for the effect on a specific location. Their configuration with respect to the location where the maximum results is desired could be further optimized.

The wave reduction caused by marsh vegetation is larger at Galveston Island than at San Leon. Apart from the different bathymetry, this is probably a result of the increased length of the vegetation field. The length of the vegetation field for marsh vegetation has increased the reduction percentage significantly. This suggest that generally, the length of the field increases the wave height reduction. Other characteristics such as stem density and vegetation height could have a similar effect.

Even in very large water depth with high waves (i.e. 1 in 500 year conditions), the marsh vegetation is able to reduce the wave height significantly. This can be explained by the fact that vegetation is able to dissipate wave energy if it 'feels' the waves. That means that the H/h ratio is important: for the same water depth, vegetation will have more effect on large waves than on small waves. As long as the marsh vegetation 'feels' the waves, it is effective in dissipating energy, due to its upright, stiff stems and its dense above-ground biomass.

The results further suggest that marsh vegetation has a range of applicability that is, hydraulically spoken, very wide. Its effect outreaches the effect of oyster reefs and seagrass meadows at both locations for all simulated conditions. However, it was assumed that the vegetation withstands the force of the waves and does not break. This might not be an realistic assumption. Large-scale breakage of stems could dwindle the reduction rate, especially for marsh vegetation, and overestimate its effect. To assess the reliability of the assumption, the effect is further investigated in section 7.3.

If the oyster reef is at a large distance of the output location, its attenuating effect at the output location is canceled out in comparison to the original wave height propagation (visible in figure 6.14, panel 3). This suggest that an optimal location could be found to maximize its effect. The results further suggest that oyster reefs are, more than the other two measures, sensitive to the water depth. This may be caused by the fact that its main reducing mechanisms in this model is increased bottom friction, which is more sensitive to the H/h ratio than vegetation-induced drag.

A seagrass meadow seems to have little effect on wave height under storm conditions. The elongated vegetation field, that was also applied for seagrass, at the Galveston Island location has not increased the percentage wave height reduction in comparison to the San Leon location, while this is indeed the case for marsh vegetation. This can be explained by the characteristics of seagrass: it is not as high and dense as marsh vegetation, thus the above ground biomass is smaller and its stems are not as stiff as the stems of marsh vegetation. Both factors influence the energy dissipation rate, so seagrass is less effective in attenuating waves.

7

Limitations and optimization of the configuration of Nature-based Solutions

In the previous chapter the effect of three Nature-based Solutions on wave propagation was investigated. Two locations were simulated for four different return periods, that represent a specific combination of input parameters (h, U_{10}, H_s and T_s). The results showed the potential of their effectiveness but also gave reason for further research on the optimization of the configuration of the NbS and on the limits of effectiveness. In the section on the interpretation of the results (section 6.5) several suggestions were made that call for further investigation. This chapter focuses on four of the suggestions for further research. In section 7.1 the location configuration of an oyster reef will be investigated. Next, in section 7.2 the influence of the length and height of a vegetation field for marsh vegetation will be looked into. Thirdly the influence of stem breakage on the effectiveness of a marsh is assessed in section 7.3. In section 7.4 the biological limits of the applications of Nature-based Solutions are discussed. The results in the previous chapter suggest that the effect of seagrass meadows is small, therefore its application will not be studied in more detail.

7.1. Location of oyster reefs

The results discussed in section 6.5 suggest that an oyster reef has potential for wave attenuation but that its effectiveness is sensitive to its distance from the output location (first line of houses). A reduction in wave height was visible directly behind the reef, but further from the reef the effect was canceled out. This might mean that the oyster reef was located too far from the output location. In order to find a better location, several configurations for the position of the oyster reef relative to output location was tested. These different scenarios were simulated with the numerical model to assess the dependence of the wave height reduction on the location.

A second important notion was the effectiveness of the reef with respect to water depth. Based on the findings, one could argue that an oyster reef is most effective in relative shallow water. Volp et al. (2012) also concluded that the influence of the reef on the waves is linearly related to the water depth and the reef height. Therefore the strongest effect is expected for the 1-10 year situation.

7.1.1. Model set-up

As the Galveston Island location is most suitable to distinguish the effect of Nature-based Solutions, this location will be used in this section. A model run where the location of the oyster reef is varied over the sloping foreshore was done. The dimensions and roughness of the reef were kept constant. The cross section overview is shown in the lowest panel of figure 7.2. The configuration where the reef is at a distance of 500 m from the output location corresponds with the original location of the oyster reef, used in the previous chapter. All other input parameters were kept similar to the original simulations at the Galveston Island location.

Table 7.1: Residual wave height for different locations of an oyster reef, for 1-in-10 year conditions.

Distance between reef and output location	**Wave height at output location [1310]** m
Without reef	0.75 (100%)
700 m	0.73 (-3%)
500 m	0.68 (-9%)
300 m	0.48 (-36%)
100 m	0.27 (-64%)

7.1.2. Results

The graphical results are shown in figure 7.2 for 1 in 10 year conditions and the resulting wave heights at the output location are shown in table 7.1. A shift in location towards the output location increases the effectiveness of the oyster reef in attenuation waves: the reduction percentage for 1 in 10 year conditions increases from 9% to 64%.

The enhancing effect of locating the reef closer to the output location can also be found for more extreme conditions (e.g. higher waves and water levels, corresponding with 50, 100 or 500 year return periods). However, the more extreme the conditions, the less pronounced the effect is. This is shown in figure 7.1, where wave height at the output location is measured against the distance between the reef and output location. The influence of the distance is strongest for the conditions with a return period of 10 year.

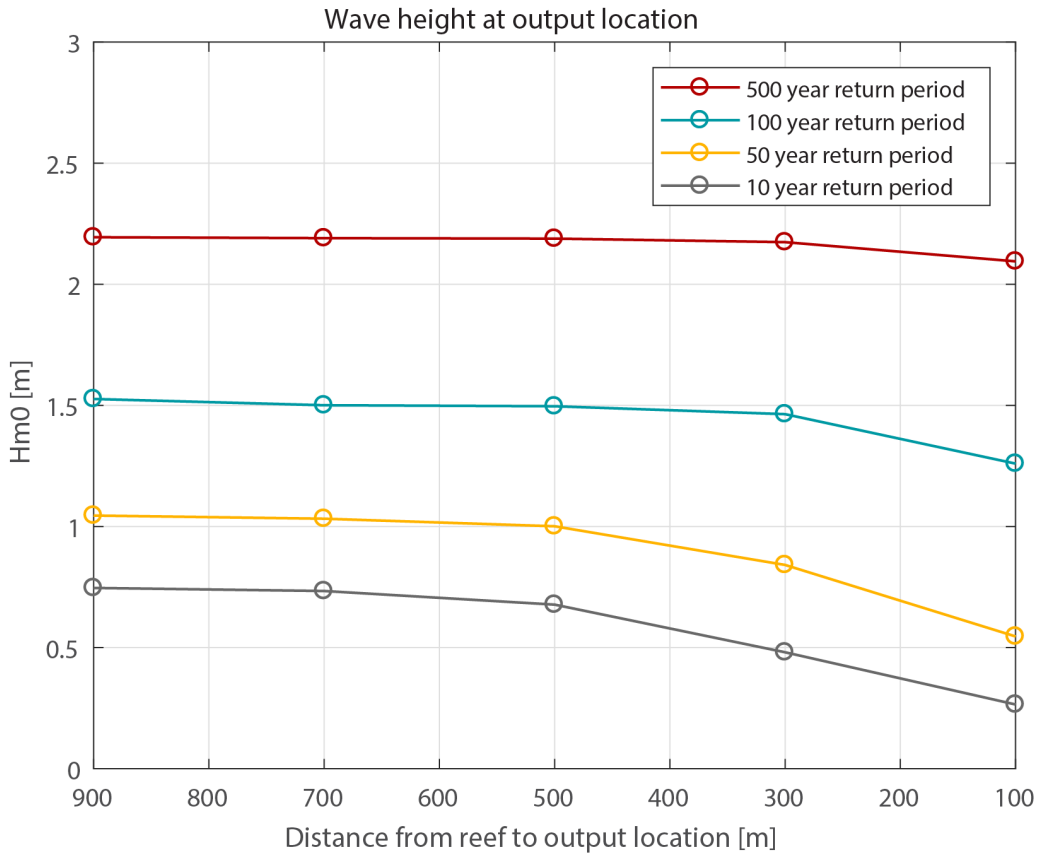

Figure 7.1: Influence of distance between oyster reef and output location on effectiveness of wave height reduction, for four return periods, at the Galveston Island location.

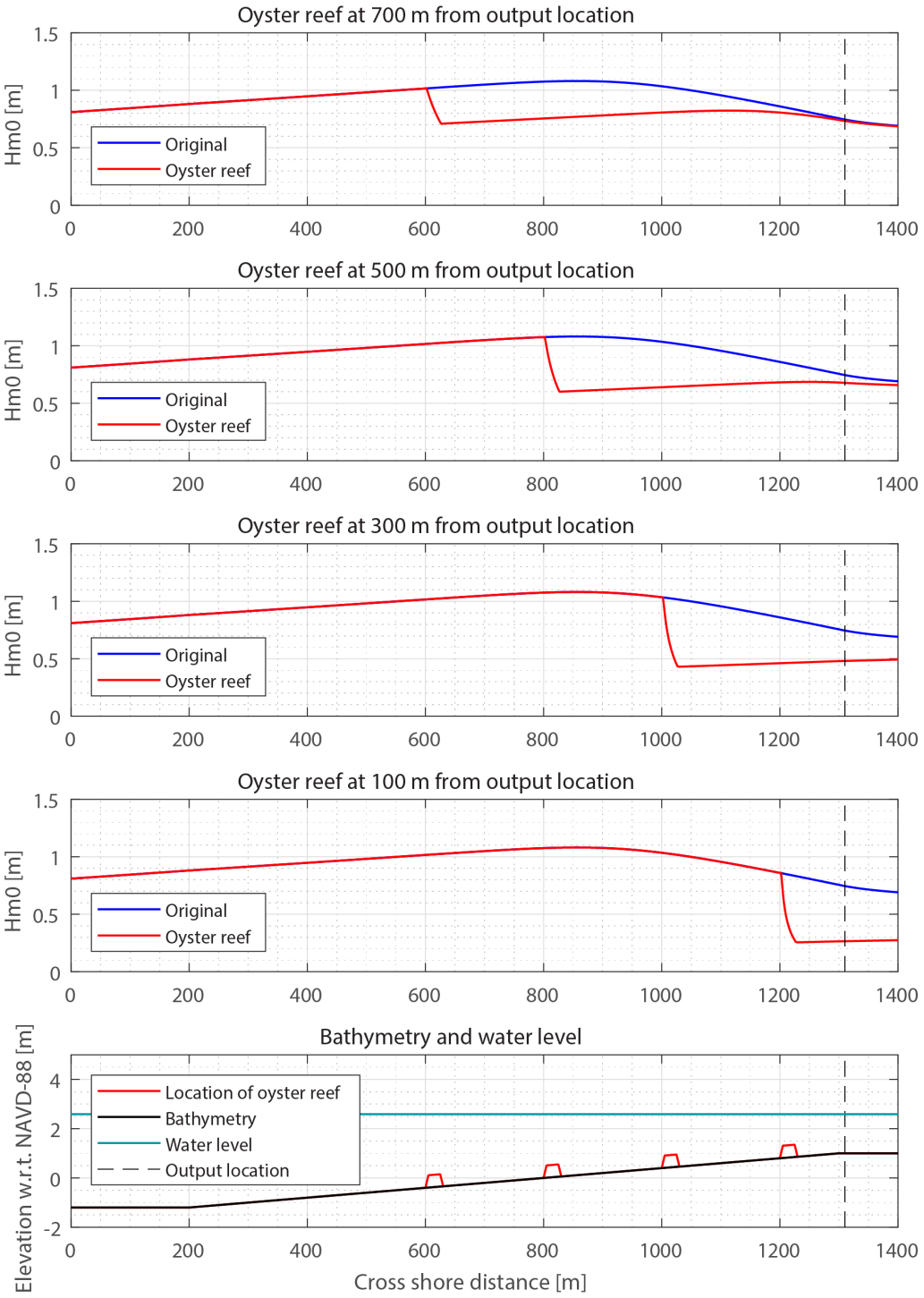

Figure 7.2: Schematized cross section of Galveston location with inclusion of an oyster reef on four different locations, 1-in-10 year conditions.

7.1.3. Conclusion

The reason for the influence of the location of the oyster reef is twofold. Firstly, the difference between the original wave height and the wave height under influence of the reef is maximum just behind the oyster reef. Further from the reef, other hydrodynamic processes such as wind generation cancel out the effect of the reef. Thus if the zone of interest (output location) is located directly behind the reef, the effect of the reef is used to its full extend. Secondly, the oyster reef reduces the wave height more if it is located higher on the slope, because the water is shallower. This is clearly visible in figure 7.2, the initial wave height reducing effect (directly behind the reef) is largest in the most shallow water. That is because higher on the slope, the wave height relative to the water depth is largest. This enhances the effect of depth-induced breaking and bottom friction, since both processes are related to the wave height over water depth ratio. The reversed effect, e.g. a small H/h ratio, might cause the decreasing effectiveness for longer return periods. This is further investigated in appendix C.

A major uncertainty is the growth ceiling of the reef. The toe of the reef on the highest location (third and fourth panel in 7.2) is located at +0.85 m MLLW, the top of the reef at +1.35 MLLW. This implies that the water level should reach to +1.35 on a daily base in order to sustain the reef. This is rarely the case at the location near Galveston Island, hence the reef would not be a realistic measure at that location. Nevertheless, the principles hold and the measure could be useful at other locations, for instance near the toe of dikes and levees or at locations with a larger tidal range.

7.2. Seasonal variation of marsh vegetation

From the results discussed in section 6.5 it follows that marsh vegetation has great potential in reducing wave height. However, in contrast with an oyster reef, the properties of a marsh vary throughout the year. Seasonal variation influences the above ground biomass of marsh vegetation in the Galveston Bay. This might influence its wave height reducing capacity. On average, marsh vegetation (e.g. Spartina Alterniflora) has a higher stem density (N_v) and a larger vegetation height (h_v) in summer. During winter, the above ground biomass is at a low point (Bouma et al., 2014).

7.2.1. Model set-up

The Galveston Island location is selected to assess the effect of seasonal variation since it is most suitable to distinguish the effectiveness of NbS. Two sets of model runs were done, one where the vegetation height varies, another where the stem density varies. Other parameters where kept constant. An overview of the vegetation parameters that were used in the runs are given in table 7.2. The simulations were done for four different return periods, the accompanying hydrodynamic conditions that were used as input for the numerical model were given in table 6.3.

Table 7.2: Marsh vegetation parameters used in the numerical model to asses influence of marsh vegetation height and marsh vegetation density.

Density N_v m^{-2}	**Stem diameter** b_v m	**Vegetation height** h_v m	**Drag coefficient** C_D
491	0.006	0 / 0.2 / 0.4 / 0.6 / 0.8	0.4
0 / 250 / 500 / 750 / 1000	0.006	0.58	0.4

7.2.2. Results

The results show that an increase in vegetation height increases the wave height reduction. As can be seen in figure 7.3 this effect holds for every return period. Figure 7.4 shows that the relative reduction is largest for a large vegetation height and a low wave height. Note that the wave height is coupled to the water depth. For an incoming wave height of 0.81 m (1 in 10 year conditions, with a water level of 2.59 m NAVD-88) and a vegetation height of 0.8 meter, the wave height is reduced to 0.14 m. The reduction in comparison with the situation without a marsh vegetation is 81%. Nevertheless, the reduction for 1 in 500 year conditions with a vegetation height of only 0.2 m is still 0.43 cm, a relative decrease of 20%.

The results of the simulations with varying stem density suggest that a higher density increases the

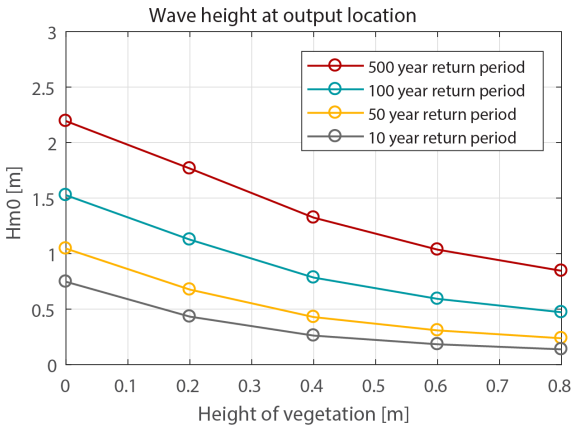

Figure 7.3: Influence of the vegetation height on the effectiveness of wave height reduction, for four return periods, at the Galveston Island location. Output location is at grid point [1310].

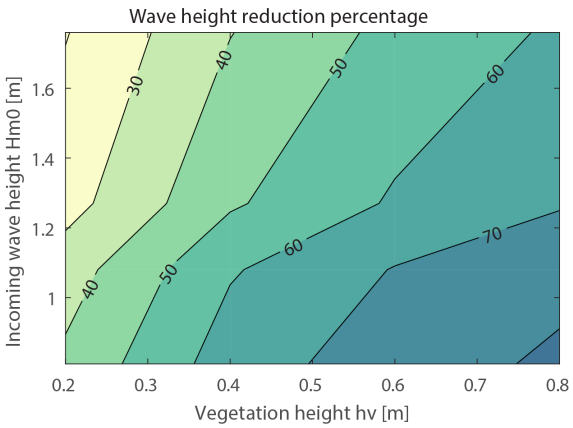

Figure 7.4: Percentage reduction for different vegetation heights in comparison with situation without marsh vegetation. Note that the incoming wave height is linearly related to the water height.

wave height reduction. Figure 7.5 shows a strong increase in wave height reduction for a higher stem density for all four return periods. Figure 7.6 shows that even for 500 year return period conditions (i.e. incoming wave height of 1.76 m and water depth of 5.34 m), the reduction of the marsh vegetation field with a density of 1000 stems per meter, at the output location, in comparison to the situation without marsh vegetation is well over 70%. Furthermore, it follows from figure 7.5 that the influence of a higher density on the wave height reduction decreases slowly with increasing density. For the conditions with a return period of 10 year, the difference in wave height reduction between a density of 500 stems per meter and 1000 stems per meter is only 0.10 m, while the difference between 0 and 500 stems is 0.56 m.

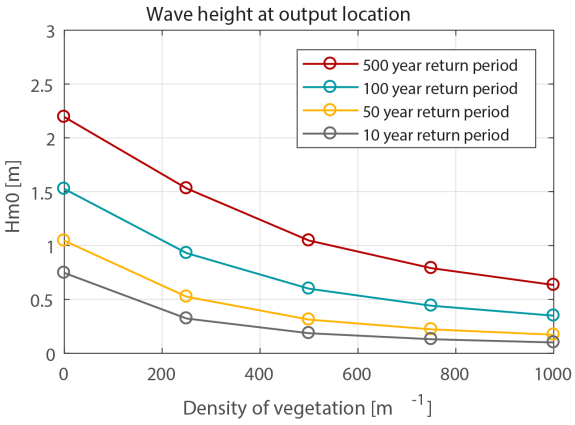

Figure 7.5: Influence of the stem density on the effectiveness of wave height reduction, for four return periods, at the Galveston Island location. Output location is at grid point [1310].

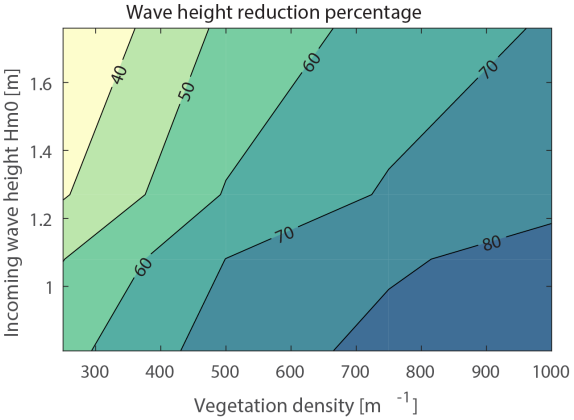

Figure 7.6: Percentage reduction for different stem densities in comparison with situation without marsh vegetation. Note that the incoming wave height is linearly related to the water height.

7.2.3. Conclusion

The results indicate that there is indeed a strong correlation between the above ground biomass, which is represented by the stem density and the vegetation height, and the wave height reduction rate of marsh vegetation. This is important for wave reduction during storm conditions in the Galveston Bay. Texas has a distinct hurricane season (i.e. June to November), in which the highest wave height and water levels are expected. If this period coincides with the summer state of the vegetation, a higher protection level due to marsh vegetation is expected. However, the results show that the reduction effect is significant even for very short or sparse vegetation in combination with extremely high water

levels and wave heights.

The effect of a higher stem density is most distinct for the first 500 stems per meter. This suggests that implementation of a marsh with a larger area and a sparser density is preferred above a small area with very high stem density. This could prove a valuable design consideration when planning a marsh restoration project.

7.3. Stem breakage of marsh vegetation

A large wave force acting on a vegetation field can cause stem breakage. This can be caused by storms and results in a vegetation field with strongly reduced capacities for wave attenuation. Because this effect is of particular relevance during extreme conditions, it makes sense to investigate the occurrence and potential severity of stem breakage in case of extreme conditions in the Galveston Bay.

Vuik et al. (2017) researched stem breakage of Spartina anglica (common cord-grass) and Scirpus maritimus (sea club-rush), both marsh vegetation species. They compared the maximum flexural stem strength with occurring wave forces and included the findings in a numerical model that simulates wave attenuation by vegetation. Observations of stem breakage in a vegetation field in the Western Scheldt in the Netherlands were used to calibrate and validate the stem breakage model.

When using this method, the maximum flexural strength of the stems is expressed in terms of a critical orbital wave velocity. This represents the maximum orbital velocity that can act on a stem before it breaks. If this value is compared to the occurring orbital velocity in a vegetation field, it can be predicted if the stem will break or not. Larger wave heights result in larger occurring orbital velocities. It is given as:

$$u_{crit} = \sqrt{\frac{\sigma_{max}\pi(b_v^4 - b_{v,in}^4)}{8A_c\rho C_D b_v^2(\alpha h)^2\cos^2\theta}} \tag{7.1}$$

with critical orbital velocity u_{crit} [m/s], maximum bending stress σ_{max} [N/m^2], stem diameter b_v [m], inner stem diameter $b_{v,in}$ [m], correction factor A_c [-], water density ρ [kg/m^3], bulk drag coefficient C_D [-], relative vegetation height α [-], water depth h [m] and maximum leaning angle of the species θ [deg].

The occurring orbital velocity can be described with:

$$u_z = \frac{\omega H}{2}\frac{\cosh(k(z+h))}{\sinh(kh)} \tag{7.2}$$

with actual orbital velocity at height z in the vegetation u_z [m/s], angular wave frequency ω [rad/s], normative wave height H [m], wave number k [m^{-1}], distance from the water surface z [m] and water depth h [m].

A few important notes on this method are:

- The normative wave height that is used for stem breakage is $H_{1/10}$ (≈1.27 H_s) because it is assumed that this wave height causes stem breakage.
- The reference level where the orbital velocities are compared is at half the vegetation height.
- The critical orbital velocity is very sensitive to the maximum leaning angle. Most types of vegetation first bend before they breaks (see figure 7.7). However, little research is available on the normative bending angle of stems of different species.
- The bulk drag coefficient C_D in expression 7.1 does not account for the bending of the vegetation, because this is accounted for separately. Therefore, the value of C_D wil be closer to 1.

For a more detailed description of the stem breakage model, the origin of the expressions and the involved parameters, please refer to Vuik et al. (2017).

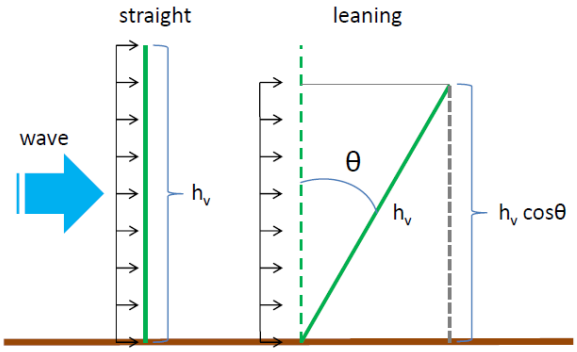

Figure 7.7: Schematic overview of stem bending. Left a straight stem with height h_v and right a stem that bends under influence of the wave load over leaning angle θ, which reduced the experienced horizontal wave load. Source: Vuik et al. (2017)

Table 7.3: Input parameters for stem breakage calculations.

Parameter	Quantity	Value	Unit	Note
σ_{max}	Maximum bending stress	12.5	[MN/m^2]	Vuik et al. (2017)
b_v	Stem diameter	0.006	[m]	
$b_{v,in}$	Inner stem diameter	0.003	[m]	Estimation
A_f	Correction factor	1.7	[-]	Vuik et al. (2017)
ρ	Water density	1025	[kg/m^3]	Salt/ brackish water
C_D	Bulk drag coefficient	1.0	[-]	Does not include bending
θ	Maximum leaning angle	51±15	[deg]	Bouma et al. (2005)
h_v	Vegetation height	0.58 and 0.40	[m]	

7.3.1. Model set-up

The test case for Galveston Island was used to investigate the potential stem breakage under extreme conditions. The occurring orbital wave velocities were derived for the four considered return periods at three locations in the vegetation field, halfway through the vegetation height. The considered species is Spartina Alterniflora. The hypothetical characteristics of the marsh vegetation that were used in the original simulations (section 6.4) were also used in this analysis. However, a species-specific maximum bending angle and maximum bending stress had to be determined.

The critical orbital wave velocity is highly sensitive to the maximum bending angle of the stem (Vuik et al., 2017). The value of 51 degrees is based upon Bouma et al. (2005), who derived it for Spartina Angelica in a flume experiment. Because it is uncertain if this value is accurate for S. alterniflora in highly energetic conditions in the Galveston Bay, and the critical orbital velocity is highly sensitivity for this parameter, the angle was varied with 15 degrees in the calculations.

The bulk drag parameter C_D, correction factor A_f and maximum bending stress σ_{max} were derived from Vuik et al. (2017). These values were originally determined for Spartina Angelica for the wave climate of the Western Scheldt.

Table 7.4: Input parameters for stem breakage calculations that depend on the return period. Given values hold for the beginning of the vegetation field (gridpoint [800]), with a vegetation height of 0.58 m.

Parameter	Quantity	10 years	50 years	100 years	500 years
h	Water depth [m]	2.59	3.17	4.09	5.34
$H_{1/10}$	Mean of 1/10 highest waves [m]	1.37	1.83	2.24	3.12
z	Distance from water surface [m]	-2.30	-2.88	-3.80	-5.05
k	Wave number [m^{-1}]	0.397	0.318	0.264	0.201
ω	Angular wave frequency [rad/s]	2.00	1.77	1.67	1.45

7.3.2. Results

The results of the comparison between the critical and actual orbital wave velocity are shown in figure 7.8. The upper panel shows the results for a vegetation height of 0.58 m and the orbital velocities are compared at a height of 0.29 m. For every return period, the occurring orbital velocity exceeds the critical velocity for a critical bending angle of 51 and 36 degrees. Indeed, for the 500 year conditions, the occurring velocity exceeds the critical threshold throughout the vegetation field. This suggest that the stems of S. Alterniflora will break during 500 year conditions near Galveston Island. If the maximum bending angle is 66 degrees, the critical velocity is substantially higher, because the vegetation will bend further before it breaks.

The lower panel shows the results for a vegetation height of 0.4 m. The critical velocities are higher because the total horizontal wave force is lower on lower vegetation. Indeed, less stem breakage is expected during all four return periods. However, with an maximum bending angle of 51 degrees, the expected stem breakage is still significant, especially for the 500 year conditions.

An important effect that is not visible in figure 7.8, is that the stem breakage and the wave attenuation rate are interdependent. The occurring orbital wave velocity is decreasing throughout the vegetation field because the vegetation dissipates wave energy. If, however, the vegetation breaks due to the high velocity, the dissipation rates will be (much) lower, and the orbital velocity will remain high. For instance, in the upper panel of 7.8 for the 100 year conditions (blue line), the occurring orbital velocity drops below the critical threshold around 280 m from the edge of the vegetation field. But that is under the assumptions that over the first 280 meter, the vegetation does not break and will dissipate wave energy, while the vegetation over that distance will most likely break and thus dissipate far less energy. The result is that for the 100 year conditions with a vegetation height of 0.58 m, the stems will probably continue to break towards the end of the vegetation field. Broken vegetation still dissipates some wave energy: the residual vegetation height for broken S. Alterniflora is approximately 0.1 m. This iterative effect could be capture well in a numerical model, as proposed by Vuik et al. (2017).

In the case for h_v = 0.40 m (lower panel in figure 7.8) the expected stem breakage is lower than h_v = 0.58 m, but the wave energy reduction capacity of the marsh is subsequently also lower. This suggest that there is an optimum for the vegetation height for which stem breakage is mostly avoided, but the wave energy reduction is maximized.

An second option to reduce stem breakage is to combine the marsh vegetation with an oyster reef. An oyster reef is not damaged by large waves and can, situated in front of the the marsh, reduce the peak wave heights. The transmitted wave height could be further reduced by the marsh vegetation. Even though the reduction rate of the oyster reef is small, it could make the difference for stem breakage in the marsh vegetation.

7.3.3. Conclusion

Because of the interdependence of wave height reduction and stem breakage, a numerical calculation would give a more accurate prediction of the stem breakage. Vuik et al. (2017) includes the stem breakage model in a numerical model that calculates the wave energy development at every gridpoint in a cross section, this should be done for the Galveston Bay as well. Furthermore, an experiment to derive input parameters for S. Alterniflora should be done to include more accurate values in the calculations. Nevertheless, several conclusion can be drawn from this preliminary assessment:

- Stem breakage is a significant process when assessing wave height reduction due to marsh vegetation. An orbital wave velocity associated with storm conditions can cause stem breakage which will reduce the marsh vegetation height and thus reduce its capacity for wave attenuation.
- For the case of the Galveston Bay with the currently applied marsh configuration, stem breakage will probably occur during hydrodynamic conditions with a return period of 100 years or longer. Particular for 500 year conditions and with a vegetation height of 0.58, stem breakage will likely occur over the total length of the vegetation field.
- The properties of the marsh vegetation can be optimized in order to reduce the expected stem breakage rate. The results suggest that an optimum for the vegetation height can be found that minimizes the stem breakage rate and maximizes wave energy dissipation. Another option to avoid stem breakage is to situate an oyster reef in front of the marsh to reduce the peak wave heights.

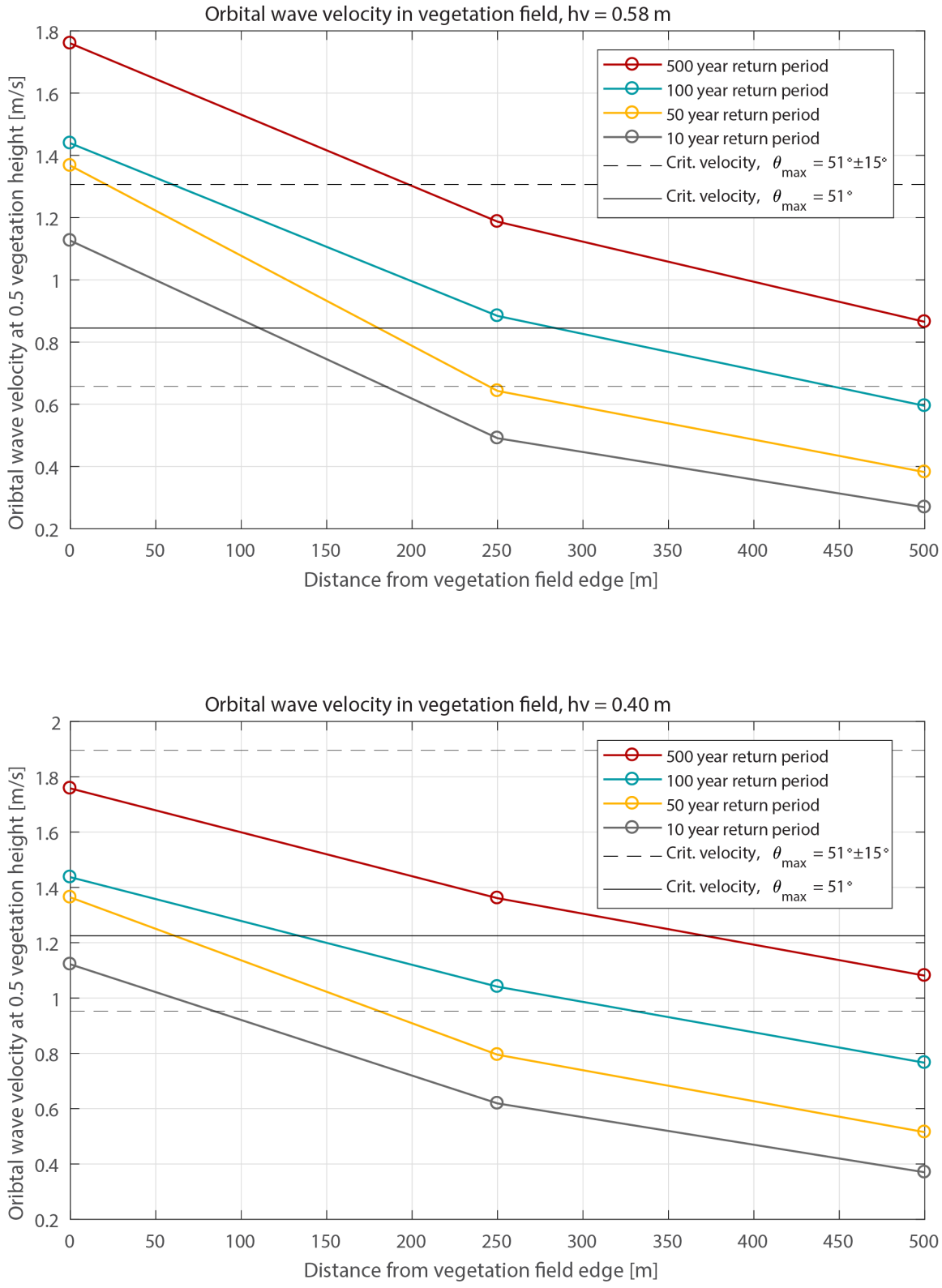

Figure 7.8: Comparison between the ciritical and acutal orbital wave velocity, which is a measure for stem breakage, in the hypothetical vegetation field at Galveston Island for four return periods and three maximum bending angles. The upper panel shows the comparison for a vegetation height of 0.58 m. The lower panel shows the comparison for a vegetation height of 0.4.

- In order to gain more insight in the extend of the stem breakage in the Galveston Bay, a numerical wave propagation model with inclusion of the stem breakage model should be used.

7.4. Biological limitations for Nature-based Solutions

The focus of the simulations in chapter 6 was on possibility of wave height reduction from a hydrodynamic point of view. However, assessment of the biological feasibility of the Nature-based Solutions was limited to the mere basics. Therefore, in this section the biological requirements for growth are discussed, in order to gain insight in the limits of application of marsh vegetation, seagrass meadows and oyster reefs in the Galveston Bay. The focus is mostly on how the optimal location of the NbS depend on the the tidal range and the water depth.

In the simulations in this research, the distribution of Nature-based Solutions for the San Leon location was on a flat foreshore with a bed around MLLW. For the Galveston Island location the distribution was on a sloping foreshore from MLLW to +1 m MLLW (over a distance of 500 meter). The cross-sections are shown in figure 7.9. The tidal range is approximately 0.4 m in the Galveston Bay. The continuous presence of wind set-up can play a role as well. For instance, at some locations in the Galveston Bay, the water level measurements from NOAA (2017) show that the water level is over 50% of the time more than a feet (0.3 m) above the predicted tidal level.

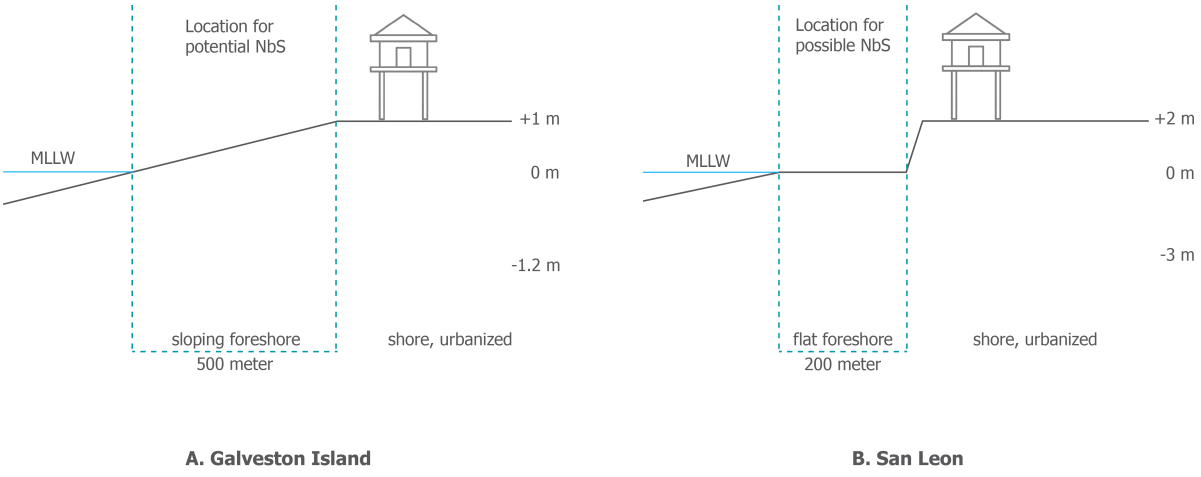

Figure 7.9: Schematic cross-section of the two test locations, Galveston Island (A) and San Leon (B).

7.4.1. Marsh vegetation

The tidal inundation is considered the primary factor of influence for the growth range of smooth cord grass (S. alterniflora). McKee and Patrick (1988) showed that the Mean Tidal Range has a strong positive correlation with the growth range of S. alterniflora. They investigated marshes along the Gulf Coast and Atlantic Coast and found that in most cases the species grows between Mean Low Water and Mean High Water with the emphasis on the higher intertidal zone.

The distribution of marsh vegetation is stressed by submergence, which means that on the long term sea-level rise can threaten a salt marsh and cause it to slowly move land-inwards. Nevertheless, at several location it has been observed that the rate of sediment accumulation by marshes can keep up with level of the sea-level rise (Bouma et al., 2014). Apart from the tidal range, several biotic and abiotic factors have found to be of influence on the distribution of marsh vegetation. This includes the salinity, temperature, nutrient levels and competition of other species (McKee & Patrick, 1988).

For the San Leon location, the hypothetical marsh on the flat foreshore is biologically feasible. At the Galveston Island location, the upper part of the slope (highest 0.3 meter) might have a submergence rate that is too low to sustain S. alterniflora.

7.4.2. Seagrass meadows

The distribution of seagrasses is stressed by emergence. Nonetheless, the species needs sunlight for photosynthesis, so it does not occur in deep water. More than for marsh vegetation and oyster

reefs, water clarity is important for seagrass, because the canopy is totally submerged and light needs to reach the leaves for photosynthesis. The maximum depth limit for growth is determined by the amount of light that penetrates the water column (Bradley & Houser, 2009).

Seagrass is known to be able to survive in shallow tidal pools or on a dry bed during ebb tide for several hours (Pedersen et al., 2016). Nevertheless, it is not clear to what extend this applies to T. testudinum (turtle grass). The strength of the solar radiation is an important factor to determine the maximum emergence period.

For the San Leon location, the hypothetical seagrass meadow on the flat foreshore is biologically feasible. At the Galveston Island location, the upper part of the slope (highest 0.3 m) is suspected to have a daily submergence rate that is too low to sustain a seagrass meadow.

7.4.3. Oyster reefs

The tidal range and salinity rate are the foremost limiting factors for the distribution of oysters. The limiting factor for growth seems to be influenced by the high water level of the tidal range. Ridge et al. (2015) found that the parts of an oyster reef that are 20 to 40% of the time emerged have the highest growth rate. They furthermore discovered a growth ceiling at 55% of the tidal range. Other sources mention a higher growth ceiling, as long as an oyster is at some point emerged and at some point submerged during the day.

In contrast to vegetation, oysters are hardly affected by seasonality. While vegetation suffers from stem breakage, oysters endure little damage during hydrodynamic storm conditions. Overall, it is a stable natural measure, although shellfish diseases are known to have decimated oyster colonies (e.g. Davis and Barber (1999)).

Taking into account the growth ceiling, the oyster reef is biologically feasible for the San Leon location. For the Galveston Island location, an oyster reef with a height of 0.5 meter is not feasible on the upper half of the slope.

7.4.4. Conclusion

The tidal range is important for the distribution pattern of the selected Nature-based Solutions. Oyster reefs and seagrass meadows are stressed by emergence, whereas marsh vegetation is mostly stressed by submergence. Marsh vegetation grows in the middle and upper tidal zone. Seagrass meadows thrive in shallow water and constant submergence, although most species can survive emergence for several hours. The growth range of oyster reefs is primarily determined by the tidal range, because the growth of oysters benefits from daily alternation of submergence and emergence. The distribution range of all three species increases with a larger tidal range. This means that the application in the Galveston Bay, which has a micro-tidal character, is limited to a relative small vertical zone. However, the Galveston Bay is located in a flat, coastal plain, which increases the potential spatial distribution of the Nature-based Solutions horizontally (this effect is illustrated in figure 7.10).

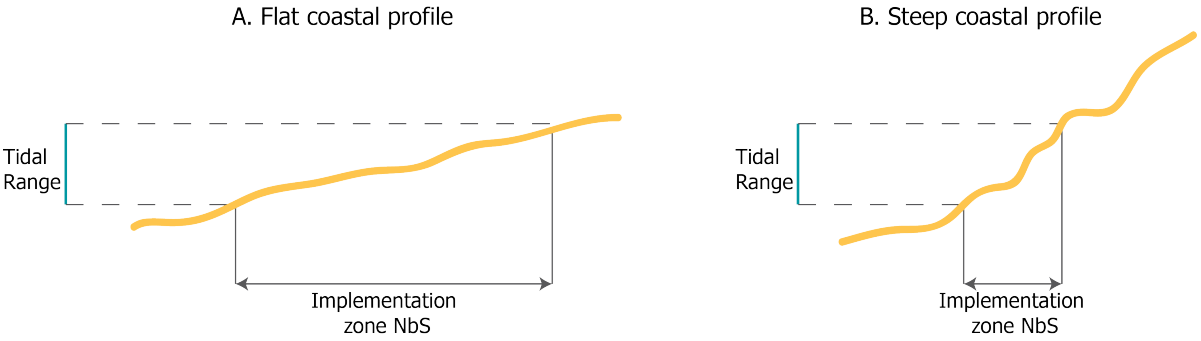

Figure 7.10: The area of influence of an oyster reef in term of water depth and wave height.

8

Applications in the Galveston Bay

This chapter aims to provide a more practical insight into the effect of Nature-based Solutions. The objective is to show with three examples how NbS can contribute to flood risk reduction in the Galveston Bay. Note that it is not the goal to provide a fully optimized design, but merely to show promising applications of Nature-based Solutions. In section 8.1, the influence of marsh vegetation on the Base Floor Elevation of houses at the northern shore of Galveston Island is discussed. In section 8.2 the influence of marsh vegetation on expected overtopping of the Texas City Hurricane Flood Protection will be analyzed. In section 8.3, it is explained how the effect of marsh vegetation can be included in a risk reduction optimization strategy.

8.1. Influence on the Base Floor Elevation at Galveston Island

The south west part of Galveston Island is one of the most flood prone areas in the Houston-Galveston Bay Region. This is visualized on the map of FEMA in figure 8.1. The cross section that is addresses in this section is located along the red line AA' in figure 8.1. Figure 8.2 summarizes the different hazard zones. The location of the case study at Galveston Island is situated in a **VE** zone. As explained in section 5.4, this means there is inundation risk with a return period of 100 years or less with additional risk due to storm waves. FEMA analyzed the location in detail and a Base Floor Elevation (BFE) of 19 feet (5.79 m) NAVD-88 was established. The BFE is the minimum level at which the floor of a house should be constructed, although the use of extra freeboard is strongly advised by FEMA.

The value of 5.79 m is the sum of the 100 year return period still water level and a value to account for waves (70% of 0.78 times the water depth). This value is compared to the calculations in this study (section 6.5). The expected water level and significant wave height with a return period of 100 year at the output location at Galveston Island without Nature-based Solutions are 4.09 m and 1.53 m. Although it is not custom in the Netherlands to add up still water level and a significant wave height, it can be concluded that the values of this study and the study by FEMA are in the same range. This suggests that the results from this study can be used to evaluate the flood zone map of Galveston Island from FEMA with a reasonable margin of accuracy.

The results for 1 in 100 year conditions from section 6.5 were used to asses the effect of marsh vegetation on the BFE at the northern shore of Galveston Island. From the results in table 6.10 it followed that for 1 in 100 year conditions, the wave height at the Galveston Island location could be reduced with 0.92 m (3 feet) if marsh vegetation was implemented in front of the shore line. The residual significant wave height at the shoreline is 0.61 (2 feet).

The wave height development is shown in the upper panel of figure 8.3, which is similar to the results that were presented in section 6.5. Additionally, the area behind the shore line is included in the graph. This shows that the wave height that was influenced by marsh vegetation remains significantly lower than the original wave height further land inward. Nevertheless, an increase in wave height is visible between [1300] and [3500]. It is unclear over what distance the effect of the marsh vegetation on wave height remains distinguishable once on shore, because the profile is interrupted with vegetation, houses and other structures. The second panel shows the absolute reduction of wave height as a result of marsh vegetation over the cross shore distance in feet. This is the input for the reduced and discrete

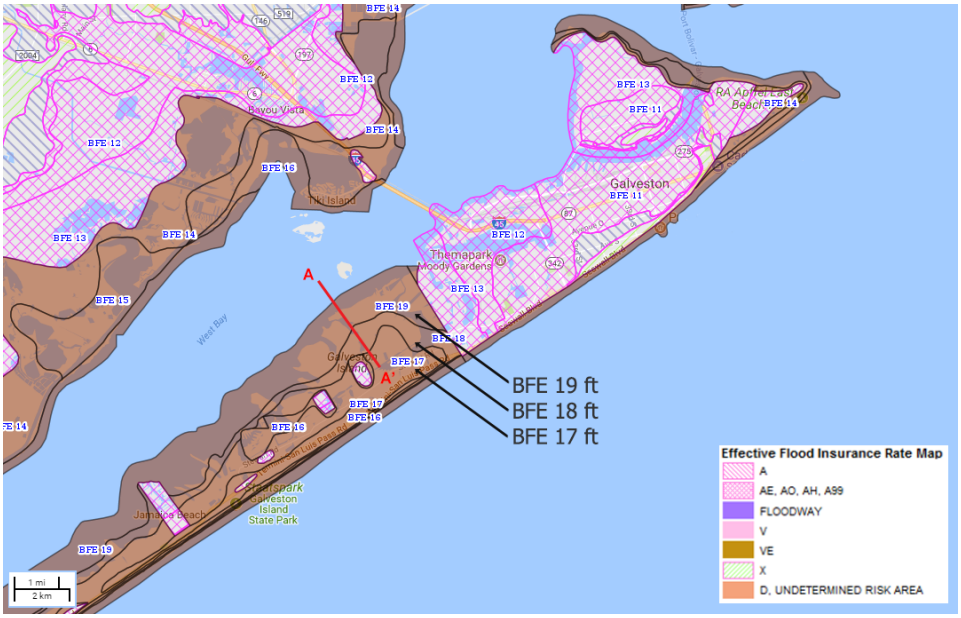

Figure 8.1: Effective flood hazard areas on Galveston Island, designated by FEMA. Pink areas are flood plains with a return period of 100 years or less. Brown areas are flood plains with additional risk due to storm waves. The cross-section AA' represent the location of the test case. The Base Floor Elevation levels are provided in the map. Adapted from (FEMA, 2017)

Base Floor Elevation zones in the third panel. The wave height reduction is transformed in discrete steps of one feet, and is subtracted from the original Base Floor Elevation.

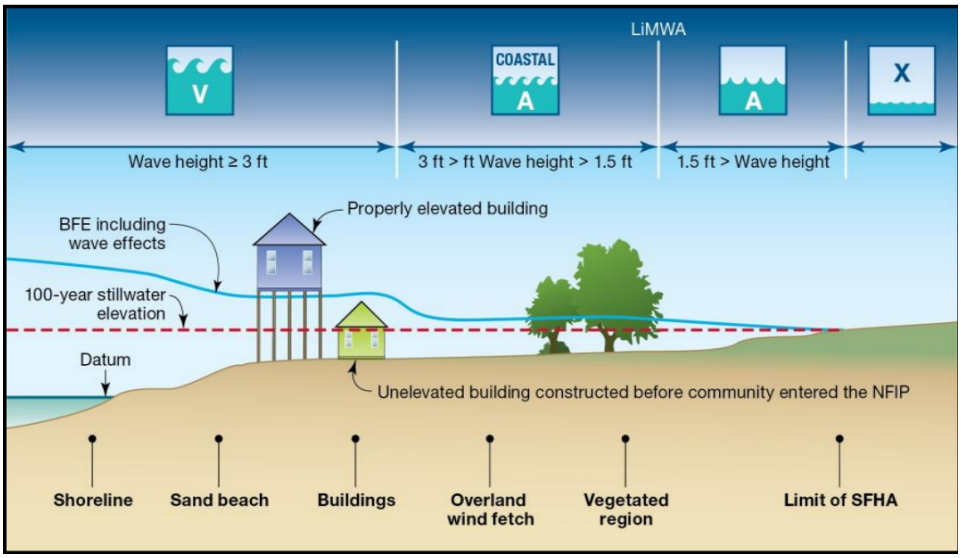

Figure 8.2: Flood hazard zones with inclusion of wave height, determined by FEMA. Soucre: (FEMA, 2017)

The results suggest that in an idealized case the influence of the marsh vegetation is significant up to 3 km land inward. Note that stem breakage is not included in this analysis, this might reduce the effect. Nevertheless it is clear that the marsh vegetation can lower the BFE based on the 100 year flood plains as determined by FEMA. The case study location at Galveston Island would no longer be in a **VE** zone that is prone to storm surge waves, because the expected wave height under influence of the marsh vegetation is lower than 3 feet. This can subsequently lead to lower flood insurance rates of the residents of the area. Additionally, marsh vegetation could decreases the expected damages in the area in case of a flooding. The percentage of elevated houses that gets hit by waves during a flood event will be lower since the expected wave height is lower.

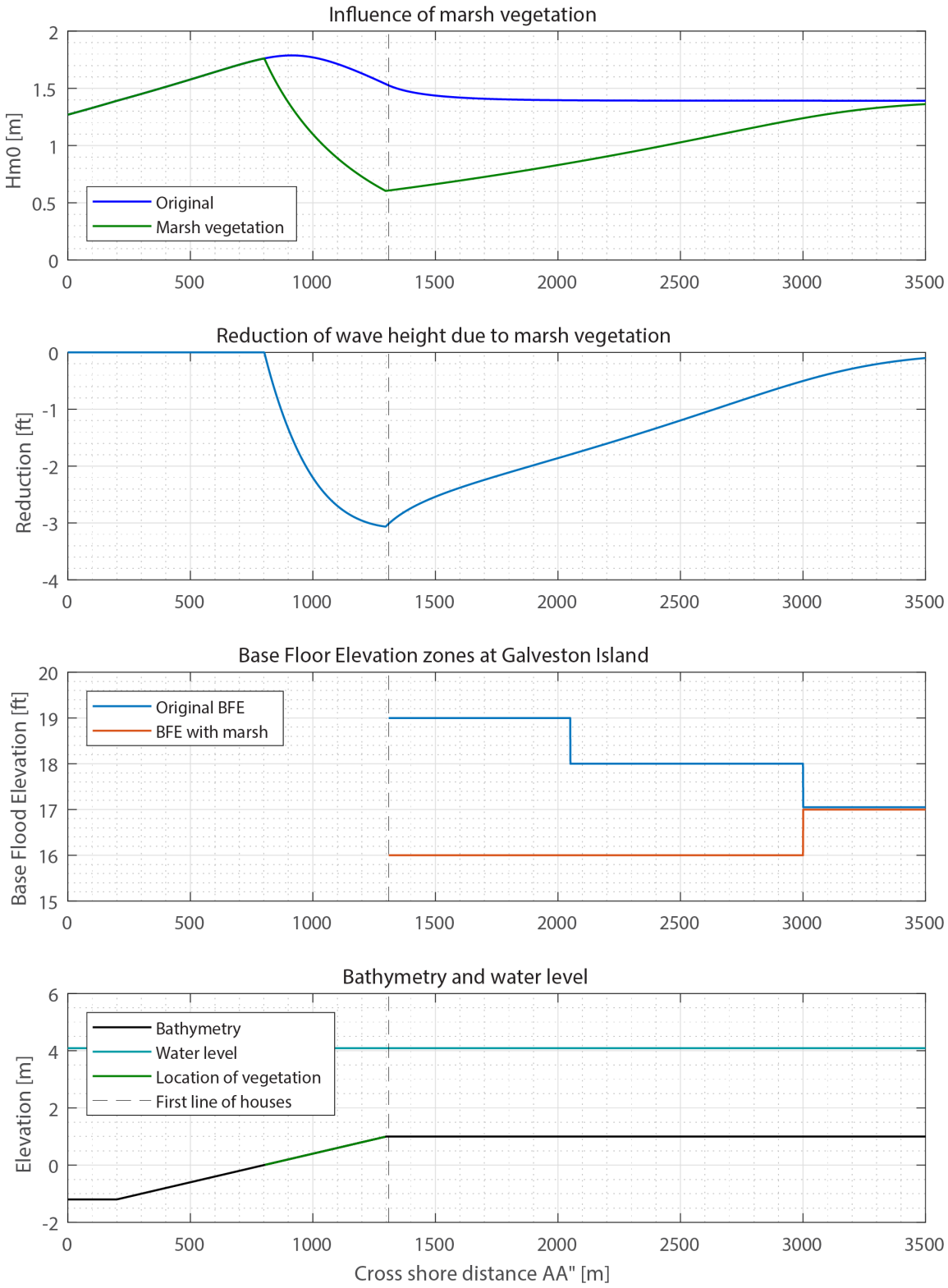

Figure 8.3: The upper panel shows the influence of marsh vegetation on the development of the significant wave height. The plot is similar to upper panel in figure 6.14, but the distance in x-direction has been elongated land inwards. The second panel shows the absolute difference in feet(!) between the original Hm0 and the Hm0 under influence of marsh vegetation. The third panel shows the original Base Floor Elevation in feet (!) along cross-section AA' (as shown in figure 8.2) and the potential Base Floor Elevation as a result of marsh vegetation. The lower panel shows the bathymetry of the cross section.

8.2. Overtopping of the Texas City Hurricane Flood Protection

In this section the effect of implementation of marsh vegetation is investigated to increase the reliability of the Texas City Hurricane Flood Protection (TCHFP). To this end, the effect of marsh vegetation on the expected overtopping rate was calculated.

Two structural flood prevention measures are present in the Galveston Bay region: the Texas City Hurricane Flood Protection and the Galveston Seawall. Their locations are shown in figure 8.4. The flood protection system at Texas City was designed to protect the greater Texas City area from 4.5 meter (15 ft) storm surge with accompanying waves. The system comprises concrete walls, earthen levees, closure structures and a precipitation drainage system for the hinterland. The crest measures 7.0 meter (23 feet) above m.s.l. at its highest point and the total length of the system is approximately 28 kilometer (17.5 miles). The northern section that faces the Bay is evaluated. A characteristic cross section of this part of the system is shown in figure 8.6, the top view at that location is shown in figure 8.5.

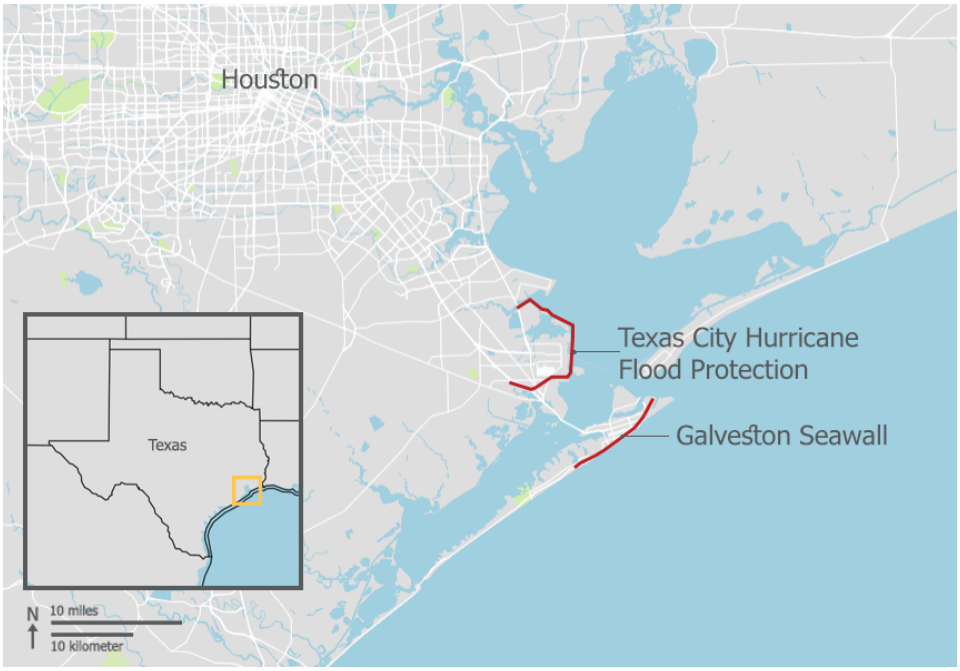

Figure 8.4: Location of structural flood protection systems in the Galveston Bay.

During Hurricane Ike in 2008, the water level came within 0.6 meter (2 ft) of the crest. This underlines the necessity of the levee system, that protects approximately 45.000 inhabitants, 4 million dollars in local property and commerce and over 20 billion dollars worth in petrochemical industry. Regular maintenance works are conducted on the system. This is mostly repairs due to erosion of the dike. Damage on the dike is caused by storm events. In 2009 repairs were made, and a new tender was issued in 2017 (Evans, 2008).

8.2.1. Determining the 1 in 100 year water level

The complete system was finalized in 1987, although large sections were completed in the 1960's. It is designed to withstand a 1-in-100 year water level, with inclusion of waves. The height of the crest was determined by adding a characteristic storm surge level, a height to account for run-up and overtopping (which is primarily based on wave height) and additional freeboard. The original design report is not available, but an environmental assessment of the project (USACE, 1979) and a review on the design (Murphy & Geelan, 1965) include the key characteristics of the different levee sections.

In the original design, the water level and wave height with a return period of 100 year were calculated, in order to construct a reliable levee. Two different institutes calculated the expected 1-in-100 year storm surge and wave height in the Galveston Bay near Texas City. This was done with the use of guidelines from the USACE and it is mentioned that the calculations for the wave height H_s

Figure 8.5: Top view of Texas City Hurricane Flood Protection at the section facing the Bay. Source: Google Maps

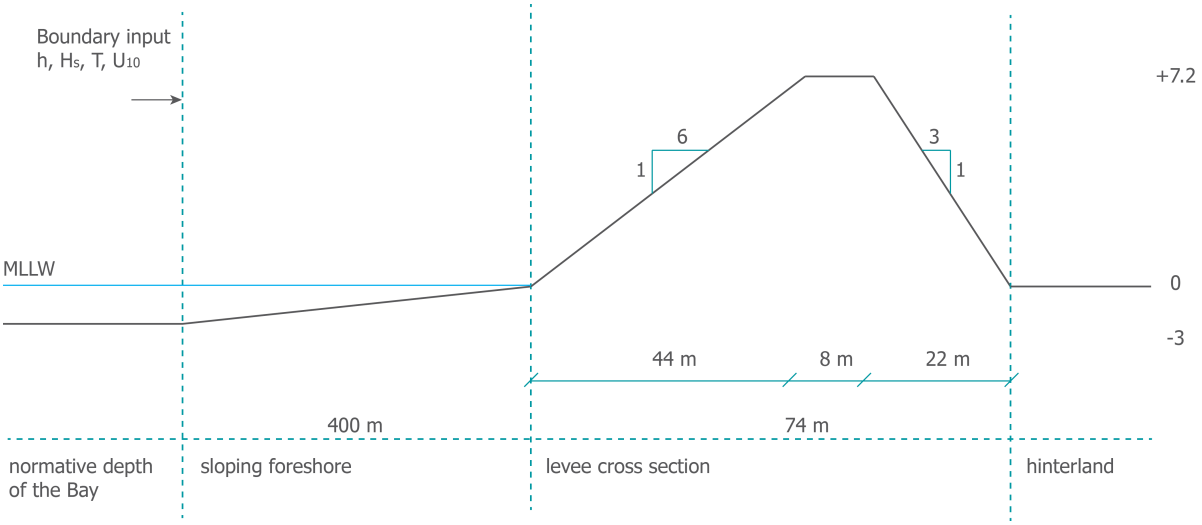

Figure 8.6: Bathymetry and cross section of Texas City Hurricane Flood Protection at the section facing the Bay (not on scale).

are based on the water depth, the wind speed and fetch length. For the calculations an -at that time- 118-year record for water level was used (Murphy & Geelan, 1965). The method or coefficients are not further specified.

The National Levee Safety Act of 2007 was passed after Hurricane Katrina devastated New Orleans. It states that federal levees should be regularly checked and accredited to make sure they can withstand a 1-in-100 year water level. The TCHFP falls within responsibility of the USACE, and in 2012 they proposed a feasibility study to assess the requirements of the dike. A civil engineering firm found in 2013 that the system still complies with the requirements for a 1 in 100 year water level, except for a short section of about fifty meter (160 ft) at the south side of the system. Details of the report were not made public, so it is unclear weather only the properties of the levee were checked, or that the hydrodynamic conditions were recalculated as well.

The hydrodynamic calculations and simulations in this study for San Leon can be applied to the part of the TCHFP that faces the Bay. The location is six kilometers south of San Leon and the bathymetry and orientation are similar, as can be seen in figure 8.4. The values that were calculated in chapter 6 are repeated in table 8.1 so that the values from this study can be compared with the original values. The value for the wave height at the toe was also calculated with the the numerical model, as shown in figure 8.7, grid point [400].

In Murphy and Geelan (1965), the wave height at the toe of the levee $H_{s,toe}$ is calculated with wind growth curves. The value for the equivalent deep water wave height $H_{s,input}$ was calculated by dividing the wave height $H_{s,toe}$ by a factor 0.92. This factor stems from a USACE guideline, but no further details on its background were provided. In this study, the value of $H_{s,input}$ was calculated in with wind growth curves (appendix E). This value serves as input parameter for the numerical model, that calculates the near shore wave transformation, and returns the significant wave height at the toe of the structure $H_{s,toe}$.

Table 8.1: Boundary input parameters for the design of the TCHFP from Murphy and Geelan (1965) and from this study.

	Return period Years	**Wind speed** m/s	**Water level** m	**Wave height** $H_{s,toe}$	**Wave height** $H_{s,input}$	**Wave length** L_0 in m	**Fetch** m
Murphy and Geelan (1965)	1-100	41.13	6.58	2.44	2.65	56.08	24,140
This study	1-100	31.3	6.66	1.83	2.21	46.51	30,000

It follows fro the comparison of the values in table 8.1 that the normative wave height at the toe of the structure varies 0.44 m (16% difference), the water level varies 0.08 m (1%). The values from this study were used for further assessment of the effect of Nature-based Solutions, because they have the smallest H/h ratio. That will lead to conservative results for the influence of marsh vegetation.

8.2.2. Inclusion of marsh vegetation

To assess the effect of marsh vegetation on the TCHFP, the numerical simulations for San Leon were used (see 6.5), although with a few alterations:

- Two model runs were done with a fictive vegetation field in front of the levee (with a length of 100 m cq. 300 meter).
- To reduce the expected stem breakage rate, a vegetation height of 0.4 m is chosen (instead of 0.58 m)
- The cross section of the levee section was included in the bathymetry.
- Oyster reefs and seagrass meadows were disregarded.

All other input parameters and conditions were kept equal. The graphical results are shown in figure 8.7. The numerical results are given in table 8.2.

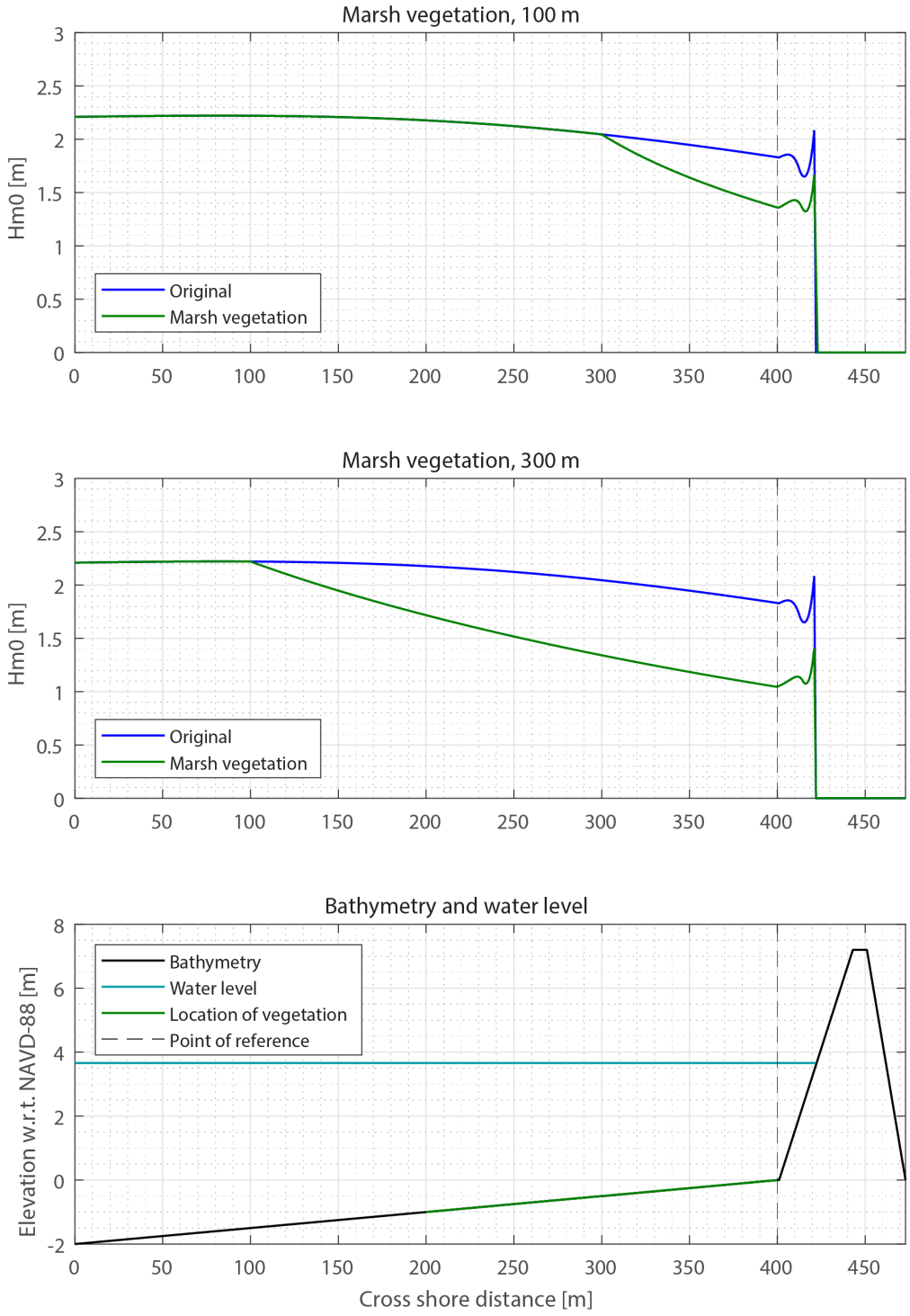

Figure 8.7: Influence of marsh vegetation (h_v = 0.4) on the development of the wave height. Wave height reduction due to 100 meter marh (upper panel), due to a 300 meter marsh (middle panel) and an overview of the bathymetry and water level (lower panel). The toe of the dike is located at gridpoint [400], this is where the wave heights are compared.

Table 8.2: Input wave height ('deep water wave height') and wave height near the toe, with and without marsh vegetation for conditions with a return period of 100 year.

Parameter	Without marsh	Marsh (100 m)	Marsh (300 m)
$H_{s,input}$	2.21	2.21	2.21
$H_{s,toe}$	1.83	1.36	1.05

8.2.3. Run-up and overtopping on the Texas City Hurricane Flood Protection

Next, values for run-up and overtopping were calculated for the levee section for both the case with and the case without marsh vegetation. All expressions were extracted from the Overtopping Manual (van der Meer et al., 2016). The formula to obtain a design run-up height is as follows:

$$\frac{R_{u2\%}}{H_{s,toe}} = min\begin{Bmatrix} 1.75 \cdot \gamma_b \cdot \gamma_f \cdot \gamma_\beta \cdot \xi \\ 1.07 \cdot \gamma_f \cdot \gamma_\beta \cdot \left((4.0 - \frac{1.5}{\sqrt{\gamma_b \cdot \xi}}\right) \end{Bmatrix} \tag{8.1}$$

with run-up height exceeded by 2% of the wave $R_{u2\%}$ [m], the wave height at the toe of the structure $H_{s,toe}$ [m], reduction factor γ and empirical design coefficients 1.75, 1.07, 4.0 and 1.5.

The reduction factors are given in table 8.3.

Table 8.3: Reduction parameters for run-up and overtopping

γ_b	berm
γ_β	oblique waves
γ_f	friction
γ_v	wall on top of crest

The ξ represents the breaker parameter (Iribarren number) and is given by:

$$\xi = \frac{\tan\alpha}{\sqrt{\frac{H_{s,toe}}{L_0}}} \tag{8.2}$$

with levee slope α and the fictive wave steepness based on the deep water wave length L_0 in [m].

The mean overtopping discharge for design conditions is given by:

$$\frac{q}{\sqrt{gH_{s,toe}^3}} = \frac{0.023}{\sqrt{tan\alpha}}\gamma_b \xi exp\left[-\left(2.7\frac{R_c}{\gamma \xi H_{s,toe}}\right)^{1.3}\right] \tag{8.3}$$

with crest freeboard R_c in [m].

The maximum overtopping for design conditions is given by:

$$\frac{q_{max}}{\sqrt{gH_{s,toe}^3}} = 0.09 * exp\left[-\left(1.5\frac{R_c}{\gamma H_{s,toe}}\right)^{1.3}\right] \tag{8.4}$$

8.2.4. Results for run-up and overtopping

An overview of the additional input parameters for wave height and overtopping is provided in table 8.4. The resulting run-up and mean and maximum overtopping discharges are given in table 8.5. As can be seen, the average overtopping during 1 in 100 year conditions is 3.07 e-04 m^3/s (0.31 liter/s) per meter levee. The maximum overtopping discharge is 0.0507 m^3/s (50.7 liter/s).

Table 8.4: Input parameters for run-up and overtopping for a 1-100 year situation.

Parameter	Quantity	Value	Unit	Note
g	gravitational acceleration	9.79	[m/s2]	Texas-based
α	angle of slope	9.5	[°]	slope 1:6
γ_b	berm factor	1.0	[-]	no berm present
γ_β	oblique waves factor	1.0	[-]	perpendicular wave attack
γ_f	friction factor	0.95	[-]	grass
γ_v	wall on crest factor	1.0	[-]	no wall on top of crest
R_c	crest freeboard	2.44	[m]	freeboard from original design

The resistance of a grass cover varies greatly, depending on it quality and maintenance. During experiments, a well-maintained closed grass cover was observed to resist a mean discharge of 0.1 m^3/s (100 liter/s), but a poorly maintained grass cover with holes and obstacles failed well below 0.005 m^3/s (5 liter/s). The design guideline from van der Meer et al. (2016) for a dike with a crest and landward slope covered with grass for the mean overtopping is 1.0 e-4 m^3/s (0.1 liter/s).

The considered section of the TCHFP is completely turfed with grass, both on the landward as the seaward side of the slope. The cover seems reasonably well maintained, although there are arid and bare patches visible, that form a risk (Google Maps). The expected values for overtopping are likely to inflict damage on the dike during 1 in 100 years storm conditions. Moreover, the wave impact ($H_{s,toe}$ = 1.83 m) is likely to cause extensive damage on the grass cover and create holes on the seaward slope.

The overtopping rates are strongly reduced by marsh vegetation. For a vegetation field of 300 meter, the average overtopping reduces to 7.92 e-06 m^3/s (0.008 liter/s) per meter levee. The expected maximum overtopping discharge is reduced to 0.0013 m^3/s (1.3 liter/s). The vegetation field in front of the dike reduces the incoming wave height with 0.78 m, the residual wave height is 1.05 m. This reduces the extend of damage due to wave impact on the seaward slope of the dike during storm conditions.

The results suggest that marsh vegetation is very effective in reducing overtopping over the levee section of the TCHFP. The implementation of marsh vegetation could greatly increase the reliability level of the dike in case of storm conditions. Marsh vegetation also counters erosion problems because it traps sediment, thus it would be an effective and sustainable maintenance measure for the levee.

Table 8.5: Resulting run-up and overtopping rates with and without marsh vegetation.

		1-100 year		
Parameter	**Unit**	**Without marsh**	**Marsh (100 m)**	**Marsh (300 m)**
$H_{s,input}$	[m]	2.21	2.21	2.21
$H_{s,toe}$	[m]	1.83	1.36	1.05
$\xi_{m-1,0}$	[-]	0.84	0.98	1.11
$R_{u2\%}$	[m]	2.57	2.22	1.94
q	[m^3/s]	3.07 e-04	5.13 e-05	7.92 e-06
q_{max}	[m^3/s]	0.0507	0.0095	0.0013

8.2.5. Comparison with other measures

In order to assess the effectiveness of marsh vegetation, it is relevant to compare the effect of a marsh with other measures that increase the reliability of the dike. A measure to reduce run-up and overtopping is to raise the crest of the dike. The effect can be simulated by increasing the crest freeboard R_c in expressions 8.3 and 8.4. The original value for R_c is 2.44 m. The raise in crest height means that the dike has be widened in order to maintain the steepness profile.

A second measure could be to replace the cover of the slopes of the dike with more rough material

than grass. The effect can be simulated by lowering the value roughness coefficient γ_f in expressions 8.3 and 8.4 (a lower coefficient means a higher slope roughness). The original value for γ_f is 0.95. A slight decrease in roughness coefficient could be obtained with a different cover layer, for instance small rubble or pitched quarry stone (approximately up to γ_f = 0.8). To increase the roughness more drastically, larger elements are necessary. For instance, a layer of Xblocs® can reduce the roughness coefficient of the slope to 0.44. Boulders and concrete cubes can also reduce the roughness coefficient to around 0.5, the exact roughness coefficient depends on the size and the distribution pattern of the elements (van der Meer et al., 2016).

The comparison between marsh vegetation, a crest raise and an increase in cover roughness are shown in table 8.6. The original effect of the marsh vegetation is shown in the upper rows. The adaptations to the crest height and the roughness that result in the same overtopping rates as the implementation of marsh vegetation are provided in the lower rows.

Table 8.6: The values for an increase in crest height and a decrease in friction coefficient in order to obtain the same effect as marsh vegetation (target values given in the upper two rows).

Parameter	**Unit**	**Without marsh**	**1-100 year Marsh (100 m)**	**Marsh (300 m)**
q	[m^3/s]	3.07 e-04	5.13 e-05	7.92 e-06
q_{max}	[m^3/s]	0.0507	0.0095	0.0013
		Raising the crest level [m]		
		-	+0.47	+0.93
		-	+1.13	+2.36
		Increasing the slope roughness [-]		
		-	0.80	0.70
		-	0.65	0.48

8.3. Marsh vegetation in a risk reduction strategy

In the introduction (section 1.3), the ongoing research to find the optimal flood risk reduction strategy for the Galveston Bay was pointed out. Van Berchum and Mobley (2017) developed a risk reduction optimization model that evaluates a range of combinations of both structural and non-structural measures. The effect of Nature-based Solutions on flood risk should be quantified to include it in this model.

8.3.1. Risk curves

Flood risk can be defined as the product of the probability of a flooding times the consequence of that flooding (e.g. damage, life loss) (Kaplan & Garrick, 1981). The relation between the two can be represented with a risk curve, that shows the expected consequence for the probability of a flood event. This is shown in the left diagram in figure 8.8. Mitigation measures for flood risk that reduce the consequence of a flood event can be visualized as a leftward shift of the curve, shown in the middle diagram in figure 8.8. A downward shift of the risk curve is realized by prevention measures that reduce the probability of a flood event. This corresponds to the right diagram in figure 8.9.

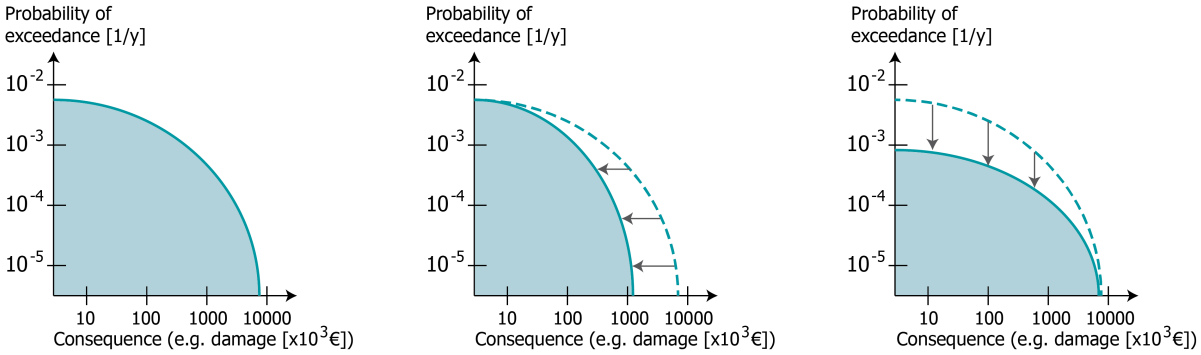

Figure 8.8: The left figure shows an example of a risk curve that visualizes the relation between the probability and the consequence of a flood event. The middle and right figure show the influence of mitigation measures that reduce the consequence cq. the probability of a flood event.

As shown in section 8.2, marsh vegetation can reduce the hydraulic load on a dike. In that context, it reduces the probability of the failure of a dike and flooding of the hinterland, which corresponds to the right diagram in figure 8.8. In section 8.1 it was explained how marsh vegetation can reduce the required Base Floor Elevation. This can be explained as a reduction in probability: for the same house elevation level, the chance that the house will be damaged is smaller. It could also be explained as a reduction of consequence: for a hurricane with the same frequency, the expected amount damage on the house is lower. Additional details on the concepts of risk are provided in appendix D.

8.3.2. Steps to include marsh vegetation in a risk reduction strategy

Four steps should be taken to include the marsh vegetation in a risk reduction optimization strategy. First, the exceedance probability (i.e. return periods) for different water levels should be determined. In the case of the Galveston Bay, this can be expressed as the Base Floor Elevation level, as it includes both the water level and the wave height. It is important to realize that here, it represents the extreme water level (and wave height) with accompanying exceedance probability, and not the required elevation of a house. The second step is to determine the effect of marsh vegetation on the required BFE. The third step is to derive a relation between the Base Flood Elevation levels and the amount of damage in an area. This results in the expected amount of damage for each increasing step in BFE in an area. The last step is to combine both diagrams in a risk curve that gives the risk reduction level due to marsh vegetation. To increase the accuracy, the investment costs of the construction of a marsh should be included in the calculations. Step 1 and 2 are visualized in the left panel in figure 8.9, step 3 is shown in the middle panel and step 4 is shown in the right panel. Note that the values in this diagram are figurative.

For the second step, namely the effect of marsh vegetation on the return period of a BFE, a generalization of the effect was derived. A relation between the exceedance probability of the wave height

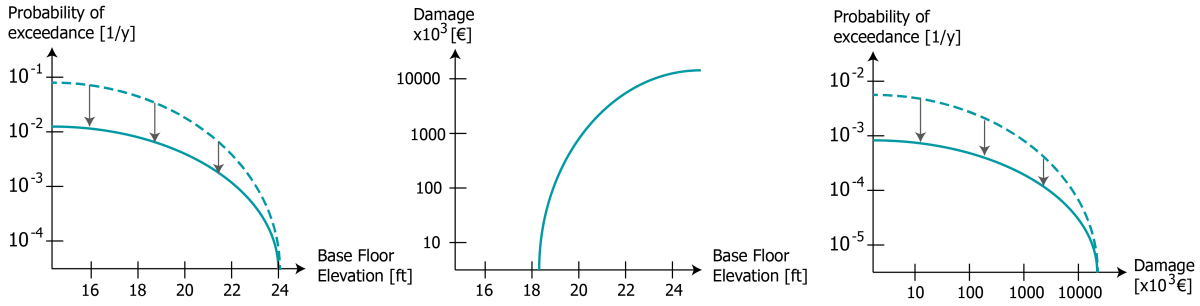

Figure 8.9: Left panel: the effect of marsh vegetation on the exceedance probability of a BFE level. Middle panel: relation between damage level and BFE level. Right panel: total effect of marsh vegetation on risk level of an area. Note that the values in this diagram are figurative.

and the water depth was derived both for the case with and the case without marsh vegetation. Figure 8.10 shows a generalization of the effect of marsh vegetation. The return periods are marked in the plot, so that it can be used in a risk reduction evaluation. The lines in the figure represent the wave height at the output location (i.e. first line of houses at Galveston Island) with and without marsh vegetation. The properties of the hypothetical marsh are N_v = 491 m^{-2}, b_v = 0.006 m, l = 500 m and C_D = 0.4. The grey line represents marsh vegetation with a height of 0.58 m, which is used in the original simulation in section 6.5. However, in section 7.3 it was found that for the longer return periods (>100 year), stem breakage will probably annul the effect. The green line shows the effect for vegetation with a height of 0.4 m, for which the expected stem breakage rate is significantly lower. This line provides more realistic expectations for the effect of marsh vegetation on the wave height.

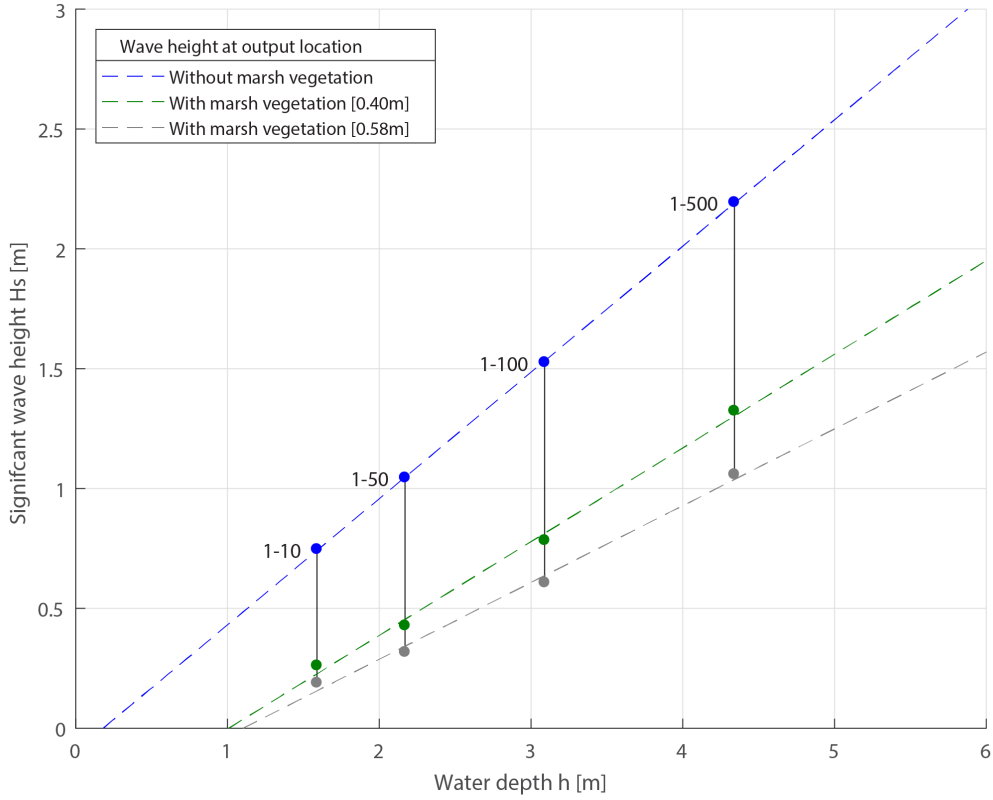

Figure 8.10: Linear trend lines for the significant wave height at the output location (i.e. first line of houses) with and without marsh vegetation. . The markers show the results for the different return periods. Coefficient of determination for the linear regression line is R^2 = 0.9999 for the blue line (without marsh vegetation), R^2 = 0.9952 for the green line (with marsh vegetation, h_v = 0.40 m) and R^2 = 0,9932 for the grey line (with marsh vegetation, h_v=0.58 m).

III

Concluding remarks

9

Conclusions

In this chapter the main conclusions of this study are presented and the research question described in the introduction will be answered. The objectives of this thesis were (1) to quantify wave height reduction by Nature-based Solutions and (2) to assess the effectiveness of Nature-based Solutions in reducing flood risk in the Galveston Bay by means of wave attenuation.

According to literature, marsh vegetation, coral and shellfish reefs, mangroves, sand nourishments and seagrass are able to reduce wave height. This list is not exhaustive, but the effectiveness of these measures has been researched and scientifically substantiated with observations. When taking into account the limitations with respect to hydraulic, environmental and climatic conditions in the Galveston Bay, marsh vegetation, oyster reefs and seagrass meadows prove promising Nature-based Solutions for further research.

Wave height reduction can be described accurately in terms of wave energy dissipation. The hydrodynamic processes that cause energy dissipation were identified in the wave attenuating mechanisms of marsh vegetation, seagrass meadows and oyster reefs. Vegetation-induced drag, expressed by Mendez and Losada (2004), proved to clearly describe wave attenuation by marsh vegetation and seagrass meadows. The reason is threefold: the selected method is flexible, it closely approximates the physical processes and it is well equipped to account for highly energetic conditions (e.g. storm and hurricanes). Furthermore, it was found that a combination of depth-induced breaking and bottom friction can describe wave attenuation by oyster reefs. Despite the validation of the selected processes with two sets of observations, no field measurements on wave attenuation by oyster reefs during extreme conditions are currently available. This implies that the results for oyster reefs should be interpreted with care. The expressions used to describe these hydrodynamic processes are included in a 1D numerical wave propagation model to increase understanding of the effect of the Nature-based Solution on the wave height. The model can subsequently be applied to predict their effectiveness in wave attenuation on arbitrary locations.

In this research, the Galveston Bay, located on the upper Texas coast, is used as a case study to investigate wave height reduction by Nature-based Solutions. This semi-enclosed bay is regularly hit by tropical storms and hurricanes, which are significant drivers for flood risk because they induce storm surge and large waves. Since no large-scale structural flood risk protection is present in the Galveston Bay, storm-induced surge can cause flooding of the hinterland and storm waves can travel inland. There, they inflict damage on houses and coastal infrastructure, especially by strong energy dissipation due to adverse wave breaking. Furthermore, storm waves are relevant in combination with dikes and levees, as they generate run-up and overtopping and cause erosion and damage to the existing structures. This indicates that storm waves contribute significantly to the level of flood risk in the Galveston Bay. Consequently, the Federal Emergency Agency identified flood hazard areas in the Bay with a return period of 100 years or shorter. Furthermore, areas with additional risk due to storm waves are marked explicitly (FEMA, 2017). In these areas wave attenuating measures could contribute to flood risk reduction.

Two different locations in the Galveston Bay, being San Leon and Galveston Island, both threatened by waves during storm conditions, were selected as a case study. For each location a stylized case was developed to simulate wave height development and assess the effectiveness of Nature-based Solutions. Overall, the effect is most promising for marsh vegetation, even deeply submerged vegetation can significantly reduce the incoming wave height. Marsh vegetation showed the strongest wave height reduction for every combination of wave height and water depth that was tested, with a reduction percentage varying from 52% to 75%. However, the results indicate that stem breakage is of significant influence on the capacity of marsh vegetation to attenuate storm waves. This is caused by the strong orbital wave velocity of storm waves that exert a force that exceeds the strength of the stems. For the case of the Galveston Bay, stem breakage will probably occur during conditions with a return period of 100 years or higher. In order to reduce the expected stem breakage rate, the properties of the marsh vegetation can be optimized. The results suggest that an optimum for the vegetation height can be found that minimizes the stem breakage rate and maximizes wave energy dissipation. Since oyster reefs are not damaged by high waves, another option that may reduce stem breakage is to situate an oyster reef in front of the marsh in order to reduce the peak wave heights.

The wave height reduction by seagrass meadows is observed to be minor and decreases even further for increasing water depths and wave heights. Thus it is concluded that seagrass is not effective in reducing wave heights during stormy conditions in the Galveston Bay.

Oyster reefs are effective at reducing wave height, provided that their location is close to the intended area of wave height reduction. The results of the simulations showed that relocating a reef to 100 meter from the output location, increases the wave height reduction at the output location from 9% to 64%. Reefs are especially effective for hydrodynamic conditions with shorter return periods (<100 years). It was found that biological conditions are also important: an oyster reef needs to be alternately submerged and emerged in order to thrive, which means that their range of application is not so flexible at locations with a small tidal range. The tidal range is furthermore important for the distribution pattern of marsh vegetation and seagrass meadows. The distribution range of all three species increases with a larger tidal range. Despite the fact that the Galveston Bay has a small tidal range (0.4 m), the potential distribution range is still of considerable size, because the Galveston Bay area is very flat.

Marsh vegetation proves especially effective in combination with a levee, since it reduces run-up and overtopping. It was found that a marsh of 100 meters in front of a dike reduces the maximum overtopping as much as a crest raise of 1.13 meter. This shows that application of natural measures can increase the reliability of existing flood protection structures, and allows new structures to be lower while maintaining the same flood safety requirements. Subsequently, the expected damage on a dike and its hinterland will be lower if marsh vegetation is implemented on its foreshore. This could be of particular interest for potential future structural measures in the Bay.

Because the Base Floor Elevation (BFE) requirement for individual houses is an important indicator for the flood risk level in the Galveston Bay, the effect of marsh vegetation on the BFE was investigated. It was found that the wave height reduction due to marsh vegetation reduces the required Base Floor Elevation with up to three feet (0.91 m). This underlines that, owing to marsh vegetation, the expected damage during flood events will be lower because the expected wave height is lower.

In summary, this research shows that Nature-based Solutions have great potential to contribute to flood risk reduction in the Galveston Bay due to their capability to contribute to wave height reduction during storm conditions. However, it is emphasized that the limitations and optimizations with respect to their location, strength and biological requirements must be taken into account in order to maximize their effectiveness.

10

Discussion

Marsh vegetation and oyster reefs can reduce wave height significantly. Particularly marsh vegetation has a great potential to contribute to protection of coastal infrastructure during extreme conditions. Since flood risk is mainly defined by small probability events, this study focused on storm conditions (e.g. high water levels and wave heights). However, these conditions rarely occur, and subsequently there is a lack of field observations of the effect of Nature-based Solutions on wave height during such conditions. To overcome this, measurements of mild to moderate hydrodynamic conditions are extrapolated to simulate the mechanisms. But by doing so, non-linear effects or unexpected behavior that only occurs during extreme conditions is not captured. These effects include for instance stem breakage of vegetation or extreme erosion during a storm event which destabilizes a Nature-based Solution.

This is even more so because during storm conditions, and particular during hurricanes, not only waves cause damage. Storm surge, precipitation and compound flooding was disregarded in this study. This makes it difficult to say something about flood risk reduction altogether. A model that investigates the effect of Nature-Based Solutions on both the effect of waves, storm surge and precipitation, leads to a more complete insight in the flood risk reduction. Especially because the combined occurrence of these hazards will probably lead to synergistic flooding effects.

On the other hand, this study also leaves the second-order benefits of Nature-based Solutions largely untouched. For instance, sediment trapping is an often heard property of marsh vegetation, seagrass meadows and oyster reefs that can contribute to coastal protection. Also, reduction of storm surge due to marsh vegetation was observed in several cases. The benefits of the simultaneous occurrence of these effects could be larger than the summation of the separately predicted effects, because they are interdependent. Although Nature-based Solutions prove to be effective in reducing wave height independently, they are particularly efficient when combined with structural measures.

Additionally, the following notions on the validity of the results are significant:

- Detailed knowledge on hydrodynamic processes tailored for oyster reefs is limited. Let alone availability of observations of their behavior during storm conditions. Their incorporation in the used numerical model is unprecedented and, although supported by findings from academic papers, should be calibrated and validated with observations during extreme hydrodynamic conditions. Since there is no measured wave data for the Galveston Bay or for oyster reefs in storm conditions, the results should be interpreted with care.

- In the Galveston Bay, 2D effects of wave propagation such as refraction and diffraction could prove significant, because the semi-enclosed Bay has an irregular coast line and bathymetry. This could locally lead to atypical water levels and wave heights.

- Wind and wave set-up were included indirectly in the water level, that was assumed horizontal along all cross-section. In reality the water level is under a small gradient due to wind set-up. This could influence the development of the wave height over the fetch length. The wave height and the water level are interconnected, thus the local wave set-up might vary per location.

11

Recommendations

This study could be expanded in a variety of ways. The recommendations are twofold: one part focuses on the quantification of wave attenuation by Nature-based Solutions in general and provides suggestions for improvement of the numerical model. The other part aims to suggest additional and relevant research in the Galveston Bay with respect to flood risk reduction by Nature-based Solutions.

Recommendations for quantifying wave attenuation by Nature-based Solutions

- Although several Nature-based Solutions were disregarded in this research, their implementation could prove effective at other locations than the Galveston Bay. The wave attenuating mechanisms of, for instance, coral reefs and mangrove forests could be schematized and included in the numerical model. The model could then be used in a wider range of locations to predict which Nature-based Solution is most effective at attenuating waves.
- Research that focuses on the behavior of one specific Nature-based Solutions could expand the knowledge on its limits of effectiveness. This could be achieved with laboratory observations under controlled conditions, so that the sensitivity of each parameter can be investigated.
- Measurements, both in the laboratory and in the field, on the wave attenuation of oyster reefs under moderate and extreme hydrodynamic conditions would improve the insight in their effectiveness of wave height reduction and would be increase the accuracy of the inclusion of an oyster reef in a numerical model.
- The current state of the model could be improved with the following aspects:
  - Expand the model to two dimensions. Two dimensional wave effects such as oblique incident waves, refraction and diffraction can be of particular significance in a semi-enclosed water body with an irregular coastline. Nature-based Solutions are often found is such sheltered areas.
  - To improve the accuracy of the model for a specific location, it should be calibrated for normative parameters with local observations. The calibration parameters for seagrass and marsh vegetation should be the bulk drag parameter C_D. For oyster reefs, the calibration parameter should be the bottom roughness K_s.
  - Expand the simulations in this study with a built-in check for stem breakage. This can be done by including the stem breakage model numerically in the wave propagation calculations.

Additional research on flood risk reduction by Nature-based Solutions in the Galveston Bay

- The joint return period for wave height and storm surge was assumed equal to the return period of the individual parameters (e.g. very high dependence). This probably overestimates the water level and wave height. The correlation of the extreme behavior of wave height and water depth

could be analyzed in order to calculate a more accurate joint return period. This will increase the accuracy of the normative wave height and water level for an arbitrary return period. The extremal dependence could be approximated with a componentwise maxima approach.

- Collecting observations of the wave climate in the Bay is essential for further research on the effectiveness of wave height reducing measures. This also holds for wave height measurements around Nature-based Solutions: in recent years several restoration projects for marshes and oyster reefs have been conducted in the Galveston Bay, but wave parameters were not monitored.
- The effect of Nature-based Solutions on the combination of storm surge and waves would be an important step towards a full analysis of the effect of NbS on flood risk in the Galveston bay. Generating synthetic storms parameters with a statistic simulation could contribute because of the limited observations.
- The suggested practical applications of Nature-based Solutions in this study can be expanded. Their application in combination with suggested flood risk protection measures could be investigated. Possible projects are the 'Ike Dike' or the SH-146 Levee (explanation on these suggested measures is provided in appendix B).
- This study focused mostly on the *probability* part of flood risk: it investigated how expected flood levels could be lowered. Mapping the consequences of a flooding in the Galveston Bay will contribute to the development of a more complete flood risk framework for the area. This could be achieved by assigning an expected damage level to the Base Floor Elevation levels in the Galveston Bay Area. A cost-benefit analysis could be used to assess the effectiveness of Nature-based Solutions in comparison to other measures.
- In order to assess Nature-based Solutions in an integral flood risk evaluation, the additional benefits of NbS should be investigated and quantified.

List of Figures

List of Tables

Appendices

A

Wave behavior

A.1. Wave transformation

The dominant transformation process in cross shore wave propagation is shoaling. Wave shoaling can be defined as the increase of wave height due to a conservation of energy flux while waves approach shallower water. As soon a wave propagates into shallow water, i.e. a water depth where the bottom affects the wave, the wave speed and wavelength starts to decrease. The wave energy is assumed constant at two separate locations outside the breaker zone, so in order to keep the energy balance, the wave height has to increase:

$$Ec_g = Enc = constant \tag{A.1}$$

here n is the ratio c_g to c.
And since:

$$E = \frac{1}{8}\rho g H_{rms}^2 \tag{A.2}$$

a decrease of wave speed c leads to an increase of wave height H_{rms}.
This can be written as follows:

$$\frac{H_2}{H_1} = \sqrt{\frac{c_1 n_1}{c_2 n_2}} \tag{A.3}$$

A.2. Wave forces

Storm surge is often the cause for coastal flooding as it can lead to significant inland water levels. During storm events, waves can cause severe damages to coastal and inland structures. Wave height is, among others, limited by water depth. Waves travel further inland in case of high surge levels. Surface waves propagating towards the coast can transport energy. Wave energy is a function of the square of the wave height, so large waves with a high celerity transfer significant energy in the direction of wave propagation. This is called the energy flux or the wave force (Bosboom & Stive, 2013). When water depth reduces towards the coast, waves start to shoal. They will heighten and steepen until maximum steepness is reached. The wave will break and the concentrated wave energy is dissipated.

Different types of wave loads can be distinguished. A breaking wave can act as a force on structures. The driving mechanism in this case is the wave pound following from the breaking of the wave. The impact generates a high pressure for a brief moment. This is shown in figure A.1 C. Furthermore, a bore can exert a force on a structure or slope. This is illustrated in figure A.1 B, where a breaking wave on a mild slope moves in the direction of wave propagation. Apart from the forces that follow from wave breaking, non-breaking waves can exert a pressure force on a structure as well. This quasi-hydrostatic pressure force follows from the fluctuating water elevation during a wave period (see figure A.1 A).

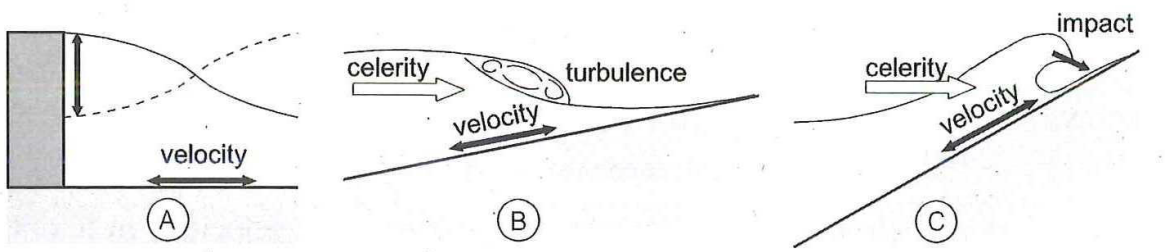

Figure A.1: Wave loads on a slope or structure. Source: Schiereck and Verhagen (2012)

A.3. Drag force

The Morison equation is a practical relation to the describe the cylinder-induced force in a non-steady flow. It can be used to describe wave forces on stiff vegetation in flow. The formula consists of the summation of an inertia force and a drag force. In the case of vegetation, the inertia force is usually negligible due to the small stem diameter over wave height ratio (Morison, O'Brien, Johnson, & Schaaf, 1950). The drag in the Morison equation is described as follows:

$$F_{M,d} = \frac{1}{2} C_D \rho A u |u| \tag{A.4}$$

where $F_{M,d}$ is the drag-induced force, C_D is the drag coefficient, ρ is the fluid density, A is the area of the object perpendicular to the flow velocity and u is the undisturbed flow velocity relative to the cylinder. This formula is used as a basis for formula 3.10. The area A in A.4 is represented by the multiplication of the b_v and N_v.

The drag coefficient C_D was originally based on the form drag, since this is the dominant drag type for rigid cylinders. Since vegetation fields can also induce significant forces due to swaying, skin drag and interference drag, the original ranges for C_D are not suitable. Therefore C_D must be calibrated for each site. For clarity, the relevant forms of drag in fluid mechanics are shown in figure A.2.

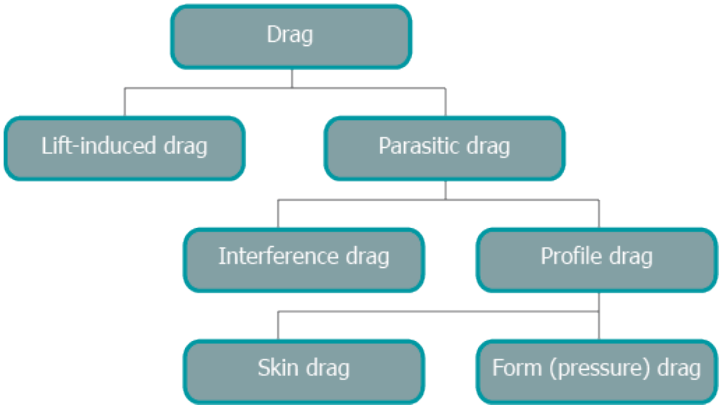

Figure A.2: Subdivision of drag types.

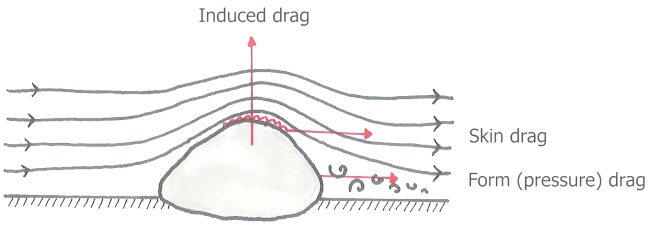

Figure A.3: Types of drag working on a structure in a flow. Interference drag is induced by a adjacent structure.

B

History of hurricanes in the Houston-Galveston Bay Region

The U.S. and especially the HGBR are frequently hit by hurricanes. Since the 1900 Galveston Hurricane, which is still the deadliest natural disaster in the U.S., the HGBR is hit by a major hurricane averagely every 10 years. Severe hurricanes with multiple fatalities and billions of USD in damages have led to adaptations and preparations in a range of aspects in society.

As in most communities, first a large disaster has to happen before action is undertaken. The 1900 Galveston hurricane sparked the design and construction of the Galveston Sea Wall. It proved effective, in the next major hurricane in 1915 Galveston was kept mostly untouched in comparison with the surrounding region.

During the 20th century, the HGBR was hit many times by hurricanes and tropical storms. The results range from a 'few' million dollars in material damage to hundreds of fatalities and billions of dollars in repairs (National Hurricane Centre, 2008). In the 1950s a study was done by the US army corps of engineers on flood risk in the region and as a result the Texas City Levee System was build. In 1979 the USACE undertook a large-scale research in the HGBR on flood risk, but ultimately none of the alternatives was implemented due to the lack of federal funding. The only other substantial structural levee system is situated near Freeport and was completed in 1982 (USACE. (2005)).

In 2001 tropical storm Allison made landfall near Freeport, Texas and looped over Houston. It induced extreme precipitation rates in the area, which let to floods in dozens of locations along its path. It sparked the establishment of the Tropical Storm Allison Recovery Project, that assessed and mapped flood risk in Harris County (in which Houston is situated). Its main focus was on precipitation-driven floods. Furthermore it aimed at more public awareness on flood risk as well as citizen having an emergency plan and flood insurance (TSARP, 2002).

Less than a month after Hurricane Katerina (2005) rampaged over New Orleans, the upper Texas Region was hit by category 5 hurricane Rita. With Katherina fresh in mind, large scale evacuations were ordered in the HGBR. In the end Rita largely missed the HGBR, but due to the chaos of the evacuations, over 100 people died. This let to an improvement of the governmental emergency and evacuation plans (GCCPRD, 2016).

When hurricane Ike hit in 2008 it was devastating, but not a worst case scenario. More than one institution realised this and in the following years several plans were made to protect the HGBR from another devastating flooding.

In 2007 the Severe Storm Prediction, Education, and Evacuation from Disasters (SSPEED) centre was founded and started to research flood risk in the HGBR. After Ike, the Texas A&M University - Galveston (TAMUG) also started a research on how to most effectively reduce flood risk in area. A political response to Hurricane Ike came in the form of a committee consisting of the six counties adjacent to the Galveston Bay that started researching the possibilities of flood risk reduction as well. This committee was then transformed in the Gulf Coast Community Protection and Recovery District (GCCPRD). In the following years the TU Delft, the Texas General Land Office (GLO), the US Army Corps of Engineers (USACE) and several other parties got involved in the search for a suitable, feasible solution.

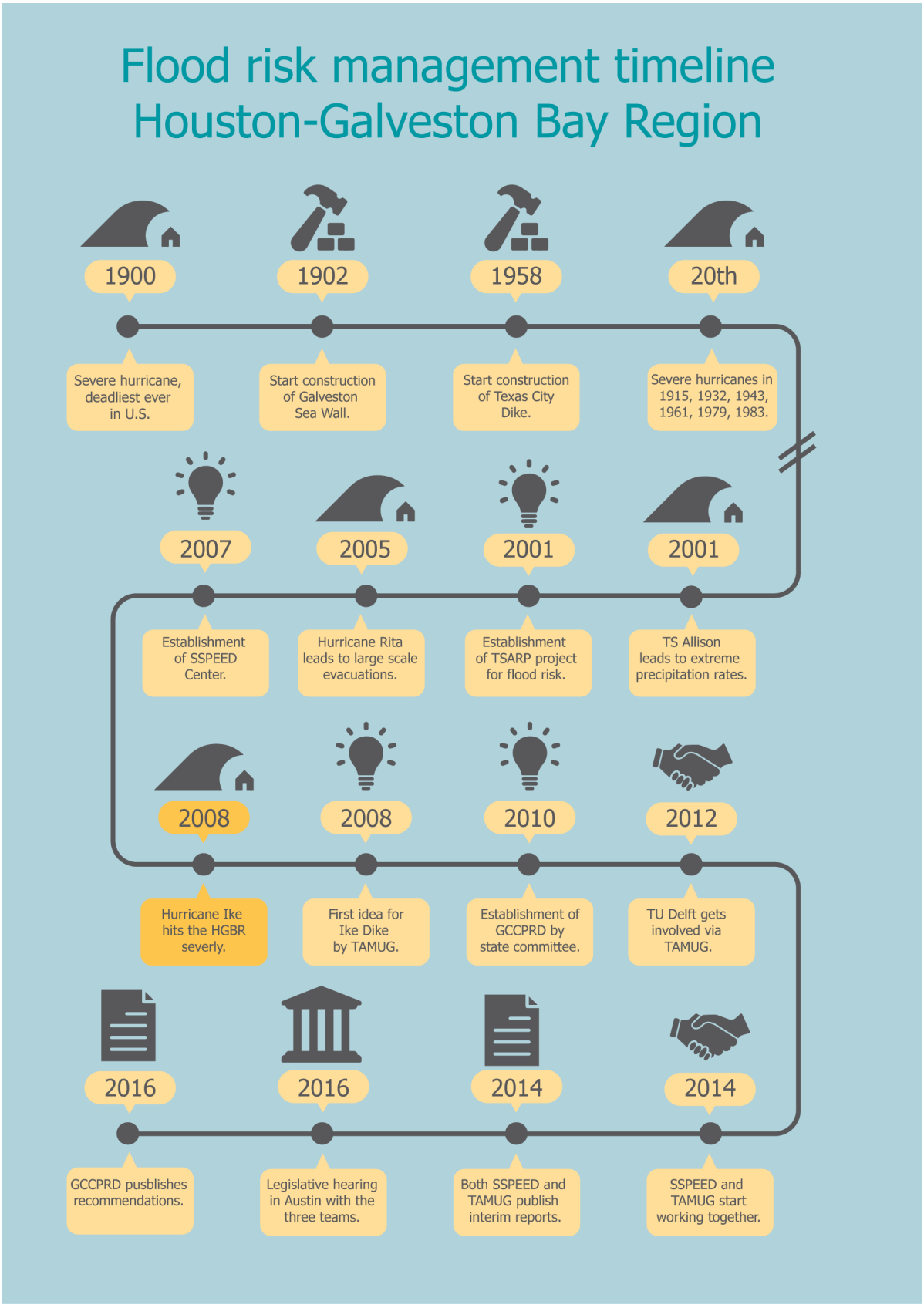

Figure B.1: Time line of important events in flood risk management in the HGBR.

In 2016 a legislative hearing in Austin, the capital of Texas, was held. The three main parties (SSPEED, TAMUG and GCCPRd) elaborated their plans and findings so far. The GLO and the USACE were present as well. Currently they are conducting two studies on the Texas coast, one of them long-term and large scale, the other focusing only on the northern part of the barrier system. (Shorto (2014), Scranton (2016), O'Neil (2015), Wray (2016))

B.1. Recent developments in flood risk reduction

Most of the previous mentioned measures have been integrated in large scale plans for the HGBR. The most significant proposed measures will be explained briefly.

Coastal spine ('Ike dike')

The coastal spine is a concept that stretches along the adjacent coasts of the Galveston bay, mainly on the barrier islands. It consists of the existing Galveston Sea Wall and several land barriers on the barrier islands. It closes of the entrances from the Gulf of Mexico to the bay via several storm surge barriers. It was first suggested by TAMUG. Some parts of the coastal spine have been researched more thoroughly than others. A preliminary design has been made for the system. (S. Jonkman et al. (2015))

Benefits:

- Significant reduce in damage in a 1-in-500 and 1-in-100 year return period case.
- A 100 percent reduction in 1-in-10 year return period case. (Hurricane Ike was classified in this category.)

Drawbacks:

- Possible negative effect on the ecological system in and around the bay.
- Possible negative effect on the fishing industry. (Second largest production in US.)
- Storm surge still able to build up in the bay due to long fetch length. This could lead for instance to high water levels in the Houston Ship Channel.
- Galveston will still be prone to flood risk from the bay side. High water levels can be induced by the rotating nature of a hurricane and also by large water volumes pushed up in the adjacent rivers returning to the bay.

Houston ship channel gate ('Centennial Gate')

This is a concept that aims to close down the Houston ship channel in case of extreme weather. There are different options and locations available for the gate system, which have been researched by SSPEED.

Benefits:

- Its a relatively cheap measure to protect the industrial assets of the port of Houston and communities along the channel.
- There will probably not be major land conflicts.

Drawbacks:

- The communities and assets adjacent to the Galveston Bay are not protected in this plan.

In-bay solutions

In order to reduce the set-up in the Galveston bay during storms and hurricanes, a mid-bay-barrier is suggested. This mid bay barrier closes of the passage through the bay. On either side of the barrier, dredge disposal sides, berms with oyster reefs or artificial islands are constructed.

Benefits:

- Dredged material from the Houston Ship Channel can be used to construct artificial islands (this has already been done by the USACE).

- This measures gives opportunity to enhance the ecosystem and implement nature based solutions in the system.

Drawbacks:

- Water can still flow around the islands in the upper bay area.
- If the total section gets closed of by a combination of islands and gates, these island have to be maintained intensively to keep the system water tight.

The SH-146 raising

This plan involves the raising of the current State Highway 146 on the west side of the bay (Collier, 2016).

Benefits:

- It is an easy route to follow, the state highway is already there. The amount of land that has to be acquired will be limited.
- Due to the highway, the levee will be multifunctional. It is possible that funds for infrastructure can be addressed.

Drawbacks:

- On the long run the land east of the levee/high would probably be lost to the bay.
- This plan only protects one part of the HGBR. For flood risk reduction everywhere in the area it should be combined with other measures.

West Levee

The west levee shows similarity to the SH-146 raising but is at some parts of the trace closer to the bay. It therefore protects more land east of the high way and thus more communities and assets. This measures has not been researched thoroughly.

Benefits

- This levee would protect all communities west of the Galveston bay.
- There will probably not be major land conflicts.

Drawbacks

- This levee will be longer than the HS-146 alternative and thus be more expensive.
- It is suspected that there will be land owner conflicts.
- This plan only protects one part of the HGBR. For flood risk reduction everywhere in the area it should be combined with other measures.

Levees on barrier islands

Several involved parties have suggested to construct additional levees in the form of walls or dunes on the barrier islands in front of the Galveston bay (Bolivar Peninsula and Galveston Island).

Benefits:

- Protection of communities on the islands.
- Reducing overflow into the Galveston Bay.

Drawbacks:

- Foreseeable land acquisition problems on the islands to construct such levees
- On its own not a suitable solution to protect the total HGBR.
- High investment costs for relatively few people.

Lone Star National Recreation Area (LSCNRA),

This plan involves the creation of a large national park stretching out over the coastal area of four counties. It would create large buffer zones for storm surge. The wetlands and barrier islands would reduce the impact of a hurricane of storm. It is unclear whether this alternative has been thoroughly studied (Archie & Terry, 2014).

Benefits:

- Eco-friendly and non-structural way of reducing flood risk in the area.
- It would increase the touristic attractiveness of the area and might generate revenues.

Drawbacks:

- Unsure if only Nature-based Solutions will reduce flood risk enough.
- This plans need a high level of collaboration and participation by different stakeholders.

Combination of measures

Most of the aforementioned measures do not sufficiently protect the total HGBR. A combination of measures could be a solution. Most of the involved parties (SSPEED, GCCPRD) suggest combinations of measures to come to a sufficient risk reduction and a favourable cost-benefit ratio (GCCPRD (2016), Blackburn, Bedient, and Dunbar (2014)).

An example of such a combination is the Houston-Galveston Area Protection System (H-GAPS) suggested by SSPEED. This combines several levees, the Houston Ship Channel gate, the SH-146 raising and several Nature-based Solutions such as oyster reefs. (SSPEED (2015))

B.2. Stakeholder analysis

The 'Texas Case' has a wide range of stakeholders. A convenient way to classify then is their public or private background. A special group of stakeholders are the 'enablers'. They are trying themselves to come up with a solution to lower the flood risk in the HGBR.

- **TAMUG group**

  The TAMUG group forms around Dr. Merrell who came up with the idea of the coastal spine ('Ike Dike'). The plan has gained a lot of attention in the media over the years and a range of local communities have endorsed the plan.

- **SSPEED group** The Severe Storm Prediction, Education, and Evacuation from Disasters Centre works closely together with Rice university. Researchers from other universities are also involved. The SSPEED centre was founed by dr. Bedient and dr. Blackburn.

  They propagate a 'mid-bay solution' including the 'Centennial Gate', a gate that protects the Houston Ship Channel from storm surge.

- **GCCPRD group** The Gulf Coast Community Protection & Recovery District was founded through a state commission for disaster recovery (which was established after Hurricane Ike). It consists among other of the judges (county heads) of the six bay counties. Its goal is to research the proposed measures and determine the most effective and feasible alternatives. In order to do so they hired engineering company Dannenbaum.

Although TAMUG and SSPEED work together since 2014, TAMUG still advocates the Coastal Spine and researchers from Rice University are still researching combinations of smaller solutions, which could be less invasive.

Two involved public agencies are the Texas General Land Office (GLO) and the United States Army Corps of Engineers (USACE) which since long have been involved in coastal projects.

In B.1 the stakeholders in the HGBR are shown. It is qualitatively shown how much interest or power a stakeholder has in implementing a large scale flood risk reduction plan. Note: this list is not complete.

Table B.1: Stakeholders in HGBR

Actor(group)	**Interest**	**Power**
Public stakeholders		
Texas General Land Office	+	++
The six bay area counties*	+	++
U.S. Army Corps of Engineers	+	++
Harris County Flood Control District	+	+
Citizens in flood prone area	++	0
Other citizens	0	-
Other state and local governments	+	++
Port authority	+	+
Recreation organizations (boating, fishing etc)	+	-
Public-private stakeholders		
Educational institutes	+	+
Environmental groups	++	0
Emergency management institutions	+	+
Private stakeholders		
Petro-chemical companies	++	++
Other port industry	++	+
Tourism branch	+	0
Fishing branch	+	-
Insurance companies	+	-
Galveston bay foundation	+	-
*Chambers, Brazoria, Galveston, Harris, Jefferson, Orange		

C

Wave height reduction due to oyster reefs

In figure C.1 the effectiveness of oyster reefs in reducing wave height for different water depths and wave heights is given. Two trends can be distinguished. The first one is that for similar water depths, the reduction percentage is higher for higher waves. This suggest that a large H/h-ratio results in a higher reduction percentage. This holds particularly for small water depths. Secondly, the simulations suggest that even though the H/h-ratio stays the same, the reduction percentage decreases with increasing water depth.

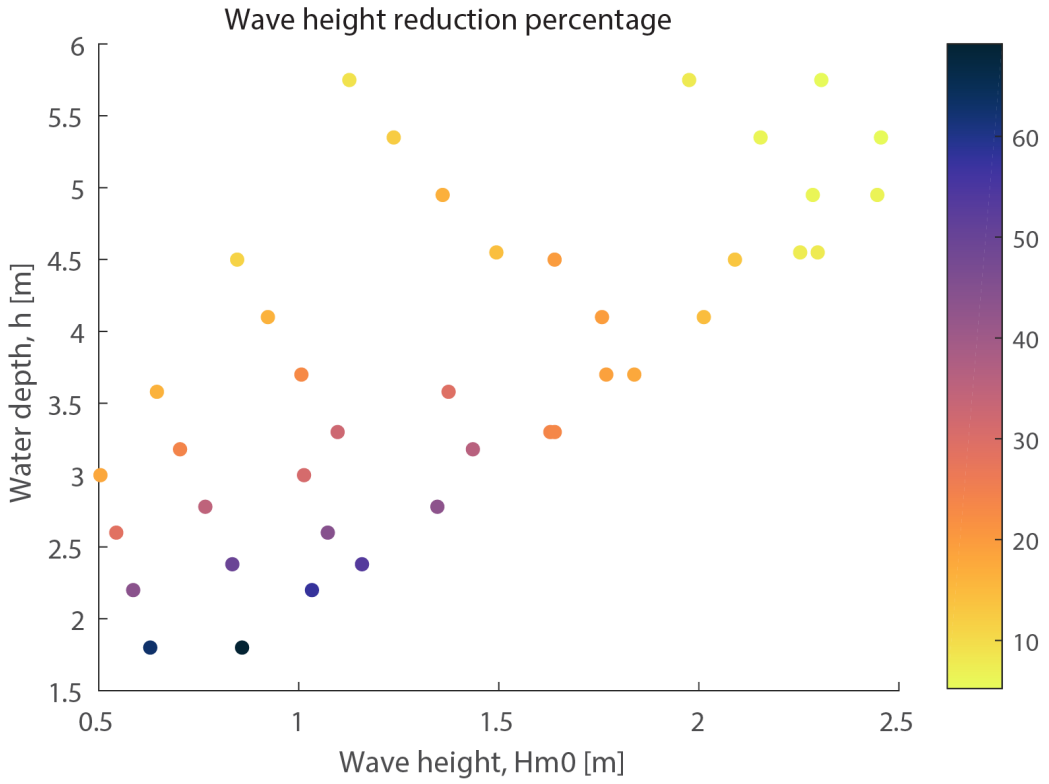

Figure C.1: The wave height reduction percentage due to oyster reefs. Percentages measured at output location in comparison with situation without an oyster reef. Wave height and water depth measured in front of the reef. Results are obtained with numerical modeling.

D

Flood risk

Literature gives various definitions for the term "risk". A generally accepted definition in Civil Engineering is that *risk* is *probability* times *consequence*. In the case of flooding this translates to the probability of a flood event times the consequence of such an event. Flood events can be categorized in coastal (from sea), fluvial (from a river) or pluvial (from precipitation) flooding. In this report the focus is on coastal flooding.

Kaplan and Garrick (1981) define risk as a combination of likelihood and hazard for certain scenarios.

$$R = \langle s_i, p_i, x_i \rangle, i = 1, 2, ..., n. \tag{D.1}$$

In which:

$s_i =$ Scenario
$p_i =$ Probability of that scenario
$x_i =$ Consequence of that scenario
$R =$ Risk

Probability is the chance that a certain event will happen, in this case the inundation of a coastal area. Several factor can affects this probability. For instance the probability of occurrence of a certain water level at sea, due to a storm or high tide. Other factors that affect the probability are the height of the hinterland or to which extent an area is protected against flooding by means of a protection system.

Note that these factors that affect the probability of a flood event, are also subject to a variety of components that influence their probability of occurrence. This process of influence is far-reaching and complex. A simplification of the situation is therefore inevitable. (For instance: the probability of flooding is influenced by the water level at sea. The water level at sea is influenced by the weather conditions. The weather conditions are influenced by the atmospheric pressure, etcetera.)

The consequence of a flood event is often expressed in damage. This can be economical damage due to loss of buildings, assets or infrastructure. Economical damage can also be indirect, for instance decreased revenue of a company due to destroyed infrastructure. Apart from economical damage, there can also be social, ecological or environmental damage. Another relevant consequence of a flood event can be fatalities or injured people.

Since risk is, in this definition, dependent on the multiplication of two variables, 'high' risk can be caused by various combinations of these variables. For instance, an unprotected, low-lying area in a coastal region with a high frequency of severe storms could lead to high flood risk because the probability of inundation of the region is high. If the region would be well-protected against flood events, but harbours a large population and vast economical assets, the flood risk would still be high,

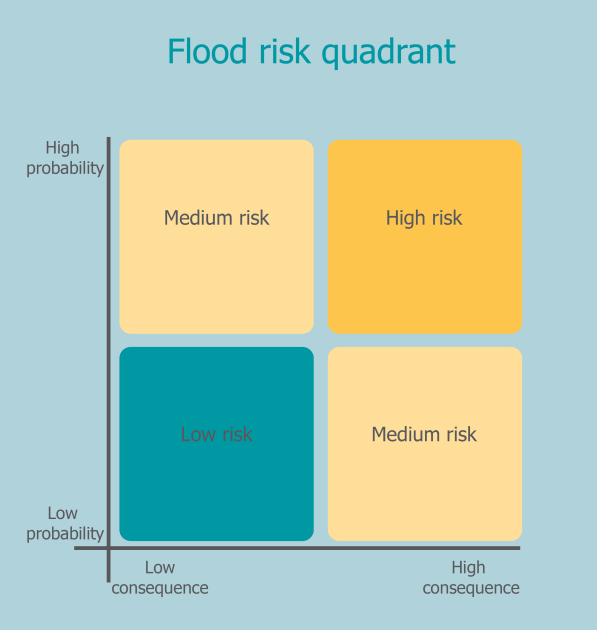

Figure D.1: A risk quadrant.

because of the potential damaging consequences of a flood event. Subsequently in a low-lying region with little protection and with a dense population and high economical value, flood risk is very high. This is shown in figure D.1.

D.1. Reducing flood risk

The list of of possible flood reduction measures is long. Each situations asks for a particular set of measures to come to an optimal solution. Measures to reduce flood risk can be classified in various ways. It is possible to make a distinction between measures that benefit the reduction of the consequences of a flooding (for instance evacuation) and measures that benefit the reduction of probability of flooding (for instance a storm surge barrier). Further there are measures to decrease the consequences as well as the probability of a flood event (for instance land use regulations) (S. N. Jonkman, Jongejan, Maaskant, & Vrijling, 2011).

Besides that, a difference can be made between structural and non-structural measures. Non-structural actions also include so called policy driven measures (awareness campaigns and such). It has to be said that 'policy driven' is not so clear a term since practically all interventions, also structural ones, are policy driven. Other often used terms are 'soft' and 'hard' mitigation measures such as in (Hutter, McFadden, Penning-Rowsell, Tapsell, & Borga, 2007).

A list of possible flood risk reducing measures and a classification in structural/non-structural and probability reducing/consequence reducing in given in figure D.2. A framework that is used in the Netherlands to manage flood risk is multi-layer safety. It is a concept that is based on three pillars ('layers'):

- Flood prevention
- Spatial solutions
- Emergency measures

The first layer, prevention, mainly focuses on reducing risk by reducing the probability of flooding. This can be done by means of dikes, levees or barriers. The second layer, spatial solutions can reduce both probability and consequence and consist of land use planning. Emergency measures focuses mainly on reducing the consequences of a flood. An example of a measure in this third layer is evacuation (S. Jonkman & Schweckendiek, 2016).

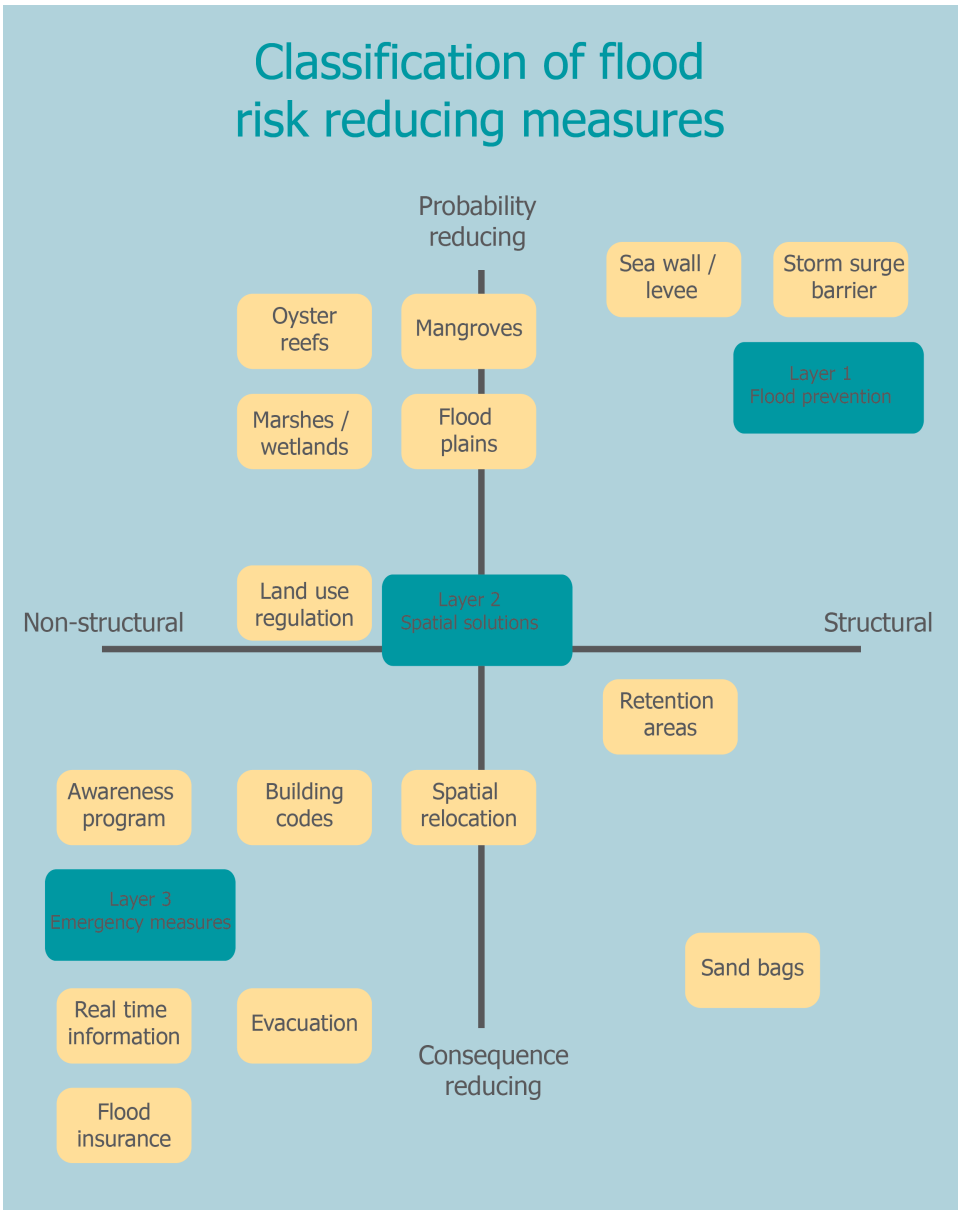

Figure D.2: Classification of flood risk reducing measures

More frameworks have been developed to classify flood risk reduction measures. Lopez (2009) describes a strategy called 'multiple lines of defense', which integrates different flood risk reducing measures and different types of habitats.

Another framework is that of the United States Army corps of Engineers (USACE), it is based on shared flood risk management and is called 'buy down risk'. Different types of stakeholders (such as federal, local, individual) all chip in in flood risk reduction via for instance insurance, structural measures or building codes (USACE., 2005).

D.2. System optimization

The earliest application of a quantitative method for decision-making on flood protection is the application of cost-benefit analysis by van Dantzig (1956).

Other optimization and decisions methods:

- Trial and error
- Cost-benefit analysis
- Risk-based approach: balance of investment and maintenance costs and potential damage reduction

To better understand flood risk and flood risk reduction research was done on combinations of measures. Nowadays flood prone areas are often complex systems. The stakes are high due to dense population and high economic value. A combinations of stakeholders with contradictory interests and the large amount of funding that is often needed for flood risk mitigation measures makes the situation even more complicated.

In order to to get more insight in optimization of combinations of flood risk measures, a research called 'MODOS' was initiated in which varying mitigation measures, risk reduction and costs are combined. Furthermore an optimization of measures is calculated.

Original economic optimization was initiated by van Dantzig (1956) in his article 'Economic decision problems for flood prevention'. Since then the economic optimization for flood risk reduction has been developing. As explained in Tsimopoulou, Vrijling, Kok, Jonkman, and Stijnen (2013) three decision types can be distinguished.

- 'Accept or reject' decision. If a solution has a positive Net Present Value, it should be accepted.
- 'Optimization' decision. A solution is optimized to have the highest possible Net Present Value.
- 'Prioritization' decision. Multiple measures are configured in such a way that a total maximum Net Present Value is obtained.

E

Wind growth curves

Numerical simulation of wave propagation is used to assess the effectiveness of oyster reefs, marsh vegetation and seagrass meadows at two location in the Galveston Bay. Hydrodynamic input parameters for the numerical model are necessary, these consist of significant wave height H_s, significant wave period T_s, water level h and wind speed U_{10}.

No comprehensive wave data are available for the Galveston Bay. The meteorologic stations in the Bay register observations of, among others, water level, wind speed, air temperature and barometric pressure. However, the sample frequency of the water level is too low to keep record of wave heights or wave periods. On the other hand, wave buoys are present off shore in the Gulf of Mexico. But since no wave penetration from the Gulf into the Bay is assumed, this data is not relevant.

A generally calm wave climate characterizes the Bay, due to its semi-enclosed features and low water depth. However, the wave height in the bay can become significant under storm conditions. This is caused by the high wind speed and the increased water depth (storm surge) in the Bay. In order to gain insight into the wave behavior, despite the lack of measurements, the characteristics of the wave climate under storm conditions in the Bay can be approximated. The water depth and the wind speed serve as input to derive the wave parameters (H_S and T_S). The characteristic values for water depth for the two locations in the Galveston Bay are available (FEMA, 2012). For the wind speed, they need to be calculated.

Thus, to obtain to the required wave parameters, first the characteristic wind speeds for the two locations are calculated. Next, the water depth and wind speed serve as input to derived the wave parameters. This is done for two locations (San Leon and Galveston Island) for four return periods (10, 50, 100, 500 years).

E.1. Wind speed

The wind speed in the Galveston Bay is one of the parameters that can be extracted directly from the NOAA database. The NOAA station near to San Leon, called Eagle Point, has kept a wind speed record since November 1995. This is one of the longest measurement periods of meteorologic stations in the Galveston Bay. However, we need the characteristic wind speed at San Leon for return periods up to 500 year, thus we need to extrapolate the observed data with Extreme Value Analysis.

In the next sections, first the methodology of deriving the characteristic wind speeds will be elaborated. Next, the input data and the assumptions will be listed. Lastly, the resulting wind speeds for San Leon and Galveston Island for four return periods will be given.

E.1.1. Methodology

Yearly wind speed records of station eagle Point were extracted from the NOAA website (NOAA, 2017) for the period 1996 - 2016. Extreme value theory (EVT) is used to investigate the extreme behaviour of the wind speed. EVT allows us to extrapolate expected values for the wind speed to very small probabilities. From these probabilities, the return periods for extreme values for wind speed were obtained.

Intermezzo: Extreme Value Theory

Extreme Value Theory is a statistical discipline concerned with the approximation of the probability of extreme events. It uses observed levels to estimate particularly high, unobserved levels. This extrapolation is done with specialized probability distributions. Attention is on maxima, since minima do not dictate design criteria in this case. However, the general theory holds equally well for minima.

A continuous random variable can be described with a distribution. For instance, wind speed tends to follow a Weibull distribution. If we have a data set of wind speed values, we can generate samples (e.g. years) from this set. The collection of maxima of these samples follow a different distribution than the original ('parent') distribution. The distribution tends to be more skewed and shifted to the right in case of maxima. If we follow the example for wind speed, its extreme value distribution will be defined by the behavior of the tail of the parent Weibull distribution.

Maxima of a data set can be obtained in two ways. A *Peak over Threshold* method includes all data points above a certain level. A *Block Maximum* method divides a data set sample and selects the maximum of each sample ('block'). An annual block maximum method is a relatively fast method, because only the maximum value of a year has to be found. A downside of the method is that the biggest part of the data set is unutilized since only one data point per year is taken into account. A Peak over Threshold method has its own downsides. The choice of threshold level is very delicate and ensuring independence of maxima can be complex.

The Generalized Extreme Values (GEV) distribution consists of a family of distributions that describe upper limit behaviour. It is a flexible distribution that combines the Gumbel, Fréchet, and Weibull distribution with three parameters: μ, σ and κ. They describe the location, scale and shape of the distribution. The GEV is applicable to a Block Maximum dataset. If the data set of observed maxima is compared to a distribution, the corresponding parameters can be found using a fitting method, such as the Maximum Likelihood Method. The purpose of this method is to estimate model parameters given the observed data. This mathematical method does so by finding the parameters that maximize the likelihood of making the particular observations. This can be done for several distributions, the one that returns the highest likelihood estimator for his parameters, describes the observed data best.

For further explanation, please refer to Coles (2001), who gives an excellent overview of statistic modeling of extreme values.

To obtain the return periods for the wind speed, the 21 maxima are sorted on frequency of occurrence so that an empirical cumulative distribution can be formed. The data set is then compared to several extreme value probability distributions. The Maximum Likelihood Method was used to investigate which distribution approximates the observed data best. It maximizes the agreement of the selected distribution with the observed data with distribution-specific parameters.

After a suitable distribution with corresponding parameters was found, its cumulative distribution was plotted (which matches the ranked observations, see figure E.4). The complementary exceedance probabilities (Complementary Cumulative Distribution Function) for the wind speed values were then extrapolated to very small exceedance probabilities (i.e. long return periods). This extrapolation of the extreme value distribution describes the upper tail of the empirical cumulative distribution function. It allows us to estimate the exceedance probabilities of very large wind speeds.

Because these exceedance probabilities with matching extreme values for wind speed are based upon yearly maxima, the annual probability of exceedance graph can be plotted. Moreover, the 'inverse' was used: extreme values plotted against the expected return period in years. The resulting return period plot is shown in figure E.5. The followed steps are summarized in figure E.1.

There is ongoing debate about the correct way of determining the plotting position of the observed data in relation to its rank position. This depends, among others, on the type of parent distribution. In this study, the method of Gringorten is followed to determine the plotting positions of the observed data points in both the return period graph (E.5) as the CDF graph (E.4). The method of Gringorten (1963) is often used in flood risk analysis and although originally aimed for the Gumbel distribution, it gives a good fit for other extreme value distributions as well.

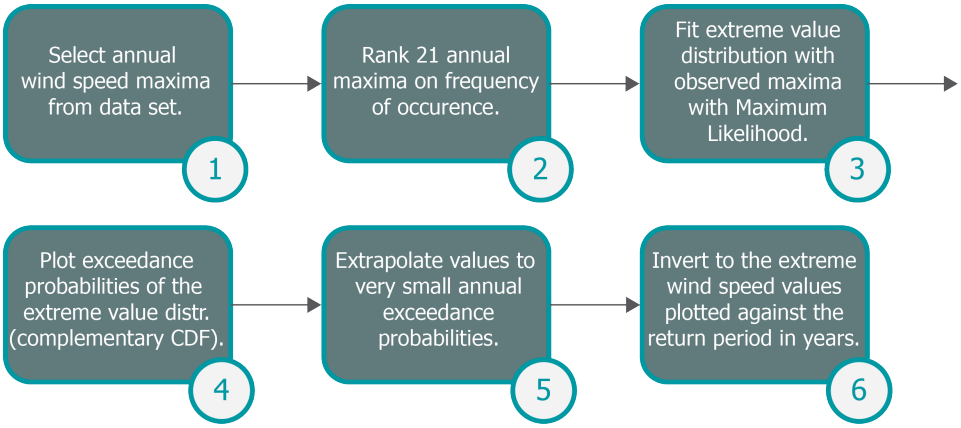

Figure E.1: Steps to calculate the wind speed for different return periods.

E.1.2. Input data

Since the wind is measured at 8 m above MSL, and the desired parameter is the wind speed at 10 m U_{10}, a small correction was applied (as described in the European Wind Atlas (Troen & Petersen, 1989)). The wind speed is a scalar average of two minutes, prior to each hour. The wind gust is the maximum five second scalar of six minutes, prior to each hour. Since 2003 the frequency has been increased to measurements each 6 minutes. Out of consistency, only the hourly data were taken into account.

The data from NOAA station Eagle Point (location is shown as a red dot in figure E.2) functions as a basis for the normative wind speeds of both the location near San Leon as Galveston Island, even though they are 25 kilometer apart. The reason is twofold. First, Eagle Point has by far the longest data record in the Bay, which makes it most suitable for extreme value analysis. Second, the fetch length that is used at San Leon is 30 kilometers and a constant wind field is assumed over this fetch. This length scale is in the same order as the distance between San Leon and Galveston Island.

Since we are interested in 1D waves propagating perpendicular to the coast line, only wind coming from the direction of the bay is taken into account. For location San Leon: 285 to 105 degrees, as shown in figure E.2. The data points that were used for the location San Leon are given in table E.1. For location Galveston Island the annual maxima wind speeds for Eagle Point between 240 to 60 degrees were extracted, as shown in figureE.3). The annual maxima with the directional limits for Galveston Island are largely similar to the the values in E.1.

The following assumptions were made:

- Only the wind coming from the Bay (180 degrees limit) is taken into account.
- The wind field is unidirectional (perpendicular to the coastline) and constant.
- Although the data base (NOAA, 2017) contains gaps of several months,the 21 annual maximum values are representative.
- The data from Eagle Point is used for both the San Leon location as the Galveston Island location.

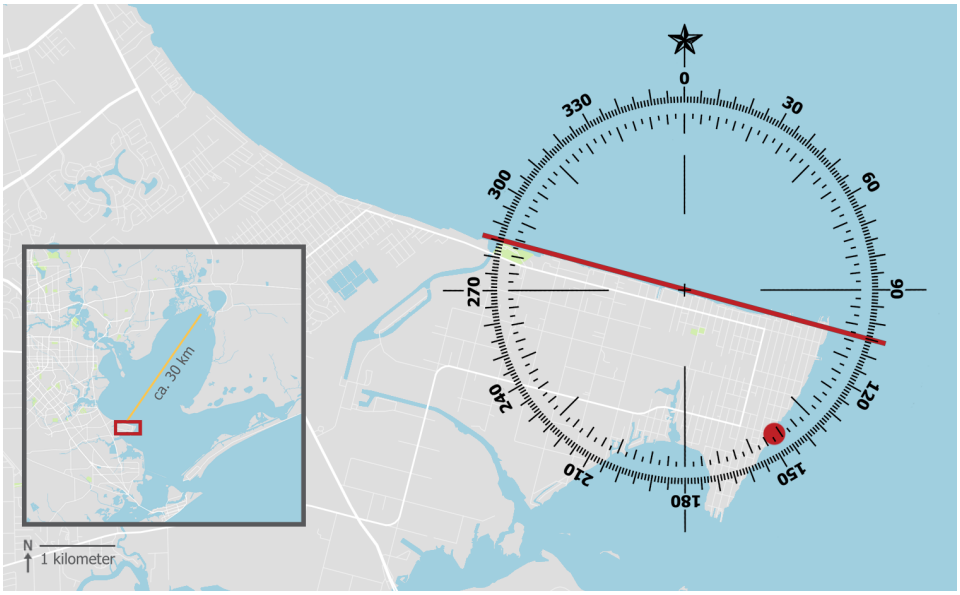

Figure E.2: Compass rose that shows relevant wind directions near San Leon.

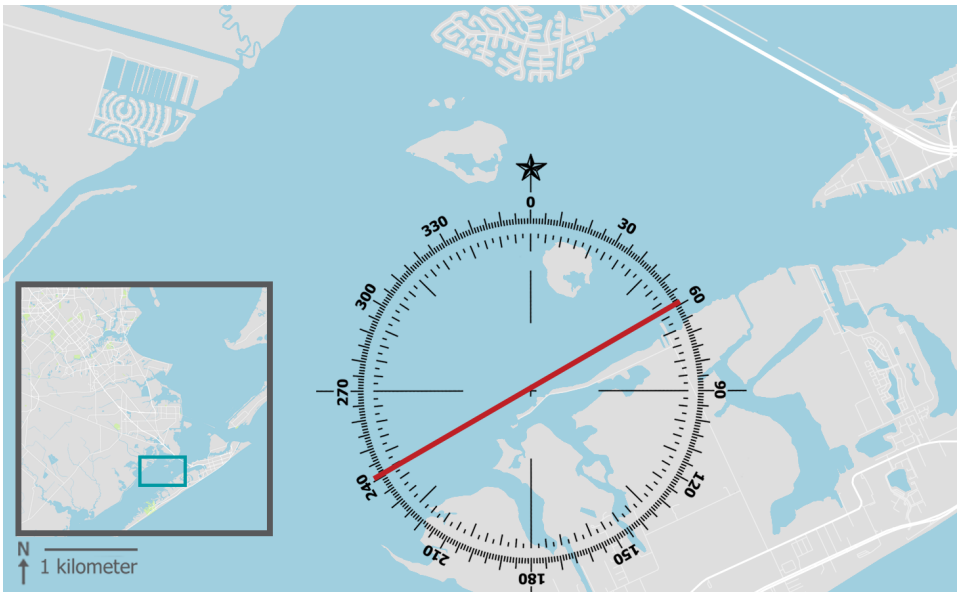

Figure E.3: Compass rose that shows relevant wind directions near Galveston Island.

Table E.1: Maximum annual wind speed values U_{10} that were used for location San Leon, extracted ftom at Eagle Point NOAA (2017)

Year	**Date**	U_{10}	**Direction**	**Gust**	**Note**
		[m/s]	[degree]	[m/s]	
1996	29-02	**14.7**	56	17.3	
1997	14-07	**19.5**	95	24.3	
1998	11-09	**18.0**	37	22.3	Tropical Storm Frances
1999	12-05	**13.9**	2	19.9	
2000	18-11	**13.7**	32	16.0	
2001	14-03	**17.4**	91	26.2	
2002	01-03	**15.5**	77	18.1	
2003	15-07	**16.6**	78	20.2	Hurricane Claudette
2004	06-04	**14.9**	88	16.7	
2005	24-09	**18.8**	347	23.5	Hurricane Rita
2006	24-12	**15.8**	47	18.7	
2007	01-09	**14.2**	66	16.6	
2008	13-09	**36.6**	25	44.7	Hurricane Ike
2009	28-04	**15.6**	91	20.2	
2010	04-02	**16.1**	72	19.0	
2011	24-12	**12.5**	41	13.8	
2012	24-04	**14.7**	7	16.7	
2013	06-02	**13.7**	98	17.0	
2014	06-10	**15.5**	57	18.6	
2015	26-09	**17.8**	62	21.8	
2016	01-04	**15.5**	66	18.1	

E.1.3. Resulting wind speed

The Generalized Extreme Value distribution proves to be the best fit for the observed maxima of the wind speed. The distribution specific parameters are given in table E.2. The cumulative distribution function for the GEV fit for the San Leon annual maximum wind speed is given in E.4. The extrapolated annual exceedance probability graph for the GEV fit for the San Leon annual maximum wind speed is given in E.5. This plot visualizes the return periods for wind speeds (from bay direction) at San Leon. The normative simulations for the wind speed with return periods 10, 50 100 and 500 year for San Leon and Galveston Island are shown in E.3.

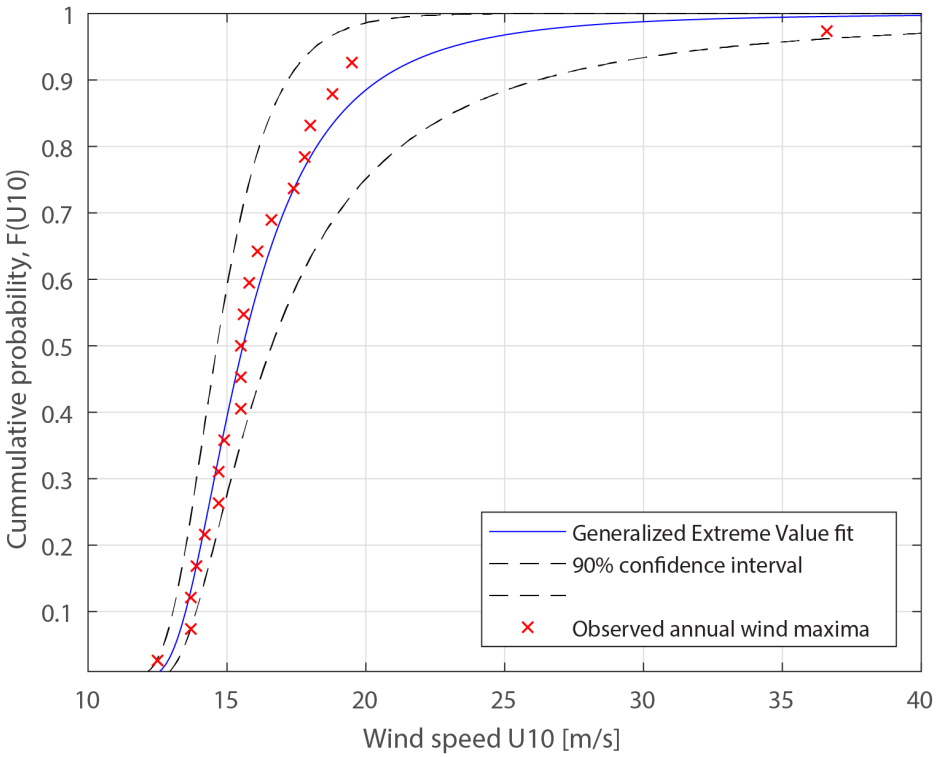

Figure E.4: Extrapolated annual exceedance probability graph for the GEV fit for the San Leon annual maximum wind speed. Observed data plotted with Gringorten method.

The simulations for normative wind speeds, given in the E.3, show that the expected wind speed at San Leon is higher than at Galveston Island. This makes sense if the wind direction is taken into account: the directional boundaries for San Leon encompass wind from open water (and 30 km fetch) while the directional boundaries for Galveston Island include mostly landward wind.

Table E.2: Generalized Extreme Value distribution parameters for the annual maximum wind speed data sets for San Leon and Galveston Island that were approximated with the Maximum Likelihood Method.

Parameter	Description	San Leon	Galveston Island
κ	shape	0.2646	0.2349
μ	location	14.8737	13.7995
σ	scale	1.8238	1.7086

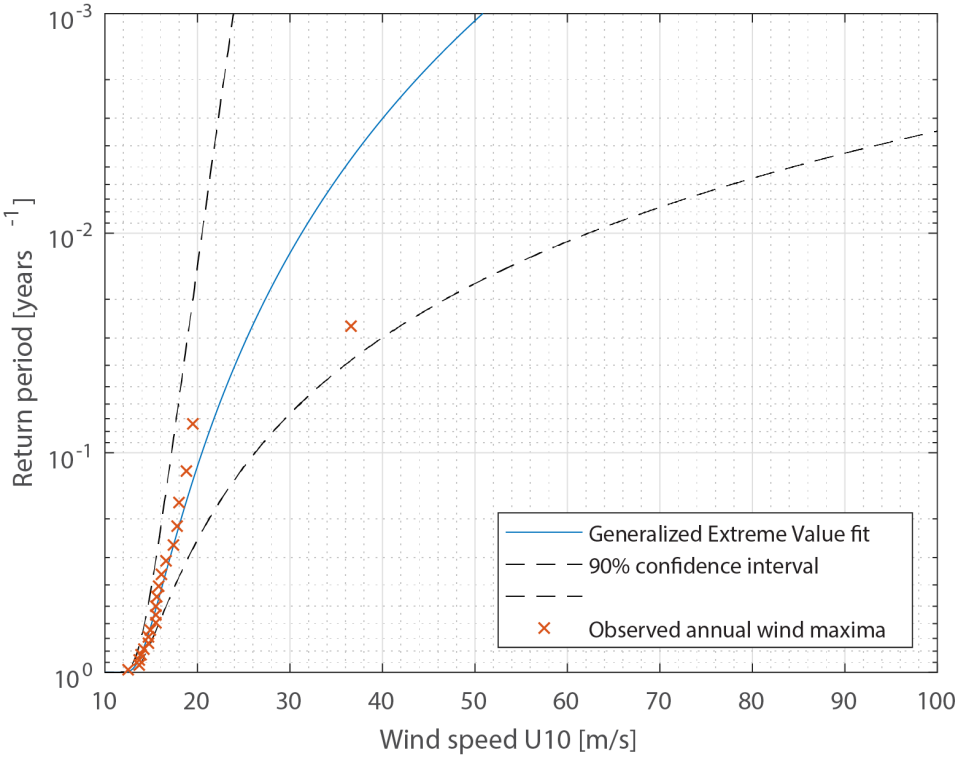

Figure E.5: Cumulative distribution function for the GEV fit for the San Leon annual maximum wind speed. Observed data plotted with Gringorten method.

Table E.3: Normative simulations for the wind speed with return period for San Leon and Galveston Island.

Return period Years	**Wind speed U_{10}, San Leon** m/s	**Wind speed U_{10}, Galveston Island** m/s
10	20.5	18.9
50	27.3	24.7
100	31.3	28.0
500	43.6	37.8

E.2. Wave height

Since no comprehensive wave data are available for the Galveston Bay, wave height values are simulated. Young and Verhagen (1996) explicate an adequate method to simulate wave growth for cases similar to the Galveston Bay. Their results were further refined by Breugem and Holthuijsen (2007). The model represents the relation between the characteristic wave height and period on the one hand, and the fetch, wind speed and water depth on the other. It is tailored to describe wave growth in enclosed water bodies with shallow water conditions.

E.2.1. Methodology and input parameters

The idealized significant wave height and wave period can be calculated with the fetch length, the water depth, wind speed. One of the key concepts is that the parameter involved in the method of Young and Verhagen (1996) are dimensionless. The original measurements and derivation of coefficients were done during mild conditions and the results can then be transposed to a larger scale. The expression for the shallow-water wave growth curves is as follows:

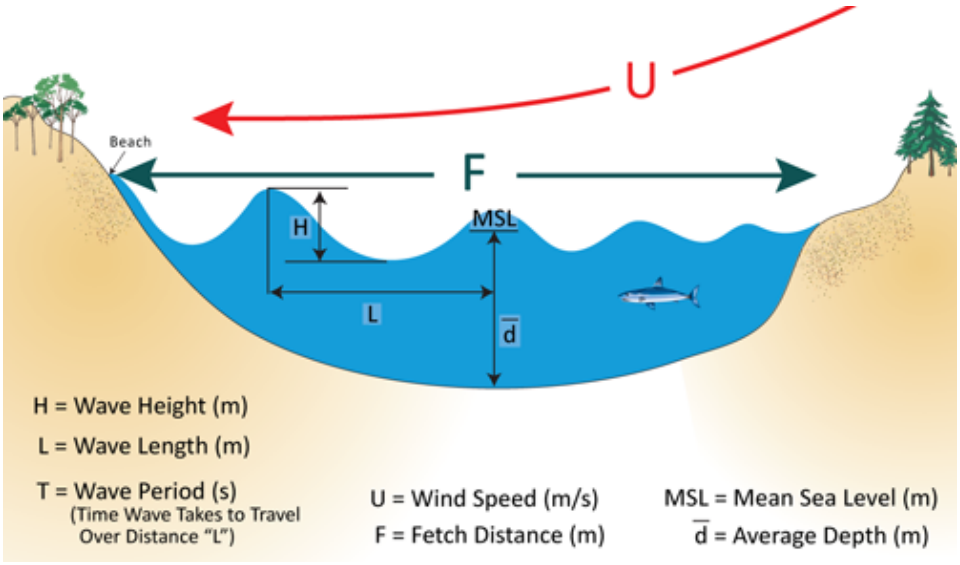

Figure E.6: An illustration of wave generation in a confined water. Source: Lee (2013).

$$\widetilde{H} = \widetilde{H}_{\infty}\left[tanh(k_3\widetilde{d}^{m_3})tanh\left(\frac{k_1\widetilde{F}^{m_1}}{tanh(k_3\widetilde{d}^{m_3}}\right)\right]^{p} \tag{E.1}$$

and for the wave period:

$$\widetilde{T} = \widetilde{T}_{\infty}\left[tanh(k_4\widetilde{d}^{m_4})tanh\left(\frac{k_2\widetilde{F}^{m_2}}{tanh(k_4\widetilde{d}^{m_4}}\right)\right]^{q} \tag{E.2}$$

in which $\widetilde{H}$, $\widetilde{T}$, $\widetilde{d}$ and $\widetilde{F}$ are made dimensionless via expression E.3 - E.6.

$$\widetilde{H}_s = \frac{gH_s}{U_{10}^2} \tag{E.3}$$

$$\widetilde{T}_s = \frac{gT_s}{U_{10}} \tag{E.4}$$

$$\widetilde{d} = \frac{gd}{U_{10}^2} \tag{E.5}$$

$$\widetilde{F} = \frac{gF}{U_{10}^2} \tag{E.6}$$

where H_s is the significant wave height [m], T_s is the significant wave period [s], d is the water depth [m], F is the fetch length [m], U_{10} is the normative wind speed and g is the gravitational acceleration [m^2 /s]. The coefficients for the wave growth curves are given in table E.4.

For a more detailed explanation of the procedure, please refer to Holthuijsen (2010).

An important note is that wave generation due to hurricanes differs from 'regular' wave generation. This is due to the structure and rotating character of a hurricane. The governing parameters are the direction, velocity and the radius to maximum wind of the eye of the hurricane. The diameter of a

Table E.4: Coefficients for wave growth curve (Young & Verhagen, 1996).

Wave height		**Wave period**	m/s
$\widetilde{H}_{\infty}$	0.24	$\widetilde{T}_{\infty}$	7.69
k_1	$4.41e^{-4}$	k_2	$2.77e^{-7}$
k_3	0.343	k_4	0.10
m_1	0.79	m_2	1.45
m_3	1.14	m_4	2.01
p	0.572	q	0.187

Table E.5: Simulated significant wave height near San Leon for idealized conditions.

	San Leon		**Galveston Island**	
Return period years	**Wind speed** U_{10} m/s	**Water depth** m	**Wind speed** U_{10} m/s	**Water depth** m
10	20.5	5.41	18.9	3.79
50	27.3	5.96	24.7	4.37
100	31.3	6.66	28.0	5.29
500	43.6	7.70	37.8	6.54
Fetch [m]	30,000		4,000	

hurricane often spans hundreds of kilometers. Because of this large scale, a wind field in the Galveston Bay is assumed to be homogeneous, even if it is generated by a hurricane.

Additionally, the normative fetch length, water depth and wind speed are used as input parameters. Water depth and wind speed are probabilistic parameters and vary for different return periods. The normative fetch length is assumed to be equal for each return period (for information on the fetch length, refer to section 6.2). The values are given in E.5.

The following assumptions were made:

- The wave height and period depend on wind speed, water depth, fetch and gravitational acceleration only.
- The fetch is small enough to assume an idealized wind field, even during hurricanes.
- Duration is taken infinitely, so that the duration becomes non-essential.
- Turbulence in the air flow, atmospheric instability and wind gusts are disregarded.

E.2.2. Resulting wave height

The resulting simulated significant wave heights and significant wave periods for idealized conditions near San Leon and Galveston Island are given in table E.6.

Table E.6: Simulated significant wave height and significant wave period for idealized conditions near San Leon and Galveston Island.

	San Leon		**Galveston Island**	
Return period years	**Wave height** H_s m	**Wave period** T_s s	**Wave height** H_s m	**Wave period** T_s s
10	1.43	4.79	0.81	3.14
50	1.87	5.34	1.08	3.55
100	2.21	5.76	1.27	3.76
500	3.07	6.61	1.76	4.32

F

Numerical model results for the Galveston Bay

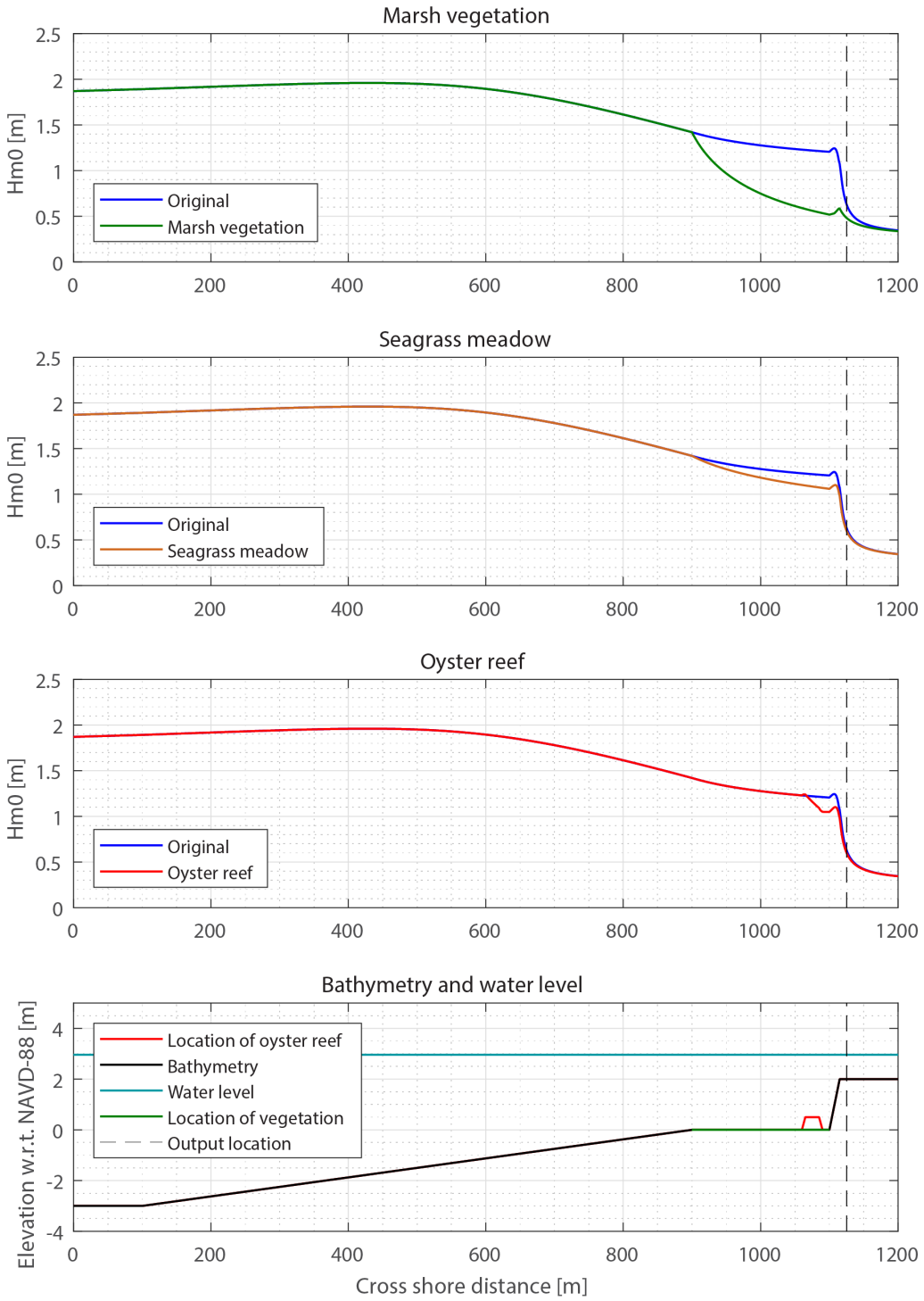

Figure F.1: Resulting significant wave heights over the San Leon cross section in a 1 in 50 years situation.

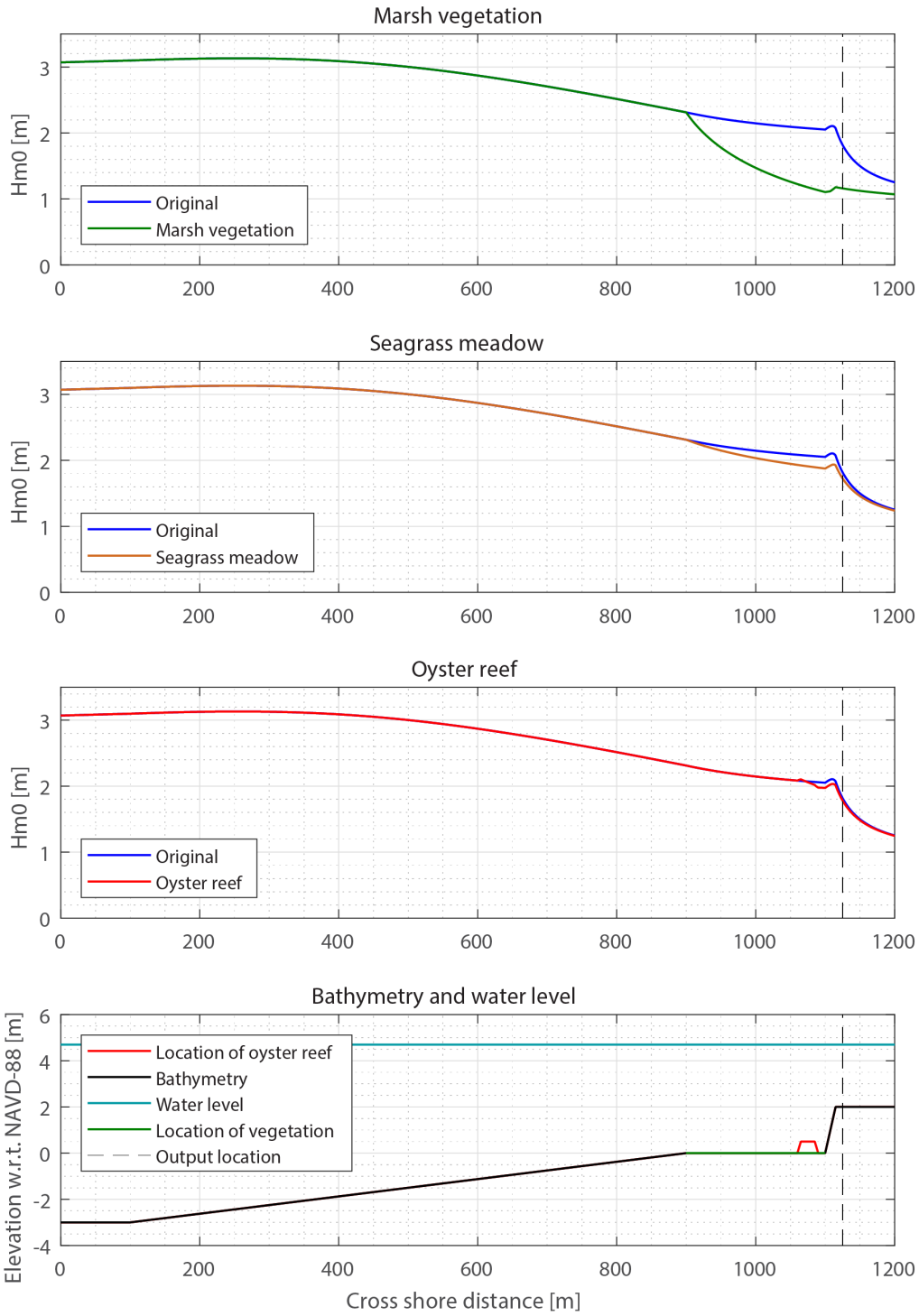

Figure F.2: Resulting significant wave heights over the San Leon cross section in a 1 in 500 years situation.

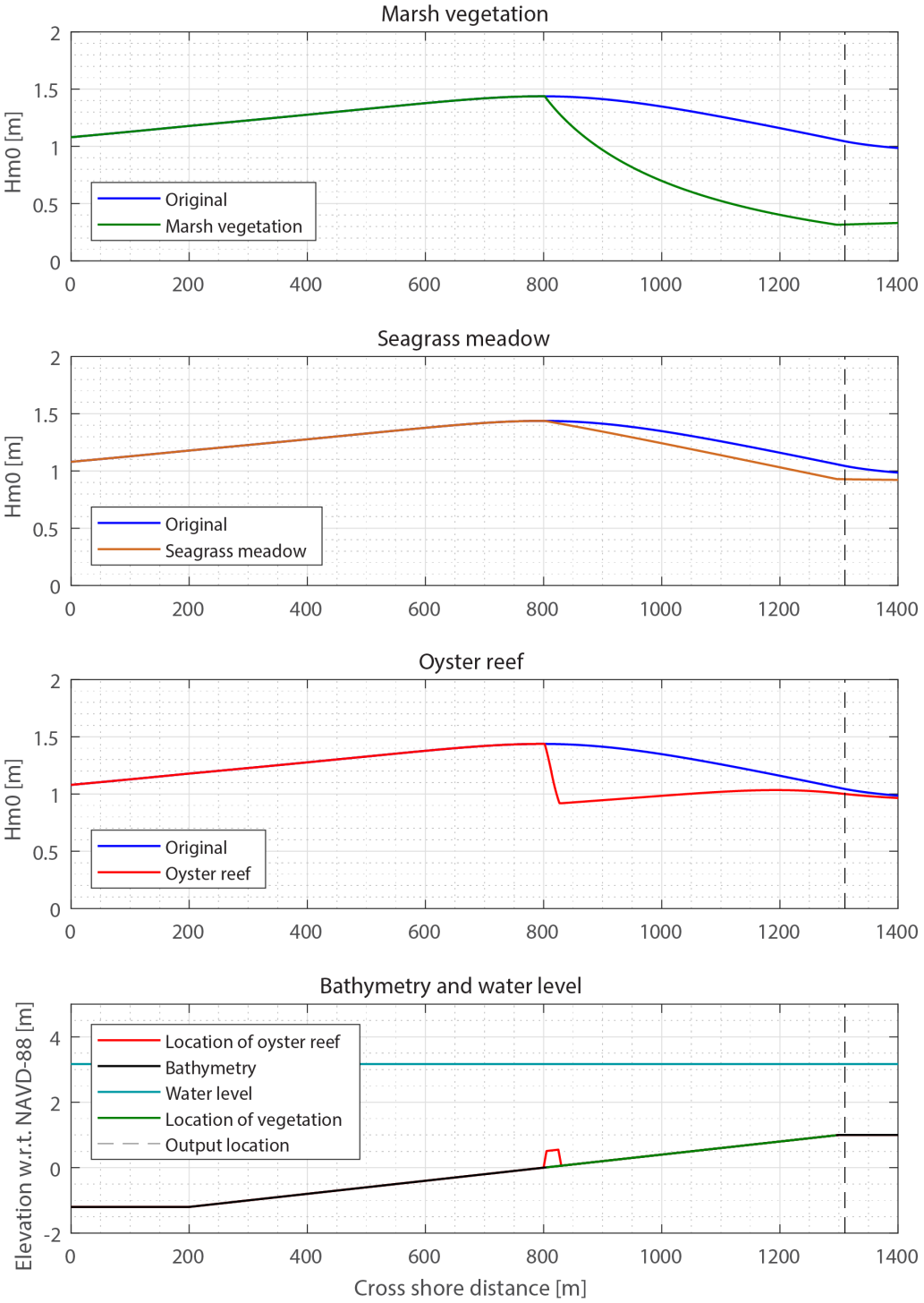

Figure F.3: Resulting significant wave heights over the Galveston Island cross section in a 1 in 50 years situation.

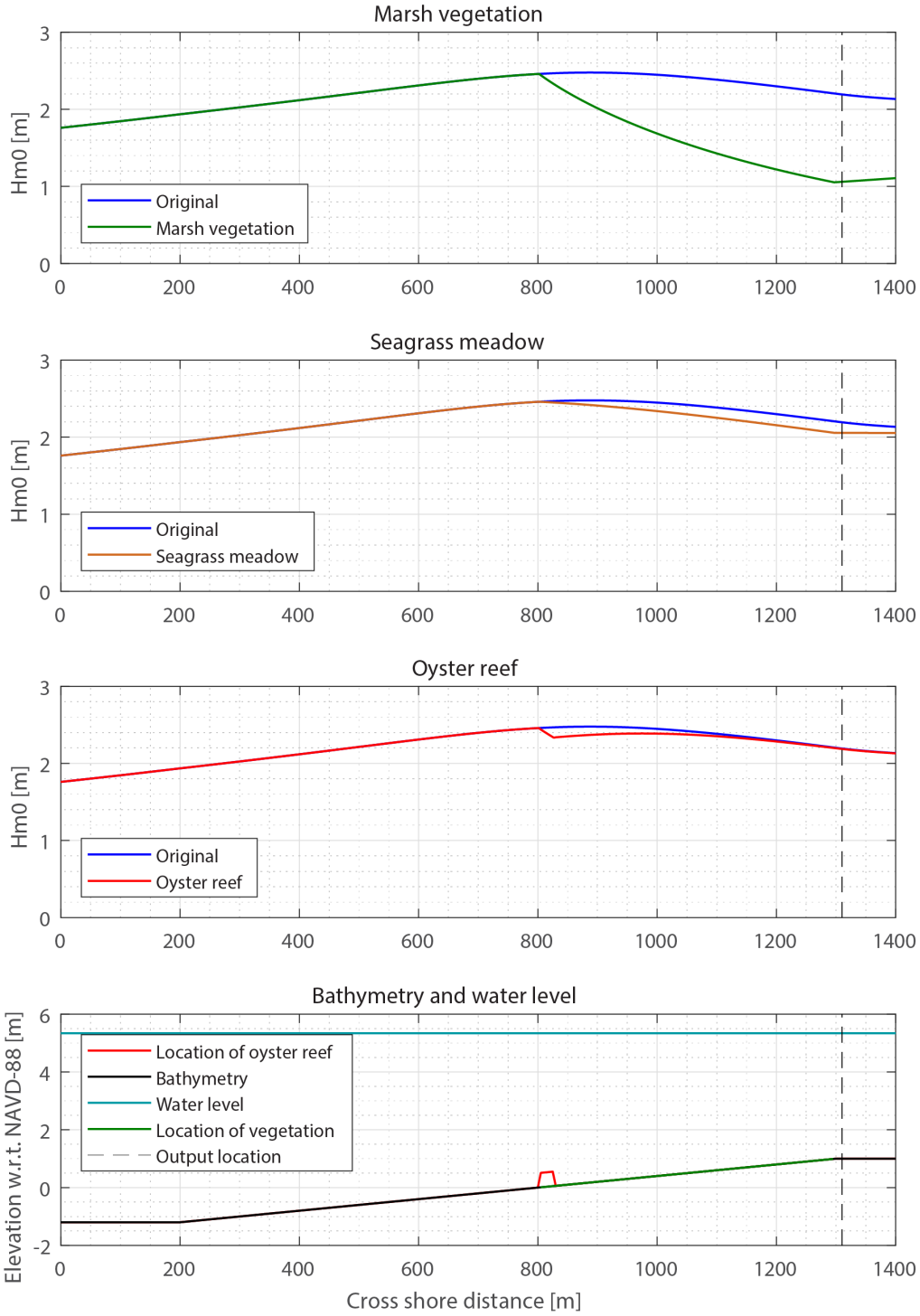

Figure F.4: Resulting significant wave heights over the Galveston Island cross section in a 1 in 500 years situation.

G

Texas City Dike

G.1. Review of calculations

In order to assess the effect of Nature-Based Solutions on the run-up and overtopping, the original calculations were reviewed and new calculations for run-up and overtopping were made.

Considering the original calculations, the first thing to notice is that for the run-up, a basic formula is used, with no corrections for local conditions. However, since the 'run-up factor' is not further specified, it is possible that this parameter includes a correction. The use of this formula is further explainable by the fact that the calculations were made in the early 1960's (Murphy & Geelan, 1965). The second important notice is that run-up, and not overtopping, is the normative criterion. It is customary in the Netherlands to choose overtopping rather than run-up as a criterion for the crest height. Also interesting is the claim that the calculated rate of overtopping would not critically damage the levee.

The reduction factors are given in table G.1.

The run-up height in the original report is calculated by multiplication of the prevailing deep water wave height and the run-up factor:

$$R = H_0 * r_u \tag{G.1}$$

with deep water wave height H_0 and 'run-up factor' r_u. The latter is given as 0.87 and not further specified. This is usually a factor based upon the Iribarren number ξ. That means that in the original design, the additional height of the crest due to run-up is 0.87 times the prevailing deep water wave height.

Overtopping is mentioned but not taken as a criterion for crest height in the report. The rate was calculated that during a design storm the maximum overtopping would be 1 cubic foot per second per linear foot crest (92.9 liter/second/meter). Over a characteristic period of three hours during a design storm, a total of 540 cubic foot per linear foot (50,156 liter / meter) would pass the crest. The report states that given these values, the levee would not be critically damaged.

Table G.1: Input parameters for run-up and overtopping for a 1-100 year situation.

Parameter	Quantity	Value	Unit	Note
g	gravitational acceleration	9.79	[m/s2]	Texas-based
α	angle of slope	9.5	[°]	slope 1:6
γ_b	berm factor	1.0	[-]	no berm present
γ_β	oblique waves factor	1.0	[-]	perpendicular wave attack
γ_f	friction factor	0.95	[-]	grass
γ_v	wall on crest factor	1.0	[-]	no wall on top of crest
R_c	crest freeboard	2.44	[m]	freeboard from original design
Values from original design				
$\xi_{m-1,0}$	breaker parameter	0.87	[-]	
H_{m0}	significant wave height	2.44	[m]	
R	run-up height	2.32	[m]	value from original design
q	mean overtopping	0.0046	[m3/s/m]	4.6 l/s (50.16 m3 / 3h)
q_{max}	maximum overtopping	0.0929	[m3/s/m]	92.9 l/s
New calculations with input from original design				
$\xi_{m-1,0}$	breaker parameter	0.87	[-]	
H_{m0}	significant wave height	2.44	[m]	
$R_{u2\%}$	run-up height	3.53	[m]	
q	mean overtopping	0.0078	[m3/s/m]	7.8 l/s
q_{max}	maximum overtopping	0.1755	[m3/s/m]	175.5 l/s
Calculations with input from San Leon values [1-100 y]				
$\xi_{m-1,0}$	breaker parameter	0.94	[-]	
H_{m0}	significant wave height	1.83	[m]	
$R_{u2\%}$	run-up height	2.86	[m]	
q	mean overtopping	0.0013	[m3/s/m]	1.3 l/s
q_{max}	maximum overtopping	0.0501	[m3/s/m]	50.1 l/s
Calculations with input from San Leon values [1-500 y]				
$\xi_{m-1,0}$	breaker parameter	0.82	[-]	
H_{m0}	significant wave height	2.40	[m]	
$R_{u2\%}$	run-up height	3.27	[m]	
q	mean overtopping	0.0044	[m3/s/m]	4.4 l/s
q_{max}	maximum overtopping	0.1646	[m3/s/m]	164.6 l/s

References

Archie, M., & Terry, H. (2014). *How the proposed lone star coastal national recreation area could attract visitors, boost business, and create jobs* (Tech. Rep.). National Parks Conservation Association. Retrieved from http://www.lonestarcoastal.org/wp-content/uploads/2014/12/opportunity-knocks.pdf

Armitage, A. R., Highfield, W. E., Brody, S. D., & Louchouarn, P. (2015, may). The contribution of mangrove expansion to salt marsh loss on the texas gulf coast. *PLOS ONE*, *10*(5), e0125404. doi: 10.1371/journal.pone.0125404

Balistreri, P., Chemello, R., & Mannino, A. M. (2015). First assessment of the vermetid reefs along the coasts of favignana island (southern tyrrhenian sea). *Biodiversity Journal*, *2015*(6), 371–376. Retrieved from http://www.biodiversityjournal.com/pdf/6(1)_371-376.pdf

Battjes, J. (2002). *Vloeistofmechnaica - lecture notes ct2100*. TU Delft.

Battjes, J., & Janssen, J. (1978). Energy loss and set-up due to breaking of random waves. *Proc. 16th Int. Conf. Coastal Engineering*.

Battjes, J. A., & Stive, M. J. F. (1985). Calibration and verification of a dissipation model for random breaking waves. *Journal of Geophysical Research*, *90*(C5), 9159. Retrieved from https://doi.org/10.1029/jc090ic05p09159 doi: 10.1029/jc090ic05p09159

Blackburn, J., Bedient, P., & Dunbar, L. (2014). *Sspeed center 2014 report* (Tech. Rep.). SSPEED. Retrieved from http://sspeed.rice.edu/sspeed/downloads/HE_Final_Report_2014.pdf

Booij, N., Ris, R. C., & Holthuijsen, L. H. (1999, apr). A third-generation wave model for coastal regions: 1. model description and validation. *Journal of Geophysical Research: Oceans*, *104*(C4), 7649–7666. Retrieved from https://doi.org/10.1029/98jc02622 doi: 10.1029/98jc02622

Borsje, B. W., van Wesenbeeck, B. K., Dekker, F., Paalvast, P., Bouma, T. J., van Katwijk, M. M., & de Vries, M. B. (2011, feb). How ecological engineering can serve in coastal protection. *Ecological Engineering*, *37*(2), 113–122. Retrieved from https://doi.org/10.1016/j.ecoleng.2010.11.027 doi: 10.1016/j.ecoleng.2010.11.027

Bosboom, J., & Stive, M. (2013). *Coastal dynamics i - lecture notes cie4305* (Version 0.4 ed.). Delft Academic Press.

Bouma, T. J., van Belzen, J., Balke, T., Zhu, Z., Airoldi, L., Blight, A. J., … Herman, P. M. (2014, may). Identifying knowledge gaps hampering application of intertidal habitats in coastal protection: Opportunities & steps to take. *Coastal Engineering*, *87*, 147–157. doi: 10.1016/j.coastaleng.2013.11.014

Bouma, T. J., Vries, M. B. D., Low, E., Peralta, G., Tánczos, I. C., van de Koppel, J., & Herman, P. M. J. (2005, aug). TRADE-OFFS RELATED TO ECOSYSTEM ENGINEERING: A CASE STUDY ON STIFFNESS OF EMERGING MACROPHYTES. *Ecology*, *86*(8), 2187–2199. doi: 10.1890/04-1588

Bradley, K., & Houser, C. (2009). Relative velocity of seagrass blades: Implications for wave attenuation in low-energy environments. *Journal of Geophysical Research*, *114*.

Bretschneider, C. (1958). Revisions in wave forecasting: Deep and shallow water. *6th Conference on Coastal Engineering*.

Breugem, W. A., & Holthuijsen, L. H. (2007, may). Generalized shallow water wave growth from lake george. *Journal of Waterway, Port, Coastal, and Ocean Engineering*, *133*(3), 173–182. doi: 10.1061/(asce)0733-950x(2007)133:3(173)

Bureau, U. C. (2016). *United states census bureau.* U.S. Department of Commerce. Retrieved from https://www.census.gov/ (Retrieved at 26-04-17)

Chung, I. K., Oak, J. H., Lee, J. A., Shin, J. A., Kim, J. G., & Park, K.-S. (2013, jan). Installing kelp forests/seaweed beds for mitigation and adaptation against global warming: Korean project overview. *ICES Journal of Marine Science*, *70*(5), 1038–1044. doi: 10.1093/icesjms/fss206

Cohen-Shacham, E., Walters, G., Janzen, C., & Maginnis, S. (Eds.). (2016). *Nature-based solutions to address global societal challenges*. IUCN International Union for Conservation of Nature. doi: 10.2305/iucn.ch.2016.13.en

Coles, S. (2001). *An introduction to statistical modeling of extreme values*. Springer London. Retrieved from https://doi.org/10.1007/978-1-4471-3675-0 doi: 10.1007/978-1-4471-3675-0

Collier, K. (2016, March). New houston hurricane plan stirs the pot. *The Texas Tribune*. Retrieved from https://www.texastribune.org/2016/03/10/new-houston-hurricane-plan-stirs-pot/

Congdon, V., & Dunton, K. (2016). *Tracking long-term trends in seagrass cover and condition in texas coastal waters* (Tech. Rep.). The University of Texas at Austin Marine Science Institute.

Dalrymple, R. A., Kirby, J. T., & Hwang, P. (1984). Wave diffraction due to areas of energy dissipation. *Journal of Waterway Port Coastal and Ocean Engineering*.

Davis, C. V., & Barber, B. J. (1999, aug). Growth and survival of selected lines of eastern oysters, crassostrea virginica affected by juvenile oyster disease. *Aquaculture*, *178*(3-4), 253–271. doi: 10.1016/s0044-8486(99)00135-0

Dean, R. G., & Dalrymple, R. A. (1991). *Water wave mechanics for engineers and scientists*. World Scientific Publishing Company. Retrieved from http://www.ebook.de/de/product/6958988/robert_g_dean_robert_a_dalrymple_water_wave_mechanics_for_engineers_and_scientists.html

de Boer, R. (2015). *Building-with-nature solutions for hurricane flood risk reduction in galveston bay - texas* (mathesis). TU Delft.

Deltacommissie. (2008, September). *Working together with water, a living land builds for its future, findings of the deltacommissie 2008.* The Hague. Retrieved from http://www.deltacommissie.com/doc/2008-09-03%20Advies%20Deltacommissie.pdf

Deltares. (2015). *https://publicwiki.deltares.nl/display/bwn1/building+with+nature.* Retrieved from https://publicwiki.deltares.nl/display/BWN1/Building+with+Nature (Accessed on 19-4-2017)

Deltares. (2016). *Nature-based flood defenses.* Retrieved from https://www.deltares.nl/en/issues/nature-based-flood-defenses/

de Vriend, H. J., van Koningsveld, M., Aarninkhof, S. G., de Vries, M. B., & Baptist, M. J. (2015, jun). Sustainable hydraulic engineering through building with nature. *Journal of Hydro-environment Research*, *9*(2), 159–171. Retrieved from https://doi.org/10.1016/j.jher.2014.06.004 doi: 10.1016/j.jher.2014.06.004

Dupuis, K. W., & Anis, A. (2013, jul). Observations and modeling of wind waves in a shallow estuary: Galveston bay, texas. *Journal of Waterway, Port, Coastal, and Ocean Engineering*, *139*(4), 314–325. doi: 10.1061/(asce)ww.1943-5460.0000160

Dupuits, E., Schweckendiek, T., & Kok, M. (2017, mar). Economic optimization of coastal flood defense systems. *Reliability Engineering & System Safety*, *159*, 143–152. doi: 10.1016/j.ress.2016.10.027

Ecoshape. (n.d.). *Building with nature toolbox - roughness module.* Retrieved from https://publicwiki.deltares.nl/display/BWN1/Tool+-+Roughness+module

EPA. (2013, April). *Level iii and iv ecoregions of the continental united states.* United States Environmental Protection Agency. Retrieved from https://www.epa.gov/eco-research/level-iii-and-iv-ecoregions-continental-united-states (Accessed on 8-6-2017)

Evans, T. (2008, November). Levee system kept texas city from flooding. *Houston Chronicle*. Retrieved from http://www.chron.com/news/hurricanes/article/Levee-system-kept-Texas-City-from-flooding-1622095.php

FEMA. (2009). *Recommended residential construction for coastal areas* (Tech. Rep.). Author. Retrieved from https://www.fema.gov/media-library/assets/documents/3972 (Principal Authors: Bill Coulbourne, Matt Haupt, Scott Sundberg, David K. Low, Jimmy Yeung, John Squerciati)

FEMA. (2012). *Flood insurance study, galveston county, texas* (Tech. Rep. No. volume 1-4). Retrieved from http://www.riskmap6.com

FEMA. (2015). *Limit of moderate wave action (limwa) fact sheet* (Tech. Rep.). Author. Retrieved from https://www.fema.gov/media-library/assets/documents/96413

FEMA. (2017). *The national flood insurance program.* online. Retrieved from https://www.fema.gov/national-flood-insurance-program

Ferrario, F., Beck, M. W., Storlazzi, C. D., Micheli, F., Shepard, C. C., & Airoldi, L. (2014, may). The effectiveness of coral reefs for coastal hazard risk reduction and adaptation. *Nature Communications*, *5*. doi: 10.1038/ncomms4794

Fonseca, M. S., & Cahalan, J. A. (1992, dec). A preliminary evaluation of wave attenuation by four species of seagrass. *Estuarine, Coastal and Shelf Science*, *35*(6), 565–576. Retrieved from https://doi.org/10.1016/s0272-7714(05)80039-3 doi: 10.1016/s0272-7714(05)80039-3

GalvestonBayFoundation. (2016). *Galveston bay report card 2016* (Tech. Rep.). Galveston Bay Foundation and HARC. Retrieved from http://www.galvbaygrade.org/

GCCPRD. (2016, June). *Storm surge suppresion study, phase 3 report, recommended acion* (Tech. Rep.). The Gulf Coast Community Protection and Recovery District. Retrieved from http://www.gccprd.com/pdfs/GCCPRD%20Phase%203%20Report%20-%20Recommended%20Actions.pdf

Gonzalez, L. A., & Lester, L. J. (2011, 12). *The state of the bay* (techreport). Houston, Texas: Galveston Bay Estuary Program. Retrieved from http://galvbaydata.org/Portals/2/StateOfTheBay/2011/

Gringorten, I. I. (1963, feb). A plotting rule for extreme probability paper. *Journal of Geophysical Research*, *68*(3), 813–814. Retrieved from https://doi.org/10.1029/jz068i003p00813 doi: 10.1029/jz068i003p00813

HerbariumNewYork. (2017). *C. v. starr virtual herbarium, new york botanical garden.* Retrieved from http://sweetgum.nybg.org/

Holthuijsen, L. H. (2010). *Waves in oceanic and coastal waters*. Cambridge University Press. Retrieved from http://www.ebook.de/de/product/9549235/leo_h_holthuijsen_waves_in_oceanic_and_coastal_waters.html

HoustonWilderness. (2007). Coastal marshes. In *Houston atlas of biodiversity.* Houston Wilderness.

Hutter, G., McFadden, L., Penning-Rowsell, E., Tapsell, S., & Borga, M. (2007). *Strategies for pre-flood risk management* (Tech. Rep.). FLOODsite. Retrieved from http://www.floodsite.net/html/partner_area/project_docs/T13_07_04_pre_flood_RM_strategies_D13_1_v1_0_p04.pdf

Infantes, E., Orfila, A., Simarro, G., Terrados, J., Luhar, M., & Nepf, H. (2012, jun). Effect of a seagrass (posidonia oceanica) meadow on wave propagation. *Marine Ecology Progress Series*, *456*, 63–72. Retrieved from https://doi.org/10.3354/meps09754 doi: 10.3354/meps09754

Jadhav, R. S., & Chen, Q. (2012, oct). FIELD INVESTIGATION OF WAVE DISSIPATION OVER SALT MARSH VEGETATION DURING TROPICAL CYCLONE. *Coastal Engineering Proceedings*, *1*(33), 41. Retrieved from https://doi.org/10.9753/icce.v33.waves.41 doi: 10.9753/icce.v33.waves.41

Jin, J., Jeong, C., Chang, K.-A., Song, Y. K., Irish, J., & Edge, B. (2010). *Site specific wave parameters for texas coastal bridges: Final report* (Tech. Rep.). Texas Transportation Institute, Texas A&M University.

Jonkman, S., Lendering, K., van Berchum, E., Nillesen, A., Mooyaart, L., de Vries, P., … Nooij, R. (2015, June). *Coastal spine system - interim design report* (Tech. Rep.). TU Delft et al. Retrieved from http://www.tamug.edu/ikedike/images_and_documents/20150620_Coastal_spine_system-interim_design_report_v06.pdf

Jonkman, S., & Schweckendiek, T. (2016). *Flood defences - lecture notes cie5314*. TU Delft.

Jonkman, S. N., Jongejan, R., Maaskant, B., & Vrijling, H. (2011, feb). New safety standards for coastal flood defences in the netherlands. *Coastal Engineering Proceedings*, *1*(32). doi: 10.9753/icce.v32.management.11

Jonsson, I. G. (1966, nov). Wave boundary layers and friction factors. In *Coastal engineering 1966.* American Society of Civil Engineers. doi: 10.1061/9780872620087.010

Kaplan, S., & Garrick, B. J. (1981, mar). On the quantitative definition of risk. *Risk Analysis*, *1*(1), 11–27. doi: 10.1111/j.1539-6924.1981.tb01350.x

Keefer, M. N. (2017). *Wetlands as a nature-based ood defense: Numerical modeling of wave attenuation by vegetation in coastal new jersey* (Tech. Rep.). Delft University of Technology.

Keim, B. D., & Muller, R. A. (2009). *Hurricanes of the gulf of mexico*. LOUISIANA STATE UNIV PR. Retrieved from http://www.ebook.de/de/product/8631032/barry_d_keim_robert_a_muller_hurricanes_of_the_gulf_of_mexico.html

Krull, W., Berry, P., Bauduceau, N., & Cecchi, C. (2015). *Final report of the horizon 2020 expert group on 'nature-based solutions and re-naturing cities* (Tech. Rep.). European Commission, Directorate-General for Research and Innovation. Retrieved from http://bookshop.europa.eu/en/

towards-an-eu-research-and-innovation-policy-agenda-for-nature-based-solutions-re-naturing-cities-pbKI0215162/

Laffoley, D., & Grimsditch, G. (2009). *The management of natural coastal carbon sinks* (Tech. Rep.). International Union for Conservation of Nature and Natural Resources. Retrieved from http://www.lighthouse-foundation.org/fileadmin/LHF/PDF/2009-038.pdf

Lee, H. S. (2013). Integrated modeling of the dynamic meteorological and sea surface conditions during the passage of typhoon morakot. *Dynamics of Atmospheres and Oceans*.

Lopez, J. A. (2009, nov). The multiple lines of defense strategy to sustain coastal louisiana. *Journal of Coastal Research*, *10054*, 186–197. doi: 10.2112/si54-020.1

Manis, J. E., Garvis, S. K., Jachec, S. M., & Walters, L. J. (2014, oct). Wave attenuation experiments over living shorelines over time: a wave tank study to assess recreational boating pressures. *Journal of Coastal Conservation*, *19*(1), 1–11. Retrieved from https://doi.org/10.1007/s11852-014-0349-5 doi: 10.1007/s11852-014-0349-5

McKee, K. L., & Patrick, W. H. (1988, sep). The relationship of smooth cordgrass (spartina alterniflora) to tidal datums: A review. *Estuaries*, *11*(3), 143. doi: 10.2307/1351966

Medina-Gómez, I. (2016, oct). Response of thalassia testudinum morphometry and distribution to environmental drivers in a pristine tropical lagoon. *PLOS ONE*, *11*(10), e0164014. Retrieved from https://doi.org/10.1371/journal.pone.0164014 (Christopher J. Madden and Jorge Herrera-Silveira and Björn Kjerfve) doi: 10.1371/journal.pone.0164014

Mendelsohn, R., Emanuel, K., Chonabayashi, S., & Bakkensen, L. (2012, jan). The impact of climate change on global tropical cyclone damage. *Nature Climate Change*, *2*(3), 205–209. doi: 10.1038/nclimate1357

Mendez, F., & Losada, I. (2004). An empirical model to estimate the propagation of random breaking and nonbreaking waves over vegetation fields. *Coastal Engineering*, *51*, 103–118.

Milazzo, M., Fine, M., Marca, E. C. L., Alessi, C., & Chemello, R. (2016). Drawing the line at neglected marine ecosystems: Ecology of vermetid reefs in a changing ocean. In *Marine animal forests* (pp. 1–23). Springer International Publishing. doi: 10.1007/978-3-319-17001-5_9-1

Milazzo, M., Rodolfo-Metalpa, R., Chan, V. B. S., Fine, M., Alessi, C., Thiyagarajan, V., … Chemello, R. (2014, feb). Ocean acidification impairs vermetid reef recruitment. *Scientific Reports*, *4*. doi: 10.1038/srep04189

Möller, I., Kudella, M., Rupprecht, F., Spencer, T., Paul, M., van Wesenbeeck, B. K., … Schimmels, S. (2014, sep). Wave attenuation over coastal salt marshes under storm surge conditions. *Nature Geoscience*, *7*(10), 727–731. Retrieved from https://doi.org/10.1038/ngeo2251 doi: 10.1038/ngeo2251

Möller, I., Spencer, T., French, J., Leggett, D., & Dixon, M. (1999). Wave transformation over salt marshes: A field and numerical modelling study from north norfolk, england. *Estuarine Coastal and Shelf Science*, *49*, 411-426.

Morison, J. R., O'Brien, M. P., Johnson, J. W., & Schaaf, S. A. (1950). The force exerted by surface waves on piles. *Petroleum Transactions*.

Murphy, W. Y., & Geelan, C. W. (1965). *Development of hurricane flood protection for texas city, texas* (Tech. Rep.). U.S. Army Engineer District Galveston.

Narayan, S., Beck, M. W., Reguero, B. G., Losada, I. J., van Wesenbeeck, B., Pontee, N., … Burks-Copes, K. A. (2016, may). The effectiveness, costs and coastal protection benefits of natural and nature-based defences. *PLOS ONE*, *11*(5), e0154735. doi: 10.1371/journal.pone.0154735

National Hurricane Centre, N. (2008). *Hurricanes in history.* Online. Retrieved from http://www.nhc.noaa.gov/outreach/history/

NationalOceanService. (2016). *Nautical chart, galveston bay, texas.* Retrieved from http://www.charts.noaa.gov (nr. 11326)

Nicholls, R. J., & Small, C. (2002). Improved estimates of coastal population and exposure to hazards released. *Eos, Transactions American Geophysical Union*, *83*(28), 301. doi: 10.1029/2002eo000216

Nielsen, P. (1992). *Coastal bottom boundary layers and sediment transport*. WORLD SCIENTIFIC PUB CO INC. Retrieved from http://www.ebook.de/de/product/7774069/peter_nielsen_coastal_bottom_boundary_layers_and_sedim.html

NOAA. (2016). *Noaa coral reef information system.* Retrieved from https://www.coris.noaa.gov/portals/flowergarden.html

NOAA. (2017). *Noaa station home page "eagle point".* Retrieved from https://tidesandcurrents.noaa.gov/stationhome.html?id=8771013

NOAACCAP. (2010). *Noaa's coastal change analysis program (c-cap).* Retrieved from https://coast.noaa.gov/ccapatlas/

O'Neil, L. (2015, September 2). Why doesn't new orleans look more like amsterdam. *The Atlantic*. Retrieved from http://www.theatlantic.com/technology/archive/2015/09/why-doesnt-new-orleans-look-like-amsterdam/402322/ (Read on January 17, 2017)

Paul, M., & Amos, C. L. (2011, aug). Spatial and seasonal variation in wave attenuation overZostera noltii. *Journal of Geophysical Research*, *116*(C8). Retrieved from https://doi.org/10.1029/2010jc006797 doi: 10.1029/2010jc006797

Pedersen, O., Colmer, T. D., Borum, J., Zavala-Perez, A., & Kendrick, G. A. (2016, feb). Heat stress of two tropical seagrass species during low tides - impact on underwater net photosynthesis, dark respiration and dielin situinternal aeration. *New Phytologist*, *210*(4), 1207–1218.

Phillips, J. D. (2005). *A sediment budget for galveston bay* (Tech. Rep.). Department of Geography, University of Kentucky.

Pulich, W., Dunton, K., Roberts, L., Calnan, T., Lester, J., & McKinney, L. (1996). *Seagrass conservation plan for texas* (Tech. Rep.). Texas Parks & Wildlife. Retrieved from https://tpwd.texas.gov/publications/pwdpubs/media/pwd_bk_r0400_0041.pdf

Rego, J. L., & Li, C. (2010, sep). Storm surge propagation in galveston bay during hurricane ike. *Journal of Marine Systems*, *82*(4), 265–279. Retrieved from https://doi.org/10.1016/j.jmarsys.2010.06.001 doi: 10.1016/j.jmarsys.2010.06.001

Ridge, J. T., Rodriguez, A. B., Fodrie, F. J., Lindquist, N. L., Brodeur, M. C., Coleman, S. E., … Theuerkauf, E. J. (2015, oct). Maximizing oyster-reef growth supports green infrastructure with accelerating sea-level rise. *Scientific Reports*, *5*, 14785. Retrieved from https://doi.org/10.1038/srep14785 doi: 10.1038/srep14785

Rijkswaterstaat. (2016, april). *The national flood risk analysis for the netherlands, vnk project.* Retrieved from https://www.helpdeskwater.nl/publish/pages/33875/vnk-rapport-eng-lr.pdf

Schiereck, G., & Verhagen, H. (2012). *Introduction to bed, bank and shore protection*. VSSD.

Scranton, R. (2016, October 7). When the next hurricane hits texas. *NY Times Sunday Review*. Retrieved from https://www.nytimes.com/2016/10/09/opinion/sunday/when-the-hurricane-hits-texas.html (Read on January 19, 2017)

Scyphers, S. B., Powers, S. P., Heck, K. L., & Byron, D. (2011, aug). Oyster reefs as natural breakwaters mitigate shoreline loss and facilitate fisheries. *PLoS ONE*, *6*(8), e22396. doi: 10.1371/journal.pone.0022396

Shorto, R. (2014, April 9). How to think like the dutch in a post-sandy world. *NY Times Magazine*. Retrieved from https://www.nytimes.com/2014/04/13/magazine/how-to-think-like-the-dutch-in-a-post-sandy-world.html?_r=1 (Read on February 1, 2017)

Smith, C. (2013). *History of the galveston bay areagalveston bay: A brief history of one of america's great waters.* http://www.galvbay.org/about/about-the-bay/history-of-the-bay/. Retrieved from http://houstonhistorymagazine.org/2013/07/galveston-bay/

Snyder, R. L., Dobson, F. W., Elliott, J. A., & Long, R. B. (1981, jan). Array measurements of atmospheric pressure fluctuations above surface gravity waves. *Journal of Fluid Mechanics*, *102*(-1), 1. Retrieved from https://doi.org/10.1017/s0022112081002528 doi: 10.1017/s0022112081002528

SSPEED. (2015). *Houston-galveston area protection system* (Tech. Rep.). Author. Retrieved from http://sspeed.rice.edu/sspeed/downloads/HGAPS_Report_08_31_15.pdf

Steneck, R. S., Graham, M. H., Bourque, B. J., Corbett, D., Erlandson, J. M., Estes, J. A., & Tegner, M. J. (2002, dec). Kelp forest ecosystems: biodiversity, stability, resilience and future. *Environmental Conservation*, *29*(04). doi: 10.1017/s0376892902000322

Stoeten, K. (2013). *Hurricane surge risk reduction for galveston bay* (Tech. Rep.).

Styles, R. (2015, jul). Flow and turbulence over an oyster reef. *Journal of Coastal Research*, *314*, 978–985. Retrieved from https://doi.org/10.2112/jcoastres-d-14-00115.1 doi: 10.2112/jcoastres-d-14-00115.1

Suzuki, T., Zijlema, M., Burger, B., Meijer, M. C., & Narayan, S. (2012, jan). Wave dissipation by

vegetation with layer schematization in SWAN. *Coastal Engineering*, *59*(1), 64–71. doi: 10.1016/j.coastaleng.2011.07.006

SWANteam. (2017). *Technical and scientific documentation of swan.* Retrieved from http://swanmodel.sourceforge.net/

Swart, D. (1974). Offshore sediment transport and equilibrium beach profiles. *Delft Hydraulic Lab Publications*, *No. 131*. Retrieved from http://resolver.tudelft.nl/uuid:057cb136-5f5b-484a-878d-5616fbaeda4e

Taylor, L., Deshotel, J., & Sunstrum, N. (2016, December). *Testimonies report to the 85th texas legislature* (Tech. Rep.). Joint Interim Committee to Study a Coastal Barrier System. Retrieved from http://www.senate.texas.gov/cmtes/84/c840/c840.InterimReport2016.pdf

Troen, I., & Petersen, E. L. (1989). *European wind atlas* (Tech. Rep.). Roskilde: Risø National Laboratory.

TSARP. (2002). *Off the charts, tropical storm allison public report* (Tech. Rep.). FEMA and Harris County FLood Control DIstrict. Retrieved from https://www.hcfcd.org/media/1351/ts-allison_pubreportenglish.pdf

Tsimopoulou, V., Jonkman, S., Kolen, B., Maaskant, B., Mori, N., & Yasuda, T. (2012, nov). A multi-layered safety perspective on the tsunami disaster in tohoku, japan. In *Comprehensive flood risk management.* Informa UK Limited. doi: 10.1201/b13715-143

Tsimopoulou, V., Vrijling, J., Kok, M., Jonkman, S., & Stijnen, J. (2013, sep). Economic implications of multi-layer safety projects for flood protection. In *Safety, reliability and risk analysis* (pp. 2583–2588). Informa UK Limited. doi: 10.1201/b15938-387

Tsimopoulou, V., Vrijling, J. K., Jonkman, S. N., & Kok, M. (2015). Cost-efficient design of multilayer safety systems against large-scale coastal disasters. In *Handbook of coastal disaster mitigation for engineers and planners* (pp. 537–559). Elsevier BV. doi: 10.1016/b978-0-12-801060-0.00025-3

USACE. (1979). *Texas city and vicinity hurricane flood protection: Environmental impact statement* (Tech. Rep.). Retrieved from https://books.google.nl/books?id=HPc0AQAAMAAJ (Galveston District)

USACE. (2005, May). *Freeport and vicinity, texas, hurricane-flood protection, draft feasibility report* (Tech. Rep.). U.S. Army Corps of Engineers District Galveston. Retrieved from http://www.velascodrainagedistrict.com/Freeport_HFP_Draft_Final.pdf

USACE. (2016). *Institute for water resources, faq.* Online. Retrieved from http://www.iwr.usace.army.mil/Missions/Flood-Risk-Management/Flood-Risk-Management-Program/Frequently-Asked-Questions/FAQ-Typical/ (Accessed on 3-3-2016)

van Berchum, E. C., & Mobley, W. (2017). *Flood risk reduction system optimization [unpublished]* (Tech. Rep.). Delft University of Technology, Texas A&M University.

van Dantzig, D. (1956, jul). Economic decision problems for flood prevention. *Econometrica*, *24*(3), 276. doi: 10.2307/1911632

van der Meer, J., Allsop, N., Bruce, T., Rouck, J. D., Kortenhaus, A., Pullen, T., … Zanuttigh, B. (2016). *Manual on wave overtopping of sea defences and related structures. an overtopping manual largely based on european research, but for worldwide application.* (Tech. Rep.). EuroTop.

van der Most, H., Tánczos, I., de Bruijn, K., & Wagenaar, D. (2014, September). New, risk-based standards for flood protection in the netherlands. *6th International Conference On Flood Management, Brazil*. Retrieved from https://www.deltares.nl/app/uploads/2014/12/ICFM6-PAP014759-Flood-protection-standards-def1.pdf

Verhagen, H. J., d'Angremond, K., & van Roode, F. (2012). *Breakwater and closure dams*. VSSD.

Vidal, L., & Basurto, M. (2003). A preliminary trophic model of bahía de la ascensión, quintana roo, mexico. *Fisheries Centre Research Reports*, *11*.

Volp, N., van Prooijen, B., Ysebeart, T., & Dijkstra, J. (2012, 12). *Design rules for oyster reefs to prevent ebd degradation on tidal flats.*

Vuik, V., Heo, H. Y. S., Zhu, Z., Borsje, B. W., & Jonkman, S. N. (2017, oct). Stem breakage of salt marsh vegetation under wave forcing: A field and model study. *Estuarine, Coastal and Shelf Science*. doi: 10.1016/j.ecss.2017.09.028

Vuik, V., Jonkman, S. N., Borsje, B. W., & Suzuki, T. (2016, oct). Nature-based flood protection: The efficiency of vegetated foreshores for reducing wave loads on coastal dikes. *Coastal Engineering*, *116*, 42–56. Retrieved from https://doi.org/10.1016/j.coastaleng.2016.06.001

doi: 10.1016/j.coastaleng.2016.06.001

Walles, B., Troost, K., van den Ende, D., Nieuwhof, S., Smaal, A. C., & Ysebaert, T. (2016, feb). From artificial structures to self-sustaining oyster reefs. *Journal of Sea Research*, *108*, 1–9. doi: 10.1016/j.seares.2015.11.007

Wray, D. (2016, October 25). The ike dike is gaining support, but will it really save us? *Houston Press*. Retrieved from http://www.houstonpress.com/news/the-ike-dike-is-gaining-support-but-will-it-really-save-us-8888737 (Read on January 17, 2017)

Wyatt, A. S. J., Lowe, R. J., Humphries, S., & Waite, A. M. (2013, jan). Particulate nutrient fluxes over a fringing coral reef: Source-sink dynamics inferred from carbon to nitrogen ratios and stable isotopes. *Limnology and Oceanography*, *58*(1), 409–427. doi: 10.4319/lo.2013.58.1.0409

Yang, S. L., Shi, B. W., Bouma, T. J., Ysebaert, T., & Luo, X. X. (2011, jul). Wave attenuation at a salt marsh margin: A case study of an exposed coast on the yangtze estuary. *Estuaries and Coasts*, *35*(1), 169–182. Retrieved from https://doi.org/10.1007/s12237-011-9424-4 doi: 10.1007/s12237-011-9424-4

Yin, F., Hayworth, J. S., & Clement, T. P. (2015, feb). A tale of two recent spills—comparison of 2014 galveston bay and 2010 deepwater horizon oil spill residues. *PLOS ONE*, *10*(2), e0118098. Retrieved from https://doi.org/10.1371/journal.pone.0118098 doi: 10.1371/journal.pone.0118098

Young, I., & Verhagen, L. (1996, dec). The growth of fetch limited waves in water of finite depth. part 1. total energy and peak frequency. *Coastal Engineering*, *29*(1-2), 47–78. doi: 10.1016/s0378-3839(96)00006-3

Ysebaert, T., Yang, S.-L., Zhang, L., He, Q., Bouma, T. J., & Herman, P. M. J. (2011, oct). Wave attenuation by two contrasting ecosystem engineering salt marsh macrophytes in the intertidal pioneer zone. *Wetlands*, *31*(6), 1043–1054. Retrieved from https://doi.org/10.1007/s13157-011-0240-1 doi: 10.1007/s13157-011-0240-1